

Stine Flage Marman

Development of Control Strategies for Demand Controlled Ventilation using IoT

Master's thesis in Energy and Environmental Engineering

Supervisor: Hans Martin Mathisen

Co-supervisor: Maria Justo Alonso

July 2022

Stine Flage Marman

Development of Control Strategies for Demand Controlled Ventilation using IoT

Master's thesis in Energy and Environmental Engineering
Supervisor: Hans Martin Mathisen
Co-supervisor: Maria Justo Alonso
July 2022

Norwegian University of Science and Technology
Faculty of Engineering
Department of Energy and Process Engineering

Abstract

With the prevalence of energy-efficient buildings, airtight constructions to reduce energy for space heating have become common in new buildings. This impacts parameters in the indoor environment which may affect occupants' health and well-being. Demand-controlled ventilation (DCV) is a common energy-saving measure, where sensors measure indoor air quality (IAQ) parameters for control of the ventilation system. The recent development in sensing technologies allows for low-cost sensors (LCSs) to be able to compete with known, reliable detectors. Hence, investigating control strategies to optimize both energy efficiency and IAQ is advantageous.

A full-scale office model is constructed and is used to conduct experiments investigating control strategies for the associated DCV system. Arduino-based low-cost sensors are used to measure CO₂, PM_{2.5}, TVOC, formaldehyde, temperature, and RH concentrations. Each control strategy is constructed by one or several control parameters, measured by the LCSs, for control of supply airflow to the rooms. Additionally, control of recirculation of air is implemented in the control strategies. The obtained data is used to validate a building model for co-simulation between EnergyPlus and CONTAM. Thus, simulations with various control strategies for DCV systems are performed and set the base for the analysis of control strategies. The analysis aims to evaluate both IAQ and energy use related to each control strategy.

The simulations indicate that changing the control parameters for ventilation control can improve both energy consumption and IAQ. By introducing recirculation to the system, indoor concentrations of outdoor generated pollutants, such as PM_{2.5}, are improved. Recirculation of air also results in larger energy savings. With regard to room airflow control, applying more control parameters to the ventilation logic showed great results. The simulations indicated that formaldehyde should be considered used for airflow control in DCV systems, while outdoor-generated pollutants may be less suited. However, what parameters are most efficient may depend on climate and building characteristics.

Sammendrag

Som et resultat av utbredelsen av energieffektive bygg, er lufttette konstruksjoner blitt vanlige i nye bygg for å redusere energibruk til oppvarming. Dette påvirker innendørs luftkvalitetsparametere og kan gi utslag på folks helse og velvære. Behovsstyrt ventilasjon (DCV) er et vanlig tiltak for å redusere energibruk, hvor sensorer brukes for å måle forskjellige parametere innendørs som brukes til kontroll av ventilasjonssystemet. Utviklingen av sensorteknologi gjør at lavkostnadssensorer nå kan konkurrere mot kjente, pålitelige detektorer. Derfor er det fordelaktig å undersøke kontrollstrategier for ventilasjon for å optimalisere både energieffektivitet og inneklima.

En full-skala kontormodell er konstruert og blir brukt til eksperimenter for å undersøke forskjellige kontrollstrategier for det tilhørende DCV-systemet. Arduino-baserte lavkostnadssensorer brukes for å måle CO₂, PM_{2.5}, TVOC, formaldehyd, temperatur og relativ fuktighet. Hver kontrollstrategi er satt sammen av en eller flere kontrollparametere, som måles av sensorene, for kontroll av luftmengde inn til rommene. I tillegg er forskjellig logikk for omluft implementert i kontrollstrategiene. Dataen fra eksperimentene brukes for å validere en bygningsmodell som brukes i samsimulering mellom EnergyPlus og CONTAM. Simuleringer av forskjellige kontrollstrategier for DCV-systemer setter dermed grunnlaget for analysen av de forskjellige kontrollstrategiene. Analysen vil basere seg på å evaluere både energibruk og inneklima.

Simuleringene indikerer at ved å endre kontrollparameterne for ventilasjonskontroll kan både energibruk og inneklima forbedres. Ved å introdusere omluft til systemet, blir innendørs konsentrasjon av utendørsgenererte forurensninger, som eksempelvis PM_{2.5}, redusert. Omluft resulterer også i større energibesparelser. Relatert til romluftskontroll vil hvilke parametere som passer best avhenge av klima og bygningskarakteristikk. Simuleringene indikerte at formaldehyd bør vurderes for bruk til kontroll av luftmengder i DCV systemer, mens utendørsgenererte forurensninger er mindre egnet.

Preface

The research in this thesis was conducted in the Department of Energy and Process Engineering of the Norwegian University of Science and Technology (NTNU), under the supervision of Professor Hans Martin Mathisen and Maria Justo Alonso during spring 2022. The research is based on experiments conducted in a test facility and simulations investigating various control strategies for demand-controlled ventilation systems. This thesis is related to the PhD of Maria Justo Alonso.

Throughout the period of this work, the research have met several challenges, resulting in delays in getting started with experiments, as the test facility have not been ready. Due to several new challenges occurring even after the facility was considered ready for experiments, simulations was introduced to the scope instead of all the experiments that were planned. Thanks to the help of many people the research could finally be finished in July 2022.

I would like to thank the people that have contributed in getting the test facility used in this thesis ready. A massive thank you to Inge Håvard Rekstad who have always offered his help, even on short notice and with any kind of problem that occurred. Halvor Haukevik, Tore Kristian Eliassen, Morten Grønli, Kent Andre Ross and Reidar Tellebon have also contributed with various solutions regarding the ventilation system, and I am thankful for their help. Also, thank you to Kaja Grotnes Edvardsen, Mona Skar Baglo and Caroline Berntsen Markeng for participating in preparatory experiments, often on short notice.

A special thank you to my supervisors Hans Martin Mathisen and Maria Justo Alonso for their valuable advise throughout. I am especially grateful for the support offered by Maria Justo Alonso, who contributed in solving the problems we met along the way, and helped with adjustments of the scope of this thesis when new challenges occurred.

Stine Flage Marman

Trondheim, July 2022

Contents

List of Figures	x
List of Tables	xvi
Abbreviations	xix
1 Introduction	1
1.1 Background and motivation	1
1.2 Problem Description	2
1.3 Research questions	3
1.4 Previous work	3
1.5 Structure	4
2 State of The Art	5
2.1 Indoor Air Quality	5

2.1.1	Health Effects of Pollutants	6
2.1.2	Limit values	15
2.1.3	Energy Savings and IAQ	15
2.2	Ventilation Systems	18
2.3	Demand Controlled Ventilation	20
2.4	Sensors for DCV Systems	26
2.4.1	Internet of Things	27
2.4.2	Low-Cost Sensing Technologies	27
2.4.3	Summary of characteristics	34
2.4.4	Sensor placement	36
3	Methodology	38
3.1	Experimental Setup	39
3.1.1	Full-Scale Test Facility	40
3.1.2	Pollution Sources	41
3.1.3	Sensors	43
3.1.4	Control System	47
3.2	Leakage Testing	48

3.2.1	Tracer Gas Tests	48
3.2.2	Air Pressure Tests	50
3.3	Experimental Procedure: Control Strategies	52
3.3.1	Control Logics	54
3.4	Simulations	56
3.4.1	Simulation Tools: CONTAM and EnergyPlus	56
3.4.2	Validation of Building Model	57
3.4.3	Simulation Procedure	58
3.5	Analysis	62
4	Results and Analysis	63
4.1	Test-Facility Leakage	63
4.1.1	Tracer Gas Testing	64
4.1.2	Air Pressure Testing	65
4.2	Control Strategy Experiments	66
4.2.1	Surrounding Environment	66
4.2.2	Recirculation Control	67
4.3	Validation of Building Model	70

4.4	Simulations	76
4.4.1	No Recirculation Control	77
4.4.2	Recirculation Control: PM _{2.5}	80
4.4.3	Recirculation Control: CO ₂ /CO ₂ and PM _{2.5}	83
4.4.4	Recirculation Control: CO ₂ and FA	87
4.4.5	Trondheim Simulations	90
4.4.6	Total Yearly Energy Consumption	93
5	Discussion	95
5.1	Sources of Error	95
5.1.1	Leakage Tests	96
5.1.2	Control Strategy Experiments	97
5.1.3	Co-Simulations	100
5.2	Evaluation of Research Questions	101
6	Conclusion	108
7	Further Work	110
	Bibliography	111

Appendix	124
A Air Pressure Test Calculations	124
A.1 Test 1.2	125
A.2 Test 2.2	126
A.3 Test 3.2	127
A.4 Test 4.2	127
A.5 Pressure Tests Results	128
B Control Strategy Experiment Figures	130
C Results: Simulations Trondheim.	140
D Formaldehyde	150
E Datasheets	151
E.1 Datasheets for the Ventilation System Components	151
E.1.1 Air Handling Unit	151
E.1.2 Onrion LØV with Sirius Supply diffuser	155
E.1.3 VAV terminal	161
E.2 Datasheets for the Sensors	167

E.2.1	Sensirion SCD30: CO ₂ , Temperature and Relative Humidity	167
E.2.2	Sensirion SPS30: Particulate Matter	173
E.2.3	Sensirion SGP30: Total Volatile Organic Compounds	179
E.2.4	The Dart Sensors WZ-S: Formaldehyde	186

F Risk Analysis **192**

List of Figures

- 2.1 Pollution sources (Su, Sutarlie, and Loh, 2020) 7
- 2.2 Principle of constant static pressure control (Mysen, Schild, and Cablé, 2017). 23
- 2.3 Principle of static pressure reset control (Mysen, Schild, and Cablé, 2017). 23
- 2.4 Principle of damper-optimized control (Mysen, Schild, and Cablé, 2017). 24
- 2.5 Principle of variable supply air diffuser control (Mysen, Schild, and Cablé, 2017). 25

- 3.1 Sketch of the methodology. 38
- 3.2 Schematic of the test facility. Credits (Sketchup Usernames): Sanju (Computer), DGL.ARUNARCH (Chair), Keino (Gas Silinder Industrial) and Suphot Jindaluang (Rotameter). 40
- 3.3 Ventilation floor plan. 41
- 3.4 Manikins. 42
- 3.5 Schematic of the setup of CO₂ bottle and rotometers. Credits (Sketchup Usernames): Keino (Gas Silinder Industrial) and Suphot Jindaluang (Rotameter). 43

3.6	Sensor Box.	44
3.7	Airflow control strategies used for experiments.	55
3.8	Recirculation control strategies used for experiments.	55
3.9	Schematic of the information exchange between CONTAM and EnergyPlus (Alonso, Dols, and Mathisen, 2022).	57
4.1	CO ₂ control without recirculation in room 1.	68
4.2	CO ₂ control with PM recirculation control in room 1.	69
4.3	CO ₂ control with CO ₂ and PM recirculation control in room 1.	70
4.4	Measured vs. simulated development of CO ₂ concentration and supply AFRs for room 1, 2, and 3.	72
4.5	Measured vs. simulated development of FA and PM _{2.5} concentration for room 1, 2, and 3.	74
4.6	Measured vs. simulated development of temperature for room 1, 2, and 3.	75
4.7	CO ₂ concentration over a year for room CSs without recirculation.	77
4.8	PM _{2.5} concentration over a year for room CSs without recirculation.	78
4.9	FA concentration over a year for room CSs without recirculation.	79
4.10	Temperature over a year for room CSs without recirculation.	80
4.11	CO ₂ concentration over a year for room CSs with PM _{2.5} as a control parameter for recirculation.	81

4.12	PM _{2.5} concentration over a year for room CSs with PM _{2.5} as a control parameter for recirculation.	82
4.13	FA concentration over a year for room CSs with PM _{2.5} as a control parameter for recirculation.	82
4.14	Temperature over a year for room CSs with PM _{2.5} as a control parameter for recirculation.	83
4.15	CO ₂ concentration over a year for room CSs with CO ₂ or CO ₂ and PM _{2.5} as control parameters for recirculation.	84
4.16	PM _{2.5} concentration over a year for room CSs with CO ₂ or CO ₂ and PM _{2.5} as control parameters for recirculation.	85
4.17	FA concentration over a year for room CSs with CO ₂ or CO ₂ and PM _{2.5} as control parameters for recirculation.	86
4.18	Temperature over a year for room CSs with CO ₂ or CO ₂ and PM _{2.5} as control parameters for recirculation.	87
4.19	CO ₂ concentration over a year for room CSs with CO ₂ and FA as control parameters for recirculation.	88
4.20	PM _{2.5} concentration over a year for room CSs with CO ₂ and FA as control parameters for recirculation.	89
4.21	FA concentration over a year for room CSs with CO ₂ and FA as control parameters for recirculation.	89
4.22	Temperature over a year for room CSs with CO ₂ and FA as control parameters for recirculation.	90

4.23	Temperature over a year for room control strategies without recirculation.	91
4.24	Temperature over a year for room control strategies with CO ₂ and PM _{2.5} as control parameters for recirculation.	92
4.25	PM _{2.5} concentration over a year for room control strategies without recirculation. . .	93
4.26	Total yearly energy consumption for simulations using Beijing weather and outdoor pollution levels.	94
B.1	CO ₂ control without recirculation in room 1.	130
B.2	CO ₂ control without recirculation in room 2.	131
B.3	CO ₂ control without recirculation in room 3.	131
B.4	CO ₂ control with PM recirculation control in room 1.	132
B.5	CO ₂ control with PM recirculation control in room 2.	132
B.6	CO ₂ control with PM recirculation control in room 3.	133
B.7	CO ₂ control with CO ₂ recirculation control in room 1.	133
B.8	CO ₂ control with CO ₂ recirculation control in room 2.	134
B.9	CO ₂ control with CO ₂ recirculation control in room 3.	134
B.10	CO ₂ control with CO ₂ and PM recirculation control in room 1.	135
B.11	CO ₂ control with CO ₂ and PM recirculation control in room 2.	135
B.12	CO ₂ control with CO ₂ and PM recirculation control in room 3.	136

B.13 CO₂ and PM control without recirculation in room 1. 136

B.14 CO₂ and PM control without recirculation in room 2. 137

B.15 CO₂ and PM control without recirculation in room 3. 137

B.16 CO₂ and PM control with CO₂ and PM recirculation control in room 1. 138

B.17 CO₂ and PM control with CO₂ and PM recirculation control in room 2. 138

B.18 CO₂ and PM control with CO₂ and PM recirculation control in room 3. 139

C.1 CO₂ concentration over a year for room control strategies without recirculation. . . 140

C.2 PM_{2.5} concentration over a year for room control strategies without recirculation. . 141

C.3 FA concentration over a year for room control strategies without recirculation. . . . 141

C.4 Temperature over a year for room control strategies without recirculation. 142

C.5 CO₂ concentration over a year for room control strategies with PM_{2.5} as control
parameter for recirculation. 142

C.6 PM_{2.5} concentration over a year for room control strategies with PM_{2.5} as control
parameter for recirculation. 143

C.7 FA concentration over a year for room control strategies with PM_{2.5} as control
parameter for recirculation. 143

C.8 Temperature over a year for room control strategies with PM_{2.5} as control parameter
for recirculation. 144

C.9	CO ₂ concentration over a year for room control strategies with CO ₂ or CO ₂ and PM _{2.5} as control parameters for recirculation.	144
C.10	PM _{2.5} concentration over a year for room control strategies with CO ₂ or CO ₂ and PM _{2.5} as control parameters for recirculation.	145
C.11	FA concentration over a year for room control strategies with CO ₂ or CO ₂ and PM _{2.5} as control parameters for recirculation.	145
C.12	Temperature over a year for room control strategies with CO ₂ or CO ₂ and PM _{2.5} as control parameters for recirculation.	146
C.13	CO ₂ concentration over a year for room control strategies with CO ₂ and FA as control parameter for recirculation.	146
C.14	PM _{2.5} concentration over a year for room control strategies with CO ₂ and FA as control parameter for recirculation.	147
C.15	FA concentration over a year for room control strategies with CO ₂ and FA as control parameter for recirculation.	147
C.16	Temperature over a year for room control strategies with CO ₂ and FA as control parameter for recirculation.	148
C.17	Total yearly energy consumption for simulations using Beijing weather and outdoor pollution levels.	149
D.1	FA measured at same place for three different sensors.	150

List of Tables

2.1	Particulate matter fraction diameter (U.S. Environmental Protection Agency, 2021b)	10
2.2	Operative temperature recommendations from TEK17 for various activity levels . . .	13
2.3	Summary of the recommended limits of the IAQ parameters	15
2.4	Minimum AFRs based on people and materials as emission sources according to TEK17 and the Guideline 444.	20
2.5	Summary of characteristics related to low-cost sensing technologies.	35
3.1	Placement of the sensor boxes in the test facility.	44
3.2	SCD30 sensor specifications for CO ₂	45
3.3	SCD30 sensor specifications for temperature.	45
3.4	SCD30 sensor specifications for RH.	45
3.5	SPS30 sensor specifications for PM _{2.5}	46
3.6	SGP30 sensor specifications for TVOC.	46

3.7	WZ-S sensor specifications for FA.	47
3.8	Tracer gas test.	49
3.9	Air pressurization tests.	50
3.10	Measurement plan.	53
3.11	Plan.	53
3.12	CSs which will be simulated.	59
3.13	Minimum AFRs calculated from TEK17 and the AFRs used in simulations.	59
3.14	Airflow control logic.	60
3.15	Recirculation control logic.	61
3.16	Definitions of subscripts from the control logics.	61
4.1	Infiltration rates calculated from tracer gas tests.	64
4.2	Calculated n_{50} values, based on air pressure tests.	65
4.3	CO ₂ generation rates per person in the simulation models.	71
4.4	Calculated MBE and RMSE.	76
A.1	Settings and achieved differential pressures for the four air pressure tests. The door between room 1 and 2 were sealed with duct tape.	124
A.2	Settings and achieved differential pressures for the four air pressure tests. The door between room 1 and 2 were not sealed with weatherstrips.	125

A.3 Calculated leakage coefficients for each building part. 128

A.4 Calculated infiltration for a 50 Pa pressure difference through each building part,
total infiltration through each room and the resulting n_{50} for each room. 129

Abbreviations

AFR Airflow Rate

AHU Air Handling Unit

CAV Constant Airflow Volume

CO₂ Carbon Dioxide

CVRMSE Coefficient Of Variance Of Root Mean Squared Error

DCV Demand - Controlled Ventilation

EC Electrochemical Cell

FA Formaldehyde

HRV Heat Recovery Ventilator

HVAC Heating Ventilation and Air Conditioning

IAQ Indoor Air Quality

IoT Internet of Things

IR Infrared

LCS Low Cost Sensors

MBE Mean Bias Error

MOS Metal Oxide Semiconductor

NDIR Non - Dispersive Infrared

NIPH Norwegian Institute of Public Health

OA Outdoor Air

PAS Photoacoustic Spectroscopy

PC-DCV Pressure Controlled DCV

PID Photoionization Detector

PM Particulate Matter

RH Relative Humidity

SBS Sick Building Syndrome

SFP Specific Fan Power

SPR-DCV Static Pressure Reset Controlled DCV

TVOC Total Volatile Organic Compounds

VAV Variable Airflow Volume

VOC Volatile Organic Compounds

VSAD-DCV Variable Supply Air Diffuser DCV

ZEB Zero Emission Building

Chapter 1

Introduction

1.1 Background and motivation

Heating ventilation and air conditioning (HVAC) systems account for 40-60 % of the total energy consumption of a building, and ventilation systems account for about 20-30 % of the total consumption (Zender–Swiercz, 2021). Demand - controlled ventilation (DCV) is a widespread method to control the supply of outdoor air and reduce energy consumption. The ventilation airflow rate (AFR) is regulated according to demand, measured by sensors inside the associated room or building. Thus, energy is saved when the demand for ventilation is low. Extensive amounts of studies have investigated the energy-saving potential of implementing a DCV system compared to a constant airflow volume (CAV) ventilation system. Hamida et al. (2019) found the potential to be up to 86 %.

The recent development in sensing technology has allowed for a wide range of low-cost sensors (LCSs) to be commercially available. Such sensors are commonly connected to the internet of things (IoT) and can thereby measure various indoor parameters in real-time and send control signals to regulate the AFRs (Demanega et al., 2021). CO₂ is the most common control parameter

and is considered a proxy for occupancy (Mysen, Schild, and Cablé, 2017). Thus, other pollutants unrelated to occupancy may not be handled efficiently by a CO₂ regulated ventilation system. Therefore, it is desirable to evaluate other control parameters for the control of DCV systems, to obtain the best attainable IAQ, while securing low energy demand.

1.2 Problem Description

This thesis will add to the work of previous project and master theses, where students have tested Arduino based sensors and RaspberryPi for measurements of indoor air quality. A selection of relevant IAQ parameters to be considered for DCV control have been recognized. Various combinations will be tested for both control of AFRs and recirculation of air.

A laboratory test facility has been established and will be used for experiments related to the development of control strategies in this thesis. CO₂, PM_{2.5}, formaldehyde, temperature, and RH are the control parameters which will be considered for the DCV control. In addition to the experiments, co-simulations between CONTAM and EnergyPlus are used to evaluate additional control strategies.

Thus, the aim of the thesis is to establish what parameters used for control of supply air and recirculated exhaust air provides adequate IAQ. The ultimate goal of the research is to develop solutions that provide healthy and good IAQ with the least possible energy consumption.

The following tasks are to be conducted:

1. State of the art of indoor pollution-related health issues, DCV regulation method, and sensors for control of ventilation systems.
2. Preparatory leakage tests to evaluate airtightness of the test facility.
3. Laboratory measurements for investigation of control strategies for DCV.

4. Validation of simulation building model.
5. Simulations for investigation of additional control strategies.
6. Evaluation of what control parameters attains best possible IAQ.
7. Analysis regarding recirculation of return air based on laboratory measurements and simulations.
8. Analysis of energy use related to the various control strategies.

1.3 Research questions

Based on the scope, the thesis will revolve around the following research questions:

- **How are other pollutants affected when CO₂ is used as the control parameter for a DCV system?**
- **Which IAQ parameters should be considered used for control of DCV systems, with regard to achieving best possible IAQ while also attaining low energy demand?**
- **What IAQ parameters are most sufficient for the purpose of regulating the ratio between recirculated air and OA in the supply?**

1.4 Previous work

This project is a continuation of the previous work of Gram (2019), Jørgensen (2020) and Buch (2021). Arduino-based low-cost sensors have been evaluated in field tests on schools in Trondheim, and in controlled environments in the laboratory at NTNU. Despite, the unveiled limitations to the low-cost sensors, they are evaluated to be sufficient for further investigation to be used for control of DCV systems.

1.5 Structure

The thesis begins with introducing theory and literature on themes relevant to the research conducted. Thus, an introduction to the various IAQ parameters and related health risks, information about DCV systems, and state-of-the-art low-cost sensing technologies are presented in Chapter 2. Thereafter, Chapter 3 gives an overview of the methods. This includes a general description of the test facility and sensors used for measurements. Then information about the experiments and simulations for the investigation of CSs for DCV systems are presented. Chapter 4 presents the results of experiments and simulations, and a comparison of the CSs with regard to IAQ and energy consumption. Continuing, Chapter 5 revolves around the research questions and discusses the results that have been found. Lastly Chapter 6 gives a conclusion to the thesis.

Chapter 2

State of The Art

This chapter provides insight into the theory and research on relevant themes including indoor air quality, pollutants, and related health risks. Additionally, regulation principles for DCV and some common low-cost sensing technologies are presented. The chapter is gathered from a preliminary project conducted by the author in autumn 2021, but the chapter has been revised for this thesis.

2.1 Indoor Air Quality

The term IAQ embraces the types and amounts of pollutants in the indoor air, as well as people's perception of the air quality. Among factors such as thermal, acoustic, and visual comfort, IAQ is recognized as a key factor in influencing occupant's satisfaction with the indoor environment (Danza et al., 2020). Furthermore, IAQ is closely related to the comfort, health, and performance of a building's occupants. The various symptoms of bad IAQ are heavily determined by the composition and concentration of the individual pollutants. Accordingly, obtaining good IAQ by monitoring and controlling the indoor pollution levels, is crucial to reduce health risks and assuring the occupant's performance and well-being (U.S. Environmental Protection Agency, 2021a). Assuring adequate ventilation is a measure to maintain good IAQ, by regulating the air temperature and diluting or

removing indoor-generated pollutants.

2.1.1 Health Effects of Pollutants

Indoor pollutants contribute to bad IAQ and can result in various health effects. High concentrations of pollutants inside a building can cause immediate discomfort, or the effects may appear later, up to many years after exposure. The acute impacts are usually minor, and such symptoms often cease when the person is removed from the exposure. Furthermore, the acute symptoms can normally be treated easily if necessary (Palmisania et al., 2021). However, more severe health effects are also associated with indoor pollutants. Palmisania et al. (2021) suggest that the severity of the symptoms is related to the following factors:

- The level of a single contaminant or mixture of contaminants.
- The inherent toxicity of the contaminants.
- The exposure time.

Accordingly, it is important to identify the impacts of the various pollutants typically found in the indoor environment, of which concentrations they become a risk to occupant's health, and how to reduce the indoor concentrations. Pollutants are released as gases or particles from various sources (U.S. Environmental Protection Agency, 2021a), and identifying the sources makes it possible to limit the emissions. Common sources include tobacco products, building materials, combustion, cleaning products, occupants, and pets. Some of them are related to activities, such as smoking and cleaning, and can therefore be limited by the user. Other sources, such as building materials, can release pollutants throughout the building's lifetime (U.S. Environmental Protection Agency, 2021a). Figure 2.1 shows an illustration of some pollution sources found in the indoor environment.

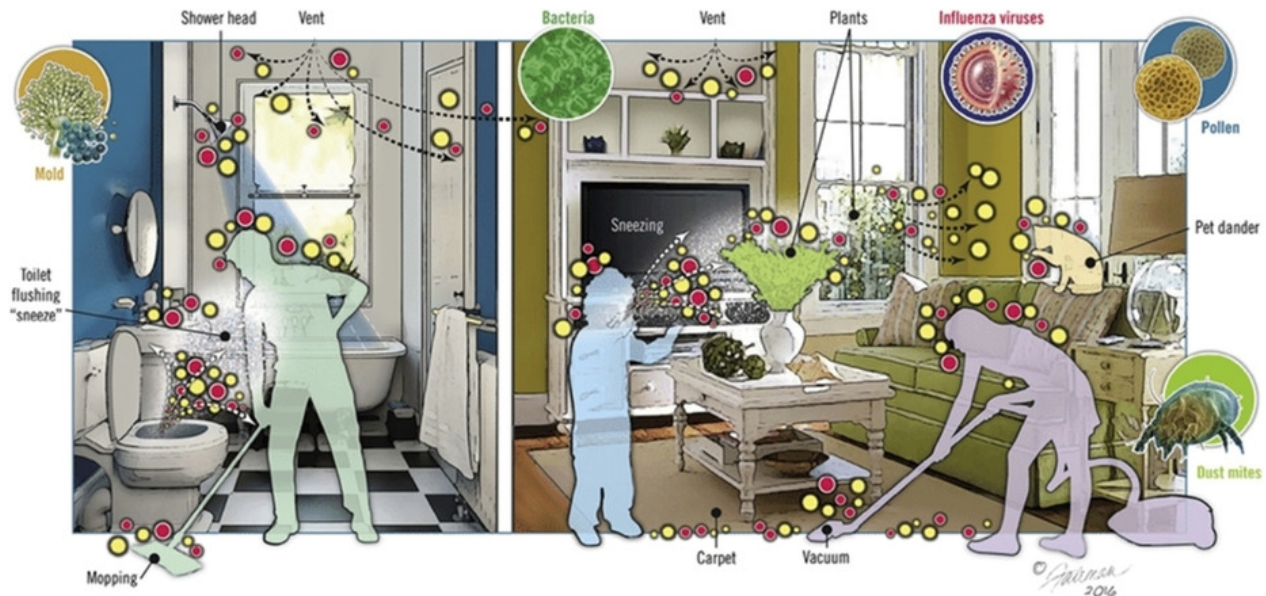


Figure 2.1: Pollution sources (Su, Sutarlie, and Loh, 2020)

Some common short-term health effects of polluted indoor air include irritation of the eyes, nose, and throat, dry skin, headaches, dizziness, and fatigue. These immediate health symptoms are associated with a number of pollutants, but since they are similar to those of several other viral diseases, it can be challenging to determine the cause of the symptoms. Relevant to building occupancy, such symptoms are included as indicators of sick building syndrome (SBS). SBS symptoms are defined as acute health and comfort effects related to time spent in the indoor environment, without being able to identify a specific illness or cause. Contributing factors to SBS symptoms include inadequate ventilation and indoor air pollutants (U.S. Environmental Protection Agency, 1991). More serious immediate effects such as asthma symptoms showing up or being aggravated are identified as having a relation to the IAQ as well. However, the long-term effects of poor IAQ are generally of larger concern. Some of the most serious long-term effects include some respiratory diseases, heart disease, and cancer (U.S. Environmental Protection Agency, 2021a). As these symptoms may show up years after exposure, it is important to maintain good IAQ even if symptoms aren't noticeable.

There are extensive amounts of research on acceptable pollution concentrations and the health impacts of pollutants. However, it can be discussed what pollutants are the most important to consider concerning IAQ-related health issues (Poirier et al., 2021). Based on a large amount of

studies, Poirier et al. (2021) have identified CO₂, relative humidity (RH), formaldehyde (FA), and fine particulate matter as relevant IAQ performance parameters for avoiding both building damage and health risks. These pollutants are all considered in this thesis, with some additional parameters being included. Thus, the IAQ parameters considered in this thesis is based on the previous work of Gram (2019), Jørgensen (2020) and Buch (2021), and consist of:

- Carbon dioxide
- Particulate matter
- Volatile organic compounds
- Formaldehyde
- Relative humidity
- Temperature

Despite not being categorized as pollutants, RH and temperature are included as they are important IAQ parameters. In addition to affecting the perceived IAQ directly, high temperature and humidity may increase the concentration level of some pollutants (U.S. Environmental Protection Agency, 2021a). They are also important factors for the survival of respiratory viruses and can therefore contribute to the transmission of various diseases (Folkehelseinstituttet, 2015). In the following, each IAQ parameter is presented in more detail.

Carbon Dioxide

Carbon dioxide (CO₂) is often considered the most important greenhouse gas concerning global warming. The major emission sources are traffic, electricity production, and industry (U.S. Environmental Protection Agency, 2022). CO₂ can be brought inside through the ventilation system, but due to normally low outdoor concentrations, this is normally not a significant contributor to the indoor CO₂ load (Folkehelseinstituttet, 2015). Outdoor concentrations depend on location and

landscape, but during April 2022 CO₂ atmospheric CO₂ levels are measured to be 420 on Hawaii (Earth's CO₂, 2022). Indoor concentrations are normally in the range of 350-2000 ppm but can vary up to 6000 ppm at most (Poirier et al., 2021). Considering CO₂ levels observed in indoor environments, humans are the main source, as CO₂ is released through respiration. Thus, the indoor CO₂ level is a direct indication of the occupancy and is therefore commonly used to estimate ventilation rates in buildings (Mysen, Schild, and Cablé, 2017). Other indoor CO₂ sources are indoor combustion such as candles, cooking, smoking, and fireplaces.

Studies have revealed that the physical health impacts directly connected to CO₂ concentrations observed in indoor environments are minimal (Mishra et al., 2020). However, a correlation between CO₂ concentrations and cognitive performance has been proven by several studies. Allen et al. (2016) did a study exposing participants to various concentrations of CO₂, in a controlled office space. They found that the participants performed worse with higher concentrations of CO₂, even when concentrations were kept at common indoor values, below 1420 ppm (Allen et al., 2016). Another study introduced the experiment participants to different environments, where the CO₂ concentrations varied up to about 2400 ppm while solving various cognitive tasks. The participants performed better when the concentration was kept below 1000 ppm, suggesting an impact of CO₂ when the concentrations exceed this threshold value (T. Hong, J. Kim, and M. Lee, 2018).

The norwegian institute of public health (NIPH) states that there are no adverse health risks associated with CO₂ levels under normal indoor conditions. They also recommend 1000 ppm as a maximum concentration, based on indicator knowledge of bad IAQ (Folkehelseinstituttet, 2015).

Particulate Matter

Particulate matter (PM) is the mixture of solid particles and liquid droplets present in the air. Traffic is the largest outdoor source, and other outdoor sources include industry and outdoor combustion. Outdoor sources are significant for indoor concentrations, but indoor activities may have an impact as well. These include indoor combustion, smoking, and cooking (Folkehelseinstituttet, 2015). PM particle sizes vary a lot, from particles that can be seen with the bare eye, such as dust and dirt,

to particles that can only be detected using microscopes (U.S. Environmental Protection Agency, 2021b). The size of fractions is used to categorize the particles. An overview of the particle fractions is presented in Table 2.1.

Table 2.1: Particulate matter fraction diameter (U.S. Environmental Protection Agency, 2021b)

Particulate matter fraction	Aerodynamic diameter, d [μm]
PM_{10}	$d \leq 10$
$\text{PM}_{2.5-10}$	$2.5 < d < 10$
$\text{PM}_{2.5}$	$d \leq 2.5$
$\text{PM}_{0.1}$	$d \leq 0.1$

Table 2.1 reveal that PM_{10} is characterized by having an aerodynamic diameter equal or inferior to $10 \mu\text{m}$. These particles can be separated into fine particles and coarse particles. The coarse particles, $\text{PM}_{2.5-10}$, define the largest particles and are deposited in the upper airways, while the smaller particles can be inhaled down to the lungs (Folkehelseinstituttet, 2015). The particles characterized by having an aerodynamic diameter equal to or inferior to $2.5 \mu\text{m}$, $\text{PM}_{2.5}$, are known as fine particles. Because of the small size of $\text{PM}_{2.5}$, they can penetrate at varying depths causing various health issues ranging from irritation of the eyes, throat, and nose, to respiratory dysfunction, infections, or even strokes. Hence, fine particles have been identified as one of the pollutants of concern by several studies (Poirier et al., 2021).

One study examined the acute health effects of fine particles emitted from cooking and burning candles. The participants were 36 young asthmatics, who entered three 5-hour exposure sessions, with various concentrations in the range $5.8-96.1 \mu\text{g}/\text{m}^3$. The study concludes that these indoor sources may affect asthmatics and that there is a health potential in reducing such emissions. Also, improving the IAQ may especially increase comfort among people with respiratory diseases (Laursen et al., 2021). Another study examined the relation between PM exposure and adverse health effects among young, healthy adults. This study also concluded that variations in concentration impacted acute respiratory-related health outcomes in healthy, young adults (Shaughnessy, Venigalla, and Trump, 2015).

In indoor air, the PM_{2.5} fraction of PM₁₀ is dominating, in addition to being more harmful than the larger particles. Guidelines from WHO state that the annual average should not exceed 5 $\mu\text{g}/\text{m}^3$, and the 24 hours average should not exceed 15 $\mu\text{g}/\text{m}^3$ more than 3-4 days per year (World Health Organization (WHO), 2022).

Volatile Organic Compounds

Volatile organic compounds (VOC) is a collective term for a variety of organic chemicals with high vapor pressure and water solubility. They are emitted as gases from certain solids or liquids (U.S. Environmental Protection Agency, 2020). Indoor sources are the main contributor to indoor concentrations and can be up to ten times higher than outdoor concentrations for some VOCs (U.S. Environmental Protection Agency, 2020). Some of the common sources include building materials, furniture, cleaning supplies, paint, lacquers, cooking, and smoking (Folkehelseinstituttet, 2015).

VOCs are recognized for having short- and long-term adverse health effects (U.S. Environmental Protection Agency, 2020). Allen et al. (2016) states that high concentrations of VOCs impact cognitive performance. Another study provides evidence suggesting that VOCs in the indoor environment may increase the risk of asthma and asthma-like symptoms. They also highlight the issue of commercial products and chemicals not being stored or used properly, contributing to unnecessary high indoor concentration of VOCs (Paterson et al., 2021). Cancer risk has also been evaluated as a result of certain VOCs. These evidences are based on data from animal testing and occupational exposure. However, the risk is considered to be low in most cases (Folkehelseinstituttet, 2015).

Due to little knowledge about each VOC, combined with indoor concentrations of the individual compounds usually being below concentrations of health impact, VOCs are often considered collectively. Total volatile organic compounds (TVOC) is a term for a group of VOCs representing the whole pool of pollutants. While FHI does not have a recommended maximum concentration value for TVOC, they advise avoiding unnecessary exposure. However, FHI has recommendation values for some of the individual VOCs, including FA (Folkehelseinstituttet, 2015).

Formaldehyde

FA is a common VOC, mainly found in indoor environments. Emissions from materials, furniture, consumer products, and combustion processes are the main sources of release. Additionally, it can be a product of oxidation or reaction of other VOCs, due to being highly reactive at room temperature. The concentration varies according to the age of the building where the release of FA decreases with time. Temperature, relative humidity, and air change rates also have an impact on the generation of FA. Outdoor air (OA) does not contribute to indoor pollution since ambient levels are generally low, typically 1-4 $\mu\text{g}/\text{m}^3$. The most important measure to control the FA concentration is the air change rate and the use of low-emitting materials and products (World Health Organization, 2010).

Many studies have investigated the influence of FA on health (K.-H. Kim, Jahan, and J.-T. Lee, 2011). Exposure is known to have wide-ranging recognized health impacts, from eye irritation to cancer risk (Poirier et al., 2021). Onyije and Avwioro (2012) assessed the effect of acute exposure to FA on medical students in Nigeria. Numerous health impacts were found to have a correlation to the exposure, including irritation of the eyes, unpleasant smell, runny or congested nose, and dizziness (Onyije and Avwioro, 2012). Another study investigated the relationship between FA exposure and allergic asthma in adults. They found a definite correlation where there was an obvious increasing risk with higher FA concentrations (Wei, Xiao-bin, and Xiao-chuan, 2004). Other studies have conducted information about the health effects of long-term exposure to FA, through occupational exposure. K.-H. Kim, Jahan, and J.-T. Lee (2011) have reviewed several studies on the effect of FA, where both acute and long-term exposure are reviewed. The American Cancer Society's Cancer Prevention Study II (cited in K.-H. Kim, Jahan, and J.-T. Lee, 2011) concluded that long-term exposure can result in a 34 % increased risk of the neurodegenerative disease ALS. Several studies on occupational exposure indicate that long-term exposure to FA results in an increased risk of several types of cancer (K.-H. Kim, Jahan, and J.-T. Lee, 2011).

WHO states that it is appropriate with a guideline for FA. The reason is that indoor exposures are the dominant contributor to personal exposures through inhalation, and indoor concentrations

may be high enough to cause adverse health effects. Thus, a short-term (30-minutes) guideline of $100 \mu\text{g}/\text{m}^3$ is recommended to prevent sensory irritation in the general population (World Health Organization, 2010). NIPH recommends the same maximum value (Folkehelseinstituttet, 2015).

Temperature

Air temperature is a crucial factor in assuring satisfaction with the room air and thermal comfort for a building's occupants. Warm air is usually associated with a perception of worse IAQ, than with lower temperatures which often give an impression of fresher air. Therefore thermal comfort, which is defined as the state of satisfaction with the thermal environment is important to the IAQ.

T. Hong, J. Kim, and M. Lee (2018) tested the impacts of various temperatures on cognitive performance. They concluded that slightly cold temperatures resulted in better performance than slightly warm (T. Hong, J. Kim, and M. Lee, 2018). Supporting this conclusion, Jaber, Dejan, and Marcella (2017) found that both hot and cold sensations can negatively affect cognitive performance, while mild cooling sensation may improve it.

TEK17 recommends keeping the air temperature below 22°C throughout the heating season. In addition, Table 2.2 present the recommendations for operative temperature for different activity levels. In addition, vertical temperature gradients and temperature variations should be limited to avoid discomfort. TEK17 recommends that the difference in temperature between feet and head level is kept below $3\text{-}4^\circ\text{C}$, and periodic or daily variations in air temperature are kept below 4°C (Direktoratet for byggkvalitet, 2017).

Table 2.2: Operative temperature recommendations from TEK17 for various activity levels

Activity level	Light work	Medium work	Hard work
Temperature [$^\circ\text{C}$]	19-26	16-26	10-26

Relative Humidity

RH is also a thermal comfort factor affecting the IAQ. It is defined as the ratio of water vapor in the air and the maximum amount of water vapor if the air was saturated. People are generally very

adaptive to variations in RH, and values between 20-60% do not normally have an impact on the perception of the indoor environment. However, too high or low values can cause damage to the building and health risks (Folkehelseinstituttet, 2015).

In the Nordic climate, low RH values are common, especially during the winter season due to the large temperature rise for space heating. There are no requirements for minimum RH values. However, very low values as those inferior to 20% have several negative effects. The low values can increase the risk of static electricity damaging equipment, in addition to health symptoms such as sensory irritation in the eyes and upper airways, the perception of dry air, and dry skin (Folkehelseinstituttet, 2015). Wolkoff, Azuma, and Carrer (2021) verifies the already known health effects, such as irritation of the eyes and airways. They found that elevating the indoor air humidity from dry indoor air conditions results in a reduction of dry eye and fatigue symptoms, fewer complaints about dry air, and less compromised work performance. Furthermore, the study found values between 40-60% RH to be optimal for health and work performance (Wolkoff, Azuma, and Carrer, 2021).

There is not a required maximum value of RH either, but high values over 70% can cause odors, fungal growth, and building damage from condensing on cold and poorly ventilated surfaces (Folkehelseinstituttet, 2015). Additionally, increasing the humidity results in increased emissions of certain VOCs from material surfaces and other typical VOC sources (Wolkoff, Azuma, and Carrer, 2021). In addition, the fungal growth can also contribute to higher VOC concentrations, as some fungi release VOCs. Several other health risks are associated with mold, including allergic reactions, infections, and symptoms related to SBS (Brambilla and Sangiorgio, 2020). For humidity levels over 80%, the viability of influenza viruses on steel surfaces is increased as well (Wolkoff, Azuma, and Carrer, 2021).

2.1.2 Limit values

Table 2.3 presents a summary of the limit values for the pollutants, and the acceptable range for temperature and relative humidity, which have already been discussed.

Table 2.3: Summary of the recommended limits of the IAQ parameters

IAQ parameter	Limit values
CO ₂	< 1000 ppm
PM _{2.5}	< 15 $\mu\text{g}/\text{m}^3$ (1 day) < 5 $\mu\text{g}/\text{m}^3$ (1 year)
TVOC	Avoid unnecessary exposure
FA	< 100 $\mu\text{g}/\text{m}^3$ (30 minutes)
Temperature	19 - 26 degrees (activity level = light work)
RH	20-60%

2.1.3 Energy Savings and IAQ

In addition to IAQ being important for assuring a healthy indoor environment, considerations regarding the reduction of global emissions have become a major focus in the building sector. The EU has a goal of 90% reduction in the emissions from the building sector by 2050. Zero emission building (ZEB)s are highly energy-efficient buildings, where on-site production of renewable energy covers the energy demand and compensates for the building's emissions. For this to be accomplished, energy-saving measures must be applied to both construction and technical systems of the building.

Poirier et al. (2021) highlights the crucial issue of "providing healthy indoor air to occupants, as well as ensuring energy efficiency". While energy savings have become a major priority in today's society, they cannot be at the expense of good air quality. This induces several considerations

when introducing energy-saving measures to buildings, as IAQ and energy efficiency are not always compatible. The performance of ventilation systems is pivotal in obtaining adequate IAQ in energy-efficient buildings (Poirier et al., 2021). In the following, some challenges and solutions to the IAQ-energy paradox will be illustrated.

Airtightness

Airtightness is a typical characteristic of ZEBs. Improving the energy performance of a building usually involves airtight constructions, due to high insulation thickness to reduce the demand for space heating and space cooling (Danza et al., 2020). Thus, improved airtightness is associated with reduced infiltration, which is defined as uncontrolled movement of air through leaks, cracks, and other openings in the building envelope. Reduced infiltration reduces the indoor concentration of pollutants that are mainly associated with outdoor sources, such as PM. However, with regard to pollutants mainly generated from indoor sources, including CO₂ and VOCs, improved airtightness may worsen the IAQ, as the pollution level may build up inside (Kempton, Daly, and Dewsbury, 2020). Studying the subject of pollutants and ventilation in ZEBs, Ng et al. (2018) concludes that adequate ventilation is especially important in airtight buildings to ensure high enough air change rates when the infiltration rates are reduced by sealed envelopes. The risk of mold growth related to airtight buildings is also a complex issue affected by many factors, including air change rates and wall constructions. However, the main challenge occurs when insufficient ventilation is provided. This may result in elevated moisture levels due to airtight constructions and may increase the risk of condensation and mold growth. (Kempton, Daly, and Dewsbury, 2020).

Recirculation of air

An energy-saving principle applied to ventilation systems is the recirculation of air. The concept is that a part of the exhaust air is reused and mixed into the supply air. The used air is normally filtered before mixed with OA and reintroduced to the building. As the system uses already heated exhaust air, it requires less energy for heating during heating season (Terry, 2021). Additionally, increased recirculation results in increased RH levels as indoor air typically contains more moisture

than OA (Norrefeldt et al., 2021). This is an advantage during the winter in cold climates as it limits the low RH values normally obtained when bringing cold OA inside. However, during summer high RH values may occur, increasing the risk of condensation.

Another risk with supplying used air to a building is the possible transfer of pollutants between rooms. The Norwegian Labor Inspection Authority states that as a main rule recirculation of air should not be accepted. The reason is that even when the air is filtrated before being reintroduced to the building, some gases, damp, and odors are difficult to remove completely, resulting in these being built up in the building. They also highlight the problem with using recirculation when no one is present in the room. Pollution can build up in the building and partly be stored in porous materials. When the recirculation then is turned off before occupancy, the concentrations may still be high (Arbeidstilsynet, 2016). TEK17 requires that recirculating air shall not be used if it results in polluting rooms where people are present. It states that the following requirements must be obtained (Direktoratet for byggkvalitet, 2017):

- Recirculation of air can be used in rooms where there are no people present, and it does not result in transferring pollutants between rooms.
- Circulating air must be filtered.

Jaakkola, Tuomaala, and Seppanen (1994) studied the effects of recirculated air on SBS. The study found that recirculated air up to 70%, when mixed with OA, can be used without adverse health effects (Jaakkola, Tuomaala, and Seppanen, 1994). During the COVID-19 pandemic, studies about how to avoid spreading the virus have impacted the research about how ventilation systems should be operated in an efficient and healthy way, as airborne transmission has been recognized as a possible transmission route (Shen et al., 2021). Whether recirculation of air contributes to the spread of the COVID-19 virus is discussed and studied. REHVA has recently issued a guidance on how to prevent the spread of the coronavirus within public and commercial buildings. They recommend no use of recirculation during COVID-19 episodes, as virus particles in return ducts can re-enter the building when a centralized air handling unit (AHU) are equipped with a recirculation

sector. If possible, systems with local circulation at room level should also be turned off (Kurnitski et al., 2020). However, there is limited information on recirculated air as a cause of COVID-19 transmission, and no reports have identified centralized HVAC systems contributing to a building-wide outbreak (Ontario Agency for Health Protection and Promotion, 2021). Furthermore, Shen et al. (2021) compared using 100% OA with using recirculation of return air filtrated by a HEPA filter, and found that these result in the same risk of getting infected by the COVID-19 virus in the same ventilation system. However, in general, limiting recirculation and bringing in OA would lower the concentration of any viral particles present in indoor air (Ontario Agency for Health Protection and Promotion, 2021)

Heat recovery

A heat recovery ventilator (HRV) is another energy-saving measure applied to the ventilation system to reduce the need for space heating. The HRV unit usually consists of two fans, one to take in the extract air and one to push out the supply air. The heat from the extract air is transferred to the supply air through a heat exchanger. Thus, less energy is required for heating the supply air. Depending on the heat-exchanger, an HRV unit can recover up to 85% of the heat in the exhaust air (Klenck, 2000).

The impact of HRVs on IAQ is less significant compared to recirculation of air, as the supply air is not mixed into the supply air but only heated through a heat exchanger. Filters in the HRV keep particles in the exhaust separate from the supply air. Unlike a recirculation system, HRVs can be more ideal for tight, moisture-prone buildings, as the moisture from the exhaust air may not be transferred to the supply air (Klenck, 2000).

2.2 Ventilation Systems

The focal responsibility of a building's ventilation system is to supply OA to the building and extract indoor air from it to ensure a healthy and safe environment. Thus, inadequate ventilation can result

in increased indoor pollution levels if insufficient supply of OA is provided to dilute emissions from indoor sources, or if indoor air pollutants are not being satisfactorily carried out of the area (U.S. Environmental Protection Agency, 2021a). Hence, dimensioning the ventilation system and estimating sufficient AFRs is crucial for assuring good IAQ.

Ventilation systems are dimensioned based on the room type, design, pollution, and moisture load from furniture, activities, and processes within a building. In Norway, the Norwegian Building Authority defines the requirements for ventilation in TEK17. It states three deciding factors for the required amount of supplied air (Direktoratet for byggkvalitet, 2017):

- (a) Personal load: Emissions from people.
- (b) Material load: Emissions from building materials, products, and installations.
- (c) Pollutants from processes and activities.

The minimum AFR is the largest value of either (1) personal and material load combined (a+b), or (2) pollutants from processes (c) (Direktoratet for byggkvalitet, 2017). The AFR that should be supplied because of emissions from people and building materials is issued in TEK17 (Direktoratet for byggkvalitet, 2017). Additionally, the Norwegian Labor Inspection Authority provides recommendations for ventilation rates in their Guideline 444 (Arbeidstilsynet, 2016). Values from both TEK17 and Guideline 444 are presented in Table 2.4. The values from TEK17 are based on some assumptions. The airflow due to people is based on the assumption that the occupants have an activity level equal to light work. The value for airflow due to emissions from materials is based on the assumption of low emitting materials, while Guideline 444 provides values for both normal emitting and low emitting materials. In Guideline 444 the minimum values are given as the air volume per second, while in TEK17 they are given as airflow per hour. However, in Table 2.4 the Guideline 444 values are calculated to l/s for comparison.

Observing Table 2.4, it is apparent that Guideline 444 and TEK17 set similar demands for minimum AFRs for both occupancy and material load. The value of 26 m³/h per person from TEK17 is defined

Table 2.4: Minimum AFRs based on people and materials as emission sources according to TEK17 and the Guideline 444.

Emission source	TEK17	Guideline 444
AFR due to personal load	26 m ³ /h per person	26 m ³ /h per person
AFR due to material load during occupied hours	2.5 m ³ /h per m ² floor area	7.2 m ³ /h per m ² floor area (normal emitting materials) 2.5 m ³ /h per m ² floor area (low emitting materials)
AFR due to material load during unoccupied hours	0.7 m ³ /h per m ² floor area	0.7 m ³ /h per m ² floor area

and estimated from the recommended maximum CO₂ concentration of 1000 ppm (Arbeidstilsynet, 2016). Additionally, the minimum AFR related to low-emitting materials provided by TEK17 is the same as stated by Guideline 444. Regarding emission from materials, the material choice contributes to the release amount. Additionally, the age of the materials does also have an impact, where the release decreases with time. TEK17 only provides a value for low-emitting materials, and emissions from newer materials are not mentioned in TEK17. However, Guideline 444 provides a value for minimum AFR due to normal-emitting materials, which is significantly larger than for low-emitting, almost three times larger. Thus, the impact of the age of the building and the materials may have a great impact on the release of pollutants, and thus the IAQ.

2.3 Demand Controlled Ventilation

The three main control principles for ventilation air supply are CAV, variable airflow volume (VAV), and DCV. The applicability of each control principle varies depending on usage, processes, occupancy pattern, and so on. Due to CAV providing constant airflow to the room, this may not be a sufficient method in places where the ventilation demand varies. Variations in ventilation demand are commonly due to varying heat load and occupancy. Constant air supply may in such situations result in overestimated AFRs in periods with low or no occupancy, and underestimated rates in

periods with high occupancy. Thus, in rooms where the heat load and occupancy vary, VAV is more sufficient. Additionally, the energy consumption is reduced as the air volume is adjusted according to the demand.

An advanced type of VAV-control is demand-controlled ventilation (DCV). It uses the building automation system to adjust the ventilation rate according to parameters measured at room level, to optimize the IAQ and energy efficiency. Sensors are used to measure the indoor air quality parameters and send control signals to adjust the ventilation rate to achieve the desired IAQ (Mysen, Schild, and Cablé, 2017). To assure that the DCV doesn't turn completely off in periods with no occupants, there is a set minimum AFR. Similarly, a maximum AFR is also set, to avoid discomfort such as draught. The AFR is then regulated between these two values according to one or more control parameters. These parameters are usually CO₂ combined with temperature, as the CO₂ concentration has a linear correlation to occupancy (Mysen, Schild, and Cablé, 2017). Consequently, the DCV provides the necessary AFR according to the occupancy in the room, assuring good IAQ while reducing the energy demand as the AFR is lowered when there are few or no occupants.

The motivation for using DCV is to reduce energy consumption while maintaining adequate IAQ. To obtain sufficient IAQ, the system must be regulated according to one or several parameters representing the IAQ in the relevant room or building. Today, most DCV systems use CO₂ as the control parameter. However, as indoor CO₂ concentration is a direct indicator of occupancy, CO₂ control does not consider pollutants unrelated to occupancy. Thus, emissions of VOCs and PM, which are commonly generated by additional pollution sources, may not be sufficiently handled by a CO₂-controlled DCV system (Demanega et al., 2021). This highlights the importance of studying multiple IAQ parameters for controlling DCV systems to obtain sufficient IAQ. Poirier et al. (2021) investigated various IAQ parameters used for control of ventilation systems, through a performance-based approach using CONTAM. The conclusion states that CO₂ is a relevant parameter for the control of ventilation systems, but should be combined with other parameters for a better consideration of the IAQ (Poirier et al., 2021). Thus, investigating what combinations of control parameters give the best IAQ, while maintaining a low energy consumption is highly

relevant.

There are also several principles for the regulation of DCV systems. The regulation principle can have a great effect on energy consumption as unnecessary throttling and imprecise regulation can result in a huge waste of energy. The four main types of solutions to regulate DCV systems are pressure control, static pressure reset, damper-optimization, and variable supply air diffuser (Fra lavenergiprogrammet, 2020).

Pressure controlled DCV

Pressure controlled DCV (PC-DCV), is the traditional and most common DCV system. The system regulates the air flows by controlling the pressure in a strategic duct position (Mysen and Schild, 2011). It regulates based on a constant pressure that is set high enough to assure sufficient air flows at all valves during maximum demand (Fra lavenergiprogrammet, 2020). The goal is to keep constant pressure on the dampers. The dampers are motorized, and control the AFRs, to meet the ventilation demand measured in each room. A change in the ventilation demand results in the damper position changing, which again influences the static pressure in the duct. A pressure sensor is connected to a controller, which it's task is to maintain constant pressure at the sensor position, by varying the fan-speed (Mysen, Schild, and Cablé, 2017). As a result of the airflow being regulated by throttling dampers, the system will accelerate and brake at the same time, most of the time during operating hours. Hence fan power is wasted regularly. Placing the pressure sensor further out in the system results in less power being wasted. Thus, accurate engineering, execution, and balancing of the system are necessary to avoid unnecessary waste of energy (Fra lavenergiprogrammet, 2020). A schematic of the PC-DCV principle is depicted in Figure 2.2.

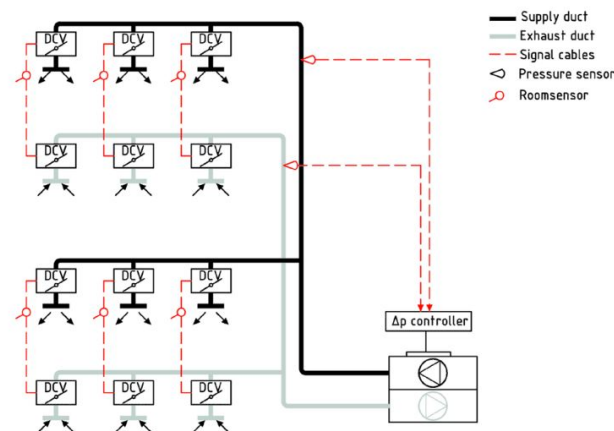


Figure 2.2: Principle of constant static pressure control (Mysen, Schild, and Cablé, 2017).

Static pressure reset DCV

Static pressure reset controlled DCV (SPR-DCV) combines pressure- and damper-control. Each zone has a motorized damper that is controlled by a pressure sensor. The damper controls the AFR, trying to maintain a constant static pressure at the pressure sensor. A controller registers the position of the damper and controls the pressure set point in the main duct, as well as the fan speed so that at least one of the dampers is in a fully open position continuously (Mysen, Schild, and Cablé, 2017).

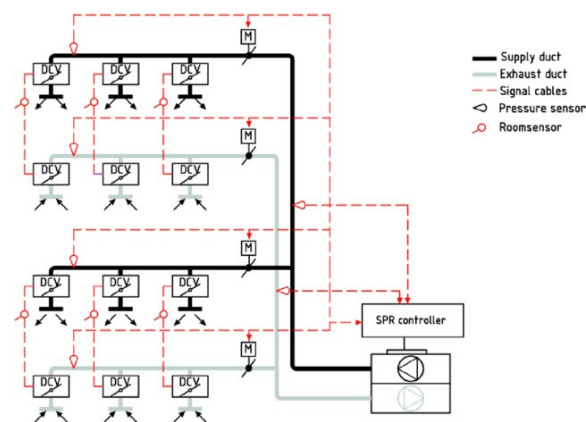


Figure 2.3: Principle of static pressure reset control (Mysen, Schild, and Cablé, 2017).

Damper-optimized DCV

Damper-optimized DCV controls the AFR in the main duct according to the position of the dampers so that at least one damper is fully open. The purpose is to ensure minimum fan energy consumption by applying a minimum pressure rise over the fan. This is achieved if the critical path is always open. The required AFR, the supplied AFR, and damper angles are recorded for all dampers, and sent to a controller which regulates the fan speed (Mysen, Schild, and Cablé, 2017).

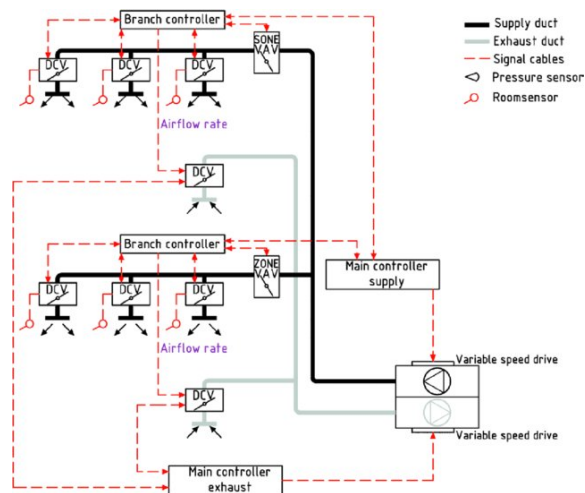


Figure 2.4: Principle of damper-optimized control (Mysen, Schild, and Cablé, 2017).

Variable Supply Air diffuser DCV

Variable supply air diffuser DCV (VSAD-DCV) is a possible variation of the damper-optimized DCV, where the DCV units are integrated into the air diffusers. The dampers are regulated by a controller connected to a bus-systems. The controller records the required AFR, supplied AFR, and the damper angle for all of the dampers. Then it regulates the fan speed such that one of the dampers is fully open on both the supply side and exhaust side. The motor-driven damper should normally remain in a fully open position, and only throttle if the pressure in the duct becomes too high relative to the working range of the dampers (Mysen, Schild, and Cablé, 2017).

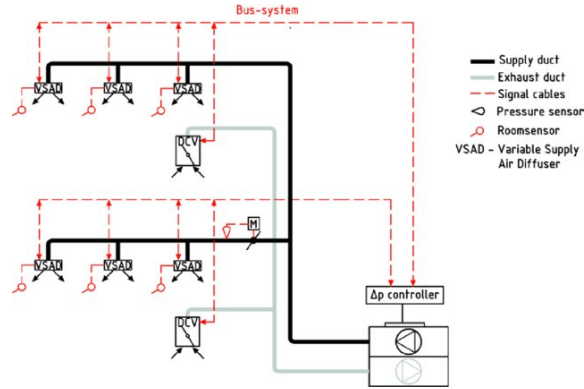


Figure 2.5: Principle of variable supply air diffuser control (Mysen, Schild, and Cablé, 2017).

Specific Fan Power

A DCV system is not necessarily energy-efficient. As mentioned, unnecessary throttling may occur and will result in energy loss. However, when implemented correctly a DCV-system can reduce the energy consumption of ventilation by more than 50% (Mysen, Schild, and Cablé, 2017). Accordingly, setting proper requirements is crucial for achieving large reductions in energy demands. Specific fan power (SFP) is a value that is appropriate to set requirements to, for obtaining an energy-efficient DCV system. This is because it can be controlled and therefore ensure an energy optimal solution (Mysen, Schild, and Cablé, 2017). The SFP indicates how efficiently the air is distributed in the building. It can be indicated as the ratio between the total electrical power to the fan motor and the airflow the ventilation system exchanges in the ventilated room, as seen from (2.1).

$$SFP = \frac{\sum \phi_{fans}}{\dot{V}} \left[\frac{kW}{m^3/s} \right] \quad (2.1)$$

Where,

- ϕ_{fans} is fan efficiency [kW]
- \dot{V} is maximum air flow rate [m^3/s]

In addition, the SFP can be expressed as the ratio between the total pressure increase in the system and the total efficiency of the fans, as described in (2.2).

$$SFP = \frac{\Delta p_{tot}}{\eta_{tot}} \left[\frac{kW}{m^3/s} \right] \quad (2.2)$$

Where,

- Δp_{tot} is total pressure increase [Pa]
- η_{tot} is total fan efficiency

In TEK17s requirements for energy efficiency a SFP value of less or equal to $1.5 \frac{kW}{m^3/s}$ is required (Direktoratet for byggkvalitet, 2017). The SFP, and hence the energy efficiency of the operation, is greatly impacted by the type of regulation method. The difference between the various methods is usually small for maximum air flows, but significant at partial load. The reason for this is that the least effective systems regulate by throttling the critical path. Hence, SINTEF Byggforsk recommends having demands for the SFP-factor both when there is maximal load and reduced load (Fra lavenergiprogrammet, 2020).

2.4 Sensors for DCV Systems

Included in DCV systems are sensors measuring control parameters representative of the IAQ in the room. The room air quality is usually assessed according to the CO₂ concentration, measured by CO₂ sensors. However, other pollutants are commonly found in hazardous concentrations in indoor environments, and should therefore be considered used for control of DCV systems. PM and VOCs are examples of pollutants not necessarily being mainly generated by people, and may therefore not be handled efficiently by a CO₂-controlled DCV system. Previously, IAQ monitoring of pollutants such as PM and VOCs has been limited to professionals with costly, certified instruments. However,

developments in sensing technologies have allowed for commercialization of low cost sensors (LCS)s (Demanega et al., 2021).

2.4.1 Internet of Things

Concerning ventilation control, LCSs typically store the measured data on IoT servers (Demanega et al., 2021). This enables continuous measurements of IAQ parameters while reading and writing data to the Cloud making the data accessible through the Internet (Coulby, A. Clear, et al., 2020). IoT-based LCSs can be used for measuring IAQ parameters and sending signals through the Internet which sets the base for the control action to be performed.

IoT is a system that allows for various devices to connect and communicate through the Internet. This enables remote operation of devices and collection of data (Gillis, 2022). IoT sensors detect information that is replaced by a signal that machines or humans may use for specific purposes. Sensors collect data from the surrounding environment and thus convert a physical quantity to a digital signal. Through an IoT gateway, the sensors are connected to the Internet and can transmit the digital signals to a cloud server. Data can then be stored and accessed through the cloud server. Through a user interface the intended action based on the measured data can be performed (Allurwar, 2022). IoT embraces many applications and a wide range of "everyday things" are today connected to the IoT, including a range of objects from ordinary household objects to sophisticated industrial tools (Oracle, 2022).

2.4.2 Low-Cost Sensing Technologies

A wide selection of low-cost air quality devices has become available on the market. These monitors are usually designed for real-time monitoring of IAQ parameters, commonly including PM, CO₂, VOCs, RH, and temperature. There are some typical sensing technologies related to the various parameters being measured. Some of the most common technologies will be discussed further in

this chapter.

LCSs have been used in a wide range of environmental studies, revealing limitations and potentialities (Palmisania et al., 2021). Generally, the main benefit of the LCSs is that they are inexpensive, which allows for scalable sensor networks where a range of sensors can provide complex data (Giordano et al., 2021). Also, their usually small size compared to laboratory units and easy handling allows for temporary and mobile installations (Palmisania et al., 2021). However, LCSs are subjected to limitations as well. Susceptibility to changes in environmental parameters, such as RH and temperature, is a common factor recognized for influencing measurements. However, the main challenges are obtaining high accuracy and precision (Palmisania et al., 2021). Precision is evaluated by comparing several measurements from the same sensors, while measurement accuracy is commonly studied by comparing the measurements with those from a reliable reference device. Drift results in less accurate measurements over time and is another common challenge for a lot of LCSs, resulting in regular calibration being necessary (Concas et al., 2021).

Coulby, A. K. Clear, et al. (2021) found several LCSs to have varying accuracy compared to reference devices. However, the sensors responded to environmental changes and followed the same measurement pattern. Thus, despite reduced accuracy, calibration of the devices could increase the accuracy due to the high precision (Coulby, A. K. Clear, et al., 2021). Moreover, it has been recognized that LCSs are subject to biases and calibration dependencies which can range from relatively straightforward to more complex procedures (Giordano et al., 2021). Gram (2019) tested sensors for measurements of several IAQ parameters, which were factory pre-calibrated. Nonetheless, most sensors were still evaluated to need calibration to obtain sufficient measurements (Gram, 2019). This shows that a major challenge for LCSs is their out-of-the-box data quality being generally low. Therefore the use of such sensors requires understanding, to be able to perform adequate calibrations (Giordano et al., 2021). Because of these potentially damaging weaknesses, a scientific evaluation of the specific sensor is essential before the collected data can be used (Palmisania et al., 2021). In the following, an overview of some common low-cost IAQ sensing technologies commonly used for the selected IAQ parameters is presented and discussed.

CO₂

Several low-cost sensing technologies for measuring indoor trace gas levels are commercially available. An example of such technology is the *non - dispersive infrared (NDIR)* sensors, which is the most common low-cost sensing technology for CO₂ measurements (Saleh and Fadillah, 2021). The technology takes basis in infrared (IR) light being absorbed by CO₂ molecules, as a result of the CO₂ absorption band being very close to the IR radiation band. By measuring the change in IR radiation in the air as it flows through a tube in the sensor, the CO₂ concentration can be estimated (*How does an NDIR CO₂ Sensor Work* 2021).

NDIR sensors are recognized for showing cross-sensitives to many gases because of the broad spectral response of solid-state-based light detectors (Palzer, 2020). However, the sensitivity can be improved by improving the IR source, the detector, and the optical design (Dinh et al., 2016). Moreover, environmental fluctuations are found to influence the performance of NDIR sensors. Therefore, they are often studied in combination with temperature and RH measurements (Saleh and Fadillah, 2021). Aging of the IR source may also cause drift in NDIR sensors over time (Dinh et al., 2016). Additionally, the sensors have high detection limits and may have trouble detecting low concentrations (Concas et al., 2021). Despite these challenges related to the NDIR technology, various sensors using the technology have shown promising results. Shah et al. (2016) evaluated the NDIR CO₂ sensing technology to be fast-responding and accurate after calibration. Additionally, the compact design is advantageous (Shah et al., 2016). The NDIR technology also has a long lifespan and little required maintenance (Concas et al., 2021).

Another technology used for monitoring CO₂, as well as other trace gases, is based on *photoacoustic spectroscopy (PAS)*. The main concept is based on converting light into sound, which can be measured and used to calculate the CO₂ concentration (Palzer, 2020). Energy from the light is absorbed in the CO₂ gas molecules and transformed into kinetic energy, which results in the production of local heat. The thermal expansion creates a pressure wave, emitting an acoustic signal (Li, Chen, and Yu, 2011). This acoustic signal can be detected with a sensitive microphone detector and used to determine the gas concentration (Qiao et al., 2019).

PAS sensors are subject to inaccuracies caused by variations in environmental factors, such as humidity, temperature, and pressure (Jin and Luo, 2021). However, several studies have had great results with PAS sensors. Qiao et al. (2019) studied a PAS sensor measuring CO₂ concentrations from several sources. The sensor showed high precision and high performance, and it was concluded to be suitable for environmental monitoring (Qiao et al., 2019). Rosenstock et al. (2013) tested the precision and accuracy of three PAS instruments, measuring several gases, including CO₂. The tests showed both higher accuracy and precision of the measurements of CO₂, than those for nitrous oxide (N₂O) and methane (CH₄). While the accuracy was within reasonable limits with a 4% lower measurement than the reference level, it is suggested that linear regression algorithms would increase the accuracy (Rosenstock et al., 2013). Jin and Luo (2021) carried out a study testing the method of multiple linear regression correction algorithms, to improve the accuracy of a PAS system measuring NO₂. The conclusion was that the multiple linear regression algorithm is efficient at improving the accuracy (Jin and Luo, 2021).

PM

The technology used for low-cost PM sensors is mainly based on light-scattering, where particle light scattering signals are converted to PM mass concentration (Tryner et al., 2021). The technology is based on the principle that when light is cast on PM in the air, the light is scattered by the particles. Thus, the amount of scattered light is proportional to the mass concentrations of PM with the same physical properties (Choi and Cho, 2020).

Light scattering sensors inhabit advantages such as small size and low cost compared to other PM sensors (Concas et al., 2021). Otherwise, they have varying accuracy and are dependent on proper calibration for achieving accurate measurements (Shao, Zhang, and Zhou, 2017). The inaccuracies related to such sensing technology, include the shape, size distribution, and density of the particles. Many light-scattering sensors fail to respond to increases in coarse particle mass. This is most likely due to particle losses in the flow path between the inlet and the light detector as well as decreases in the amount of light scattered over the angular detection range per unit mass (Tryner et al., 2021). They are also known to have problems detecting very small particles (Concas et al., 2021).

Research has also uncovered several environmental impacts on PM LCS performance, where especially RH is recognized as an influential factor (Shao, Zhang, and Zhou, 2017). G.-H. Hong et al. (2021) tested the impact of RH on three light scattering sensors. A varying dependency of RH for the individual sensors was recognized. Bulot et al. (2020) found indications of varying sensor performance with various pollution sources, which may have implications for their potential use in different locations. The source dependency may be partly attributed to the size distribution of the PM sources. Hence, some sensors may be better suited than others to track specific sources of pollution (Bulot et al., 2020). As there are several possible environmental impacting factors, calibration of the devices is advised to be performed in the environment where they are used (G.-H. Hong et al., 2021).

VOC - TVOC and Formaldehyde

Similar to PM, VOCs are emitted from several sources which are unrelated to occupancy. Thus, VOC sensors are desirable to study in combination with CO₂ sensors for monitoring the DCV system to best consider the IAQ. Low-cost FA and TVOC sensing are generally based on the same technologies. As there is a wide selection of technologies for VOC monitoring, some of the most common ones are selected and described further. This includes photoionization detector (PID), electrochemical cell (EC) and metal oxide semiconductor (MOS) (Khan, Calvé, and Newport, 2020).

PIDs use an ultraviolet (UV) light source to ionize VOCs in the air, creating positive and negative ions. The sensor then detects the charge of the ionized gas. The charge is a function of VOC levels in the air and can therefore be used to calculate the concentration. After being measured, the gas ions recombine to the original gas. Thus, the VOC levels are not changed because of the sensor (TSI Incorporated, 2021).

PIDs have high sensitivity and short response time (Concas et al., 2021). Additionally, they are recognized for being highly precise (Khan, Calvé, and Newport, 2020). However, several factors are influencing the measurements of PIDs. They are known to suffer from cross-sensitivity to

confounding compounds (Demanega et al., 2021). This is supported by Xu et al. (2020), which studied the influence of several influencing gases. The study also found evidence of sensitivity towards temperature and RH, where RH was recognized as the main influence (Xu et al., 2020). Additionally, they have a major disadvantage in that they are not selective, meaning they are not able to ionize different VOCs equally which creates a problem when measuring TVOC (Baldelli, 2021). PIDs are on the more expensive side relative to other low-cost technologies (Khan, Calvé, and Newport, 2020). Additionally, PIDs are subject to drift (Concas et al., 2021).

MOSs operate by oxygen reacting with gasses to change the resistance of the semiconductor. The change is proportional to the VOC concentration and can therefore be measured to obtain the concentration (Coulby, A. K. Clear, et al., 2021). MOSs are generally very low cost and have a compact design. Fast response, high sensitivity, and long lifetime are also typical for MOSs (Concas et al., 2021). However, they are usually sensitive to environmental factors, as well as a range of other pollutants and gases (Coulby, A. K. Clear, et al., 2021). They can respond to inorganic gases and should therefore not be used for measurements where these gases are present in higher concentrations. MOSs are also prone to low accuracy and drift. Therefore, regular re-calibration of MOSs may be necessary (Concas et al., 2021).

Electrochemical sensors are classified according to the formation of their electrical characteristics (Alan, 2020). The individual categories of ECs will however not be discussed in this thesis, but a general overview is presented. The principle of ECs is based on an electrochemical reaction occurring inside the sensor when the measured gas enters. The reaction induces a current or voltage signal output which can be used to calculate the gas concentration (Alan, 2020). Electrochemical gas sensors inhabit several advantages, including linear output and sufficient accuracy after calibration (Raninec, 2019). ECs are also highly sensitive (Concas et al., 2021). However, they typically have major issues with short lifetime and drift (Khan, Calvé, and Newport, 2020). They usually need to be replaced within one to three years (Alan, 2020). In addition, the sensors suffer from cross-sensitivity to other gases and are impacted by temperature (Raninec, 2019).

Temperature

There are three main types of temperature sensors: Resistance Temperature Detectors (RTDs), thermocouples, and thermistors, where thermistors and thermocouples are considered low-cost. Thermocouples use two metal wires, that are joined together to produce voltage when one side of the circuit is at a higher temperature than the other. The voltage is measured by a voltmeter and can be used to determine the temperature. They are typically the most robust type of temperature sensor and have a wide temperature range. They are also the cheapest choice and provide the fastest response to temperature changes. However, depending on the specific sensor, thermocouples may lack accuracy. Additionally, thermocouples are prone to drift due to chemical changes in the sensor (Omega, n.d.).

Thermistors detect and measure temperature changes by the change in resistance in a resistor inside the sensor. This is a similar concept to the more expensive RTDs. However, thermistors use ceramic or polymer resistors, while RTDs use metal resistors. Thermistors have the best performance at temperatures below 150 degrees out of the three technologies, even better than RTDs which are known for their high accuracy. The great performance is mostly due to the high sensitivity of thermistors. Additionally, they typically have a fast response time. Thermistors do not have linear output and can measure a smaller range of temperatures than thermocouples (Omega, n.d.). However, they cover temperatures found in normal indoor environments by large margins.

Humidity

RH sensors are typically divided into capacitive and resistive sensors. Capacitive sensors use two electrodes to monitor the capacitance of a thin dielectric material that is placed between the electrodes. The change in the material's capacitance is directly proportional to the change of humidity in the environment (Jost, 2019). Capacitive RH sensors are used for a wide range of applications, with HVAC systems being one of them. They are known to be able to detect a wide range of RH concentrations, provide stable results over long periods of use, and the output voltage is near linear. In addition, capacitive sensors are cost-effective and small in size (Anusha,

2017). Additionally, capacitive humidity sensors have high sensitivity. However, they inhabit some challenges as well, including slow response time and temperature dependency (C.-Y. Lee and G.-B. Lee, 2005).

The principle that resistive RH sensors are based on is the fact that the conductivity in non-metallic conductors is dependent on their water content. A resistive sensor typically contains a low resistivity material placed on top of two electrodes. When the top layer material absorbs water, the resistivity between the material and electrodes changes. This change can be measured by a simple electrical circuit and used to find the RH. Similar to the capacity sensors, resistive sensors are cost-efficient and small in size (Anusha, 2017). Also, high sensitivity and good linearity are recognized characteristics for resistive sensors (C.-Y. Lee and G.-B. Lee, 2005). On the other hand, resistive sensors are sensitive to chemical vapors and other contaminants (Anusha, 2017). Similar to capacitive sensors, resistive sensors also have a relatively slow response, in addition to being prone to drift (C.-Y. Lee and G.-B. Lee, 2005).

2.4.3 Summary of characteristics

Table 2.5 presents a summary of the known limitations and advantages of the sensing technologies mentioned. This gives an overview of the characteristics that some common sensors for IAQ monitoring inhabit. However, it is important to acknowledge that these characteristics are based on a limited fraction of all studies conducted on sensing technology. Thus, the individual sensing technologies include but are not limited to the characteristics presented in Table 2.5.

Table 2.5: Summary of characteristics related to low-cost sensing technologies.

Technology	Limitations	Advantages
NDIR	Sensitivity to environmental factors Cross-sensitivity to other gases Drift High detection limit	Accurate Fast-responding Compact Long lifespan Little maintenance
PAS	Sensitive to environmental factors	High precision High accuracy
Light-Scattering	Varying accuracy Sensitivity to size distribution of particles Sensitivity to environmental factors Limited detection range	Small size Low cost
PID	Cross-sensitivity to other gases Sensitivity to environmental factors Not selective Cost Drift	High precision High sensitivity Fast response
MOS	Sensitivity to environmental factors Cross-sensitivity to other gases Drift Low accuracy	High precision High sensitivity Compact design Fast response
EC	Drift Short lifetime Cross-sensitivity to other gases Sensitivity to temperature	Linear output High accuracy High sensitivity
Thermocouple	Various accuracy Drift	Wide temperature range Fast response
Thermistor	Narrow ranges Non-linear output	High sensitivity High accuracy Fast response
Capacitive	Slow response Sensitivity to temperature High sensitivity	Wide range of detection Low drift Near linear output Small in size
Resistive	Sensitive to chemical vapors and other contaminants Slow response Prone to drift	Small in size High sensitivity Linear response

2.4.4 Sensor placement

When sensors are used to control the DCV system, they must be placed in locations representative of the IAQ in the room. The contamination level within an occupied space may vary for different locations. Therefore, locations for sensor placement can be a deciding factor in whether the sensors and ventilation systems perform efficiently (Pei et al., 2019). Mysen, Schild, and Cablé (2017) points to the following factors influencing adequate sensor placement:

- Air distribution strategy
- Air diffuser location
- Contaminant source location and characteristics
- Temperature conditions
- Room geometry
- Sensor type

Guidelines for sensor placement of CO₂ and temperature sensors are available as these are most commonly used. Mysen, Schild, and Cablé (2017) highlights two points to consider for placement of a combined CO₂ and temperature sensor: 1) the sensors should not be placed in direct sunlight or a place where they can be affected by radiation from a heater in the room and 2) should be located away from any door that is open during normal operation. These may apply to sensors measuring other IAQ parameters as the temperature is shown to be influencing several low-cost sensing technologies, and open doors may affect the local concentrations of all pollutants. Particle room distribution is dependent on the particle size and may be less uniform than for gases. Coarse particles are found to disperse with the airflow in the room, while fine particles spread more evenly (Lin et al., 2020). This is something to consider when deciding the sensor location.

Adequate sensor placement is dependent on the ventilation strategy. When there is mixing ventilation, theoretically the sensor can be placed anywhere in the room since the contaminant levels should be homogeneous. A prerequisite would be that it is not too close to a contaminant source or the supply diffuser. But since complete mixing is unattainable, concentration gradients will occur in rooms with mixing ventilation as well. Thus, optimal sensor placement would be centrally in the room. However, due to being highly impractical because it would require the sensor hanging from the ceiling, this is not a realistic option (Mysen, Schild, and Cablé, 2017). Högdahl (2018) investigated the placement of TVOC sensors in an apartment and an office to locate where the sensor should be placed to measure the average concentration in the room. Due to the no-slip principle and more stagnant air, avoiding corners as a location for sensor placement is recommended. Similarly, because of the probable non-uniform concentration distribution close to surfaces, placing sensors on the walls is not preferred either. However, measuring IAQ parameters a few centimeters out from the wall or ceiling could result in values significantly closer to the average of the occupied zone (Högdahl, 2018).

Mou, Cui, and Khoo (2021) have identified locations near the ceiling as proper sensor placement of CO₂ sensors when there is mixing ventilation. The reason is that the air is better mixed and hence reflects the true CO₂ concentration hotspots within the indoor space near the ceiling (Mou, Cui, and Khoo, 2021). According to Pei et al. (2019), placing the CO₂ sensor at the room exhaust yield good accuracy. A prerequisite to placing the sensor in the exhaust is that the conditions at the exhaust are representative of the conditions in the room, which may not always be the case as the concentration in the room may increase at a faster rate (Mysen, Schild, and Cablé, 2017).

For displacement ventilation, where cool air is supplied with a low velocity close to the floor, the sensor should be placed in the breathing zone (1,1 m above the floor), so that one gets good ventilation efficiency up to and in the breathing zone (Mysen, Schild, and Cablé, 2017). However, Pei et al. (2019) found that placing CO₂ sensors near occupants could result in large errors under displacement ventilation. The conclusion stated that placement at breathing height performs well for constant occupancy conditions, but yields errors with varying occupancy (Pei et al., 2019).

Chapter 3

Methodology

The research aims to investigate CSs for DCV systems. The motivation behind the investigation is to reduce energy consumption while maintaining sufficient IAQ in buildings. Experiments in a test facility and simulations regarding the investigation of CSs for DCV systems are performed and are described in this chapter. However, several other tasks must be performed before experiments and simulations can be conducted. Thus, Figure 3.1 summarizes the general method of this thesis.

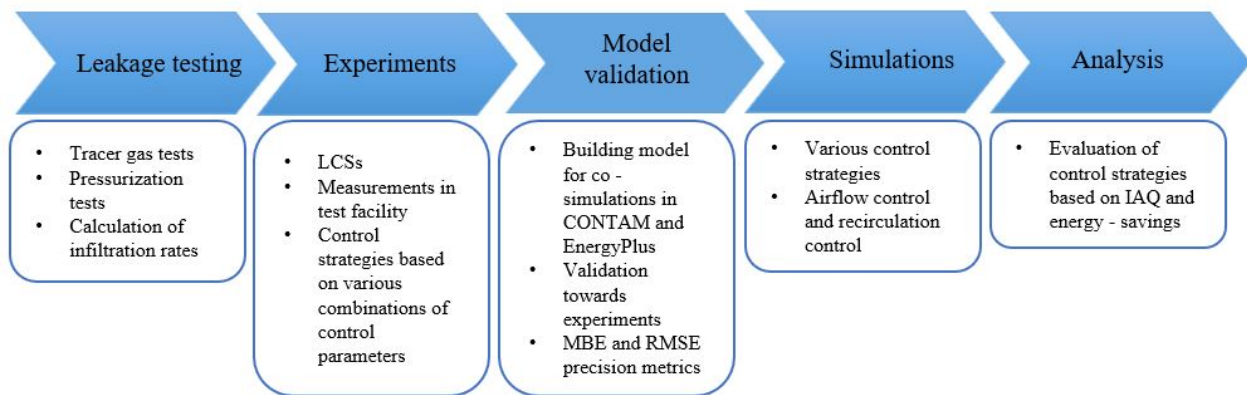


Figure 3.1: Sketch of the methodology.

Preliminary tests revealed high infiltration rates, which have been attempted to decrease with several measures to the test facility. Therefore, leakage tests are conducted before the various CSs are investigated, to see if the infiltration rates have been improved. Both tracer gas tests and

pressurization tests are conducted and used to calculate infiltration rates.

The test facility is then used as the location to perform experiments testing several CSs. The various CSs are based on combinations of measured concentrations of CO₂, PM_{2.5}, and FA, as well as temperature. While TVOC and RH are considered in the literature review, they will not be used as a control parameter during the experiments, nor for the simulations. RH is excluded due to not having any moisture generation sources available for the experiments. TVOC is excluded due to the difficulty of having a controlled generation of TVOC as there is a range of sources because it consists of a range of various gases. In addition, no calibration data are available for the TVOC sensors, and it is therefore uncertain if the sensors are sufficiently accurate.

During the experiments, LCSs are used to measure each control parameter at room level in a full-scale test facility. Further, the measured data are used to validate a building model to be used for simulating a large variation of CSs. The analysis revolves around the simulations, but some additional thoughts and results from the experiment may also be included. Both IAQ and energy savings are aspects considered when evaluating the CSs.

Thus, this chapter includes a description of the full-scale test facility, the associated ventilation system, and the sensors used for measurements. Additionally, preparatory air leakage tests and the procedure of the CS experiments are described in this chapter. Lastly, the simulation tools and simulation procedure are described.

3.1 Experimental Setup

The experimental setup for the CS experiments and the air leakage tests are described in the following. It includes information about the construction and ventilation system in the test facility, in addition to key information about each type of sensor used for the measurements performed in the facility.

3.1.1 Full-Scale Test Facility

Information about the test facility is gathered from the previous work in Buch (2020). However, some adjustments have been made to the facility and the following descriptions are therefore revised since Buch (2020).

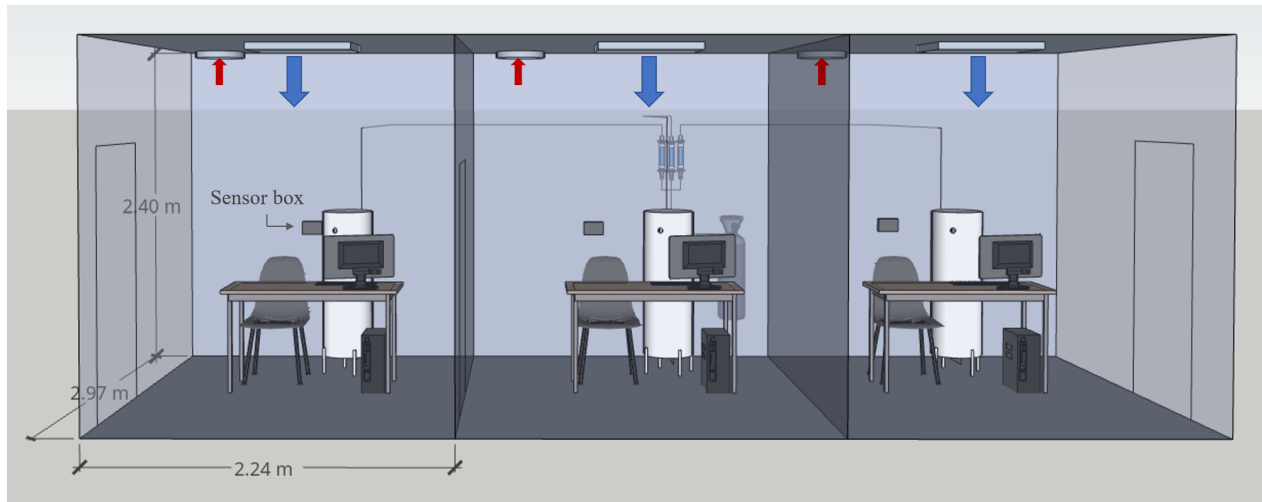


Figure 3.2: Schematic of the test facility. Credits (Sketchup Usernames): Sanju (Computer), DGL.ARUNARCH (Chair), Keino (Gas Silinder Industrial) and Suphot Jindaluang (Rotameter).

The test facility is constructed to investigate and develop CSs for DCV using LCSs, in an office environment. Furthermore, the test facility consists of 3 similar offices as depicted in Figure 3.2. Each office is 7 m^2 according to inside measurements and is furnished with a desk, a chair, a computer, and a computer screen. Additionally, a manikin representing a human is placed in each room. The rooms are hereafter referred to as room 1, 2, and 3, corresponding to the depicted rooms from left to right in Figure 3.2

The facade and the roof are constructed from Glava EPS S80 insulation plates with steel plates covering both the inside and outside. Moreover, the inner walls separating the offices also consist of Glava EPS S 80 insulation plates. As the preliminary work during autumn 2021 revealed noticeably infiltration between the rooms, plastic sheets have been mounted on both sides of both inner walls to limit these leaks.

The ventilation system in the test facility is a DCV system with mixing air distribution. The AHU is of the type UNI 3 from Flexit. A schematic of the ventilation system is depicted in Figure 3.3, where blue marks supply and red marks extract. A system to control the recirculation of return air is integrated into the ventilation system, represented by the purple duct in Figure 3.3. Based on measured pollution levels, a damper adjusts the ratio of OA and recirculated air in the supply. Additionally, a HEPA filter is applied to the recirculation duct for filtering the exhaust air which is being reintroduced to the rooms.

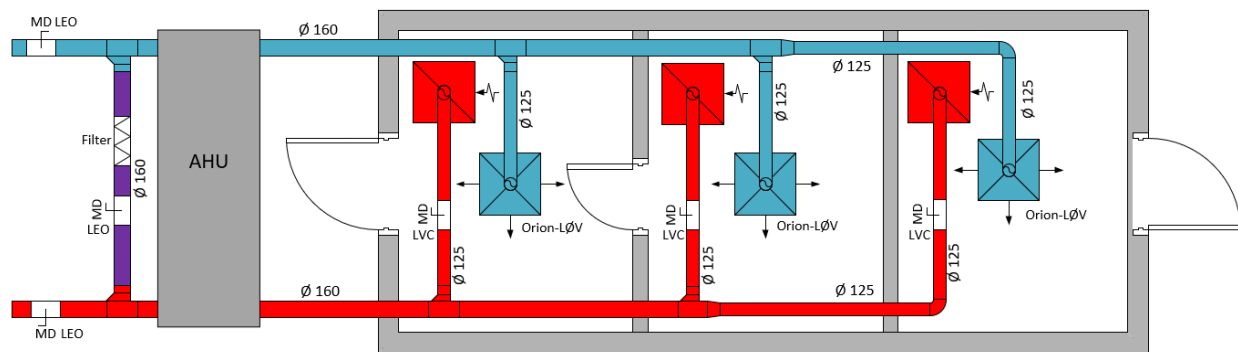


Figure 3.3: Ventilation floor plan.

The main ducts have a diameter of 160 mm, and the ducts connecting the supply- and exhaust ducts to the diffusers have a diameter of 125 mm. There is an Orion-LØV supply terminal and an LVC exhaust terminal in each room. The dampers at the main inlet, main outlet, and the recirculation duct are of the type LEO. The datasheets for all the mentioned components are found in Appendix E.1. It should be noticed, that the air that is being supplied to the facility is extracted from and exhausted to the HVAC laboratory at NTNU, as the facility is located inside the laboratory. Therefore the supply air has some deviations from normal OA with both higher temperature and pollution levels.

3.1.2 Pollution Sources

As previously mentioned, each room contains a typical office setup with a chair, desk, and computer. Additionally, a manikin is placed in each room. For the generation of particles, a mosquito coil is placed outside the facility. Each of these elements is described in more detail in the following.

Manikins are used to represent the humans in the offices during the CS experiments. These are depicted in Figure 3.4. The manikins are metal cylinders able to release heat and CO₂. Thus, a tube connects a CO₂ bottle to each manikin through a hole in the bottom of the cylinders. There is also a hole near the top of the cylinder, at breathing height, where the CO₂ is intended to be supplied from the cylinder to the room. As CO₂ weighs more than air, a 100 W light bulb is placed inside the cylinder with the outlet of the tube supplying CO₂. The thermal plume created by the light bulb helps avoid the CO₂ falling to the ground and out of the cylinder through the hole in the bottom. The thermal plume from the light bulb will make sure that the CO₂ rises and is let out through the intended hole. The heat created by the light bulb also functions to heat the cylinder itself. Thus, the manikins release heat, such as humans.

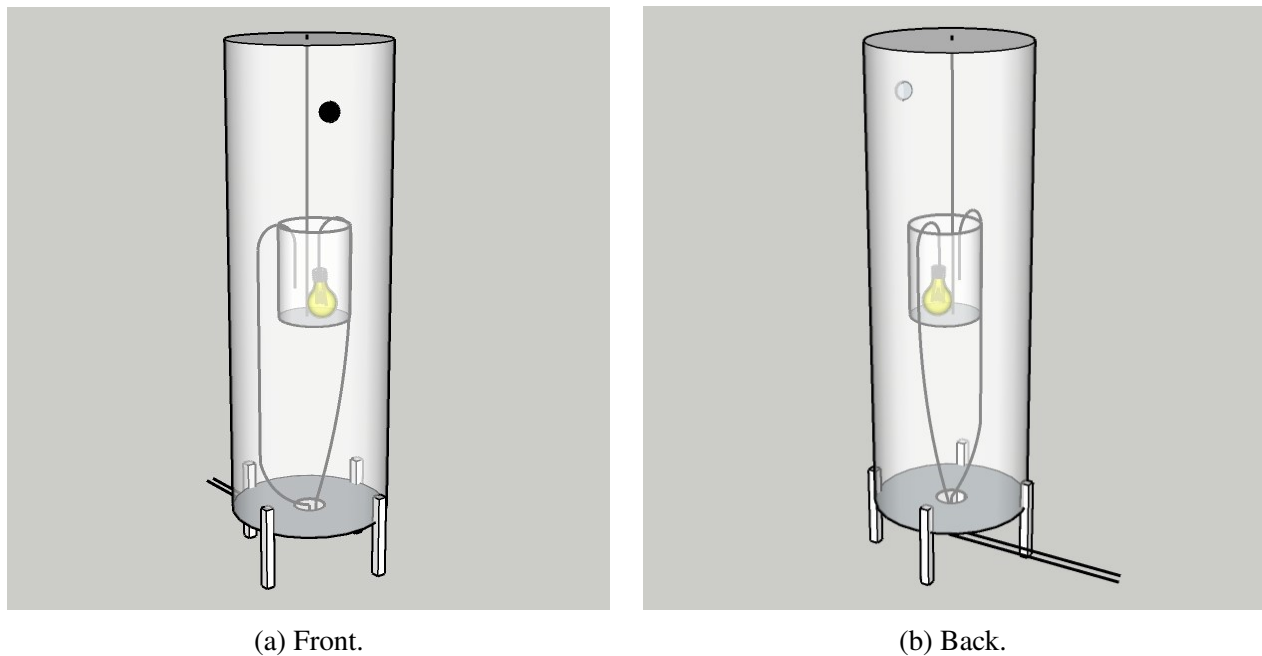


Figure 3.4: Manikins.

Connected to the CO₂ bottle supplying the CO₂ to the manikins are three rotameters allowing for adjustment of the flow of CO₂ into each room. According to ASHRAE an activity level of 1.2 met, corresponding to sedentary persons, generally results in a CO₂ generation rate of 0.3 l/min (ASHRAE, 2018). Thus, the rotameters will be used to supply CO₂ at a rate of approximately 0.3 l/min per person. A sketch of the setup of flowmeters and CO₂ bottle is depicted in Figure 3.5.

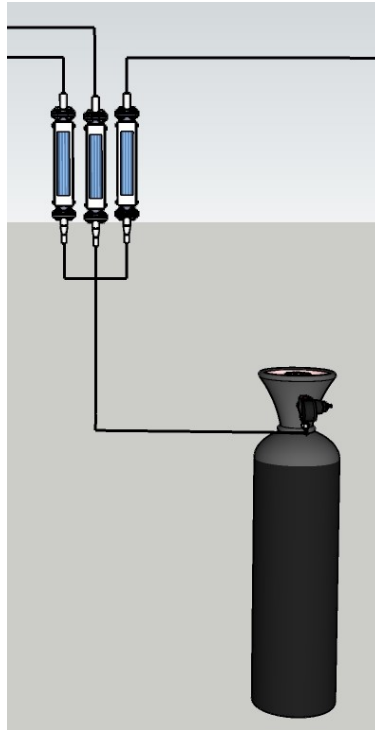


Figure 3.5: Schematic of the setup of CO₂ bottle and rotameters. Credits (Sketchup Usernames): Keino (Gas Silinder Industrial) and Suphot Jindaluang (Rotameter).

As particles are commonly found in higher concentrations outside compared to indoor environments, especially in cities, a source of particles is placed outside the test facility. A mosquito coil serves this purpose and assures that particles are brought inside the test facility through the supply air.

3.1.3 Sensors

A selection of sensors measuring CO₂, PM, TVOC, FA, temperature, and RH is placed in the test-facility to measure the control parameters which sets the base for the various CSs for DCV systems. The sensors used for measuring the specified IAQ parameters are mounted in what will be referred to as a sensor box hereafter. Figure 3.6 shows one of the sensor boxes. The specific sensor boxes used for the experiment in this thesis are referred to by their ID number: ID360360, ID123465, ID987654, ID314159, and ID420420. Their specific locations during the experiments are listed in Table 3.1. The following information about the individual sensors is gathered from the

associated datasheets, presented in Appendix E.2.

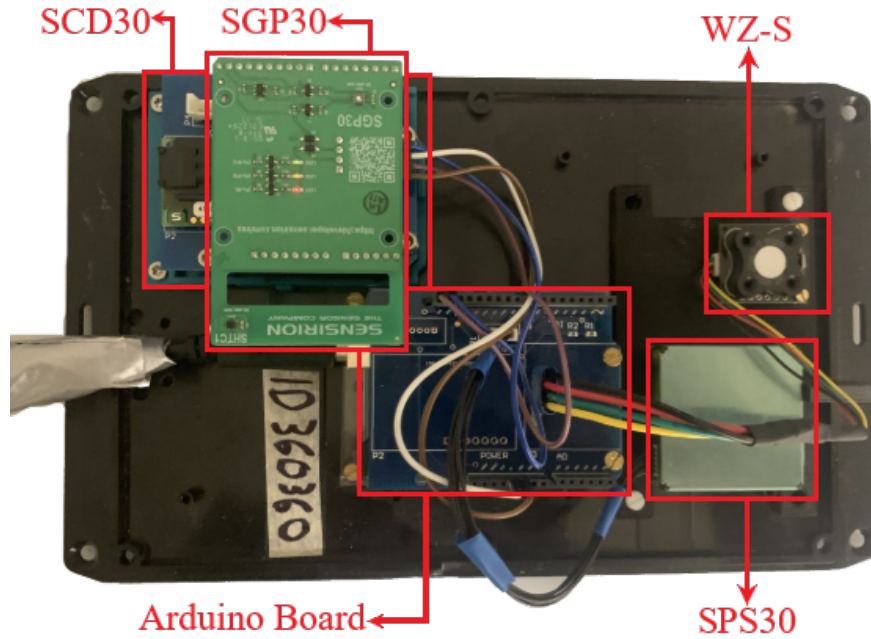


Figure 3.6: Sensor Box.

Table 3.1: Placement of the sensor boxes in the test facility.

ID	Location
360360	Room 1
123465	Room 2
987654	Room 3
314159	Main inlet
420420	Main outlet

Sensirion SCD30: CO₂, Temperature and Humidity

The Sensirion SCD30 sensor consists of an NDIR sensor for CO₂ measurements, with integrated temperature and RH sensors. The temperature sensor is a thermistor and the RH sensor is capacitive. Some of the key specifications for the SCD30 sensor obtained from the associated datasheet, is given in Table 3.2, Table 3.3 and Table 3.4 for the measurement of CO₂, temperature and RH, respectively.

Table 3.2: SCD30 sensor specifications for CO₂.

Parameter	Conditions	Value
CO ₂ measurement range	-	0 - 40 000 ppm
Accuracy	400 - 10 000 ppm	± (30 ppm + 3%)
Accuracy drift over lifetime	400 - 10 000 ppm	± 100 ppm

Table 3.3: SCD30 sensor specifications for temperature.

Parameter	Conditions	Value
Temperature measurement range	-	-40 - 70°C
Accuracy	0 - 50°C	± 0.3°C
Accuracy drift over lifetime	-	< 0.03°C/year

Table 3.4: SCD30 sensor specifications for RH.

Parameter	Conditions	Value
Humidity measurement range	-	0 - 100 % RH
Accuracy	25 °C, 0 - 100 % RH	± 2 % RH
Accuracy drift over lifetime	-	< 0.25 % RH/year

Sensirion SPS30: PM

The Sensirion SPS30 is a laser-based light-scattering sensor, which is used for measuring PM₁, PM_{2.5}, PM₄ and PM₁₀. Sensor specifications is presented in Table 3.5. More info is available in the datasheet in Appendix E. The values in Table 3.5 applies for temperature of 25°C and 5 V supply voltage.

Table 3.5: SPS30 sensor specifications for PM_{2.5}.

Parameter	Conditions	Value
Mass concentration range	-	0 - 1000 $\mu\text{g}/\text{m}^3$
Mass concentration accuracy	0 - 100 $\mu\text{g}/\text{m}^3$	$\pm 10 \mu\text{g}/\text{m}^3$
Lifetime	24 h/day operation	> 8 years

Sensirion SGP30: TVOC

The Sensirion SGP30 is a MOS sensor measuring TVOC. Some sensor specifications are listed in Table 3.6, and more information is found in the datasheet in Appendix E.

Table 3.6: SGP30 sensor specifications for TVOC.

Parameter	Signal	Value
Measurement range	Ethanol signal	0 - 1000 ppm
	H ₂ signal	0 - 1000 ppm
Specified range	Ethanol signal	0.3 - 30 ppm
	H ₂ signal	0.5 - 3 ppm
Accuracy	Ethanol signal	typ.: 15% of measured value
	H ₂ signal	typ.: 10% of measured value
Long-term drift	Ethanol signal	typ.: 1.3% of measured value
	H ₂ signal	typ.: 1.3% of measured value

Dart Sensors WZ-S: FA

The Dart Sensors WZ-S is a micro fuel cell sensor measuring FA. Some of the key sensor specifications for the WZ-S sensor are listed in Table 3.7 and more information is found in the datasheet in Appendix E.

Table 3.7: WZ-S sensor specifications for FA.

Parameter	Value
Detection range	0-2 ppm
Operating temperature range	-20 - 50°C
Operating humidity range	10 - 90%
Lifetime	5 years in air

3.1.4 Control System

In each sensor box, one copy of each of the sensors described is mounted. The sensors are connected to a RaspberryPi, which calculates and sends the control signals for the control action to be performed. To maintain adequate IAQ, the AFRs are adjusted according to the conditions in the rooms. Additionally, the recirculation is regulated according to the condition of the return air and supply air. Thus, one sensor box is placed in each room, in the supply duct and recirculation duct. AFRs are measured by the dampers in each location.

The ventilation system can work as a DCV system, but it can also be set to supply constant AFRs. However, due to the ventilation system not being dimensioned correctly, there are low pressure differences in the ducting system, resulting in the fans not being able to regulate according to the measured pressure as a normal PC-DCV system. This resulted in a solution where the control is manually programmed in Python. It is regulated such that when the LCSs measure a value above the set limits for the chosen control parameters, the inlet valves open to a position specified in the Python code. Then the outlet valves adjust according to the inlet valves to balance the airflow. When the outlet valves are adjusted, they change with 8% of their current opening until the difference

between supply and extract AFRs is below $2 \text{ m}^3/\text{h}$ in the related room. For each control strategy, there are typically three various positions set in the Python code for the inlet valves to open and close between according to the measured values of the control parameters.

3.2 Leakage Testing

Before conducting experiments evaluating CSs for the DCV system, some leakage tests are conducted. This is due to the results from preliminary work related to this thesis revealed high infiltration rates in the full-scale office model. Since then, attempts have been made to seal the office model with sealant and duct tape. Additionally, plastic sheets sealed with duct tape have been mounted to cover all the inner walls to reduce the infiltration between the rooms. Therefore, several tests are performed to confirm that the airtightness has been improved to a satisfactory level. TEK17 requires $n_{50} \leq 0.6 \text{ h}^{-1}$. The n_{50} parameter indicates the air volume being transferred through the building envelope per hour when there is a pressure difference of 50 Pa between indoor and outdoor environments. First tracer gas tests under normal conditions are conducted. Then pressurization tests with 50 Pa overpressure in various rooms are conducted to compare n_{50} values to the TEK17 requirement. The tests are described in detail in the following. During the leakage tests, CAV is used as air supply method for constant conditions.

3.2.1 Tracer Gas Tests

The infiltration rates can be estimated using the tracer gas technique. It will be used to estimate the infiltration rates of the test facility under normal conditions with minimal pressure differences between the rooms. CO_2 is used as tracer gas supplied through the manikins in each room. Four tests are performed with a ventilation rate of about $30 \text{ m}^3/\text{h}$. During all tests, the CO_2 concentration in all rooms is monitored and each test lasts for about 2.5 hours until steady-state CO_2 concentrations are obtained. The tests are described shortly in Table 3.8. Each test, except test 4, is performed

twice; One time with duct tape on the door between room 1 and 2, and one time without.

Table 3.8: Tracer gas test.

Test 1	Room 1 is supplied with a rate of 0.3 l/min CO ₂
Test 2	Room 2 is supplied with a rate of 0.3 l/min CO ₂
Test 3	Room 3 is supplied with a rate of 0.3 l/min CO ₂
Test 4	Room 1, 2 and 3 is supplied with a rate of 0.3 l/min CO ₂ each

To calculate the infiltration rates CO₂ mass balances for each room during each test are created. The mass balances from all the performed tests make a system of equations, which can be solved to obtain the infiltration rates through each part of the facade and the two inner walls. The mass balances are on the form (Gyasi, 2021):

$$C_r Q_{vent} + C_r Q_{f_exf} + \sum_{i=1}^n C_r Q_{w_exf_i} = E + C_{amb} Q_{vent} + C_{amb} Q_{f_inf} + \sum_{i=1}^n C_i Q_{w_inf_i} \quad (3.1)$$

where,

- C_r is the CO₂ concentration in the associated room [kg/m^3].
- C_{amb} is the ambient CO₂ concentration [kg/m^3].
- C_i is the CO₂ concentration in adjacent room i [kg/m^3].
- Q_{vent} is the AFR of the ventilation air in the associated room [m^3/s].
- Q_{f_exf} is the AFR of the air exfiltrating from the associated room through the facade [m^3/s].
- $Q_{w_exf_i}$ is the AFR of the air exfiltrating from the room through a wall between the room and adjacent room i [m^3/s].
- Q_{f_inf} is the AFR of the air infiltrating into the room through the facade [m^3/s].

- $Q_{w_inf_i}$ is the AFR of the air infiltrating into the room through the wall between the room and adjacent room i [m^3/s].
- E is the tracer gas injection rate [kg/s].
- n is number of adjacent rooms.

3.2.2 Air Pressure Tests

Air pressure testing is used to estimate the airtightness of a building. The ventilation system is used to create overpressure in the individual rooms by supplying more air than is being extracted in the room where the overpressure is intended. The differential pressure between the rooms is measured by a micromanometer, of the type dpm RS232. The tests summarized in Table 3.9 are performed. Again, all tests except test 1, is performed one time with duct tape covering the leaks from the door between room 1 and 2, and one time without. It is not considered necessary to perform test 1 with the door being taped as there should be even pressure throughout all three rooms.

Table 3.9: Air pressurization tests.

Air pressure test #	Description
1	50 Pa overpressure in the whole test-facility relative to ambient
2	50 Pa overpressure in room 1 relative to room 2
3	50 Pa overpressure in room 3 relative to room 2
4	50 Pa overpressure in room 2 relative to room 1 and 3

Test 1 aims to estimate the leakage through the facade and thus all three rooms have an overpressure of 50 Pa compared to the outside of the office model. Test 2, 3, and 4 pressurize room 1, 3, and 2 respectively with an overpressure of 50 Pa compared to the adjacent room(s) to estimate the leakage between the rooms.

When 50 Pa overpressure is achieved, the ventilation system settings are noted for further calculations of the infiltration rates. The power law, (3.2), is commonly used for infiltration calculations. The

flow coefficient, n , varies from 0.5 to 1 for turbulent or laminar flow respectively, and is commonly set to an assumed value of 0.67. The leakage coefficient, C , is however unknown and must be determined (Thamban, 2020). Thamban (2020) provides 3.3 which in combination with the power law are used to create a system of equations that are solved to obtain values for the infiltration rates and the leakage coefficients C (Thamban, 2020).

$$q_{m_i} = C(\Delta P)^n \quad (3.2)$$

$$\sum_{i=1}^N q_{m_i} + \sum_{j=1}^2 q_{mv_j} = 0 \quad (3.3)$$

where,

- q_{m_i} is the infiltration rate through building part i [m^3/s]
- C is the leakage coefficient [$m^3/(sPa^n)$]
- ΔP is the differential pressure [Pa]
- n is the flow coefficient
- q_{mv_j} is the mechanical AFRs for supply and extract [m^3/s]

When all leakage coefficients are obtained by solving the system of equations, n_{50} values can be calculated for the three rooms using 3.4.

$$n_{50} = \frac{Q(\Delta P = 50)}{V} \quad (3.4)$$

where Q is the total infiltration rate and V is the volume of the corresponding room.

3.3 Experimental Procedure: Control Strategies

The CS experiments are performed with various scenarios for control strategies. The goal is to find which combinations of IAQ parameters used for control achieve the best IAQ while also limiting the energy consumption. To achieve even lower energy consumption, a system for recirculation of air is implemented in the ventilation system in the test facility. Thus, investigating the IAQ parameters most suitable for recirculation control is also desirable. Some CSs will be tested through the experiments described in this chapter. However, the purpose of the experiments is mainly to validate a simulation model such that simulations of various CSs can be conducted.

During the experiments, the ventilation system is controlled by measurements of the various IAQ parameters. When a measured control factor reaches a set limit, more air is supplied to the respected room. In addition to each scenario of airflow control being performed without recirculation of air, various parameters for recirculation control are applied. Thus, one CS is composed of two types of control, hereafter referred to as airflow control and recirculation control.

Due to some limitations regarding control and availability of sources of several of the IAQ parameters, it was not possible to perform all the intended experiments. Thus, only the parameters which can be sufficiently controlled are used as control parameters during the experiments. The various CS scenarios for each experiment are summarized in Table 3.10. Additional scenarios will be simulated.

Table 3.10: Measurement plan.

Scenario	Airflow control	Recirculation control
1	CO ₂	No recirculation
2	CO ₂	PM _{2.5}
3	CO ₂	CO ₂
4	CO ₂	CO ₂ and PM _{2.5}
5	CO ₂ and PM _{2.5}	No recirculation
6	CO ₂ and PM _{2.5}	CO ₂ and PM _{2.5}

Each experiment lasts for two and a half hours, and the occupancy schedule during this time is illustrated in Table 3.11. As there may be varying occupancy in an office during the day, there is included a time slot with two people in room 1, and with no one in room 3.

Table 3.11: Plan.

Time	Room 1	Room 2	Room 3
0:00 - 0:15	1	0	0
0:15 - 0:30	1	0	1
0:30 - 1:15	1	1	1
1:15 - 1:45	2	1	0
1:45 - 2:00	1	1	1
2:00 - 2:15	0	1	1
2:15 - 2:30	0	0	1

The emission sources described in Chapter 3.1.2 are used to create somewhat similar conditions during all experiments. The purpose of the emission sources is to create a setting similar to where people are present and if the building were placed outside. Therefore, the CO₂ is turned on and off according to Table 3.11, where 1 person equals 0.3 l/min. The mosquito coil is lit 10 minutes before the beginning of the experiment to achieve a relatively high PM concentration from the beginning, as would be more realistic than a sudden rapid increase at the beginning of the experiment. However, due to safety reasons related to CO₂ supply, it is not possible to enter the rooms after the beginning

of the experiment. Thus, the heat production from the manikins and the lamps all starts at the beginning of the experiments and not when the people enter the specific rooms.

The full-scale test facility is thoroughly ventilated in between measurements. All valves are set to fully open and all the doors are opened as well. This is done for about 1 hour. Sometimes more time is needed to obtain sufficient start concentrations of certain contaminants. This must be evaluated before starting each test.

3.3.1 Control Logics

The CS scenarios listed in Table 3.10 are created by a combination of one airflow control and one recirculation control. When creating the control strategies, the control limits are decided according to the recommended maximum threshold values. To avoid exceeding these thresholds, they are set a little bit below the recommended values. The resulting types of airflow control are illustrated in Figure 3.7, and the three types of recirculation control strategies are illustrated in Figure 3.8. When OA is set to a percentage lower than 100%, it shall be understood that the return air covers the rest of the supply air.

The PM_{2.5} limits used for the experiments are 8 and 15 $\mu\text{g}/\text{m}^2$ which corresponds to the old guidelines from WHO and FHI (Folkehelseinstituttet, 2015). The reason for not using the updated lower value of 5 $\mu\text{g}/\text{m}^2$ is due to several experiments being conducted during the same day, which induced some difficulties in reducing the PM_{2.5} concentration to lower than 5 $\mu\text{g}/\text{m}^2$. Additionally, renovation work is conducted in the laboratory during the days, which also elevates the indoor PM_{2.5} concentration. Therefore, to have a larger range, 8 $\mu\text{g}/\text{m}^2$ is used instead. However, during the simulations, 5 $\mu\text{g}/\text{m}^2$ will be used as the limit.

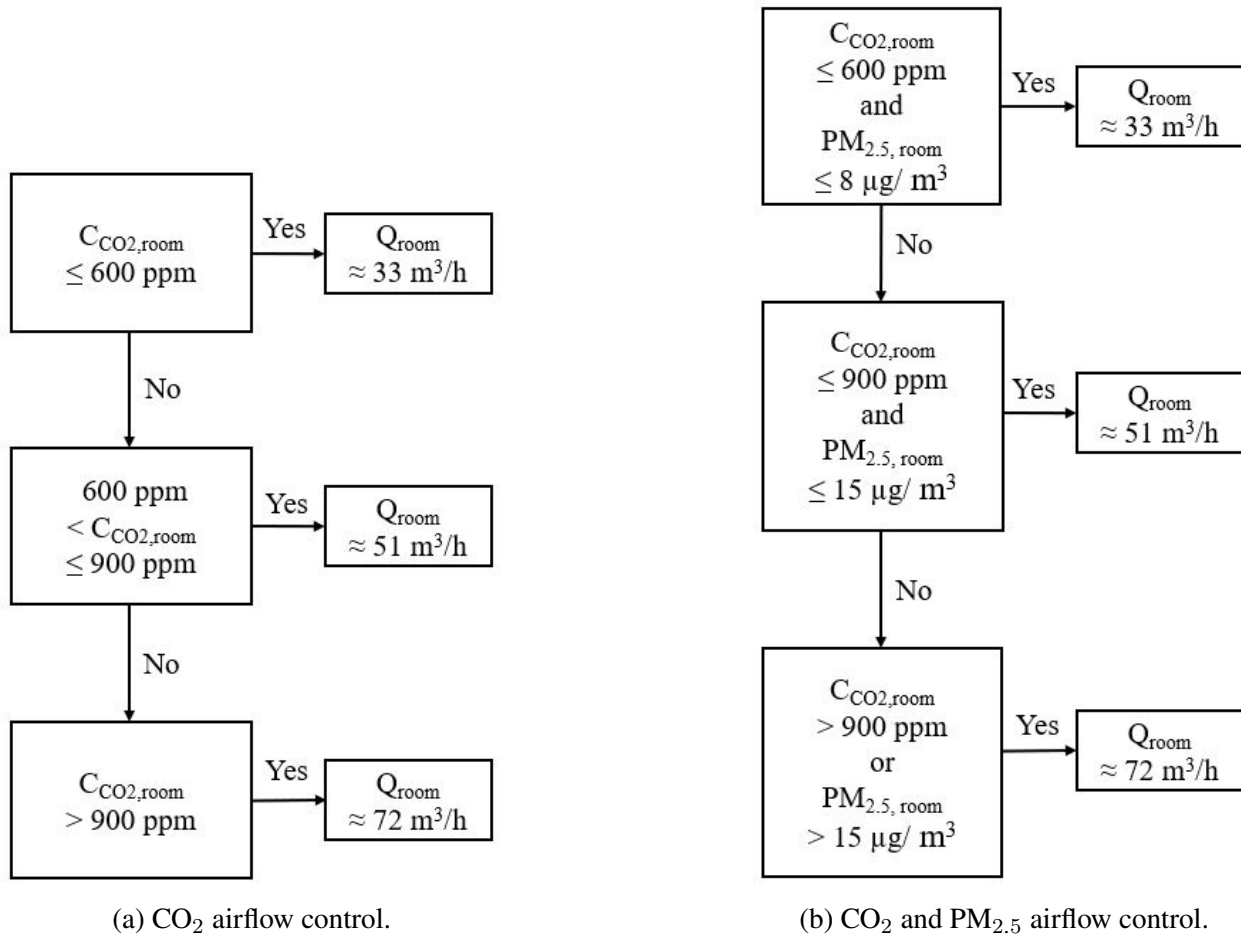


Figure 3.7: Airflow control strategies used for experiments.

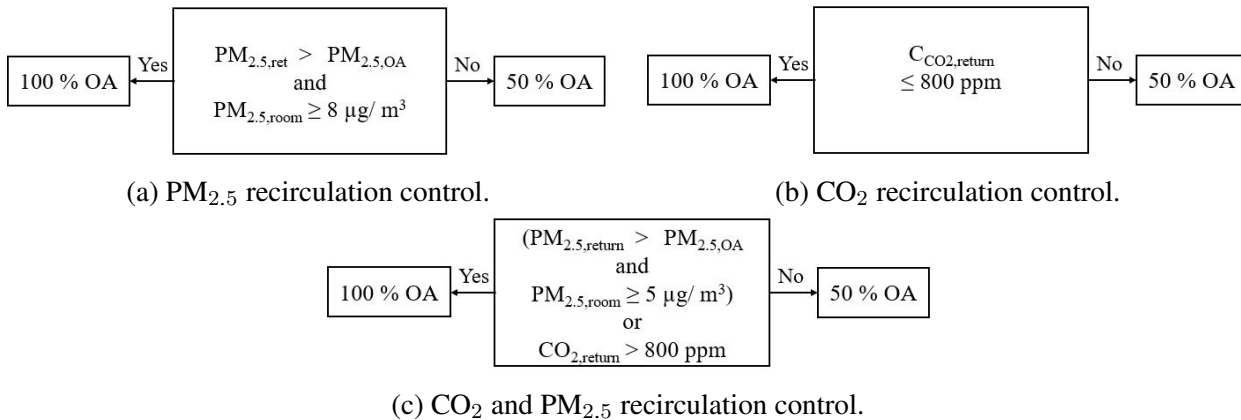


Figure 3.8: Recirculation control strategies used for experiments.

3.4 Simulations

This chapter will present the tools used for simulations and descriptions of the performed simulations. Co-simulation between CONTAM and EnergyPlus is used to evaluate additional CSs for DCV to those tested through the experiments described above. Both IAQ and energy consumption is analyzed. CONTAM is used to simulate the IAQ and airflow patterns in the test facility, while EnergyPlus can be used to simulate the energy demand for the various CSs. First, a short introduction to the tools is presented, before the procedures of model validation and simulations are presented.

3.4.1 Simulation Tools: CONTAM and EnergyPlus

CONTAM is a computer program developed by the National Institute of Standards and Technology (NIST) used to analyze IAQ and ventilation. Thus, some of the software applications include determining airflows, contaminant concentrations, and predictions of personal exposure in multi-zone building models. CONTAM can cooperate with several energy analysis programs, including EnergyPlus, for more complex analyses (National Institute of Standards and Technology, 2018). EnergyPlus is a building energy simulation program used to model energy flows. It is developed through a collaborative effort between Berkeley Lab's Simulation Research Group, the University of Illinois at Urbana-Champaign, the U.S. Army Construction Engineering Research Laboratory, and other research organizations. Some of its capabilities include heat transfer calculations and multi-zone airflow analyses (Intellectual Property Office, n.d.).

In this thesis, co-simulations between CONTAM and EnergyPlus are conducted. This is necessary to capture the mutual dependence of airflow and heat transfer, and allows for the sharing of these data between the simulation tools. The coupled building model requires information exchange between the two programs. The information exchange is summarized in Figure 3.9. Information exchange occurs at each simulation time step. Interzone and infiltration AFRs are shared with EnergyPlus from CONTAM. In turn, CONTAM gets indoor temperatures and system airflows from EnergyPlus

and performs the contaminant transport calculations. (Alonso, Dols, and Mathisen, 2022).

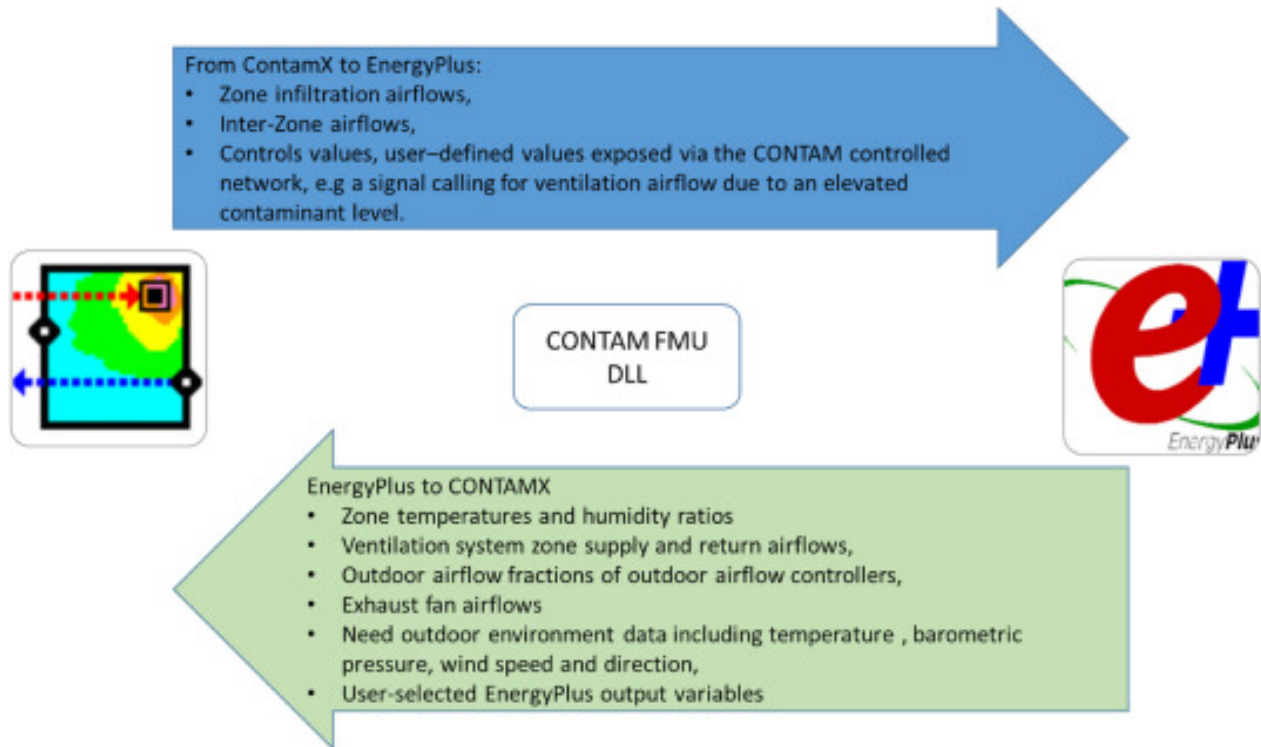


Figure 3.9: Schematic of the information exchange between CONTAM and EnergyPlus (Alonso, Dols, and Mathisen, 2022).

3.4.2 Validation of Building Model

Before investigating the various CSs through simulations, the co-simulation model is compared to the measurements previously described in Chapter 3.3. The building model is intended to recreate the test facility used for the experiments, concerning geometry, technical systems, and pollution sources. Infiltration rates are obtained from the leakage tests. The performed experiments are used as reference measurements to verify the model, which then can be used to simulate additional CSs than the ones performed experimentally.

The simulations use outdoor temperatures, humidity, and pollution levels in the calculations. This data is obtained from a weather file and a pollution file. For the validation of the model, input values in these files are decided based on measured values from the experiments. Then the indoor

pollution loads and internal gains are adjusted until the simulations fit the measured indoor values. Simulations and measurements are compared on graphs until a well fit is observed. Then the fit must be quantified to make sure the building model is fitted properly.

Two commonly used precision metrics, mean bias error (MBE) and coefficient of variance of root mean squared error (CVRMSE), are used to quantify the fit between measured and simulated values for the validation of the building model. These metrics are prescribed by ASHRAE Guideline 14 for testing the predictive performance of energy models. MBE and CVRMSE are calculated according to (3.5) and (3.6), respectively. The MBE values are recommended to be below $\pm 10\%$ and the CVRMSE values below 30 % when using hourly data (Chakraborty and Elzarka, 2017).

$$MBE = \frac{\sum_{i=1}^N (C_{sim} - C_{LCS})}{N} \cdot \frac{100}{C_{LCS,avg}} \quad (3.5)$$

$$CVRMSE = \frac{100}{C_{LCS,avg}} \cdot \sqrt{\frac{\sum_{i=1}^N (C_{sim} - C_{LCS})^2}{N}} \quad (3.6)$$

where,

- C_{sim} is simulated concentration
- C_{LCS} is concentration measured by LCSs
- $C_{LCS,avg}$ is the average of N observations measured by LCSs

3.4.3 Simulation Procedure

When the model is validated with the measured data from the experiments, additional simulations may be conducted. Table 3.12 shows a list of the various CSs to be simulated. Hereafter, when refer-

ring to a specific CS the name is on the form RoomControlParameters_RecirculationControlParameters. For example, CS 7.5 from Table 3.12, with airflow control parameters being CO₂, temperature, PM_{2.5}, and FA, and recirculation control parameters being CO₂ and FA, is called CO2TempPMFA_CO2FA.

Table 3.12: CSs which will be simulated.

CS	Room control	Recirculation control
1	CO ₂	1) No recirc, 2) PM _{2.5} , 3) CO ₂ , 4) CO ₂ , PM _{2.5} , 5) CO ₂ , FA
2	CO ₂ , Temperature	1) No recirc, 2) PM _{2.5} , 3) CO ₂ , 4) CO ₂ , PM _{2.5} , 5) CO ₂ , FA
3	CO ₂ , PM _{2.5}	1) No recirc, 2) PM _{2.5} , 3) CO ₂ , 4) CO ₂ , PM _{2.5} , 5) CO ₂ , FA
4	CO ₂ , FA	1) No recirc, 2) PM _{2.5} , 3) CO ₂ , 4) CO ₂ , PM _{2.5} , 5) CO ₂ , FA
5	CO ₂ , Temperature, PM _{2.5}	1) No recirc, 2) PM _{2.5} , 3) CO ₂ , 4) CO ₂ , PM _{2.5} , 5) CO ₂ , FA
6	CO ₂ , Temperature, FA	1) No recirc, 2) PM _{2.5} , 3) CO ₂ , 4) CO ₂ , PM _{2.5} , 5) CO ₂ , FA
7	CO ₂ , Temperature, PM _{2.5} , FA	1) No recirc, 2) PM _{2.5} , 3) CO ₂ , 4) CO ₂ , PM _{2.5} , 5) CO ₂ , FA

Table 3.14 and 3.15 shows the control logic for the various airflow CSs and recirculation CSs, respectively. The control parameter limits are based on recommended indoor threshold values. To avoid exceeding the thresholds, the limits are set somewhat lower than the actual threshold. The specific AFRs are set to satisfy the minimum requirements from TEK17. However, as the material load in the test facility can not be considered low-emitting, the AFRs are set considerably higher than the calculated minimum values from TEK17. Table 3.13 illustrates the calculated TEK17 values, and the ones used during simulations.

Table 3.13: Minimum AFRs calculated from TEK17 and the AFRs used in simulations.

Occupancy	TEK17 minimum AFR [m ³ /h]	Simulation AFR [m ³ /h]
0	5	5
1	44	65
2	70	97

Table 3.14: Airflow control logic.

Airflow control parameters	Logic for airflow control	AFR [m ³ /h]
CO ₂	IF (CO _{2_r} <= 600) ELSE IF (CO _{2_r} <= 900) ELSE IF (CO _{2_r} > 900)	5 65 97
CO ₂ , Temp	IF (CO _{2_r} <= 600 & Temp_r <= 22) ELSE IF (CO _{2_r} <= 900 & Temp_r <= 24) ELSE IF (CO _{2_r} > 900 Temp_r > 24)	5 65 97
CO ₂ , PM _{2.5}	IF (CO _{2_r} <= 600 & PM _{2.5_r} <= 5) ELSE IF (CO _{2_r} <= 900 & PM _{2.5_r} <= 5) ELSE IF (CO _{2_r} > 900 PM _{2.5_r} > 5)	5 65 97
CO ₂ , FA	IF (CO _{2_r} <= 600 & FA_r <=80) ELSE IF (CO _{2_r} <= 900 & FA_r <= 100) ELSE IF (CO _{2_r} > 900 & FA_r > 100)	5 65 97
CO ₂ , Temp, PM _{2.5}	IF (CO _{2_r} <= 600 & Temp_r <= 22 & PM _{2.5_r} <= 5) ELSE IF (CO _{2_r} <= 900 & Temp_r <= 24 & PM _{2.5_r} <= 5) ELSE IF (CO _{2_r} > 900 Temp_r > 24 PM _{2.5_r} > 5)	5 65 97
CO ₂ , Temp, FA	IF (CO _{2_r} <= 600 & Temp_r <= 22 & FA_r <= 80) ELSE IF (CO _{2_r} <= 900 & Temp_r <= 24 & FA_r <= 100) ELSE IF (CO _{2_r} > 900 Temp_r > 24 FA_r > 100)	5 65 97
CO ₂ , Temp, PM _{2.5} , FA	IF (CO _{2_r} <= 600 & Temp_r <= 22 & PM _{2.5_r} <= 5 & FA_r <= 80) ELSE IF (CO _{2_r} <= 900 & Temp_r <= 24 & PM _{2.5_r} <= 5 & FA_r <= 100) ELSE IF (CO _{2_r} > 900 Temp_r > 24 PM _{2.5_r} > 5 FA_r > 100)	5 65 97

Table 3.15: Recirculation control logic.

Recirculation control parameters	Logic for recirculation control	OA percentage [%]
No recirculation	Always	100
PM _{2.5}	IF (PM _{2.5_out} > PM _{2.5_amb} & PM _{2.5_out} > 5) ELSE	100 30
CO ₂	IF (CO _{2_out} > 800) ELSE	100 30
CO ₂ and PM _{2.5}	IF ((CO _{2_out} > 800) (PM _{2.5_out} > PM _{2.5_amb} & PM _{2.5_out} > 5)) ELSE	100 30
CO ₂ and FA	IF ((CO _{2_out} > 800) (FA_out > FA_amb & FA_out > 80)) ELSE	100 30

Each CS implemented in the simulations are constructed of one scenario for airflow control from Table 3.14 and one scenario of recirculation control from Table 3.15. In Table 3.16 some explanations to subscripts and symbols used in the control logics in Table 3.14 and 3.15 are listed.

Table 3.16: Definitions of subscripts from the control logics.

Subscript/Symbol	Meaning
r	Measured values at room level
out	Measured values in the air transferred out of the rooms
amb	Measured values at ambient level
	Or

3.5 Analysis

The results are analyzed to obtain the best CS both concerning IAQ and energy consumption. Thus, boxplots describing the temperatures and concentrations of CO₂, PM_{2.5}, and FA are used for comparison of each CS and the resulting IAQ. The boxplots give a statistical overview with information about average values, median, maximum and minimum values. Additionally, the total yearly energy consumption is compared for all CSs. Due to both energy consumption and IAQ being highly dependent on climate, various climates should be considered. Thus, simulations are performed for two different cities. Beijing is a large, highly polluted city with relatively high outdoor temperatures. Simulations from Beijing sets the basis for the analysis, and all results from all mentioned CSs are presented and analyzed. Simulations from Trondheim, a colder, less polluted city, are used to supplement the analysis when considered necessary to add more depth to the analysis.

Chapter 4

Results and Analysis

The results obtained from performing the experiments described in Chapter 3 are presented in the following. First, the calculated infiltration rates are presented to indicate the state of the test facility. Then some of the results from the CS experiments are discussed, before being used to validate the building simulation model which is used for co-simulations of a variety of CSs. The various CSs are analyzed throughout the presentation of the simulation results.

4.1 Test-Facility Leakage

Two types of leakage tests are conducted to calculate infiltration rates under normal pressure conditions, and related n_{50} values for comparison to TEK17 requirements. The results are presented in the following.

4.1.1 Tracer Gas Testing

The tracer gas tests are used to calculate infiltration rates at normal conditions with minimal pressure differences between the rooms. It is however important to acknowledge that the pressure differences between the rooms change according to several factors and is certainly not constant. However, the results give an indication of the extent of leakage in the test facility. The tracer gas tests were performed twice, one time with duct tape covering the door between room 1 and 2, and one time without duct tape to see the impact of the door. The infiltration rates for each building part are calculated and added together to get the infiltration for the whole rooms. Table 4.1 presents all individual infiltration rates.

Table 4.1: Infiltration rates calculated from tracer gas tests.

Building part	Infiltration rates [m^3/s] (with duct tape)	Infiltration rates [m^3/s] (without duct tape)
Facade 1	0.00038	0.00550
Facade 2	-0.00371	0.00354
Facade 3	-0.00120	-0.00251
Inner wall (R1-R2)	-0.00064	0.00170
Inner wall (R3-R2)	-0.00002	0.00161
Total room 1	-0.00026	0.00720
Total room 2	- 0.00306	0.00023
Total room 3	- 0.00123	-0.00090

The results provide some negative numbers, which means that a higher amount of air is infiltrating into the room than the amount exfiltrating out of the room. Thus, in room 3 the total amount of air is infiltrated independent of whether there s duct tape on the door between room 1 and 2.

There is little consistency between the infiltration rates calculated for the facades. This may be due to the infiltration rates changing between the two tests, and more likely due to uncertainties related to the calculations. The infiltration rate through the inner wall between room 1 and 2 is significantly

higher without the duct tape on the door, as would be expected. By comparing these values, an indication of the amount of air exchange through the door can be observed. The difference in infiltration rates through the inner wall between room 2 and 3 was not expected to change drastically depending on duct tape or not. However, a significant difference is observed. Again, this is most likely due to calculation uncertainties. These are discussed further in Chapter 5.1.1.

4.1.2 Air Pressure Testing

Air pressure tests are performed using overpressure of 50 Pa. The method in Chapter 3.2.2 is used to calculate infiltration rates and leakage coefficients. The resulting n_{50} values are listed in Table 4.2. More details about the tests and calculations are provided in Appendix A.

Table 4.2: Calculated n_{50} values, based on air pressure tests.

Room	n_{50} [h^{-1}] (with duct tape)	n_{50} [h^{-1}] (without duct tape)
1	2.10	3.84
2	2.34	4.35
3	2.03	2.30
Total		1.51

Table 4.2 reveals values much higher than the TEK17 requirement of $n_{50} \leq 0.6 h^{-1}$. However, as attempts have already been made concerning sealing the facility, the facility must be used for the CS experiments despite the high infiltration rates. The high infiltration rates are probably mostly due to the construction of the facility, which is very simple compared to real buildings.

It is observed that the n_{50} value for the whole facade is lower than for each room. This indicates that infiltration through the inner walls is a major contributor to the high values associated with the three rooms. Additionally, a lot of factors regarding the air pressure experiments may have had an impact on the calculations, resulting in higher values than in reality. The sources of errors are discussed further in Chapter 5.1.1.

The inner walls generally seem to have higher infiltration rates than the facade as room 2 seems to leak the most despite having a facade of a smaller area. However, during the tests with duct tape, the obtained values are relatively similar for all three rooms, and the variations may also be due to uncertainties in the calculations. The results of the tests without duct tape on the door, support the hypothesis of the door being a major leak, as the n_{50} for room 1 and 2 increases considerably when removing the duct tape. The value for room 3 increases some as well, but that is most likely due to calculation uncertainties.

4.2 Control Strategy Experiments

The experiments described in Chapter 3.3 is performed. Due to challenges in maintaining a controlled environment when conducting the control strategy experiments, simulations are chosen instead to form the analysis of the various CSs. Some indications of various tendencies related to the CSs can still be made from the experiments and will be discussed in the following. However, the data from the experiments are also used to validate a building model which will be used for simulations of various CSs for room airflow control and recirculation control. In this chapter some of the findings from the experiments will be presented, however, the main analysis regarding CSs will be related to the simulations. Figures for all experiments performed, including those not mentioned in this chapter, can be found in Appendix B. In this chapter, only some of the measurements will be discussed.

4.2.1 Surrounding Environment

Due to challenges with controlling several of the parameters intended to investigate, only some of the parameters were possible to control and evaluate. Thus, the main focus will be on the CO_2 and $\text{PM}_{2.5}$ concentrations. As the supply temperature was high during all experiments, the measurements show minimal variations in temperature. Thus control dependent on temperature was

not considered applicable and is therefore not included. Due to large variations in FA concentration in the OA during the various experiments, comparing the CSs handling of FA is challenging. There was observed higher FA concentration in OA than inside the rooms due to the facility being located inside another laboratory. This is usually not the case as typical FA sources are building materials, furniture, and respiration. FA is not included as a control parameter in any of the experiments, due to the large variations in concentrations, which makes it insufficient for comparison of CSs.

The generation of humidity also occurred to be a problem. Initially, candles were intended to be used for moisture production. However, as it showed little differences in the RH, in addition to producing additional CO₂ and particles, it was discarded. Then humidifiers were tested, despite the probability of them producing more moisture than humans normally do in an office environment. However, the humidifiers also showed disappointing results. Recognized as a limitation to light scattering particle low-cost sensors is the influence of humidity. This was observed when using humidifiers, as the measured PM_{2.5} concentration increased massively. Thus, no source of moisture production could be used during the experiment.

The remaining IAQ parameters of interest are therefore CO₂ and PM_{2.5}, which were to some degree possible to control. The CO₂ injection from the bottle through the rotameters and then the manikins functioned well. The mosquito coil was harder to use as a controlled source of particles. Therefore, the particle concentration in the OA supplied to the test facility during the experiments, fluctuated both during the experiments and between them.

4.2.2 Recirculation Control

As the simulations will be the main focus of the analysis of the CSs, only a brief analysis of the results from the experiments is included. The main tendencies observed from the experiments are related to the various recirculation control strategies. Therefore, recirculation strategies are the focus of the experimental analysis, while airflow control strategies are discussed in relation to the simulations instead.

It is evident that in places with high outdoor $PM_{2.5}$ concentrations, using DCV with no recirculation and only CO_2 as a control parameter for airflow control into rooms, may result in the concentration of certain pollutants exceeding its recommended limit. Figure 4.1 shows that during the experiment with CO_2 as airflow control parameter and no recirculation, the indoor $PM_{2.5}$ concentration exceeds the recommended limit when outdoor concentrations of $PM_{2.5}$ is in the range of $10\text{-}20 \mu\text{g}/\text{m}^3$.

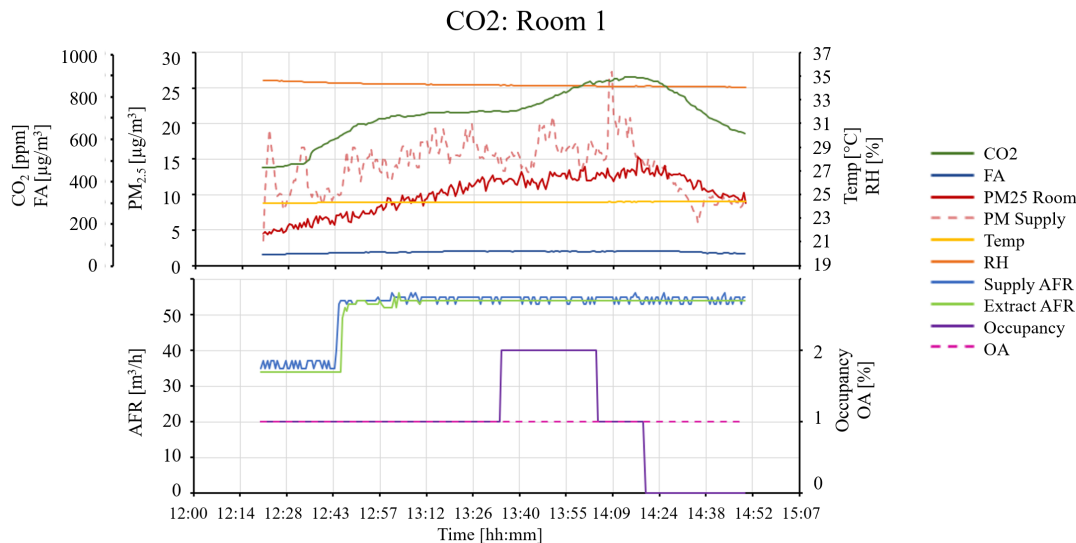


Figure 4.1: CO_2 control without recirculation in room 1.

These results indicate a need for recirculation control in areas with high outdoor pollution levels. To test this hypothesis, an experiment with $PM_{2.5}$ as a control parameter for recirculation was performed, still with CO_2 as the airflow control parameter. Figure 4.2 shows the results of this experiment in room 1. The results show that when using $PM_{2.5}$ as a control parameter for recirculation, the recirculation was kept on the whole time due to the high outdoor concentrations. Additionally, the indoor concentrations still exceeded the recommended maximum threshold values. This may however be due to higher outdoor concentration, and comparisons to the previous experiment are therefore not necessarily straightforward. However, due to the recirculation, CO_2 builds up inside the room and even exceeds the 1000 ppm limit. The 1000 ppm limit is also approached in room 2 and 3. Thus, even with a maximum of one person present in these rooms, the recirculation based on particles results in the buildup of CO_2 .

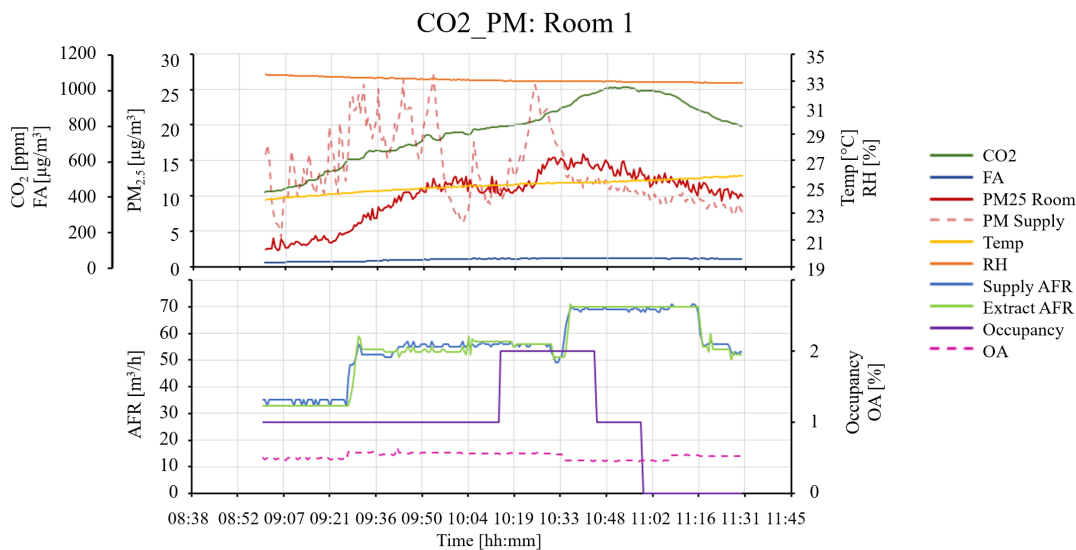


Figure 4.2: CO₂ control with PM recirculation control in room 1.

Figure 4.3 shows the results from room 1 when CO₂ and PM_{2.5} are both used as control parameters for recirculation. CO₂ is still the control parameter for airflow into rooms. Introducing CO₂ as a control parameter for recirculation results in the levels in the rooms being kept below 1000 ppm throughout the experiment. Also, the dual recirculation control seems to have a positive effect on the indoor PM concentration. However, the values are still too high in all rooms. It is however important to notice that the outdoor concentration is very high, in addition to the building used in this case having trouble with leakage, allowing for outdoor generated pollutants to enter the facility through infiltration. Thus in a more realistic setting, the impacts of this dual recirculation control may have been more evident on both CO₂ and PM_{2.5} concentrations.

As there are several factors resulting in difficulties in comparing the performed experiments, the CSs will be discussed further in relation to the simulations, where the surrounding environment will be the same throughout all simulations. However, the experiments are used for validating the model in which the simulations are performed.

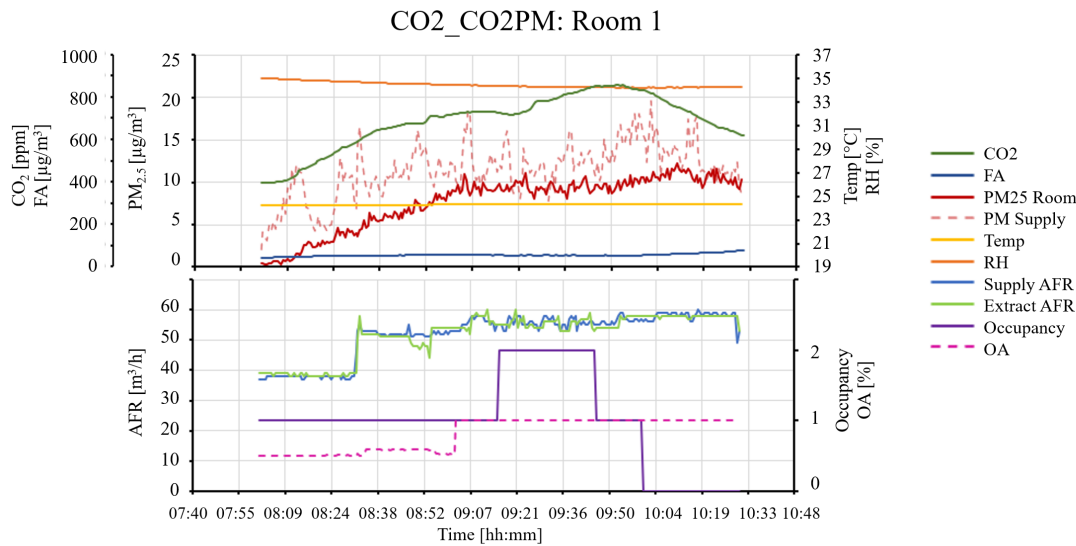


Figure 4.3: CO₂ control with CO₂ and PM recirculation control in room 1.

4.3 Validation of Building Model

To validate the building model two cases are used. One model is validated with an experiment where there were highly polluted OA with especially high concentrations of PM_{2.5} and FA which is generated from a mosquito coil. The other case is validated using an experiment with cleaner OA. However, the clean case is still quite polluted due to the OA being extracted from inside the laboratory where the test facility is located. The simulations are fitted to the measurements of CO₂, PM_{2.5}, temperature, and FA, in addition to supply AFRs. Thus, the resulting building model, which will be used for co-simulations in CONTAM and EnergyPlus, is validated according to real measurements in the test facility. The experiments are performed with CO₂ as a control parameter and no recirculation. Due to not having any moisture produced during the experiment, RH is not used to validate the model. It will therefore not be analyzed as a control parameter for CSs in the co-simulations either. Despite temperature and FA not being used as control parameters during the experiments, the values are still measured and can be used for validation of the model. Thus, these parameters can also be included in the CSs to be simulated.

Figure 4.4a-4.6a shows the validation curves for the three rooms during the experiment with highly

polluted OA. A mosquito coil is the main contributor to the high concentrations of FA and $PM_{2.5}$ in the air. However, due to the OA being extracted from a laboratory inside a building, other uncontrolled sources are also contributing. Figure 4.4b-4.6b depicts the validation curves for all rooms during the experiment with clean OA. While referring to the air as clean, it is still drawn from inside a laboratory and thus it contains higher concentrations of some pollutants than what is typically found in OA. However, the pollution level in the supply air during this experiment is much lower than during the experiment related to case 2, and will therefore be referred to as clean.

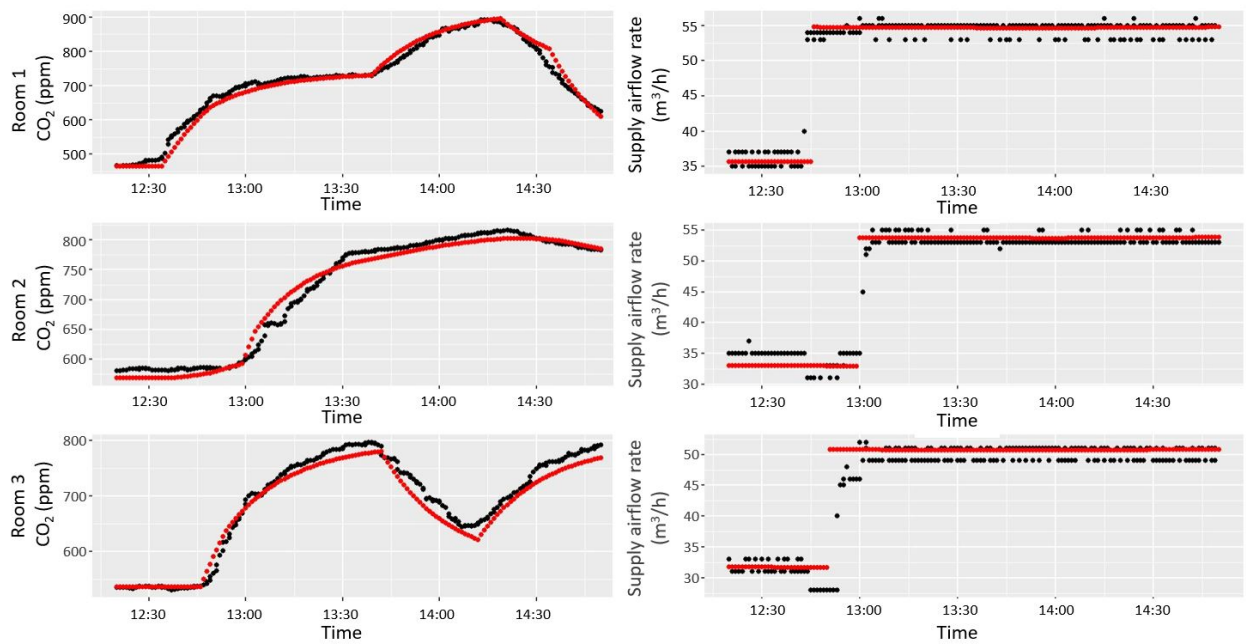
Figure 4.4 contains the curves for CO_2 and AFRs. The simulated curve for CO_2 is fitted by adding CO_2 sources in the building model which corresponds to what was injected into each room during the experiment. Some adjustments to the generation rates are done in the building model for a better fit. The chosen generation rates are listed in Table 4.3.

Table 4.3: CO_2 generation rates per person in the simulation models.

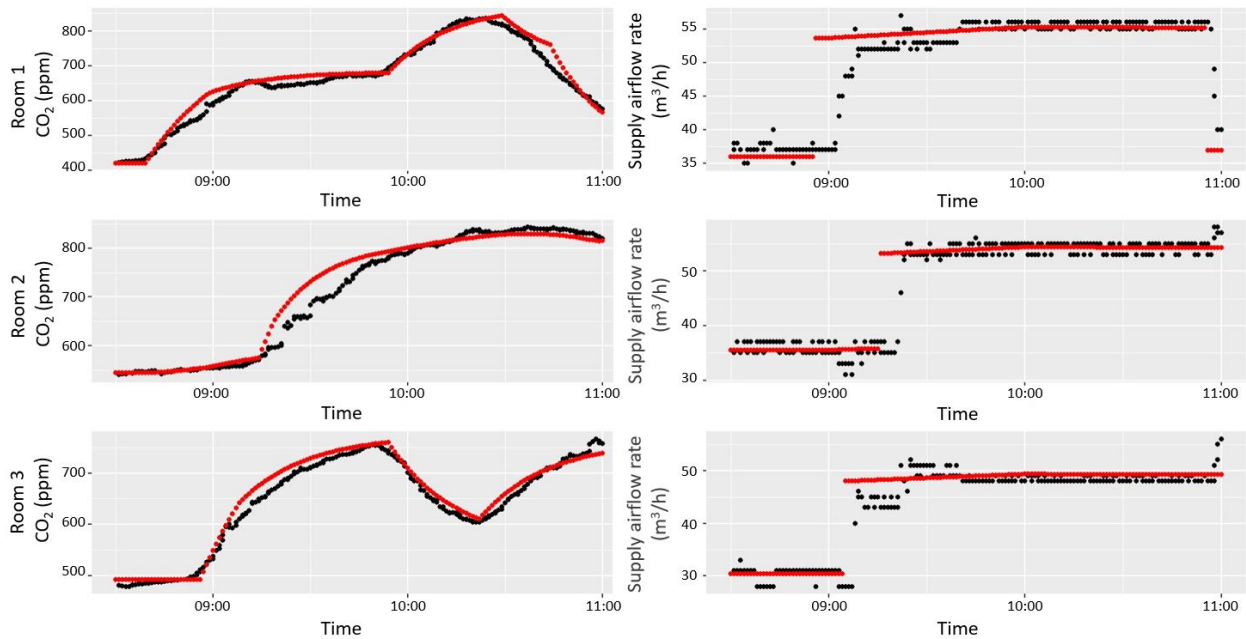
Room number	CO_2 generation [l/min per person]	
	Polluted OA case	Clean OA case
1	0.27	0.24
2	0.31	0.32
3	0.28	0.26

The experiments revealed some delay in the injection of CO_2 , as the increase of CO_2 only began after minutes of the CO_2 bottle being opened. Thus, to achieve the great fit of the curves in Figure 4.4, the time had to be adjusted by 5 minutes.

Implementing the same CS to the simulations as were used during the experiment resulted in the simulated airflows achieving a great fit to the measured ones, as can be seen in Figure 4.4. Some deviations are however observed. This is mostly due to the valves not always being able to change positions when their current position is with a small opening. Thus, sometimes this had to be done manually, which resulted in the valves adjusting sometime after they were supposed to.



(a) Polluted OA.

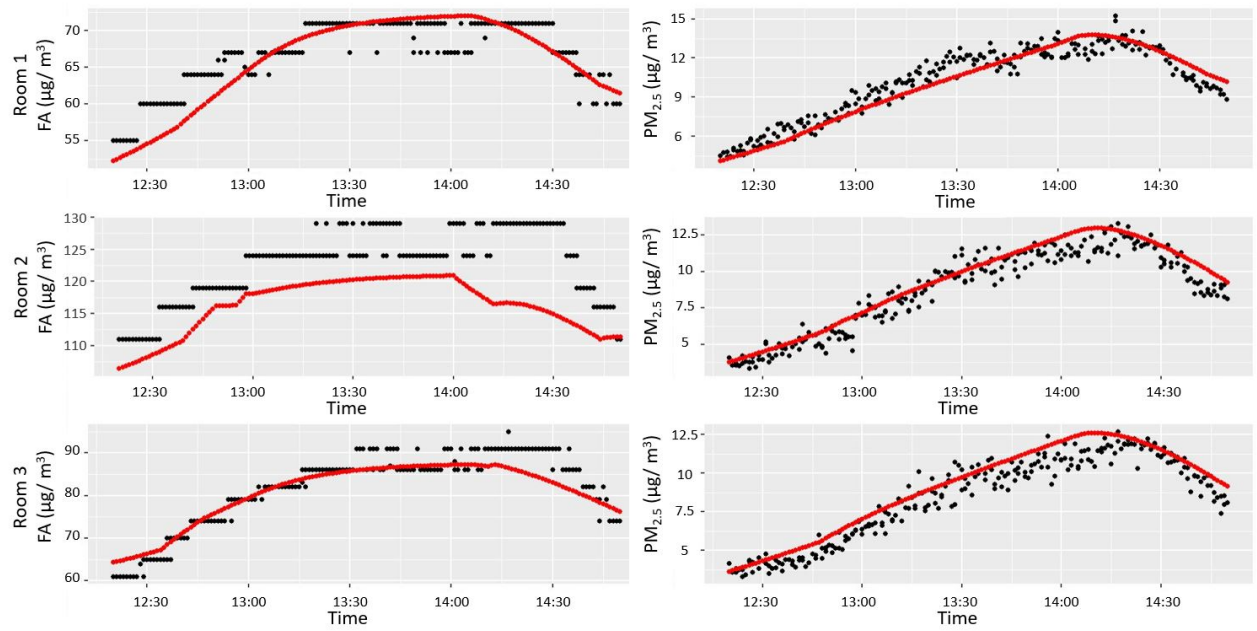


(b) Clean OA.

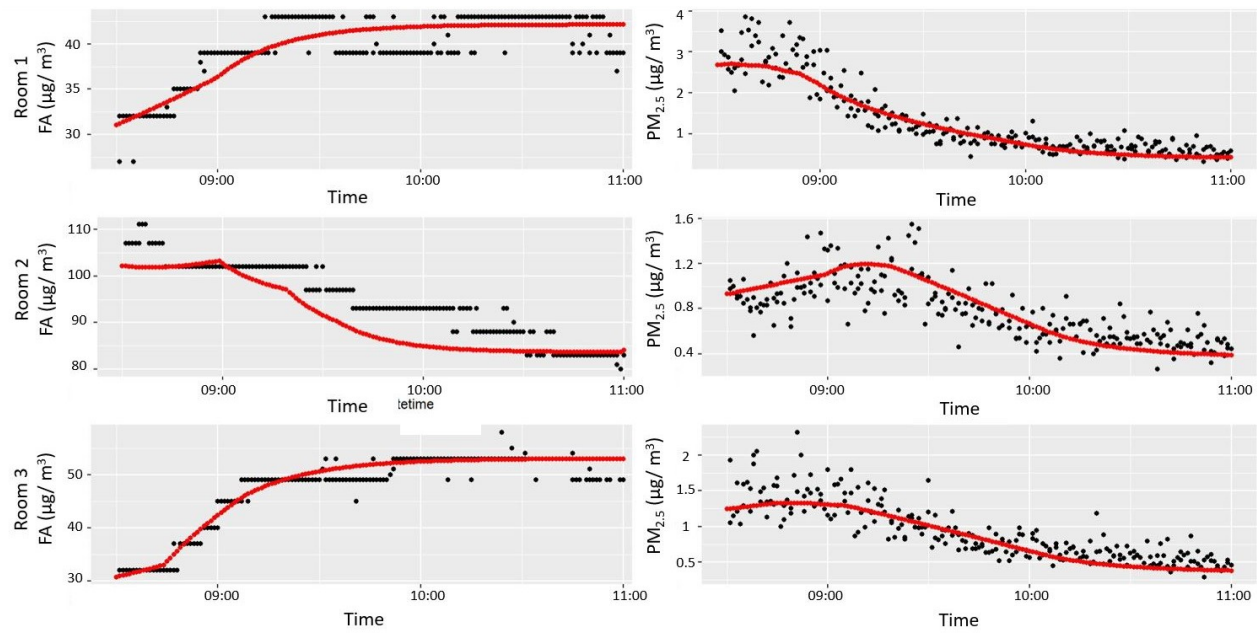
Figure 4.4: Measured vs. simulated development of CO₂ concentration and supply AFRs for room 1, 2, and 3.

Figure 4.5 shows the concentrations of FA and $PM_{2.5}$. During the experiment, both pollutants were mainly brought inside the rooms from the outside. Thus, outdoor sources have also been the main contributor to the increase of FA and $PM_{2.5}$ in the simulations. Due to the large variations in FA concentration between the rooms, larger constant indoor sources have been added to room 2 and 3 to scale the concentration up to the measured level.

Through all the experiments performed, there were always measured significantly higher FA concentrations in room 2 compared to room 1 and 3, hinting at sensor variations. Thus, a simple test was performed comparing the three formaldehyde sensors placed in the rooms during the experiments. A description and the results from the test are included in Appendix D. The results revealed that the FA sensor in the ID123465 sensor box, normally located in room 2, measures higher concentrations than the ID360360 and ID987654 FA sensors when being placed in the same location. As it can not be known which of the sensors measures most correctly without comparing with a reliable instrument, which is not available, the measurements will be used as they are. However, these differences between the sensors may be kept in mind.



(a) Polluted OA.



(b) Clean OA.

Figure 4.5: Measured vs. simulated development of FA and $PM_{2.5}$ concentration for room 1, 2, and 3.

Figure 4.6 shows the temperatures in the three rooms during the experiment along with the simulated ones. Due to the high OA temperature, the temperatures are high throughout the experiment. The outdoor temperatures in the weather files used for these validations are set similar to those measured in the laboratory where the facility is located. Additionally, internal gains from the 100 W light bulb in the manikins, contribute to the temperature rise. Relatively similar temperatures were observed in the three rooms during both experiments. There seems to be a great fit when internal gains are adjusted.

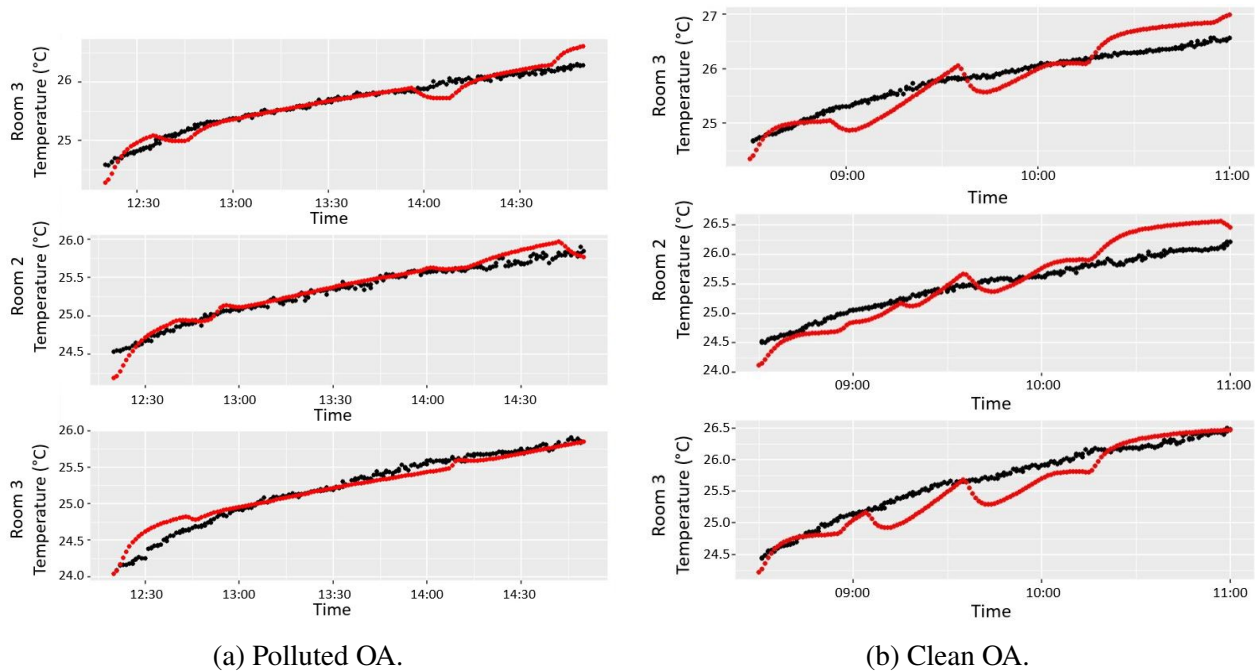


Figure 4.6: Measured vs. simulated development of temperature for room 1, 2, and 3.

To quantify the accuracy of fit between the measured and simulated values, (3.5) and (3.6) are used to calculate the MBE and CVRMSE, respectively. Table 4.4 shows the calculated values for MBE and CVRMSE for all parameters in the various rooms. These numbers indicate the fitted model's accuracy with the measurements. All values are within acceptable limits, as all MBE values are below $\pm 10\%$ and the RMSE values below 30 %. The building model is thereby sufficiently validated and can be used for further simulations.

Table 4.4: Calculated MBE and RMSE.

(a) Polluted OA.				(b) Clean OA.			
		MBE [%]	RMSE [%]			MBE [%]	RMSE [%]
CO ₂	R1	-0.196	2.278	CO ₂	R1	1.885	3.117
	R2	-4.013	6.157		R2	1.312	3.369
	R3	-1.526	2.484		R3	1.522	2.340
AFR	R1	-0.922	3.497	AFR	R1	0.972	9.223
	R2	0.338	4.330		R2	1.508	7.713
	R3	3.098	8.177		R3	2.333	7.774
FA	R1	-1.325	4.129	FA	R1	0.455	5.091
	R2	-3.640	4.905		R2	-4.038	5.444
	R3	-1.029	4.208		R3	0.967	3.772
PM _{2.5}	R1	-2.354	8.658	PM _{2.5}	R1	-6.896	24.382
	R2	4.460	9.208		R2	0.031	21.781
	R3	7.369	11.126		R3	-9.139	24.810
Temp	R1	0.118	0.297	Temp	R1	0.023	1.059
	R2	0.277	0.465		R2	0.291	1.059
	R3	0.076	0.512		R3	-0.502	0.849

4.4 Simulations

In the following, the results from co-simulations between CONTAM and EnergyPlus are presented. As the optimal CS is highly affected by the climate, it is considered advantageous to simulate various climates, adding more complexity to the analysis. Thus, a large more polluted city such as Beijing is compared with a less polluted, colder, and less humid city, which is Trondheim. However, many of the results are relatively similar for both cities and it is therefore not considered necessary to include all results. The results for simulations using weather- and pollution files for Beijing are all presented. Additionally, where it is considered helpful in obtaining a more complex analysis,

results from simulations of Trondheim are included for comparison. However, all figures from the Trondheim results are included in Appendix C

4.4.1 No Recirculation Control

Figure 4.7 shows the resulting CO₂ concentrations in all three rooms over a year for all CSs without recirculation. All CSs reveal sufficient CO₂ concentrations throughout the year for this specific case. Thus, concerning the indoor CO₂ concentrations, there seems to be no need to include other parameters in the control. Some variations associated with the various strategies can still be observed. Especially, CO2PM, CO2TempPM, and CO2TempPMFA result in both low average concentrations, and somewhat lower peaks than the others.

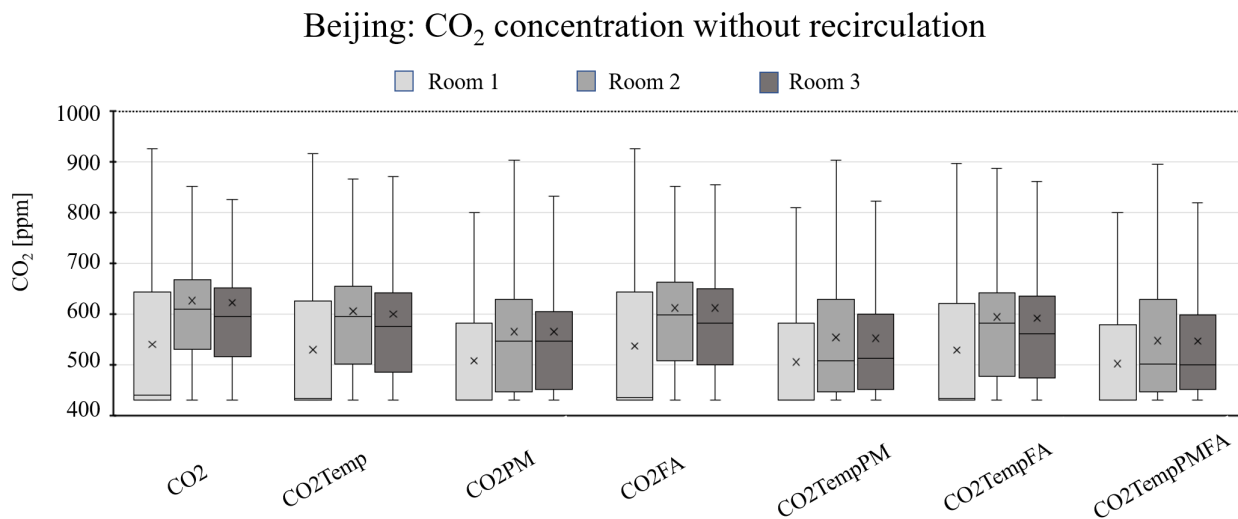


Figure 4.7: CO₂ concentration over a year for room CSs without recirculation.

In Figure 4.8 the PM_{2.5} results for all simulations without recirculation of air are depicted. All CSs result in high peaks up to over 18 $\mu\text{g}/\text{m}^3$ in one or more rooms. The short-time threshold of 15 $\mu\text{g}/\text{m}^3$ is exceeded in room 1 for all CSs. Additionally, all three CSs where PM_{2.5} is included as a control parameter, exceed the threshold in all three rooms. This indicated that PM_{2.5} is not suitable

for control of supply airflows to rooms and buildings. This is expected as $PM_{2.5}$ is normally found in higher concentrations in OA compared to indoor air. Thus, when the threshold for control of airflows to the rooms is exceeded, more OA is supplied to the rooms, which again may contain a high amount of $PM_{2.5}$, resulting in increased levels. In addition to the high peaks, all the associated CSs exceed the yearly average of $5 \mu g/m^3$ in one or more rooms. Thus, Figure 4.8 illustrates the need for recirculation in highly polluted areas, such as big cities, to limit the number of particles inside.

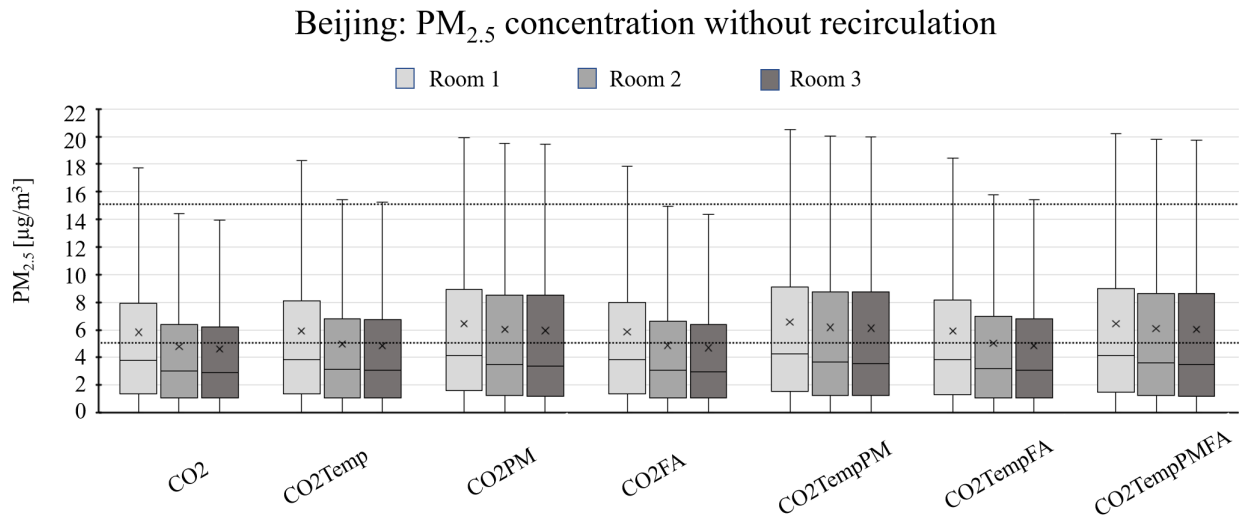


Figure 4.8: $PM_{2.5}$ concentration over a year for room CSs without recirculation.

Illustrated in Figure 4.9 are the FA concentrations for all the CSs simulated without recirculation. The CO2, CO2Temp, and CO2PM CSs exceed the FA concentration limit of $100 \mu g/m^3$ in at least one room. All the other strategies are below $100 \mu g/m^3$ in all rooms at all times. This amplifies the hypothesis of combining CO_2 with other parameters for the control of DCV systems to get a better IAQ. These specific results suggest that FA may be a favorable parameter for airflow control, as all CSs with FA included as control parameter results in sufficient FA concentrations. However, the generally high FA concentrations are reflected by the fact that the building model is based on the test facility which is located inside the laboratory at NTNU. The results may therefore reveal higher

concentrations of FA than what is normally the case. However, they give an insight into what CS is best suited for buildings with high FA generation, such as newer buildings. Additionally, the results can be extended to pollutants of similar generation patterns.

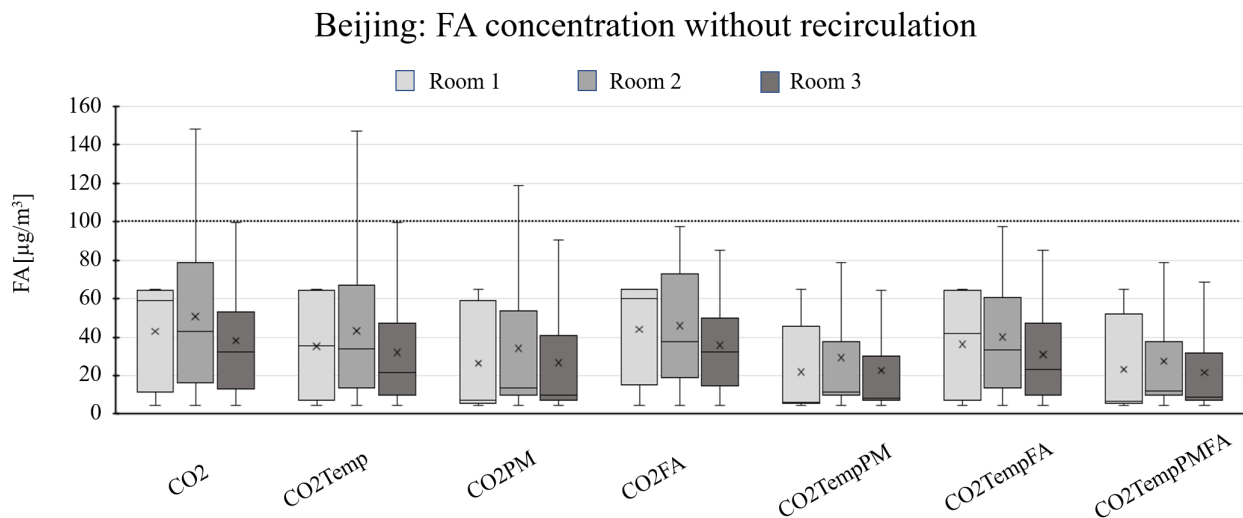


Figure 4.9: FA concentration over a year for room CSs without recirculation.

Figure 4.10 shows the temperatures for all CSs without recirculation. The average values are sufficient for all CSs, while both the upper and lower temperature thresholds are exceeded for all cases. The high infiltration rates make keeping the temperature within the limits difficult. However as this is due to the construction of the test facility, which does not replicate a real office building, the results may have been better in a real building. Nonetheless, the results can give indications on whether the temperatures rise or decrease, have large variations, or not according to each CS. Especially, using both CO_2 and $\text{PM}_{2.5}$ as control parameters reveal both higher peaks and lower minimum temperatures than the rest, again suggesting $\text{PM}_{2.5}$ not to be suitable for room control.

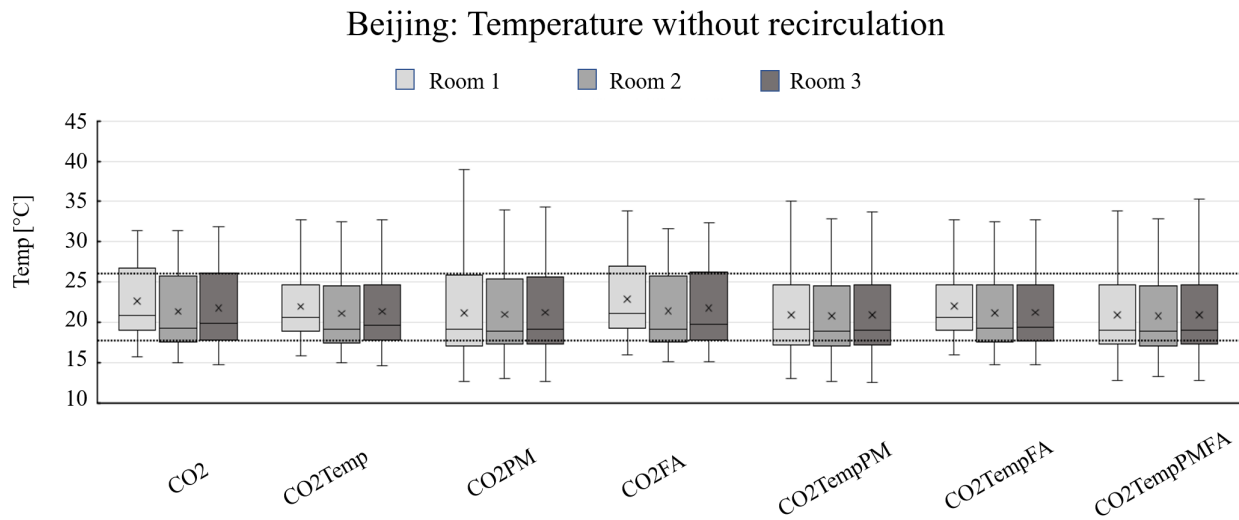


Figure 4.10: Temperature over a year for room CSs without recirculation.

4.4.2 Recirculation Control: $PM_{2.5}$

Figure 4.8 demonstrated that there may be necessary to use recirculation of air to improve the IAQ by reducing the indoor $PM_{2.5}$ concentration. In the following, several CSs for recirculation are presented. As $PM_{2.5}$ is a pollutant mainly supplied from the outside, it may be interesting to see what impact using $PM_{2.5}$ as a control parameter for recirculation has. Thus, this chapter focuses on $PM_{2.5}$ as a control parameter for recirculation.

Not surprisingly, $PM_{2.5}$ for recirculation control results in some large peaks in CO_2 levels, especially in room 1, where the threshold of 1000 ppm is exceeded for every airflow CS. This is illustrated in Figure 4.11. However, the average values are still maintained at decent levels between 600 and 700 ppm. The CSs with FA included as a control parameter for airflow control, are showing better results than the rest, again suggesting FA to be a suitable control parameter for airflow control. The dual airflow control with CO_2 and FA as control parameters continues to show great results for handling indoor CO_2 concentrations.

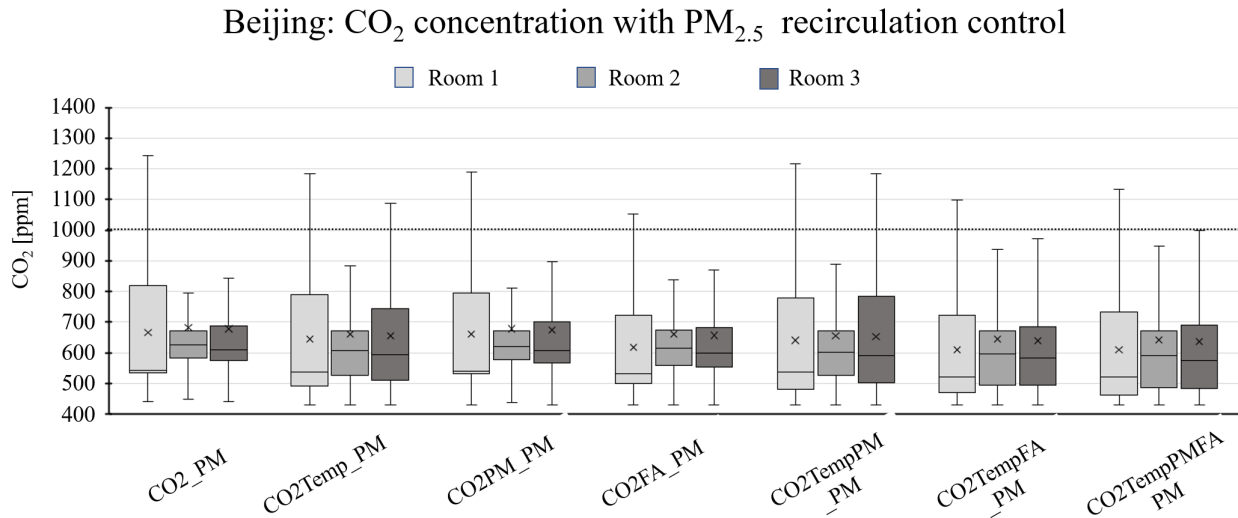


Figure 4.11: CO₂ concentration over a year for room CSs with PM_{2.5} as a control parameter for recirculation.

PM_{2.5} as a control parameter for recirculation shows great results on the indoor PM_{2.5} concentration. As shown in Figure 4.12, the yearly average concentration is well below $5 \mu\text{g}/\text{m}^3$ for all strategies, and the peaks are also kept at low levels. There are not much difference in PM_{2.5} concentrations between the various CSs. As expected this recirculation strategy reduces the indoor levels of outdoor generated pollutants considerably.

Recirculation of air also affects the FA concentrations. Figure 4.13 reveals increased concentrations compared to the results of no recirculation. However, the room CSs where FA is included as a control parameter show considerably better results than the rest. The peaks go just above $100 \mu\text{g}/\text{m}^3$, and this happens during non-occupied hours. Thus, the three CSs where FA is included as a control parameter show sufficient control of indoor FA concentrations. This result supports that if recirculation is to be used, FA should be included in the control of airflow into the rooms.

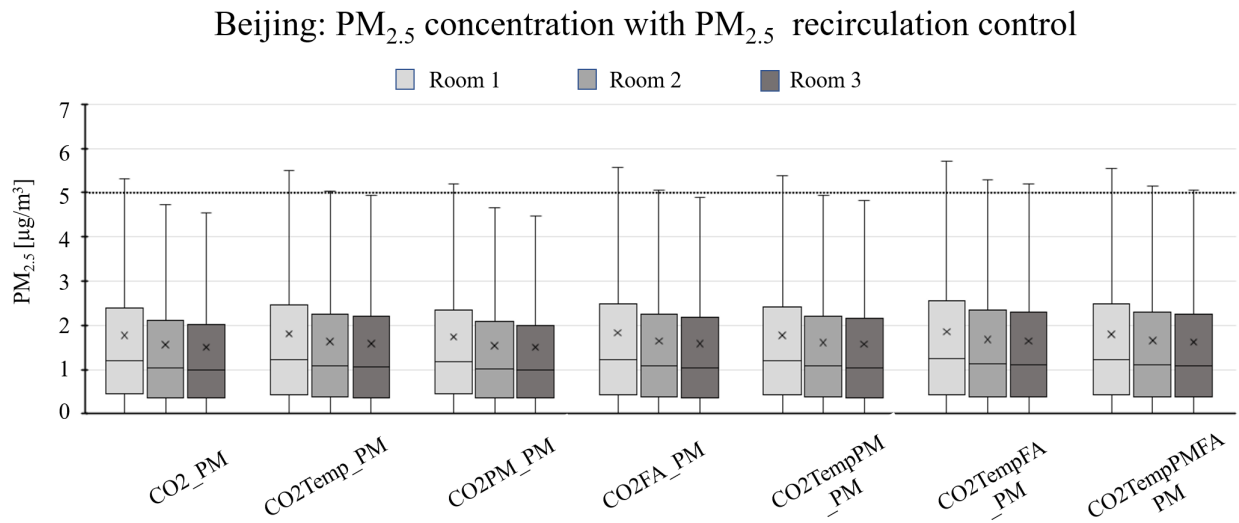


Figure 4.12: PM_{2.5} concentration over a year for room CSs with PM_{2.5} as a control parameter for recirculation.

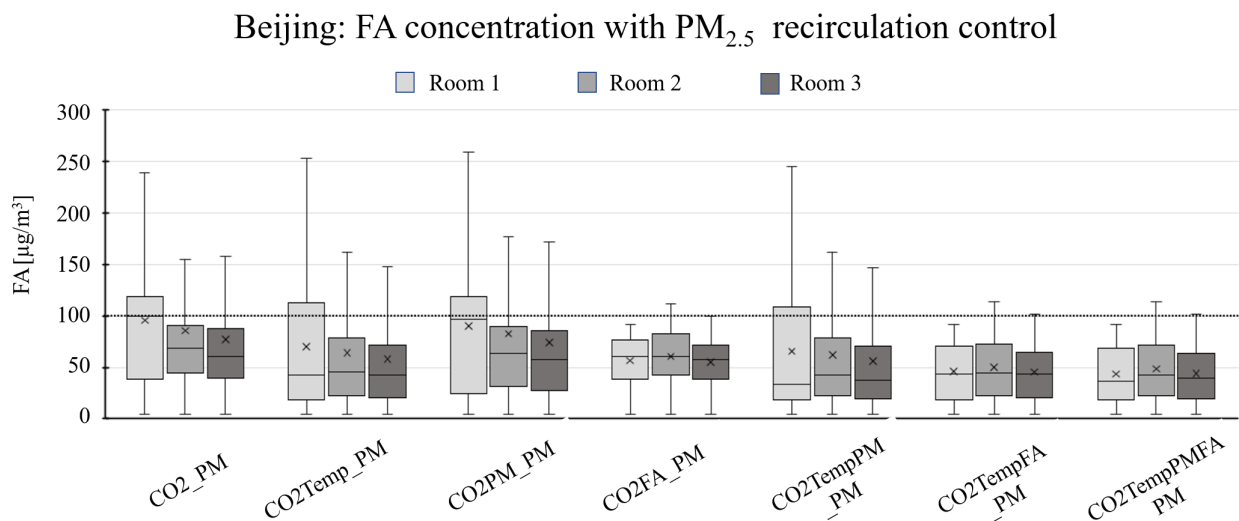


Figure 4.13: FA concentration over a year for room CSs with PM_{2.5} as a control parameter for recirculation.

With recirculation being implemented to the CSs, the lowest temperatures that were observed when having no recirculation are avoided, and the average temperatures are somewhat elevated. There does not seem to be any significant differences between any of the control strategies when $PM_{2.5}$ is used for control for recirculation, as observed in Figure 4.14. During these simulations, the recirculation mode is on most of the time.

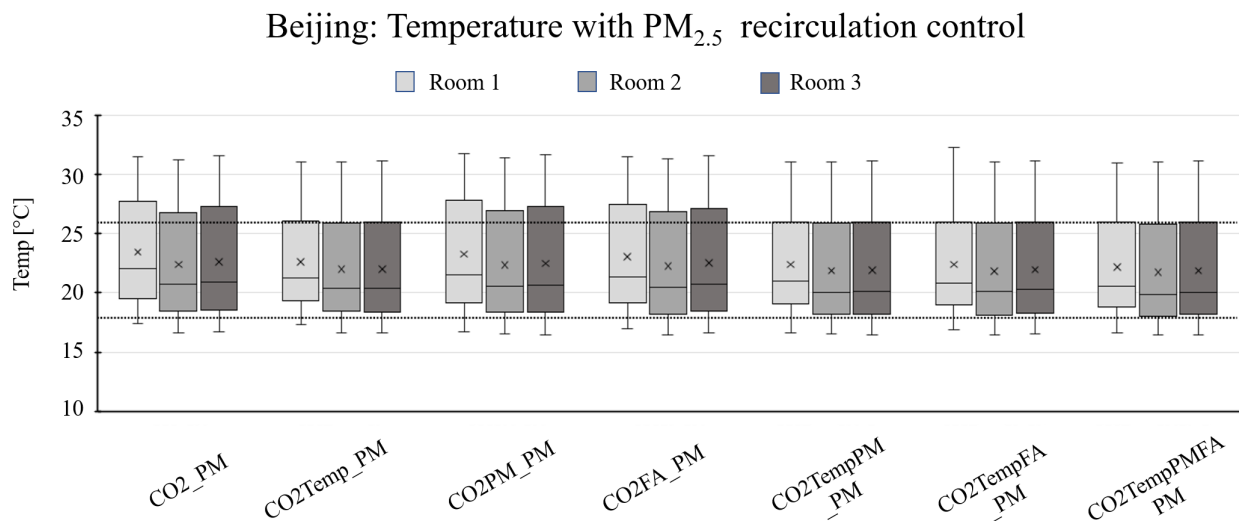


Figure 4.14: Temperature over a year for room CSs with $PM_{2.5}$ as a control parameter for recirculation.

4.4.3 Recirculation Control: CO_2/CO_2 and $PM_{2.5}$

Despite the $PM_{2.5}$ recirculation control assuring low levels of indoor particles, the indoor generated pollutants showed elevated concentrations. To assure sufficient levels of CO_2 and FA, other control parameters for recirculation are also tested.

When several parameters are used for control there may occur contradicting logic or one parameter may be the controlling factor, leaving the other or others as excess. This can happen specific to a case, and may not necessarily mean that it will happen for another building or system or in

another climate. The results from the simulations with CO_2 and $\text{PM}_{2.5}$ as control parameters for recirculation showed a case where $\text{PM}_{2.5}$ as control parameter appeared to be redundant. This is due to the CO_2 threshold limits being exceeded before the ones for $\text{PM}_{2.5}$. Therefore the simulations with recirculation control with CO_2 and $\text{PM}_{2.5}$ as control parameters give the exact same results as the ones with only CO_2 as a control parameter for recirculation. Thus, the results are presented in the same figures in the following.

CO_2 concentrations are elevated when using recirculation of air. This becomes evident when comparing the results with recirculation in Figure 4.15 with those without recirculation in Figure 4.7. Using CO_2 as control parameter for recirculation, either in combination with $\text{PM}_{2.5}$ or not, results in the limit of 1000 ppm being exceeded in two or more rooms for all CSs. The average is kept relatively similar for all CSs at acceptable levels. The airflow control with CO_2 and FA still shows somewhat better results than the rest, but in this case with small margins.

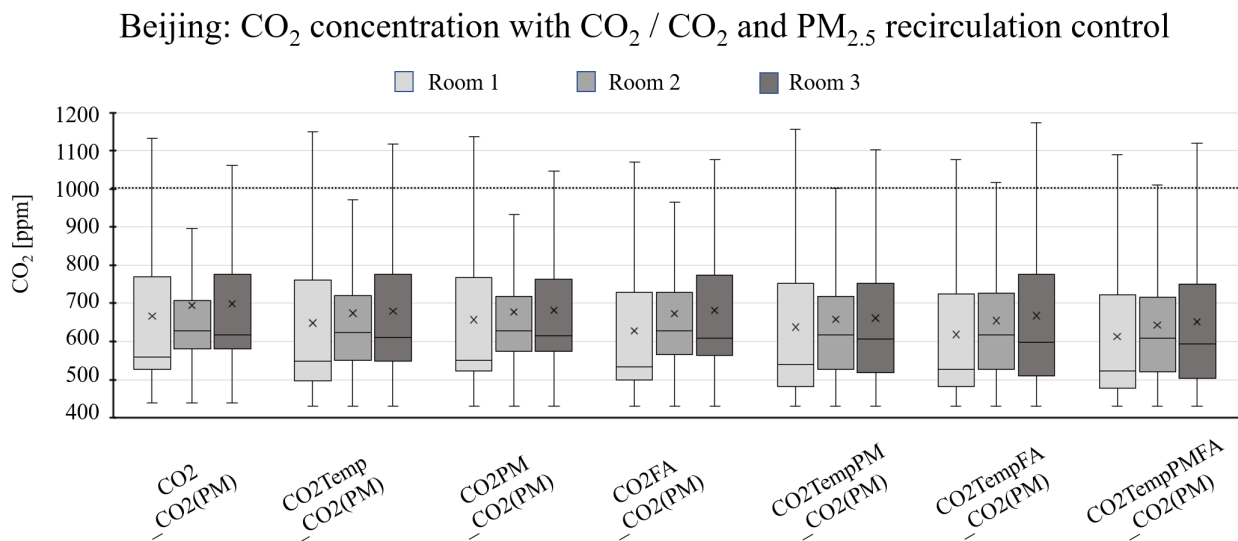


Figure 4.15: CO_2 concentration over a year for room CSs with CO_2 or CO_2 and $\text{PM}_{2.5}$ as control parameters for recirculation.

Despite the recirculation control with CO_2 as control parameter resulting in high CO_2 concentrations, Figure 4.16 reveals promising results for the $\text{PM}_{2.5}$ concentration. The $\text{PM}_{2.5}$ concentration is maintained at sufficient levels when CO_2 and $\text{PM}_{2.5}$, or just CO_2 , is used for recirculation control, as seen in Figure 4.16. While the peaks for some of the strategies are noticeably higher than during the $\text{PM}_{2.5}$ recirculation control, they do not reach the limit of $15 \mu\text{g}/\text{m}^3$. However, it is evident that the CSs with $\text{PM}_{2.5}$ included in the airflow control results in a little bit lower $\text{PM}_{2.5}$ concentration peaks. The annual average is below the threshold of $5 \mu\text{g}/\text{m}^3$ for all strategies.

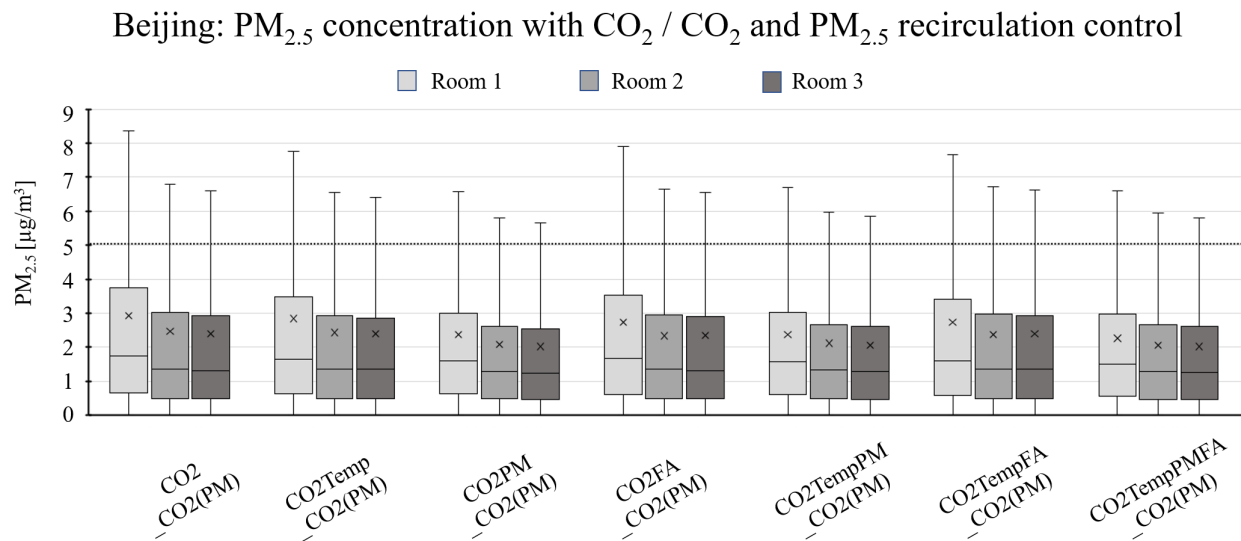


Figure 4.16: $\text{PM}_{2.5}$ concentration over a year for room CSs with CO_2 or CO_2 and $\text{PM}_{2.5}$ as control parameters for recirculation.

Figure 4.17 reveals that the FA concentrations show a similar pattern, but with somewhat lower peaks, as when using $PM_{2.5}$ for recirculation control. The levels are elevated compared to when there is no recirculation, but the strategies with FA included in the airflow control still perform relatively well. While the limit of $100 \mu\text{g}/\text{m}^3$ is exceeded in room 2 in all cases, it has been proven that the sensor in room 2 measures higher concentrations than the two others, causing the high concentrations in room 2 during the simulations

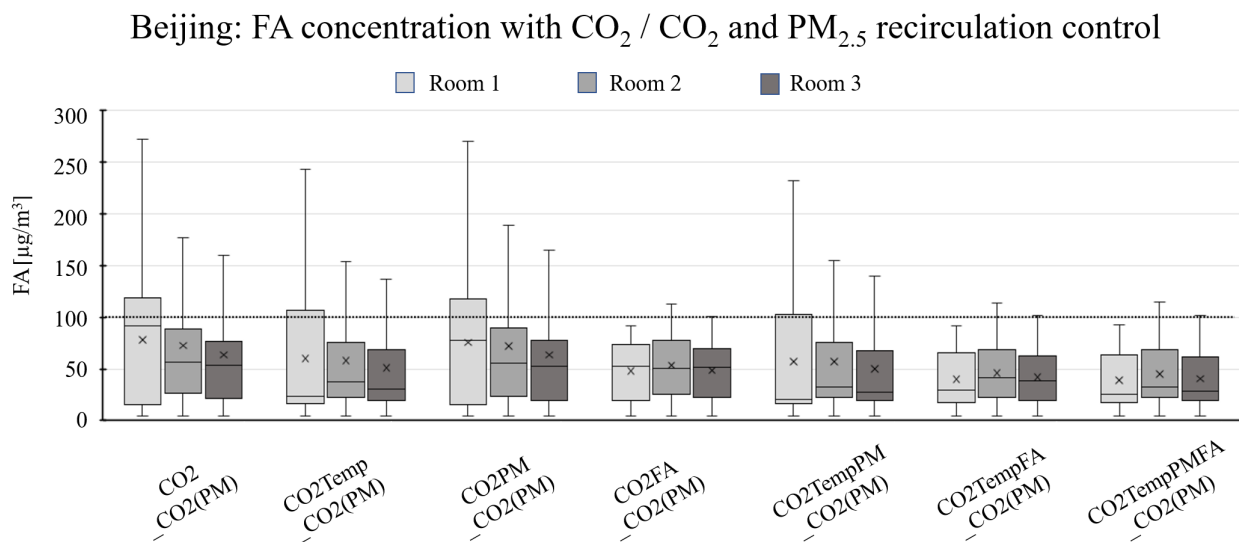


Figure 4.17: FA concentration over a year for room CSs with CO_2 or CO_2 and $PM_{2.5}$ as control parameters for recirculation.

Temperatures are kept at similar levels for all CSs with CO_2 as a recirculation control parameter, as seen from Figure 4.18. The recirculation lifts the average temperatures in all cases. While this may not necessarily be better in this specific case, as the average temperatures were already good without recirculation, it illustrates how recirculation can contribute to energy savings related to heating in other cases.

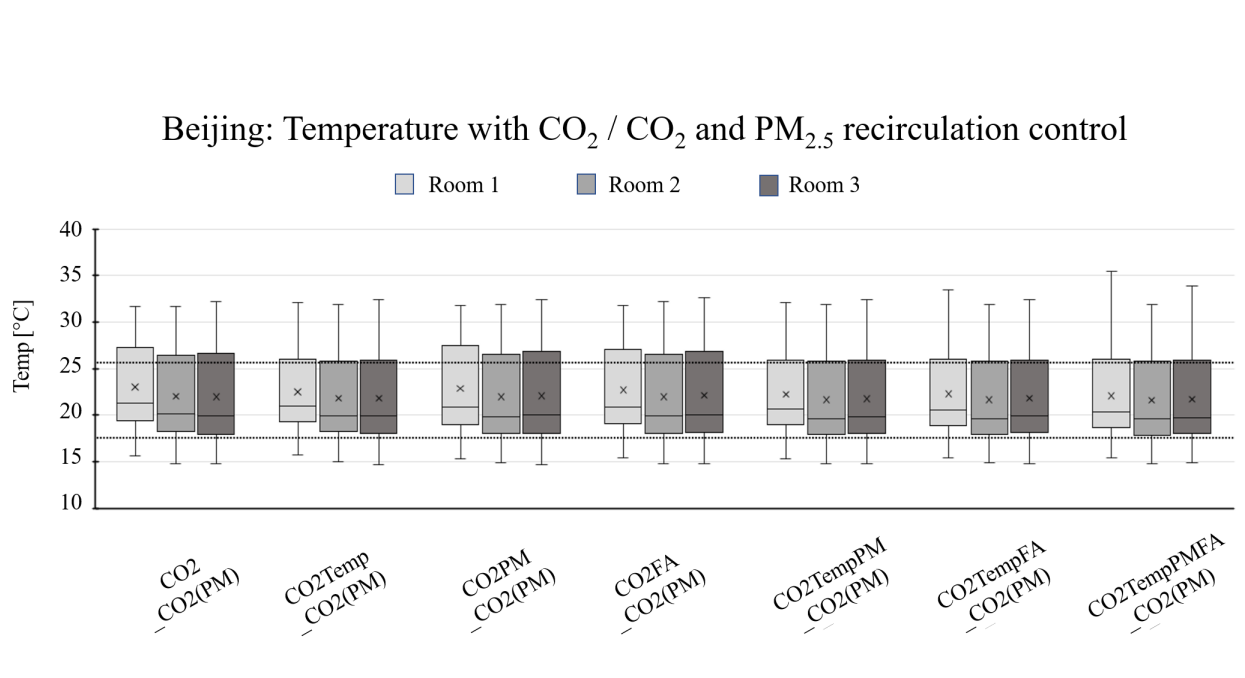


Figure 4.18: Temperature over a year for room CSs with CO₂ or CO₂ and PM_{2.5} as control parameters for recirculation.

4.4.4 Recirculation Control: CO₂ and FA

It has been confirmed that FA may be a convenient parameter for control of supply airflow. However, it may be interesting to investigate the use of FA for recirculation control. It is used together with CO₂ to account for occupancy as well.

Figure 4.19 shows generally better results on CO₂ concentrations than the other scenarios with the use of recirculation. The threshold is exceeded in some cases, but only a little above 1000 ppm. Thus, by doing small adjustments to the ventilation logic, by for example having a little bit higher ventilation rates, the concentrations may stay below the threshold of 1000 ppm. This is also the case for all previously mentioned results, as the CSs are not optimized. The control parameter limits are based on recommended threshold values and the AFRs are based on minimum requirements from TEK17. Therefore when a CS results in some of the parameters exceeding their limits, this may be improved by optimizing the control limits, AFRs, and OA percentage during recirculation. This has not been focused on in this thesis.

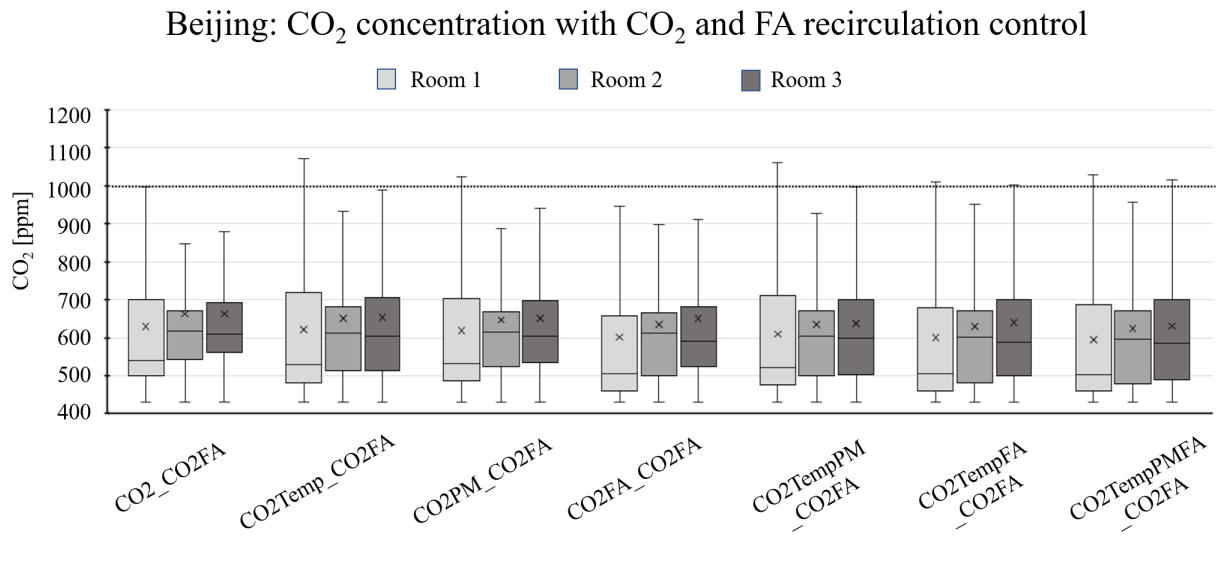


Figure 4.19: CO₂ concentration over a year for room CSs with CO₂ and FA as control parameters for recirculation.

Dual CO₂ and FA recirculation also handle PM_{2.5} well, similar to all the other strategies with recirculation. The highest peak is just below 12 $\mu\text{g}/\text{m}^3$ and the average in all cases is below 5 $\mu\text{g}/\text{m}^3$. The results are depicted in Figure 4.20.

With regard to the FA concentrations, the pattern when using dual CO₂ and FA recirculation control is the same as for the other recirculation control strategies: Recirculation of return air is not beneficial to indoor FA concentrations and may result in health risks, though with the exception of when FA is included in the airflow control. This is illustrated in Figure 4.21.

There is not much difference in the temperature for any of the CSs when using CO₂ and FA recirculation control. Large variations in temperature for all CSs result in both the upper and lower limits being compromised. The results are depicted in Figure 4.22.

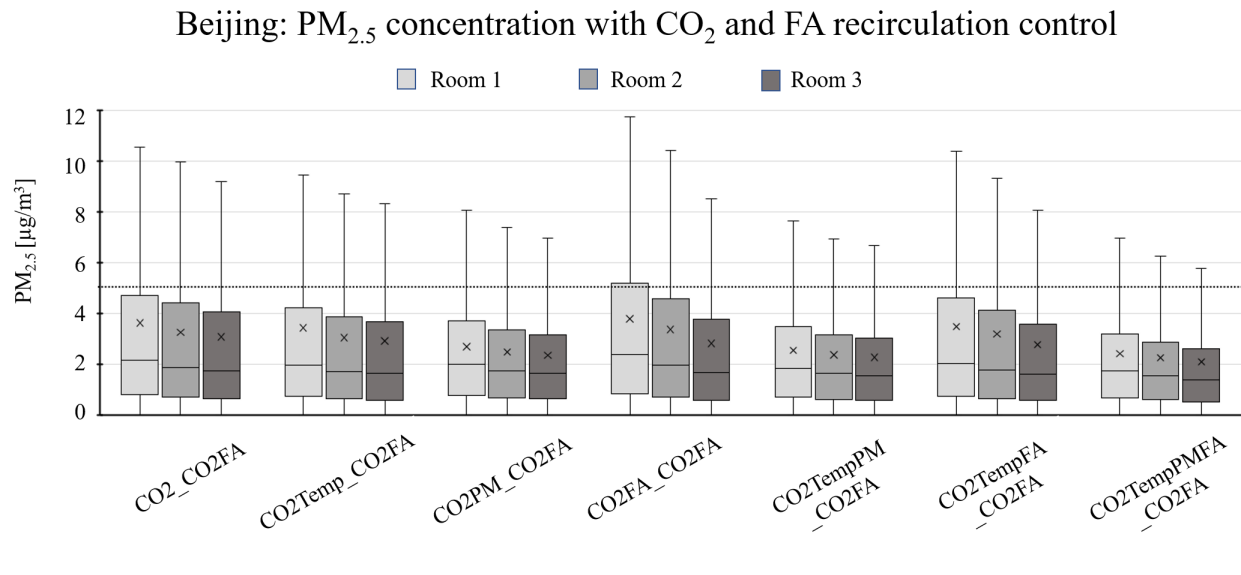


Figure 4.20: PM_{2.5} concentration over a year for room CSs with CO₂ and FA as control parameters for recirculation.

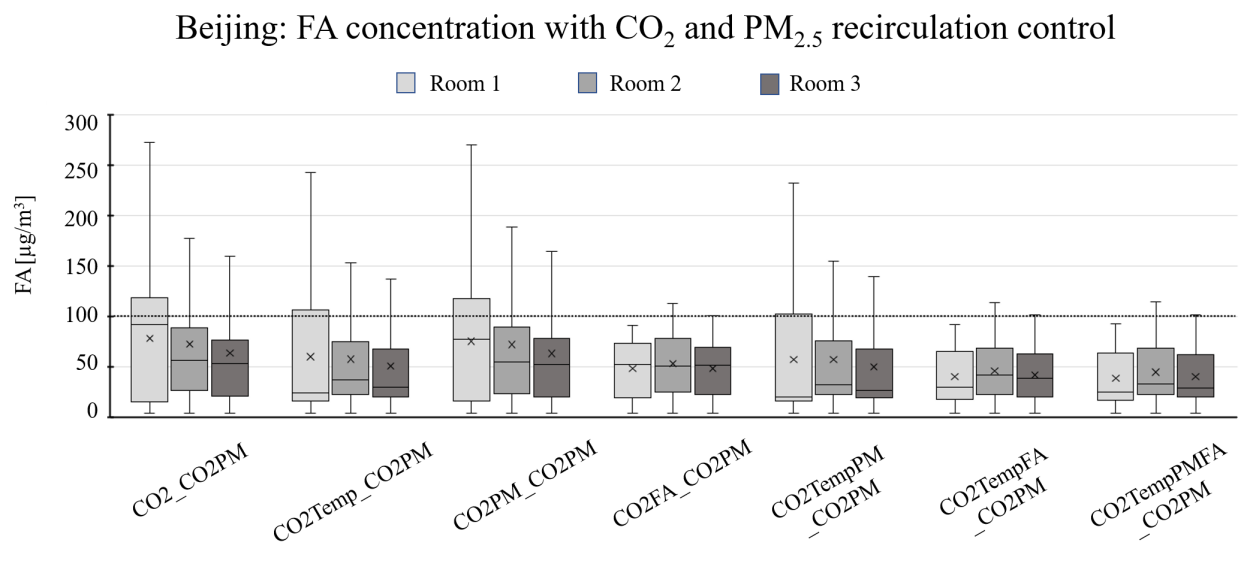


Figure 4.21: FA concentration over a year for room CSs with CO₂ and FA as control parameters for recirculation.

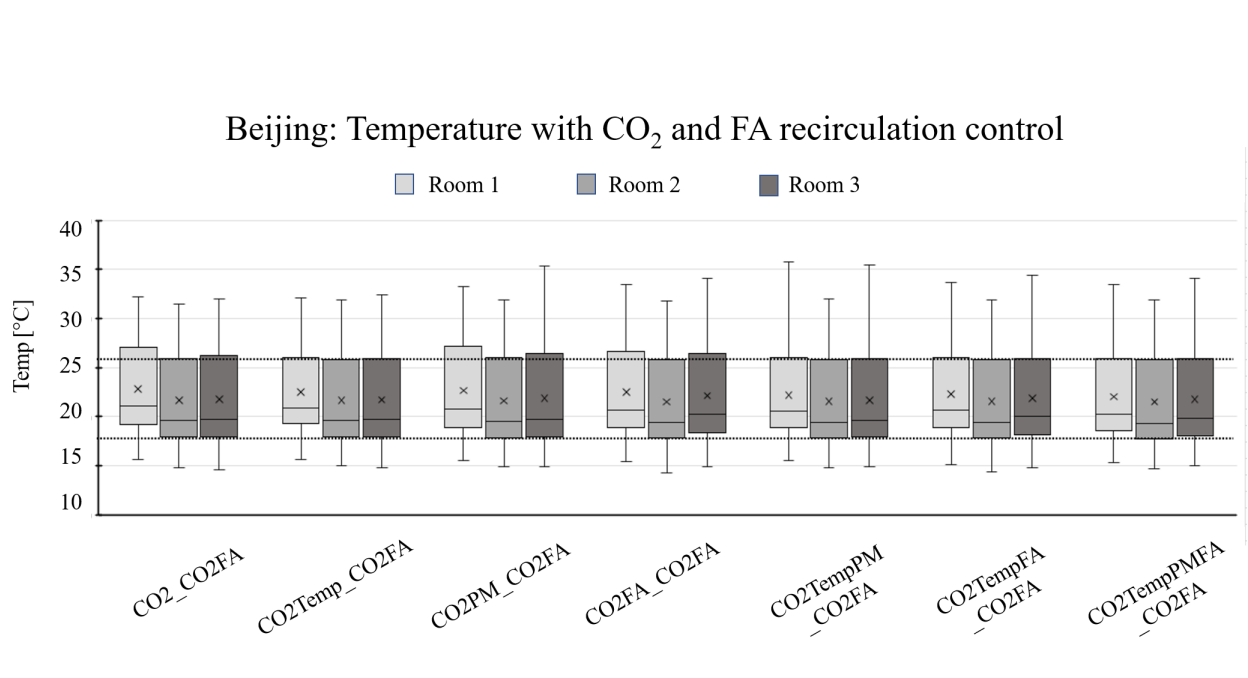


Figure 4.22: Temperature over a year for room CSs with CO₂ and FA as control parameters for recirculation.

4.4.5 Trondheim Simulations

The simulations using Trondheim weather gave similar results as those using Beijing weather concerning the various CSs effect on FA and CO₂ concentrations. Therefore, all results related to Trondheim are placed in Appendix C. However, the temperature results illustrated the effect of recirculation better than the temperature results from Beijing due to the higher outdoor temperatures in Beijing. Also, the results showing PM_{2.5} concentrations are different depending on location and reflect that the outdoor concentrations are much lower in Trondheim than in Beijing.

Trondheim Temperature

Figure 4.23 illustrates the results when recirculation is not implemented in the DCV system. Thus, low temperatures below 19 degrees are observed. Beijing simulations showed that the lowest temperatures were avoided by introducing recirculation or return air, however, it had little effect on the upper temperatures. Figure 4.24 shows the Trondheim temperatures when dual recirculation

control with CO₂ and PM_{2.5} or just CO₂ recirculation control is introduced. The temperatures are elevated and within both limits. More comfortable average temperatures are also achieved, and the maximum temperatures do not exceed the threshold of 26 degrees, such as in the Beijing simulations.

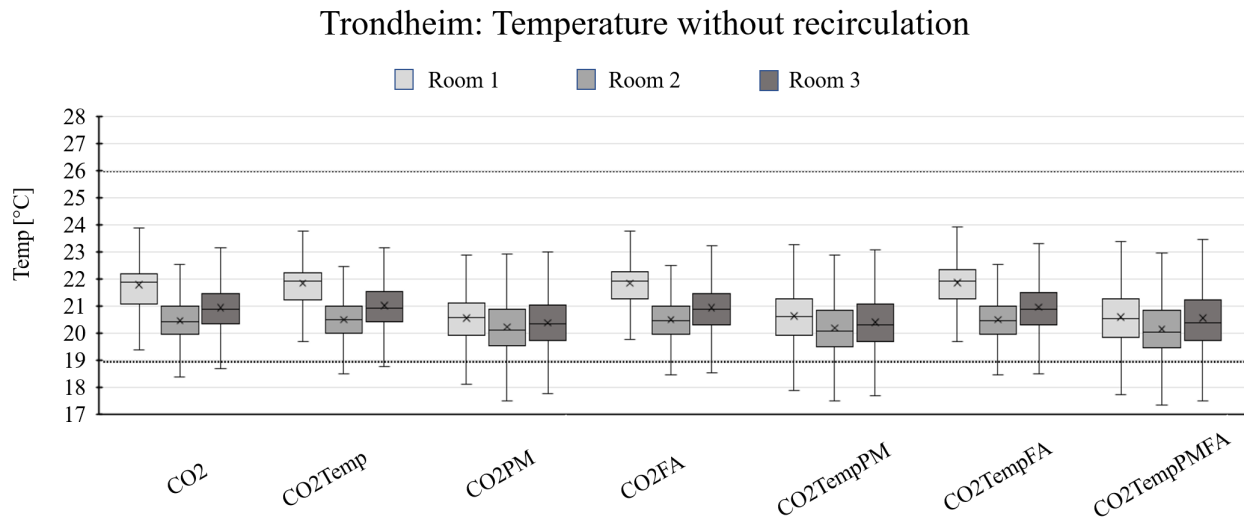


Figure 4.23: Temperature over a year for room control strategies without recirculation.

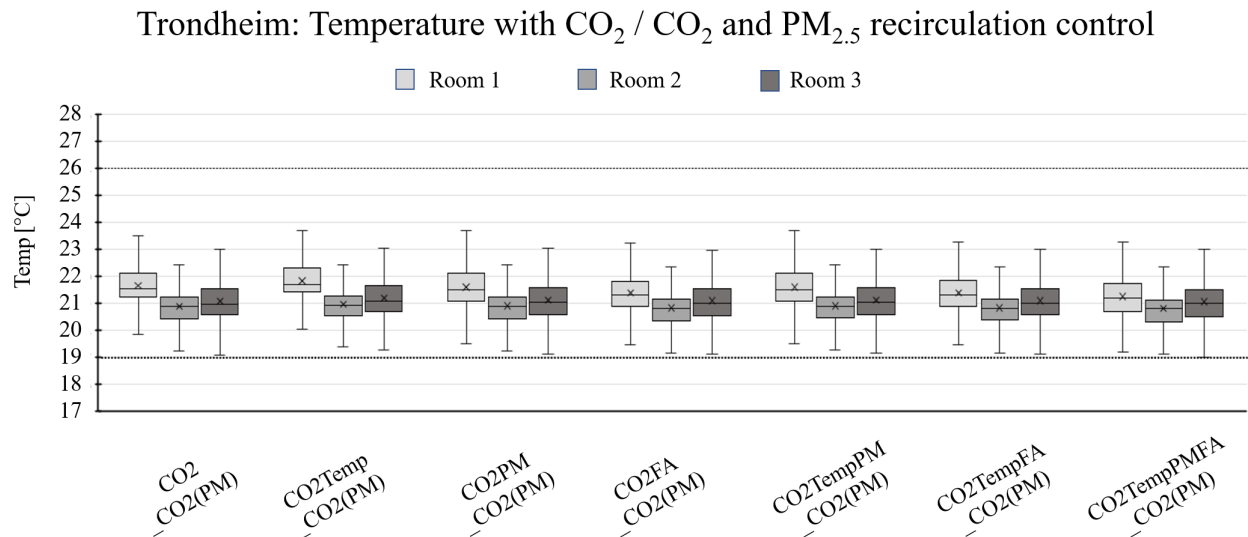


Figure 4.24: Temperature over a year for room control strategies with CO₂ and PM_{2.5} as control parameters for recirculation.

Trondheim PM_{2.5}

Trondheim has great OA concerning air quality, and the low pollution level reflects on the results regarding PM_{2.5} concentrations. Figure 4.25 shows that indoor PM_{2.5} levels are maintained at low levels even without recirculation. The annual average is below the limit for all CSs and the highest peaks are just almost approaching the short-time limit of 15 $\mu\text{g}/\text{m}^3$. Thus, recirculation is not necessary in this case, and the results of those simulations are not discussed further. They are however included in Appendix C.

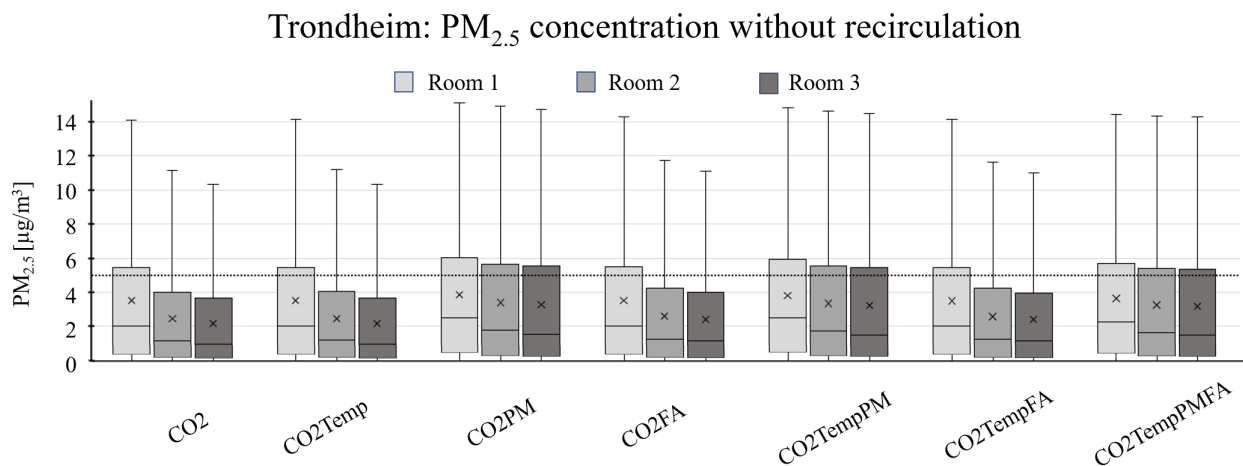


Figure 4.25: PM_{2.5} concentration over a year for room control strategies without recirculation.

4.4.6 Total Yearly Energy Consumption

Figure 4.26 gives insight into the energy use related to the various CSs for the simulations using Beijing weather and pollution files. On the y-axis, the room control methods are listed, and the various colors represent the different recirculation CSs. A similar graph for Trondheim is depicted in Appendix C, and shows a similar pattern as observed in Figure 4.26.

It is evident that the pattern of energy use is highly dependent on the type of recirculation control, where no recirculation results in higher energy consumption. Especially for the three airflow control strategies including PM_{2.5} as a control parameter, the energy consumption becomes very high when there is no recirculation. This makes sense as PM_{2.5} is generally brought inside through the OA. Thus, when the indoor concentration rises, and PM_{2.5} is used as a control parameter for airflow control, there is a constant need for increased supply airflow, which again only leads to higher indoor concentration. Hence, this combination does not work, neither for sufficient IAQ or energy consumption.

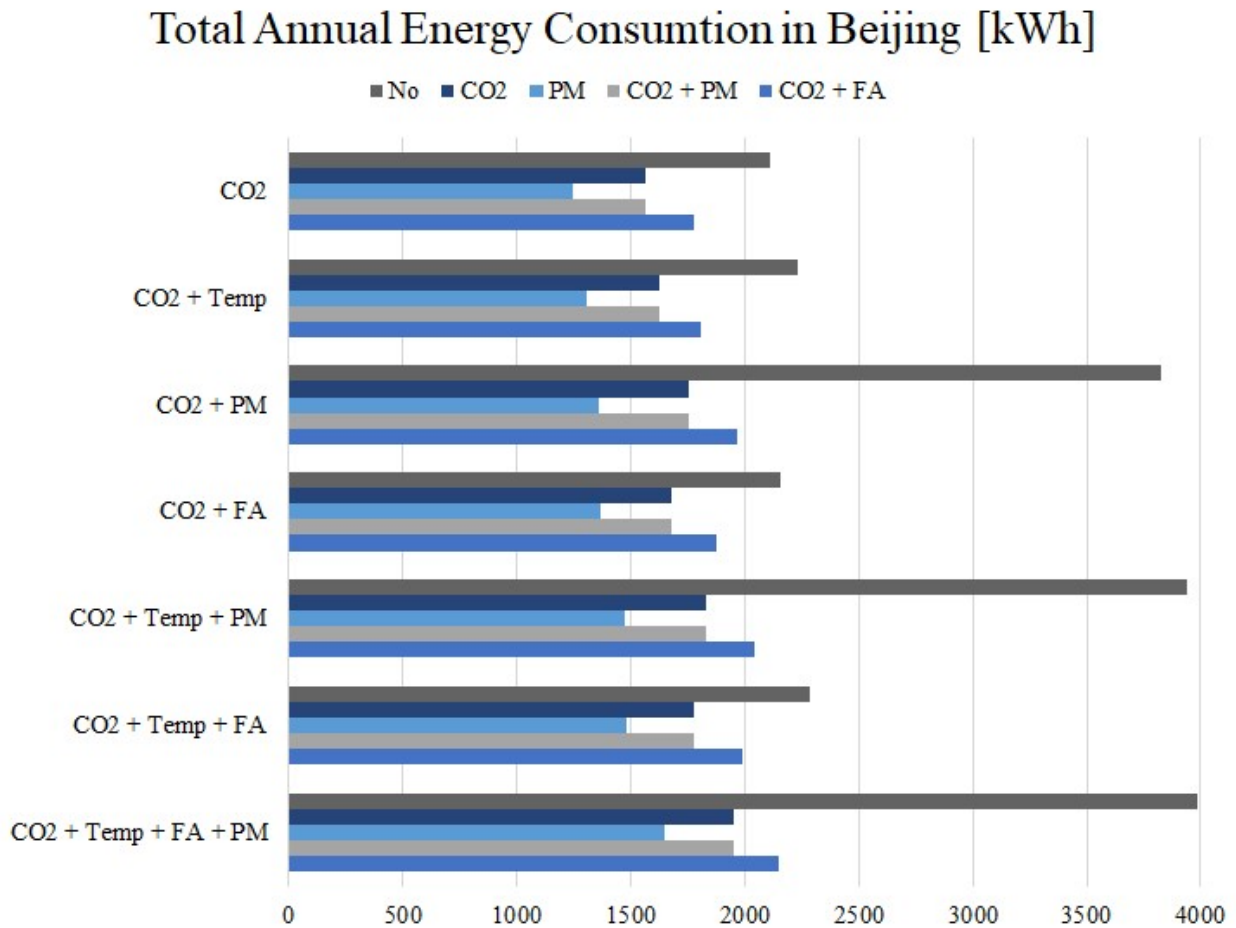


Figure 4.26: Total yearly energy consumption for simulations using Beijing weather and outdoor pollution levels.

On the other side of the scale, $PM_{2.5}$ for recirculation control results in the lowest yearly energy consumption. However, previous results showed high values for CO_2 and FA when using $PM_{2.5}$ as the only control parameter for recirculation control. It is also evident that the recirculation control strategies including both CO_2 and $PM_{2.5}$ give the same results as CO_2 as the only control parameter, revealing CO_2 to be the controlling factor over $PM_{2.5}$ for this specific case. Despite this being the case for this specific simulation model, this may be different for other cases.

It can also be observed that the energy consumption increases with additional control parameters to the CSs, however, these are not significant. Other than what is already mentioned, there are not any significant variations in energy consumption between the room airflow CSs.

Chapter 5

Discussion

Some of the most important findings have already been discussed throughout the analysis of the results. However, a general discussion based on the research questions is conducted in this chapter. The discussion takes basis in the findings from the results and relevant literature. Additionally, a summary of sources of errors related to the experiments and simulations is included.

5.1 Sources of Error

There are various factors affecting the procedures conducted in this thesis, resulting in deviating measurements and calculations. Thus, certain aspects of the findings may not be completely representative of a real setting. The sources of error concerning the leakage tests, CS experiments, and CS simulations are discussed in the following.

5.1.1 Leakage Tests

The leakage tests performed in the test facility revealed high infiltration rates. This is somewhat expected due to the construction of the facility which is very simple and does not replicate a typical office building. However, the leakage tests are subject to several errors which may have an impact on the calculated infiltration rates.

The mass balance equations used to calculate infiltration rates based on the tracer gas tests include three types of parameters: AFRs, CO₂ concentrations, and the CO₂ injection rate. All three elements are subject to limitations that may impact the calculations and resulting infiltration rates. First, the AFRs are measured by the inlet and outlet dampers in the ventilation system, which lacks accuracy. Also due to the inlet valves not being able to measure AFRs below 26 m³/h, there were generally high AFRs during the experiments, and it would have been beneficial with lower rates. The infiltration between rooms may not show up correctly because the ventilation rates in adjacent rooms to where CO₂ is supplied have high AFRs, which would be enough to remove small injections of CO₂.

The steady-state CO₂ concentrations are also used in the calculations. These are measured by the Sensirion SCD30 sensor which may also lack accuracy. The datasheet presents an accuracy of ± (30 ppm + 3%), however, due to the sensors not being re-calibrated recently a larger difference can be expected due to drift. The last parameter affecting the calculations of infiltration rates is the CO₂ injection rate. The rotameters used for adjusting the CO₂ supply contain a small disruption in the accuracy of ± 1.25 % (Platon, n.d.). Additionally, since they are adjusted by the author it may also be subject to human errors which may affect detailed reading of the injection rates. Also, since the CO₂ is first supplied to the manikins, which then will release into the room, the rate may be a little bit lower than intended as CO₂ may fall to the ground or build up inside the manikin. Thus, all three parameters in the mass balance equations are subject to errors, and the infiltration rates are therefore probably lacking accuracy as well.

Related to the pressurization tests, there were also several factors impacting the results. First,

the manometer has limited detailing and only gives pressure differences in whole pascals. This makes for possibly large errors in the calculation of infiltration rates, as small differences in input values may have a major impact on the results. Additionally, the AFRs measured by the inlet and outlet valves lack preciseness as well, which may also affect the calculations of infiltration rates. Additionally, the flow exponent, n , in the power law is assumed to be 0.67, which probably is not correct as it is just a value commonly used, and not specific to the test facility. Again, all elements including the formulas used to calculate the infiltration rates are subject to specific limitations which may impact the resulting values.

5.1.2 Control Strategy Experiments

Allocating the sources of errors regarding the experiments is pivotal in understanding why simulations are used instead of experiments to evaluate various CSs. As the simulation model is validated by data from experiments, some of the sources of errors related to the experiments may also affect the simulation results.

Maybe the most obvious aspect of the experiments which makes them deviate from a real office environment is that the test facility is located inside the HVAC laboratory at NTNU, and not outside like a real building. As already touched upon, this results in the supply temperature being much higher than what it would be realistically and does also affect the composition of the whole pool of pollutants. As the experiments were conducted during a time when the HVAC laboratory was being renovated, it was especially high levels of certain pollutants in the air, including FA and particles. This resulted in large variations in pollution levels in the supply air, depending on what type of renovation that was conducted each day. Also, it was generally lower pollution levels in the morning and late evenings than during the day when renovation tasks were performed.

The simple construction of the facade of the test facility is another aspect making the facility deviate from a typical office building. Most evident are the large infiltration rates, which in addition to being calculated, were observed during the experiments. Due to the use of a mosquito coil to generate

particles, the $PM_{2.5}$ generation was concentrated around the location of the mosquito coil. Thus, the concentration varied a lot in the air surrounding the test facility, being higher close to room 1 where the mosquito coil was located. The indoor $PM_{2.5}$ concentration was observed to increase earlier and more rapidly in room 1, compared to room 2 and 3.

The ventilation system was originally supposed to be a PC-DCV system. However, due to the too low pressure differences in the ductwork, due to wrong dimensioning of the system in the building stage of the facility, the pressure system was not able to regulate the DCV system satisfactorily. Thus, the DCV system is programmed manually, such that when the measured concentration of a control parameter exceeds a set limit, the inlet valves to the corresponding rooms are programmed to open to a certain percentage of the full opening. As the system was programmed to open the valves to specific percentages, the AFRs differed a little between each experiment, and between each room as well. Room 1, generally got higher AFRs than the other rooms due to being placed closest to the main inlet. It was made an effort to limit these differences when programming the control logic, but there were still noticeable differences during the experiments.

Another major error regarding the experiments is related to the set AFRs. TEK17 requires a minimum ventilation rate of $4.9 m^3/h$ for rooms of $7 m^2$ during unoccupied periods. Thus, ideally, the AFR should be close to $5 m^3/h$ in periods when the measured value(s) of the control parameter(s) is below the lowest limit. However, due to the Orion-LØV supply dampers not being able to measure AFRs lower than $26 m^3/h$, the lowest AFR during the experiments was set to $26-30 m^3/h$, instead of $5 m^3/h$. This results in building-generated pollutants not being able to build up at a similar rate as they would naturally in an office building during unoccupied hours. Additionally, indoor-generated pollutants reduce at a higher rate than they would with a lower ventilation rate when the occupancy reduces.

As already mentioned, the sensors may be subject to reduced accuracy. Especially the FA sensors, which have never been calibrated due to lack of reliable equipment, induce uncertainty. A test comparing the measurements of three of the FA sensors supports this statement as it indicates that the individual sensors measure different concentrations at the same location. This test is shortly

presented in Appendix D. While the other sensors are previously calibrated during the autumn of 2021, their accuracy is probably also reduced due to drift, which is a common problem for LCSs. While calibration equations are used to calibrate the data, there may still be deviations in the sensor readings.

While the pollution sources used during the experiment are chosen to obtain a somewhat controlled environment, they differ from the sources realistically found in an office environment. The pollution pattern is most likely not similar to real office spaces, and the relationship between when what parameter increases is therefore different. Most obvious is the difference in using a manikin instead of a real human being. First, the absence of movement influences the airflow and pollution flow inside the room. The heat generated from the manikins is also higher than from a normal human being, as a 100 W light bulb is used. According to ASHRAE Fundamentals Handbook the sensible heat given off by humans conducting moderately active office work is 75 W, and 70 W for very light work (*Heat Gain from People, Lights, and Appliances* n.d.). The heat production is also constant from the beginning of the experiment and does not begin at the time of arrival as it should. Unlike humans, manikins do not generate moisture. Humidifiers were tested for moisture production, but due to the droplets having a large impact on the particle sensors resulting in major PM_{2.5} measurements, they could not be used. Candles were also tested for moisture production. However, the combination of having little effect on the RH in the rooms, and producing more CO₂ and particles, they were not a good fit either.

The mosquito coil also resulted in a concentrated generation of PM_{2.5} resulting in uneven concentrations in the air surrounding the facility. In normal OA, the pollution is more evenly spread. The mosquito coil also resulted in very high PM_{2.5} concentrations, and it was difficult to maintain a constant concentration in the OA. Therefore, during the experiments, there are large peaks of PM_{2.5} concentrations, which differ between each experiment obstructing the controlled environment that was intended.

5.1.3 Co-Simulations

As the simulation model is based on the test facility and is validated with data from the experiments, some of the same sources of errors as discussed above are present in the simulation results as well. This mainly includes the aspects of the test facility which make it a lot different than a normal office building. However, as they are already mentioned, they will not be discussed any further. Other errors such as those related to sensor accuracy and AFRs are more accurately represented in the simulations.

During the experiments, the CO₂ is supplied with a delay. This means that the gas starts to increase in the room a couple of minutes after the CO₂ bottle is opened. Therefore, during the validation of the simulation model, the time is adjusted to fit measured and simulated values better. Thus, the values are fitted at what seems to be the best fit and are subject to human error.

The control logic used for each CS is based on recommended threshold values and minimum required AFRs. The results show that some pollutants still reach high levels and would probably benefit from optimizing the set limits in the control logic and the AFRs. This has not been prioritized in this thesis, due to the relatively large amount of CSs which would have made optimization very time-consuming. Additionally, as the research aims to compare and evaluate the various CSs, the used limits are considered satisfactory for this purpose. While some of the thresholds are exceeded by a lot, the various CSs can still easily be compared. However, to get the best evaluation of the most promising CSs they should be evaluated after being optimized.

The main capability of the simulations, making them suitable for evaluating various CSs is that all simulations are based on the same conditions. While they still may not be completely similar to a real case, it is great for comparison which is the main point of the research. Then, when the comparison and evaluation of CSs are done, experiments in a real setting may give additional information for use in real life.

5.2 Evaluation of Research Questions

The research questions form the foundation of the research. They may be answered based on the results. However, the results based on the experiment and simulations are heavily affected by various factors specific to the case studied. This may include climate, pollution sources and patterns, and ventilation strategies. However, some general conclusions may still be reasonably made, and extended to other cases. In addition, relevant literature may give supplementary information on the topics of interest. Thus, the research questions are discussed in the following.

Q.1. How are other pollutants affected when CO₂ is used as the control parameter for a DCV system?

Indoor CO₂ concentrations are commonly used as an indicator for the IAQ. However, it can only indicate limited aspects of the IAQ and does not provide an overall representation. Due to CO₂ being the most commonly used IAQ parameter for control of DCV systems, it is desirable to evaluate the efficiency of such control, concerning other parameters.

Several experiments are performed in the test facility with CO₂ as the only control parameter for airflow control. Depending on what type of recirculation is used, the general results from the experiments show that CO₂ control may not sufficiently handle other pollutants. Thus, it is not a comprehensive indicator of the total IAQ. During the experiments, temperatures, FA and PM_{2.5} concentrations exceeded the recommended thresholds. However, the high values are highly affected by the test facility being located inside a laboratory, and the findings from the experiments should therefore be verified by simulations. The PM concentrations were reduced with the introduction of recirculation of air, due to the outdoor concentrations being higher than inside. However, the high infiltration rates still resulted in very high indoor PM_{2.5} concentrations.

Additionally, several simulations are performed using CO₂ for control of airflow into the rooms. Due to the simulations having the same conditions compared to one another, unlike the experiments, these are more sufficient in comparing CSs and how the different IAQ parameters are handled by the

various control parameters. $PM_{2.5}$ concentrations are heavily determined by recirculation control and are only to a small extent affected by the type of airflow control. However, the CS with CO_2 as a control parameter for airflow and no recirculation results in high $PM_{2.5}$ concentrations.

Due to the small variations in temperatures for all the CSs it difficult to evaluate the parameter. Additionally, other defined factors such as temperature setpoints and ventilation system settings have a large impact on the achieved temperatures, and can be set accordingly to achieve adequate thermal conditions. However, as temperature is partly occupant-generated, and other sources, such as technical equipment, also mainly contribute to the heat generation during occupied hours, CO_2 DCV could be sufficient in controlling temperatures.

FA values are generally high, exceeding the threshold value when using CO_2 control, independent of recirculation control. As FA is usually generated constantly throughout the day and night, it is not surprising that high concentrations are observed when using a control dependent on CO_2 , which is mainly generated during occupied hours. Thus, especially in the mornings when the ventilation rates have been low throughout the night, the FA density may be high. The high FA levels will then only start to decrease after some time of occupancy when CO_2 levels rise. Hence, the simulations confirmed what the experiments indicated; That non-occupancy generated pollutants, especially FA, are not handled sufficiently by a CO_2 controlled DCV system. Therefore, other solutions may be advantageous to consider.

Concerns about occupant-related indicators used for control of DCV systems being inadequate to maintain sufficient concentrations of non-occupant-related pollutants have been a concern for many years. A. Persily, Braun, et al. (2003) acknowledges the insufficiency of CO_2 controlled DCV systems and provides some recommendations for their application. An analysis of non-occupant generated contaminants is suggested as the most ideal measure, as it can provide indications of appropriate minimum ventilation rates and other IAQ control technologies to handle the resulting contaminants. However, this is not available in all cases (A. Persily, Braun, et al., 2003). A morning purge is suggested as another measure to limit the concentration of building-generated pollutants which builds up overnight. This limits the exposure during the first few occupied hours before

CO₂ concentrations reach the threshold values in which the DCV system provides more OA to the building in the mornings (Emmerich and A. K. Persily, 2001). FA is a typical pollutant subject to such buildup overnight as it is often generated by building materials and furniture.

A. Persily, Musser, et al. (2003) used VOCs to assess the impact of a CO₂ DCV system on non-occupant related pollutants. Buildup during non-occupied hours showed to be the major problem. Increasing the minimum AFR during non-occupied periods is suggested as a solution (A. Persily, Musser, et al., 2003). However, a higher minimum AFR equals less energy savings. Therefore, it may be more beneficial to introduce other control parameters, instead of increasing the minimum airflow rate.

Q.2. Which IAQ parameters should be considered used for control of DCV systems, concerning achieving the best possible IAQ while also attaining low energy demand?

The paradox at the center of this thesis revolves around better air quality vs. lower energy consumption. More parameters included in a CS may be expected to give the best results concerning IAQ, as more aspects of the IAQ are considered. However, a more complex system may need more energy. Thus, finding a balance between obtaining the highest possible energy savings and clean IAQ must be the goal.

By involving more parameters in the control, it is more likely that one threshold is exceeded. Thus, more supply air is needed making the fan run at a higher speed using more energy. This specific trend showed in the simulation results. Subtle variations in energy demand between the various airflow CSs were observed. Some specific CSs did however stand out as significantly bad with regard to energy demand. PM_{2.5} as a control parameter for airflow control when no recirculation is included in the CS result in much higher energy demands than for the rest of the CSs. This combination of airflow and recirculation strategies is therefore not recommended. This is also supported by the obtained IAQ data from the simulations, which showed high indoor concentrations of CO₂ and FA for these specific control strategies.

While the main energy savings are already accomplished by implementing a DCV system, recircu-

lation of air also contributes some to the savings by reducing the need for heating of the supply air. The variations in energy consumption related to the various recirculation control strategies investigated in this thesis are more apparent in the simulation results than in the airflow control strategies. PM_{2.5} as the single control parameter for recirculation control, obtained the lowest energy demand. However, this strategy can not be recommended, due to the resulting bad IAQ. Thus, the other recirculation strategies are preferred instead as they resulted in better indoor conditions.

Concerning the IAQ, the simulations indicated that FA may be an appropriate control parameter for airflow control. Supporting this statement, Johnston et al. (2019) conducted simulations revealing that DCV systems using FA as a control parameter improved IAQ and reduced energy consumption by 3 % in Danish homes. However, the FA concentrations were generally high in all simulations conducted in relation to this thesis, which they may not be in all cases. Thus, including FA as a control parameter may not always be necessary, and will vary according to the specific building and case of interest. The results, however, indicate that building-generated pollutants can be considered used for airflow control in DCV systems.

When constructing a CS several considerations should be made to obtain a good balance between IAQ and energy use. First, the pollution sources and generation patterns should be assessed for the specific case, in order to choose control parameters. Then several characteristics must be set. A. Persily, Braun, et al. (2003) states that when selecting control limits for a CO₂ DCV system, they have to be low enough to provide adequate ventilation rates, and high enough to achieve some energy savings. The same goes for control limits for other control parameters. The limits used in the simulations are based on the recommended maximum threshold values for each control parameter and are adjusted a little lower in an attempt to avoid exceeding the recommended threshold too much. Additionally, the set AFRs can be increased to attain a faster decrease of pollutants when a new control limit is exceeded, and to obtain lower maximum concentrations of pollutants. Also, the ratio of OA and recirculated air in the supply can be adjusted for better results. These three aspects can be optimized to obtain more efficient control strategies. This is not done in this thesis, but the results show that some of the IAQ parameters would have benefited from some adjustments, to avoid the concentration peaks exceeding the recommended threshold values.

Q.3. What IAQ parameters are most sufficient for the purpose of regulating the ratio between recirculated air and OA in the supply?

With the introduction of recirculation of air, there are several advantages. Most evident is the advantage of energy savings. From the Trondheim simulations the potential of elevating indoor temperatures by using recirculation of return air was illustrated. Thus, energy can be saved on heating of ventilation air. Additionally, recirculation has a protective effect on the indoor concentration of outdoor-generated pollutants. Especially during periods of high outdoor levels of particles, which may occur in large cities and during rush hours with a lot of traffic, recirculation can be pivotal in keeping the concentration below the preferred indoor limits. In such periods ventilation systems without the possibility of recirculating return air can be a major health risk. Increased indoor particle levels occur as the need for more OA increases due to high concentrations in the OA. Thus, when the ventilation system is dependent on indoor CO₂ concentrations, more particles are supplied when occupancy and CO₂ levels rise.

The main challenge with recirculation is the possible buildup of indoor-generated pollutants in the indoor environment. However, using low-cost sensing technology to monitor the return air may be a measure for safer use of recirculated air. The simulations show various results concerning the use of recirculation. They highlight the importance of choosing adequate control parameters for recirculation control, which consider all aspects of the IAQ. For example, recirculation control with PM_{2.5} as a single control parameter resulted in constant low indoor PM_{2.5} concentrations. However, CO₂ and FA levels were unacceptably high. This was expected as PM_{2.5} is generally found in higher concentrations outside, and this type of recirculation control, therefore, results in recirculation being on almost all the time. However, coupling PM_{2.5} with an indoor-generated pollutant such as CO₂ to control the recirculation improves the control. This combination showed better results for both indoor CO₂ and FA concentrations. However, the results were identical to only using CO₂ as a control parameter for recirculation. The question that arises is therefore if it is necessary to include outdoor generated pollutants in the recirculation control at all?

As mentioned, to avoid indoor-generated pollutants to rise above limits, CO₂ is preferred to be

included in the recirculation control. Due to the fast increase of CO₂, the CO₂ limit showed to be the triggering factor for turning the recirculation off when CO₂ and PM_{2.5} were used for control of recirculation in the simulations. Looking at this specific recirculation control for the case investigated in this thesis, the CO₂ and PM_{2.5} will generally have contradicting interests. Ideally, to keep the PM_{2.5} concentrations as low as possible, recirculation should always be turned on. To maintain CO₂ at the lowest possible concentrations, recirculation should ideally always be turned off. Thus, one of the two parameters has to be the trigger in eventually turning the recirculation off. Based on how the control logic of this specific case is constructed, which is defined in Table 3.15, the trigger parameter will always be CO₂. This is due to the outdoor concentration of PM_{2.5} always being higher in the supply air than the return air.

The results suggest that CO₂ may be sufficient alone for control of recirculation. Thus, outdoor-generated pollutants which are always maintained at a higher level outside compared to inside, become redundant when coupled with an indoor-generated pollutant as recirculation control parameters. However, if there is a case where the outdoor-generated pollutant varies between higher concentrations inside than outside, and vice versa, a combination of an indoor-generated and outdoor-generated pollutant would probably be more sufficient for recirculation control.

The dual recirculation control with CO₂ and FA as control parameters also showed sufficient results regarding all the considered pollutants. FA as a recirculation control parameter becomes an extra safety to avoid high concentrations of building-generated pollutants. While achieving adequate IAQ, FA as a recirculation control parameter may also result in the reduction of possible energy savings. The simulation results show that this dual recirculation control has the highest energy consumption out of the evaluated recirculation control strategies. As FA often is mainly building-generated, high concentrations can be observed during unoccupied periods, when the state of the IAQ is less critical than during occupancy. FA as a control parameter may therefore turn the recirculation off due to high FA concentrations when there are no occupants, and recirculation would have been beneficial. However, adjustments to the control logic may be a solution to this particular challenge. Implementing a control where the FA control parameter only functions during occupied periods, either decided by schedules or CO₂ levels, can be a way to incorporate FA in recirculation control to

avoid high concentrations during occupancy, while also not wasting energy. Thus, FA as a control parameter for recirculation control may be a field to consider for further investigations.

Chapter 6

Conclusion

Experiments and simulations have been performed in this thesis to evaluate CSs for DCV systems. The experiments were conducted in a test facility consisting of three 7 m² offices, where low-cost sensors were used to measure CO₂, PM_{2.5}, FA, temperature, and RH. Using the results from the experiments, a simulation model was validated to perform co-simulation between EnergyPlus and CONTAM for the investigation of additional CSs.

Results showed that changing the control parameters in the ventilation logic can improve both a building's energy use and the IAQ by limiting the hours outside recommended threshold values for indoor pollutants and temperature. FA as a control parameter for airflow control showed promising results. PM_{2.5} should on the other hand not be used for airflow control. This statement can be extended to other pollutants that are mainly generated outside as well.

Recirculation had a positive effect on PM_{2.5} concentrations. However, recirculation control parameters must be determined carefully to assure that CO₂, FA, and temperatures are kept at acceptable levels. The results imply that outdoor generated pollutants which are always maintained at a higher level outside compared to inside, become redundant when coupled with an indoor generated pollutant as recirculation control parameters. However, if an outdoor generated pollutant is to be used for recirculation control, it should be coupled with CO₂ to avoid exposure risks.

While these conclusions are definite for the specific case investigated, it is important to assess the pollution sources and strengths for the specific case to be able to construct the best CS for the building of interest.

Chapter 7

Further Work

In this thesis, various parameters have been investigated for control of airflow into rooms and recirculation of air in the supply air. It has been concluded that FA as a control parameter for airflow control shows the best results for this specific case. However, what control strategy works best may be specific to the individual building, and experiments and simulations in other environments should therefore be investigated. More measurements in real buildings, as opposed to simulations, will also solidify the findings and make them more applicable to a real setting. However, simulations are great for comparison, due to having the same conditions for all scenarios, and are a great tool to verify measurements.

For a better comparison of the control strategies, the control logic and system settings should also be optimized. To optimize the control strategies, an investigation of what limits to set for the various control parameters, what ratios of recirculated and OA in the supply air, and what AFRs give the best results, should be conducted.

Bibliography

Alan (2020). *Introduction to Electrochemical Sensors*. URL: <https://www.utmel.com/blog/categories/sensors/introduction-to-electrochemical-sensors#2>.

Allen, J. G., MacNaughton, P., Satish, U., Santanam, S., Vallarino, J., and Spengler, J. D. (2016). “Associations of Cognitive Function Scores with Carbon Dioxide, Ventilation, and Volatile Organic Compound Exposures in Office Workers: A Controlled Exposure Study of Green and Conventional Office Environments”. In: *Environmental Health Perspectives* 124 (6). URL: <https://ehp.niehs.nih.gov/doi/10.1289/ehp.1510037>.

Allurwar, N. (2022). *How does IoT work?- explanation of IoT Architecture layers*. URL: <https://iotdunia.com/iot-architecture/>.

Alonso, M. J., Dols, W., and Mathisen, H. M. (2022). “Using Co-simulation between EnergyPlus and CONTAM to evaluate recirculation-based, demand-controlled ventilation strategies in an office building”. In: *Building and Environment*. URL: <https://www.sciencedirect.com/science/article/pii/S0360132321011264>.

Anusha (2017). *Humidity Sensor - Types and Working Principle*. URL: https://www.electronicshub.org/humidity-sensor-types-working-principle/#Working_of_Capacitive_RH_Sensors.

Arbeidstilsynet (2016). *Veiledning om Klima og luftkvalitet på arbeidsplassen*. URL: <https://www.arbeidstilsynet.no/contentassets/3f86f6d2038348d18540404144f76a22/luftkvalitet-pa-arbeidsplassen.pdf>.

- ASHRAE (2018). *Ventilation for Acceptable Indoor Air Quality*. URL: https://www.ashrae.org/File%5C%20Library/Technical%5C%20Resources/Standards%5C%20and%5C%20Guidelines/Standards%5C%20Addenda/62.1-2016/62_1_2016_d_20180302.pdf.
- Baldelli, A. (2021). "Evaluation of a low-cost multi-channel monitor for indoor air quality through a novel, low-cost, and reproducible platform". In: *Measurement: Sensors* 17, p. 100059. URL: <https://www.sciencedirect.com/science/article/pii/S2665917421000222>.
- Brambilla, A. and Sangiorgio, A. (2020). "Mould growth in energy efficient buildings: Causes, health implications and strategies to mitigate the risk". In: *Renewable and Sustainable Energy Reviews* 132, p. 110093. URL: <https://www.sciencedirect.com/science/article/pii/S1364032120303841>.
- Buch, J. T. (2020). *Utilizing IoT Technology for Healthy and Energy Efficient Improvement of Existing Ventilation Systems: Case Study of Indoor Air Quality in Primary School Classroom Using Arduino Sensors and CONTAM Simulations*. Specialization Project. Norwegian University of Science and Technology.
- (2021). *Control and Optimization of Ventilation in Zero Emission Buildings Using IoT*. Master's Thesis. Norwegian University of Science and Technology.
- Bulut, F. M. J. et al. (2020). "Laboratory Comparison of Low-Cost Particulate Matter Sensors to Measure Transient Events of Pollution". In: *Sensors* 20 (8), p. 2219. URL: <https://www.mdpi.com/1424-8220/20/8/2219/htm>.
- Chakraborty, D. and Elzarka, H. (2017). *Performance testing of energy models: are we using the right statistical metrics?* URL: <https://www.tandfonline.com/doi/full/10.1080/19401493.2017.1387607>.
- Choi, J.-H. and Cho, H.-S. (2020). "A Study on the Development of a Light Scattering Particulate Matter Sensor and Monitoring System". In: *Computer Science and Information Systems* 17 (3), pp. 867–890. URL: <http://www.doiserbia.nb.rs/img/doi/1820-0214/2020/1820-02142000025C.pdf>.

- Concas, F., Mineraud, J., Lagerspetz, E., Tarkoma, S., Varjonen, S., Puolamäki, X. L. K., Nurmi, P., and Tarkoma, S. (2021). *Low-Cost Outdoor Air Quality Monitoring and Sensor Calibration: A Survey and Critical Analysis*. University of Helsinki. URL: https://www.researchgate.net/publication/337944305_Low-Cost_Outdoor_Air_Quality_Monitoring_and_Sensor_Calibration_A_Survey_and_Critical_Analysis.
- Coulby, G., Clear, A., Jones, O., Young, F., Stuart, S., and Godfrey, A. (2020). “Towards remote healthcare monitoring using accessible IoT technology: state-of-the-art, insights and experimental design”. In: *BioMedical Engineering OnLine* 19.80. URL: <https://biomedical-engineering-online.biomedcentral.com/articles/10.1186/s12938-020-00825-9>.
- Coulby, G., Clear, A. K., Jones, O., and Godfrey, A. (2021). “Low-cost, multimodal environmental monitoring based on the Internet of Things”. In: *Building and Environment* 203, p. 108014. URL: https://www.sciencedirect.com/science/article/pii/S0360132321004170?casa_token=omsRPH08HSAAAAA:4nG-1CnVpEQP5YFUAHzMtja9yiRbGbZcW2XIF9xXr2wPRn0IO6bQJ5sxx2CHTbib26.
- Danza, L., Barozzi, B., Bellazzi, A., Belussi, L., Devitofrancesco, A., Ghellere, M., Salamone, F., Scamoni, F., and Scrosati, C. (2020). “A weighting procedure to analyse the Indoor Environmental Quality of a Zero-Energy Building”. In: *Building and Environment* 183, p. 107155. URL: <https://www.sciencedirect.com/science/article/pii/S0360132320305291>.
- Demanege, I., Mujan, I., Singer, B. C., Anđelković, A. S., Babich, F., and Licina, D. (2021). “Performance assessment of low-cost environmental monitors and single sensors under variable indoor air quality and thermal conditions”. In: *Building and Environment* 187, p. 107415. URL: <https://www.sciencedirect.com/science/article/pii/S0360132320307836>.
- Dinh, T.-V., Choi, I.-Y., Son, Y.-S., and Kim, J.-C. (2016). “A review on non-dispersive infrared gas sensors: Improvement of sensor detection limit and interference correction”. In: *Sensors and Actuators B: Chemical* 231, pp. 529–538. URL: <https://www.sciencedirect.com/science/article/pii/S0925400516303343>.

- Direktoratet for byggkvalitet (2017). *Byggteknisk forskrift (TEK17) med veiledning*. URL: <https://dibk.no/regelverk/byggteknisk-forskrift-tek17/>.
- Earth's CO2 (2022). *Atmospheric CO2 April 2022*. URL: <https://www.co2.earth/>.
- Emmerich, S. J. and Persily, A. K. (2001). *State-of-the-Art Review of CO2 Demand Controlled Ventilation Technology and Application*. URL: https://tsapps.nist.gov/publication/get_pdf.cfm?pub_id=860846.
- Folkehelseinstituttet (2015). *Anbefalte faglige normer for inneklima*. URL: <https://www.fhi.no/globalassets/dokumenterfiler/rapporter/2015/anbefalte-faglige-normer-for-inneklima-pdf.pdf>.
- Fra lavenergi programmet (2020). "Hvordan skal ventilasjonsanlegget reguleres". In: *Byggbloggen*. URL: <https://www.tekna.no/fag-og-nettverk/bygg-og-anlegg/byggbloggen/hvordan-skal-anlegget-reguleres/>.
- Gillis, A. S. (2022). *What is the internet of things (IoT)?* URL: <https://www.techtarget.com/iotagenda/definition/Internet-of-Things-IoT>.
- Giordano, M. R., Malings, C., Pandis, S. N., Presto, A. A., McNeill, V., Westervelt, D. M., Beekmann, M., and Subramanian, R. (2021). "From low-cost sensors to high-quality data: A summary of challenges and best practices for effectively calibrating low-cost particulate matter mass sensors". In: *Journal of Aerosol Science* 158. URL: <https://www.sciencedirect.com/science/article/pii/S0021850221005644>.
- Gram, O. K. (2019). *Use of Low Cost Pollutant Sensors for Developing Healthy Demand Controlled Ventilation Strategies: A Case Study in Four Primary School Classrooms*. Master's Thesis. Norwegian University of Science and Technology.
- Gyasi, P. (2021). *Air Infiltration Measurement by Tracer Gas and Pressurization Techniques*. URL: https://www.researchgate.net/publication/349026156_Air_Infiltration_Measurement_by_Tracer_Gas_and_Pressurization_Techniques<https://www>.

researchgate.net/publication/4256465_A_Sparse_Robust_Model_for_a_Linz-Donawitz_Steel_Converter.

Hamida, A. A., Johansson, D., Wahlström, Å., and Fransson, V. (2019). “The impact of a DCV-system on the IAQ, energy use, and moisture safety in apartments - a case study”. In: *International Journal of Ventilation*. URL: <https://www.tandfonline.com/action/showCitFormats?doi=10.1080%5C%2F14733315.2020.1818375&area=000000000000000001>.

Heat Gain from People, Lights, and Appliances (n.d.). URL: <https://engineer-educators.com/topic/5-heat-gain-from-people-lights-and-appliances/>.

Högdahl, S. (2018). *Placing VOC Sensors for Assessing Air Quality*. Master’s Thesis. KTH Royal Institute of Technology in Stockholm. URL: <https://kth.diva-portal.org/smash/get/diva2:1233872/FULLTEXT01.pdf>.

Hong, G.-H., Le, T.-C., Tu, J.-W., Wang, C., Chang, S.-C., Yu, J.-Y., Lin, G.-Y., Aggarwal, S. G., and Tsai, C.-J. (2021). “Long-term evaluation and calibration of three types of low-cost PM_{2.5} sensors at different air quality monitoring stations”. In: *Journal of Aerosol Science* 157, p. 105829. URL: <https://www.sciencedirect.com/science/article/pii/S0021850221005607>.

Hong, T., Kim, J., and Lee, M. (2018). “Integrated task performance score for the building occupants based on the CO₂ concentration and indoor climate factors changes”. In: *Applied Energy* 228. URL: <https://www.sciencedirect.com/science/article/pii/S0306261918310912>.

How does an NDIR CO₂ Sensor Work (2021). URL: <https://www.co2meter.com/blogs/news/6010192-how-does-an-ndir-co2-sensor-work>.

Intellectual Property Office (n.d.). *EnergyPlus: Energy Simulation Software for Buildings CR-2118*. URL: <https://ipo.lbl.gov/lbnl2118/>.

Jaakkola, J. J., Tuomaala, P., and Seppanen, O. (1994). “Air recirculation and sick building syndrome: A blinded crossover trial”. In: *American Journal of Public Health* 84 (3), pp. 422–8. URL: https://www.researchgate.net/publication/15070312_Air_recirculation_and_sick_building_syndrome_A_blinded_crossover_trial.

- Jaber, A. R., Dejan, M., and Marcella, U. (2017). “The Effect of Indoor Temperature and CO2 Levels on Cognitive Performance of Adult Females in a University Building in Saudi Arabia”. In: *Energy Procedia* 122, pp. 451–456. URL: <https://www.sciencedirect.com/science/article/pii/S187661021732982X>.
- Jin, H. and Luo, P. (2021). “Study on the accuracy of photoacoustic spectroscopy system based on multiple linear regression correction algorithm”. In: *AIP Advances* 11. URL: <https://aip.scitation.org/doi/10.1063/5.0060595>.
- Johnston, C. J., Andersen, R. K., Toftum, J., and Nielsen, T. R. (2019). “Effect of formaldehyde on ventilation rate and energy demand in Danish homes: Development of emission models and building performance simulation”. In: Abstract retrieved from. URL: https://www.researchgate.net/publication/335185407_Effect_of_formaldehyde_on_ventilation_rate_and_energy_demand_in_Danish_homes_Development_of_emission_models_and_building_performance_simulation.
- Jørgensen, T. B. (2020). *Utilizing IoT Technology for Healthy and Energy Efficient Improvement of Existing Ventilation Systems: Case Study of Indoor Air Quality in Primary School Classroom Using Arduino Sensors and CONTAM Simulations*. Master’s Thesis. Norwegian University of Science and Technology.
- Jost, D. (2019). *What is a Humidity Sensor*. URL: <https://www.fierceelectronics.com/sensors/what-a-humidity-sensor>.
- Kempton, L., Daly, D., and Dewsbury, M. (2020). *What impacts does increasing airtightness have on mould, condensation and measures of indoor air quality?* CRC Low Carbon Living. URL: <https://apo.org.au/sites/default/files/resource-files/2020-09/apo-nid310391.pdf>.
- Khan, S., Calvé, S. L., and Newport, D. (2020). “A review of optical interferometry techniques for VOC detectionnce evaluations in ambient air”. In: *Sensors and Actuators A: Physical* 302, p. 111782. URL: <https://www.sciencedirect.com/science/article/pii/S0924424719300652>.

- Kim, K.-H., Jahan, S. A., and Lee, J.-T. (2011). “Exposure to Formaldehyde and Its Potential Human Health Hazards”. In: *Journal of Environmental Science and Health, Part C* 29 (4), pp. 277–99. URL: https://www.researchgate.net/publication/51820816_Exposure_to_Formaldehyde_and_Its_Potential_Human_Health_Hazards.
- Klenck, T. (2000). *How It Works: Heat Recovery Ventilator*. Popular Mechanics. URL: <https://www.popularmechanics.com/home/interior-projects/how-to/a149/1275121/>.
- Kurnitski, J. et al. (2020). *REHVA COVID-19 guidance document*. URL: https://www.rehva.eu/fileadmin/user_upload/REHVA_COVID-19_guidance_document_ver2_20200403_1.pdf.
- Laursen, K. R., Rasmussen, B. B., Rosati, B., Gutzke, V. H., Østergaard, K., Ravn, P., Kjærgaard, S. K., Bilde, M., Glasius, M., and Sigsgaard, T. (2021). “Acute health effects from exposure to indoor ultrafine particles—A randomized controlled crossover study among young mild asthmatics”. In: *Indoor Air* 31, pp. 1993–2007. URL: <https://onlinelibrary.wiley.com/doi/10.1111/ina.12902>.
- Lee, C.-Y. and Lee, G.-B. (2005). “Humidity Sensors: A Review”. In: *Sensor Letters* 3 (1-4), pp. 1–15. URL: https://www.researchgate.net/publication/233616035_Humidity_Sensors_A_Review.
- Li, J., Chen, W., and Yu, B. (2011). “Recent Progress on Infrared Photoacoustic Spectroscopy Techniques”. In: *Applied Spectroscopy Reviews* 46 (6), pp. 440–471. URL: https://www.researchgate.net/publication/232922383_Recent_Progress_on_Infrared_Photoacoustic_Spectroscopy_Techniques.
- Lin, H.-H., Yuan, C.-S., Chen, W.-K., Chang, C.-T., and Chen, P.-S. (2020). “On-site measurement and simulation of indoor particulate matter distributed in a single room with stratified flow field”. In: *Indoor and Built Environment* 30 (7), pp. 886–905. URL: <https://journals.sagepub.com/doi/full/10.1177/1420326X20919788>.
- Mishra, A., Schiavon, S., Wargoeki, P., and Tham, K. W. (2020). *Carbon dioxide and its effect on occupant cognitive performance: A literature review*. URL: <https://www.researchgate.net>.

- net/publication/341255340_Carbon_dioxide_and_its_effect_on_occupant_cognitive_performance_A_literature_review.
- Mou, J., Cui, S., and Khoo, D. W. Y. (2021). “Numerical investigation of airflow field and CO2 distribution inside a seminar room for sensor placement”. In: *Measurement: Sensors* 18, p. 100119. URL: <https://www.sciencedirect.com/science/article/pii/S2665917421000829>.
- Mysen, M. and Schild, P. G. (2011). “Requirements for well functioning Demand Controlled Ventilation”. In: *Rehva*. URL: https://www.rehva.eu/fileadmin/hvac-dictio/05-2011/rj1105_p14-18_requirements-for-well-functioning-demand-controlled-ventilation.pdf.
- Mysen, M., Schild, P. G., and Cablé, A. (2017). *Demand-controlled ventilation - requirements and commissioning*. URL: https://www.researchgate.net/publication/281633644_DEMAND-CONTROLLED_VENTILATION_-_REQUIREMENTS_AND_COMMISSIONING_Guidebook_on_well-functioning_and_energy-optimal_DCV.
- National Institute of Standards and Technology (2018). *CONTAM Introduction*. URL: <https://www.nist.gov/el/energy-and-environment-division-73200/nist-multizone-modeling/software/contam>.
- Ng, L., Poppendieck, D., Dols, W., and Emmerich, S. (2018). “Evaluating IAQ and Energy Impacts of Ventilation in a Net-Zero Energy House Using a Coupled Model”. In: *Science and Technology for the Built Environment* 24 (2), pp. 124–134. URL: <https://www.tandfonline.com/doi/full/10.1080/23744731.2017.1401403>.
- Norrefeldt, V., Mayer, F., Herbig, B., Ströhlein, R., and Lei, P. W. and Fang (2021). “Effect of Increased Cabin Recirculation Airflow Fraction on Relative Humidity, CO2 and TVOC”. In: *Aerospace* 8 (15). URL: <https://www.mdpi.com/2226-4310/8/1/15>.
- Omega (n.d.). *Temperature Probes*. URL: <https://www.omega.co.uk/temperature/z/thermocouple-rtd.html>.

- Ontario Agency for Health Protection and Promotion (2021). “Heating, ventilation and air conditioning (HVAC) systems in buildings and COVID-19”. In: *Queen’s Printer for Ontario*. URL: <https://www.publichealthontario.ca/-/media/documents/ncov/ipac/2020/09/covid-19-hvac-systems-in-buildings.pdf?la=en>.
- Onyije, F. and Avwioro, O. (2012). “Excruciating effects of formaldehyde exposure to students in gross anatomy dissection laboratory”. In: *The International Journal of Occupational and Environmental Medicine* 3 (2), pp. 92–5. URL: <https://theijoem.com/ijoem/index.php/ijoem/article/view/125/272>.
- Oracle (2022). *What is IoT?* URL: <https://www.oracle.com/internet-of-things/what-is-iot/>.
- Palmisania, J., Gilioa, A. D., Viana, M., Gennaro, G. de, and Ferro, A. (2021). “Indoor air quality evaluation in oncology units at two European hospitals: Low-cost sensors for TVOCs, PM2.5 and CO2 real-time monitoring”. In: *Building and Environment* 205, p. 108237. URL: <https://www.sciencedirect.com/science/article/pii/S0360132321006387>.
- Palzer, S. (2020). “Photoacoustic-Based Gas Sensing: A Review”. In: *Sensors* 20 (9), p. 2745. URL: <https://www.ncbi.nlm.nih.gov/pmc/articles/PMC7248969/>.
- Paterson, C., Sharpe, R., Taylor, T., and Morrissey, K. (2021). “Indoor PM2.5, VOCs and asthma outcomes: A systematic review in adults and their home environments”. In: *Environmental Research* 202, p. 111631. URL: <https://www.sciencedirect.com/science/article/pii/S0013935121009257>.
- Pei, G., Rim, D., Schiavon, S., and Vannucci, M. (2019). “Effect of sensor position on the performance of CO2-based demand controlled ventilation”. In: *Energy and Buildings* 202, p. 109358. URL: <https://www.sciencedirect.com/science/article/pii/S0378778819305377>.
- Persily, A., Braun, J., Emmerich, S., Mercer, K., and Lawrence, T. (2003). *Recommendations for Application of CO2-Based Demand Controlled Ventilation, Including Proposed Guidance for ASHRAE Standard 62 and California’s Title 24*. URL: https://www.researchgate.net/publication/242724599_Recommendations_for_Application_of_CO_2_Based_

Demand_Controlled_Ventilation_Including_Proposed_Guidance_for_ASHRAE_Standard_62_and_California%5C%27s_Title_24_Letter_Report_on_Task_315a_and_316a_of_CEC-EEB_.

Persily, A., Musser, A., Emmerich, S., and Taylor, M. (2003). *Simulations of Indoor Air Quality and Ventilation Impacts of Demand Controlled Ventilation in Commercial and Institutional Buildings*.

URL: <https://www.govinfo.gov/content/pkg/GOVPUB-C13-d0e00d62acbc1522b60c13fa24765378/pdf/GOVPUB-C13-d0e00d62acbc1522b60c13fa24765378.pdf>.

Platon (n.d.).

Poirier, B., Guyot, G., Woloszyn, M., Geoffroy, H., Ondarts, M., and Gonze, E. (2021). “Development of an assessment methodology for IAQ ventilation performance in residential buildings: An investigation of relevant performance indicators”. In: *Journal of Building Engineering* 43, p. 103140. URL: <https://www.sciencedirect.com/science/article/pii/S2352710221009980>.

Qiao, S., Qu, Y., Ma, Y., He, Y., Wang, Y., Hu, Y., Yu, X., Zhang, Z., and Tittel, F. K. (2019). “A Sensitive Carbon Dioxide Sensor Based on Photoacoustic Spectroscopy with a Fixed Wavelength Quantum Cascade Laser”. In: *Sensors* 19 (19), p. 4187. URL: <https://www.mdpi.com/1424-8220/19/19/4187>.

Raninec, M. (2019). *Overcoming the Technical Challenges of Electrochemical Gas Sensing*. URL: <https://www.analog.com/en/technical-articles/overcoming-the-technical-challenges-of-electrochemical-gas-sensing.html>.

Rosenstock, T. S. et al. (2013). “Accuracy and precision of photoacoustic spectroscopy not guaranteed”. In: *Global Change Biology* 19 (12), pp. 3565–3567. URL: <https://onlinelibrary.wiley.com/doi/full/10.1111/gcb.12332>.

Saleh, T. A. and Fadillah, G. (2021). “Efficient detection of CO₂ by nanocomposites: Environmental and energy technologies”. In: *Trends in Environmental Analytical Chemistry* 32, e00142. URL: <https://www.sciencedirect.com/science/article/pii/S2214158821000295>.

- Shah, D. S., Fuke, M., Upadhyay, S., Verma, A., and Rehman, S. U. (2016). “Development and characterization of NDIR-based CO₂ sensor for manned space missions”. In: *Proceedings 9880*. URL: <https://www.spiedigitallibrary.org/conference-proceedings-of-spie/9880/98801H/Development-and-characterization-of-NDIR-based-CO2-sensor-for-manned/10.1117/12.2228226.full>.
- Shao, W., Zhang, H., and Zhou, H. (2017). “Fine Particle Sensor Based on Multi-Angle Light Scattering and Data Fusion”. In: *Sensors* 17 (5), p. 1033. URL: <https://www.mdpi.com/1424-8220/17/5/1033>.
- Shaughnessy, W. J., Venigalla, M. M., and Trump, D. (2015). “Health effects of ambient levels of respirable particulate matter (PM) on healthy, young-adult population”. In: *Atmospheric Environment* 123 (A), pp. 102–111. URL: <https://www.sciencedirect.com/science/article/pii/S1352231015304568>.
- Shen, J., Kong, M., Dong, B., Birnkrant, M. J., and Zhang, J. (2021). “A systematic approach to estimating the effectiveness of multi-scale IAQ strategies for reducing the risk of airborne infection of SARS-CoV-2”. In: *Building and Environment* 200, p. 107926. URL: <https://www.sciencedirect.com/science/article/pii/S0360132321003309>.
- Su, D. X., Sutarlie, D. L., and Loh, P. X. J. (2020). “Sensors and Analytical Technologies for Air Quality: Particulate Matters and Bioaerosols”. In: *Chemistry – An Asian Journal* 15, p. 4241. URL: <https://onlinelibrary.wiley.com/doi/10.1002/asia.202001051>.
- Terry, J. (2021). *The Energy-Saving Role of Heat Recovery and Recirculation in Ventilation Systems*. URL: <https://www.esmagazine.com/articles/101471-the-energy-saving-role-of-heat-recovery-and-recirculation-in-ventilation-systems>.
- Thamban, A. (2020). *Analysis of infiltration in buildings using LES and airflow network models*. Master’s Thesis. Delft University of Technology.
- Tryner, J., Phillips, M., Quinn, C., Neymark, G., Wilson, A., Jathar, S. H., Carter, E., and Volckens, J. (2021). “Design and testing of a low-cost sensor and sampling platform for indoor air quality”.

- In: *Building and Environment* 206, p. 108398. URL: <https://www.sciencedirect.com/science/article/pii/S0360132321007952>.
- TSI Incorporated (2021). *Photo-Ionization Detection (PID) Technology*. URL: https://tsi.com/getmedia/e6812861-60a7-4dee-82a7-09b1ea9f734c/TSI-147_Photo_Ionization_Detection_Technology?ext=.pdf.
- U.S. Environmental Protection Agency (1991). *Indoor Air Facts No. 4 Sick Building Syndrome*. URL: https://www.epa.gov/sites/default/files/2014-08/document/sick_building_factsheet.pdf.
- (2020). *What are volatile organic compounds (VOCs)?* United States Environmental Protection Agency. URL: <https://www.epa.gov/indoor-air-quality-iaq/what-are-volatile-organic-compounds-vocs>.
 - (2021a). *Introduction to Indoor Air Quality*. United States Environmental Protection Agency. URL: <https://www.epa.gov/indoor-air-quality-iaq/introduction-indoor-air-quality>.
 - (2021b). *Particulate Matter (PM) Basics*. URL: <https://www.epa.gov/pm-pollution/particulate-matter-pm-basics#PM>.
 - (2022). *Sources of Greenhouse Gas Emissions*. URL: <https://www.epa.gov/ghgemissions/sources-greenhouse-gas-emissions>.
- Wei, Y., Xiao-bin, J., and Xiao-chuan, P. (2004). “Relationship between indoor air formaldehyde exposure and allergic asthma in adults”. In: *Chinese Journal of Public Health* 20 (8), pp. 904–906. URL: <http://zgggws.xml-journal.net/en/article/id/16356>.
- Wolkoff, P., Azuma, K., and Carrer, P. (2021). “Health, work performance, and risk of infection in office-like environments: The role of indoor temperature, air humidity, and ventilation”. In: *International Journal of Hygiene and Environmental Health* 233, p. 113709. URL: <https://www.sciencedirect.com/science/article/pii/S1438463921000225?via%5C%3Dihub#bib116>.

- World Health Organization (2010). *WHO Guidelines for Indoor Air Quality: Selected Pollutants*. URL: https://www.euro.who.int/__data/assets/pdf_file/0009/128169/e94535.pdf.
- World Health Organization (WHO) (2022). *WHO Air Quality Guidelines*. URL: https://www.c40knowledgehub.org/s/article/WHO-Air-Quality-Guidelines?language=en_US.
- Xu, W., Cai, Y., Gao, S., Hou, S., Yang, Y., Duan, Y., Fu, Q., Chen, F., and Wu, J. (2020). “New understanding of miniaturized VOCs monitoring device: PID-type sensors performance evaluations in ambient air”. In: *Sensors and Actuators B: Chemical* 330, p. 129285. URL: <https://www.sciencedirect.com/science/article/pii/S0925400520316257>.
- Zender–Swiercz, E. (2021). “A Review of Heat Recovery in Ventilation”. In: *Energies* 14 (6), p. 1759. URL: <https://www.mdpi.com/1996-1073/14/6/1759>.

Appendix A

Air Pressure Test Calculations

Table A.1 and A.2 summarizes the the measured values used for infiltration rate calculations.

Table A.1: Settings and achieved differential pressures for the four air pressure tests. The door between room 1 and 2 were sealed with duct tape.

	Air Pressure Test 2.1	Air Pressure Test 3.1	Air Pressure Test 4.1
Pressures [Pa]	$P_1 - P_2 = 50$ $P_1 - P_o = 151$	$P_3 - P_2 = 50$ $P_3 - P_o = 132$	$P_2 - P_1 = 50$ $P_2 - P_3 = 49$ $P_2 - P_o = 120$
	Airflow rates [m^3/h]		
Main inlet	175	160	147
Main outlet	78	68	87
Inlet room 1	104	0	0
Outlet room 1	38	10	11
Inlet room 2	0	0	97
Outlet room 2	14	10	38
Inlet room 3	0	98	0
Outlet room 3	14	41	11

Table A.2: Settings and achieved differential pressures for the four air pressure tests. The door between room 1 and 2 were not sealed with weatherstrips.

	Air Pressure Test 1.2	Air Pressure Test 2.2	Air Pressure Test 3.2	Air Pressure Test 4.2
Pressures [Pa]	$P_1 - P_o = 50$ $P_2 - P_o = 50$ $P_2 - P_o = 50$	$P_1 - P_2 = 50$ $P_1 - P_o = 162$	$P_3 - P_2 = 50$ $P_3 - P_o = 95$	$P_2 - P_1 = 51$ Pa $P_2 - P_3 = 50$ $P_2 - P_o = 136$
	Airflow rates [m^3/h]			
Main inlet	193	183	157	187
Main outlet	126	57	71	91
Inlet room 1	61	119	0	0
Outlet room 1	33	21	10	14
Inlet room 2	59	0	0	138
Outlet room 2	33	15	10	47
Inlet room 3	60	0	92	0
Outlet room 3	35	15	40	14

Using (3.2) and (3.3) with the values from Table A.1 and Table A.2, a system of equations is obtained which can be solved to estimate the infiltration rates. Test 1.2 is included in both the calculation with the duct tape on the door and the one without. This is due to that the test with overpressure in all three rooms only was conducted one time, as there should be no difference in infiltration through the facade, whether the door is taped or not. The full calculation for the tests without duct tape are illustrated below. While some of the same names for parameters are used for several tests, their value may vary between each test.

A.1 Test 1.2

Calculating $q_{fi} = C_{fi} \cdot (\Delta P)^n = -\sum q_{mvi}$ for all rooms to get the infiltration rates when the door between room 1 and 2 is not sealed. Thus, values from Table A.2 is used. AFRs are calculated as

$[m^3/s]$.

$$q_f = C_f \cdot 50^{0.67} = 0.016944 - 0.009167 + 0.016389 - 0.01 + 0.016667 - 0.009722 = 0.021111 m^3/s$$

$$q_{f1} = C_{f1} \cdot 50^{0.67} = 0.016944 - 0.009167 = 0.007778 m^3/s$$

$$q_{f2} = C_{f2} \cdot 50^{0.67} = 0.016389 - 0.01 = 0.006389 m^3/s$$

$$q_{f3} = C_{f3} \cdot 50^{0.67} = 0.016667 - 0.009722 = 0.006944 m^3/s$$

Solving for the leakage coefficients:

$$C_f = 0.001535 m^3/sPa^n$$

$$C_{f1} = 0.000566 m^3/sPa^n$$

$$C_{f2} = 0.000465 m^3/sPa^n$$

$$C_{f3} = 0.000505 m^3/sPa^n$$

A.2 Test 2.2

Equation 3.3 with input values from Test 2.2 gives the total infiltration rates for room 1. Using the power law, (3.2) for the infiltration through the facade, the infiltration through the inner wall is obtained:

$$q_{f1} + q_{w1} = 0.033056 - 0.005833 = 0.027222 \quad q_{w1} = 0.027222 - q_{f1} = 0.027222 - 0.000566 \cdot 162^{0.67} = 0.010125$$

$$q_{w1} = C_{w1} \cdot 50^{0.67} = 0.010125$$

Solving for the leakage coefficient:

$$C_{w1} = 0.000736$$

A.3 Test 3.2

Test 3.2 is solved similarly as test 2.2:

$$q_{f3} + q_{w2} = 0.025556 - 0.011111 = 0.014444$$

$$q_{w2} = 0.014444 - q_{f3} = 0.014444 - 0.000505 \cdot 95^{0.67} = 0.003769$$

$$q_{w2} = C_{w2} \cdot 50^{0.67} = 0.003769$$

$$C_{w1} = 0.000274$$

A.4 Test 4.2

The last test is in theory redundant as the leakage coefficients for all parts of the facade and both inner walls are already obtained. It can however be used as a check to see if the same leakage coefficients for the inner walls are found when pressurizing room 2.

$$q_{f2} + q_{w1} + q_{w2} = 0.038333 - 0.010833 = 0.0275$$

First, the leakage coefficient for the inner wall between room 1 and 2 is calculated: $q_{w1} = 0.0275 - q_{f2} - q_{w2} = 0.0275 - 0.000465 \cdot 136^{0.67} - 0.000736 \cdot 50^{0.67} = 0.011241$

$$C_{w1} = 0.000807$$

Then for the wall between room 2 and 3:

$$q_{w2} = 0.0275 - q_{f2} - q_{w1} = 0.0275 - 0.000465 \cdot 136^{0.67} - 0.000274 \cdot 51^{0.67} = 0.004884$$

$$C_{w2} = 0.000366$$

A.5 Pressure Tests Results

A summary of the calculated leakage coefficients, in addition to the ones when there were duct tape on the door, is presented in Table A.3.

Table A.3: Calculated leakage coefficients for each building part.

	With duct tape	Without duct tape
C_f		0.001535
C_{f1}		0.000566
C_{f2}		0.000465
C_{f3}		0.000505
C_{w1}	0.000147	0.000736
C_{w2}	0.000184	0.000274
(C_{w1})	0.000175	0.000807
(C_{w2})	0.000212	0.000355

The infiltration rates through all building parts are calculated for a differential pressure of 50 Pa using the power law. All values are presented in Table A.4. The values are now given in m^3/h . n_{50} values calculated using (3.4), and are also presented in Table 2.2.

Table A.4: Calculated infiltration for a 50 Pa pressure difference through each building part, total infiltration through each room and the resulting n_{50} for each room.

Parameter	With duct tape	Without duct tape
$q_f(p = 50)$		76
$q_{f1}(p = 50)$		28
$q_{f2}(p = 50)$		23
$q_{f3}(p = 50)$	25	25
$q_{w1}(p = 50)$	7.28	36.45
$q_{w2}(p = 50)$	9.09	13.56
$q_{r1}(p = 50)$	35.28	64.45
$q_{r2}(p = 50)$	39.37	73.02
$q_{r3}(p = 50)$	34.09	38.57
n_{50_r1}	2.10	3.84
n_{50_r2}	2.34	4.35
n_{50_r3}	2.03	2.30
n_{50_tot}		1.51

Appendix B

Control Strategy Experiment Figures

Due to the challenges in maintaining a controlled environment when conducting the control strategy experiments, simulations are chosen instead to form the analysis of the various CSs. Some indications of various tendencies related to the CSs could be made from the experiments, and have been discussed in Chapter 4.2. The results of the rest of the CS experiments are depicted below.

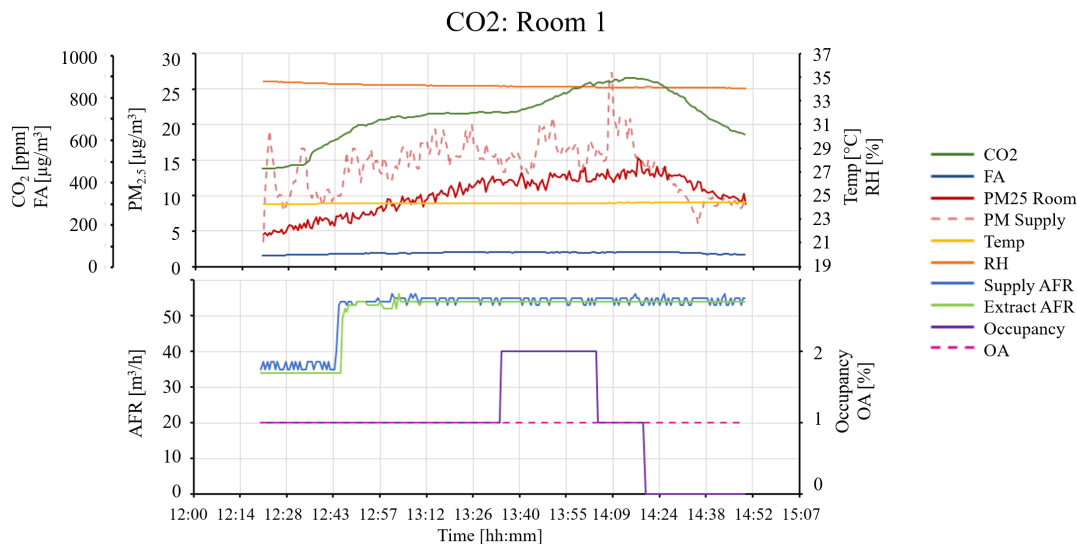


Figure B.1: CO2 control without recirculation in room 1.

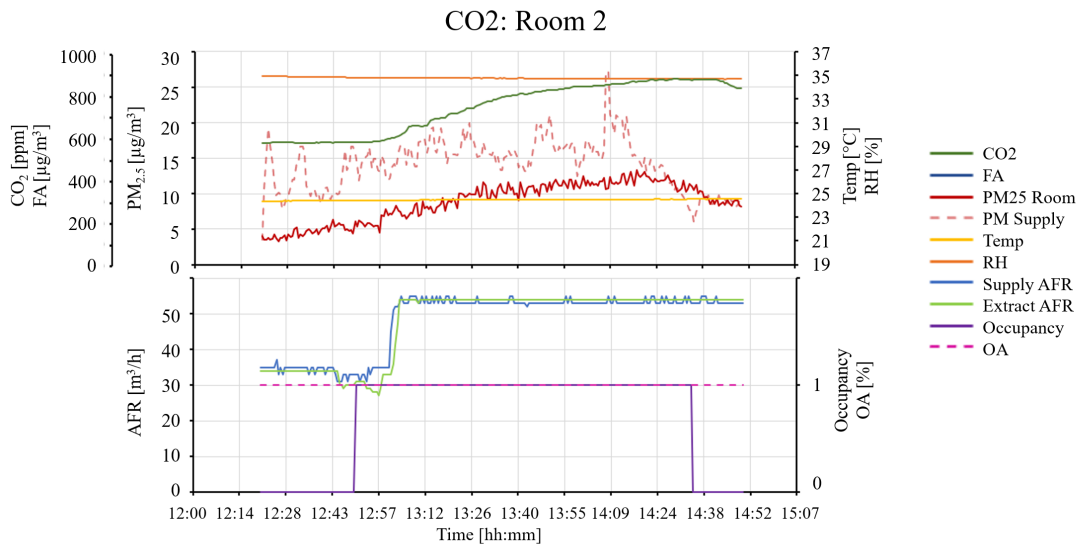


Figure B.2: CO₂ control without recirculation in room 2.

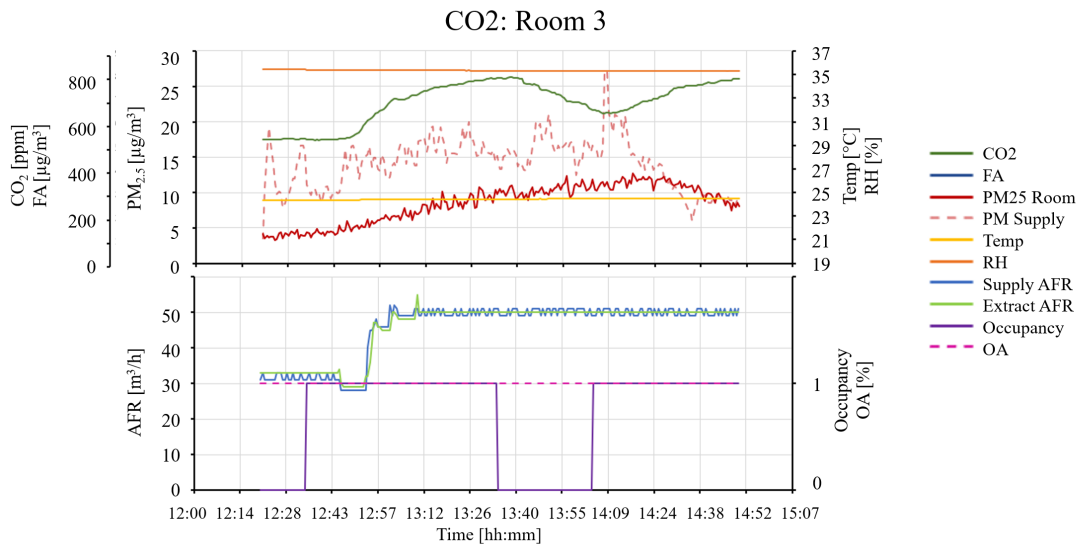


Figure B.3: CO₂ control without recirculation in room 3.

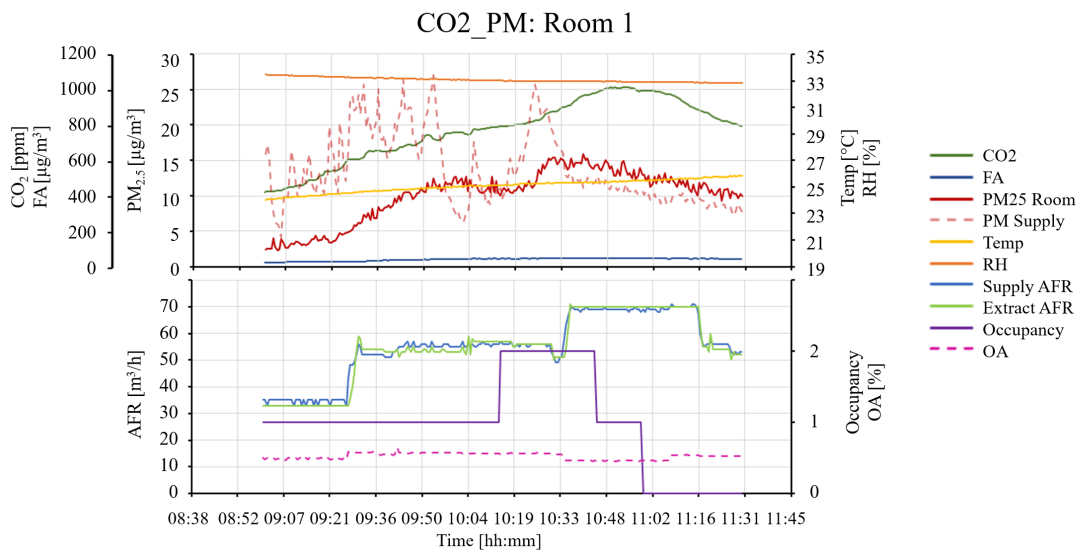


Figure B.4: CO₂ control with PM recirculation control in room 1.

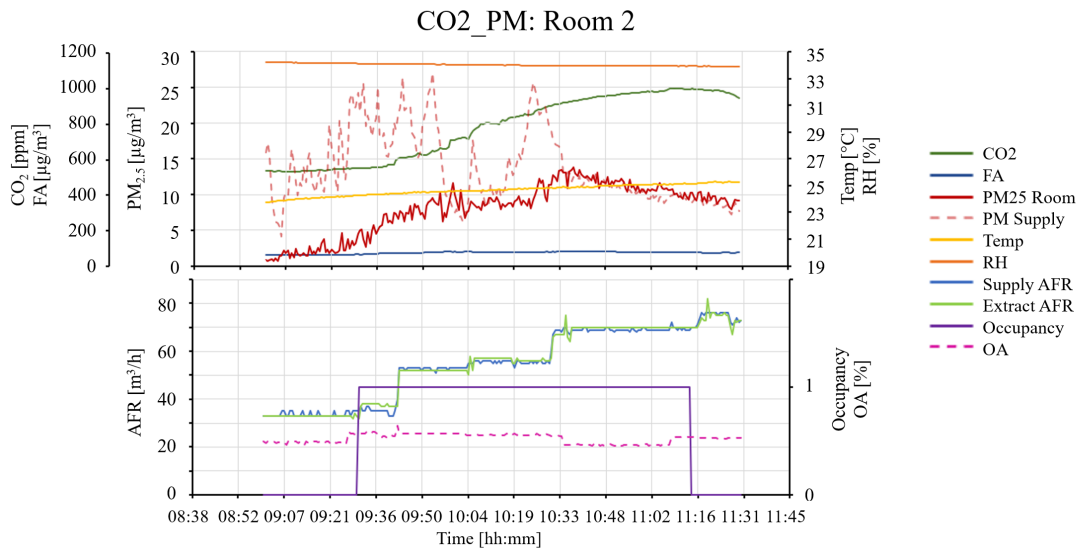


Figure B.5: CO₂ control with PM recirculation control in room 2.

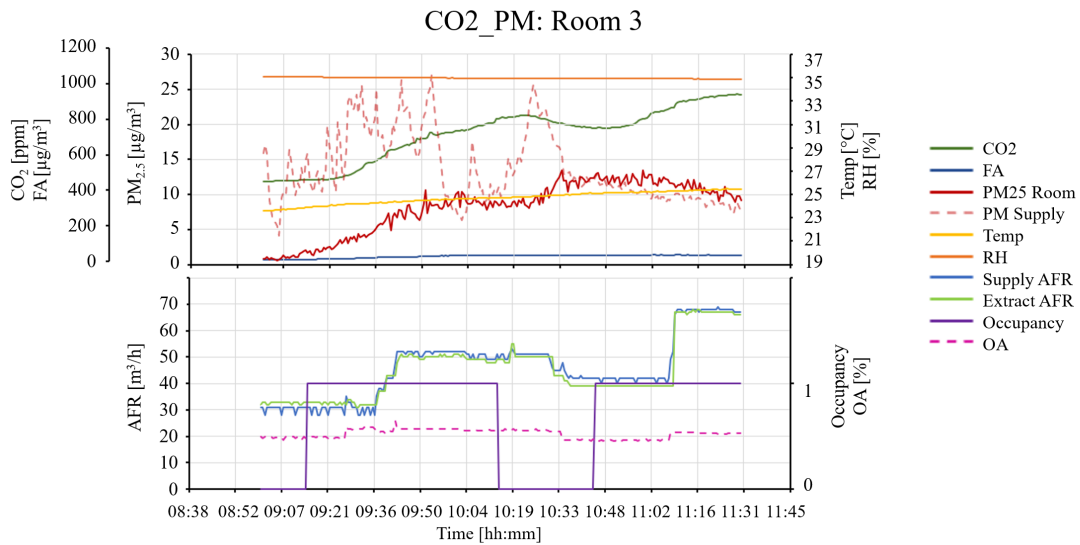


Figure B.6: CO2 control with PM recirculation control in room 3.

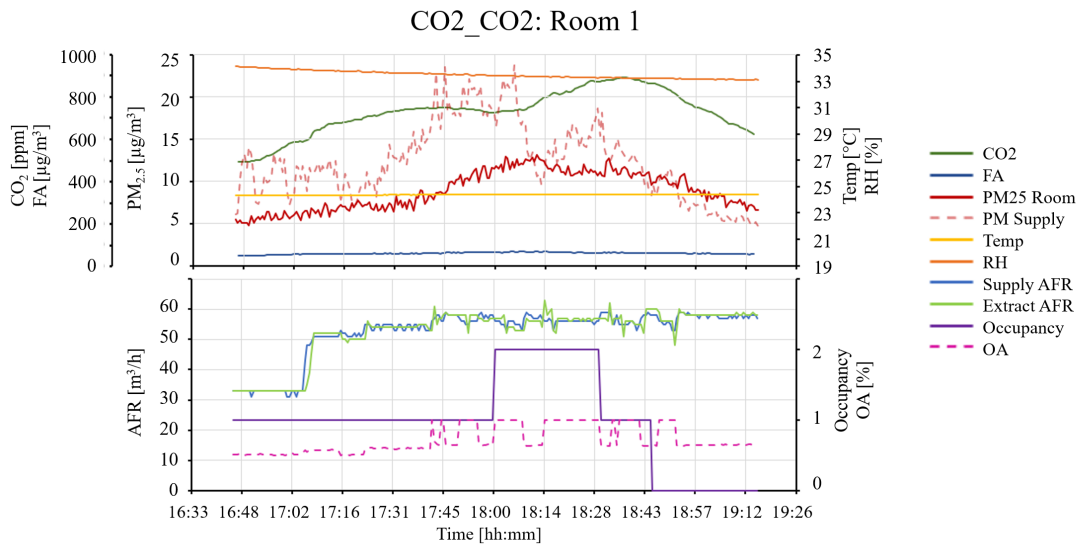


Figure B.7: CO2 control with CO2 recirculation control in room 1.

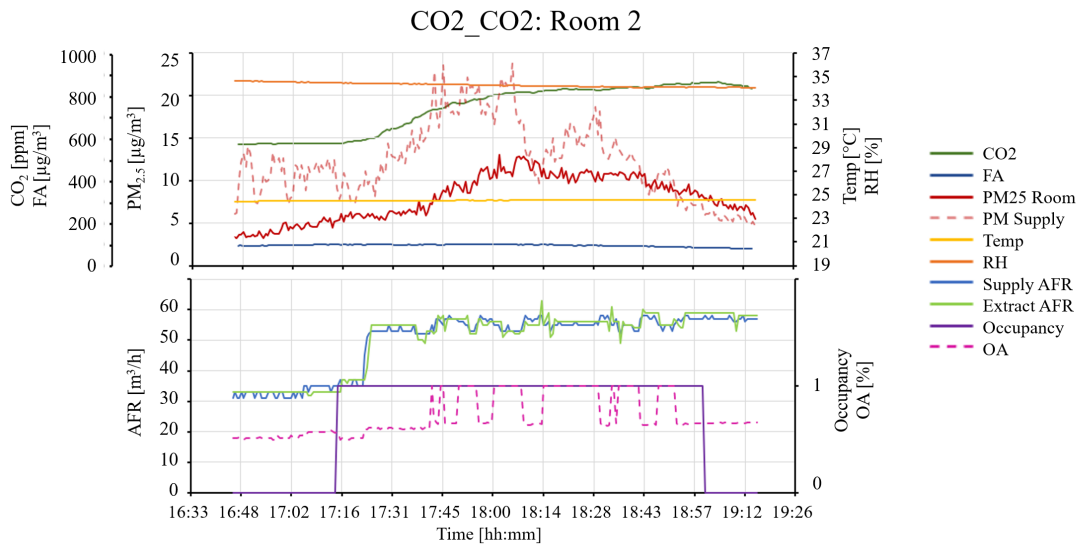


Figure B.8: CO₂ control with CO₂ recirculation control in room 2.

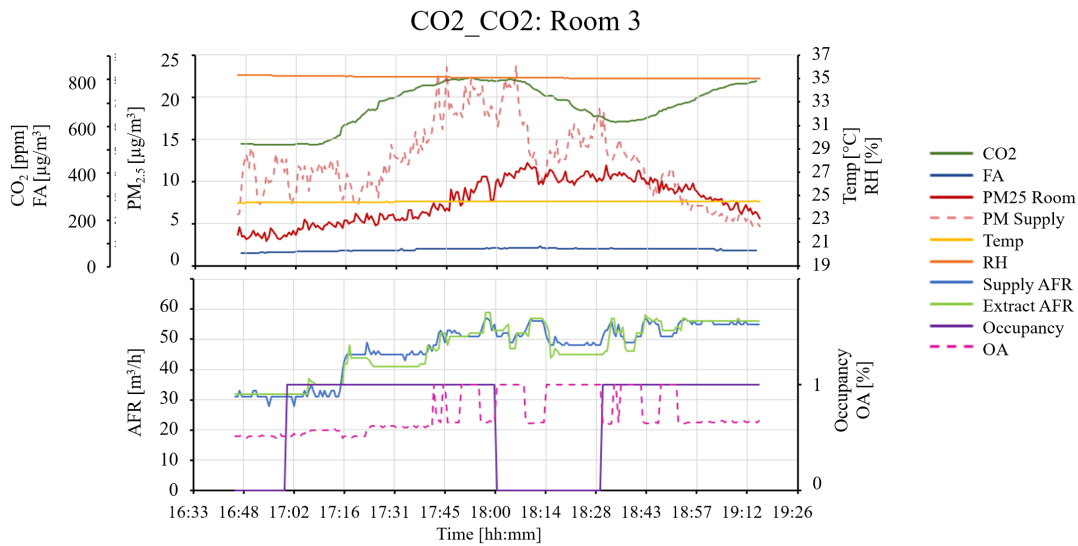


Figure B.9: CO₂ control with CO₂ recirculation control in room 3.

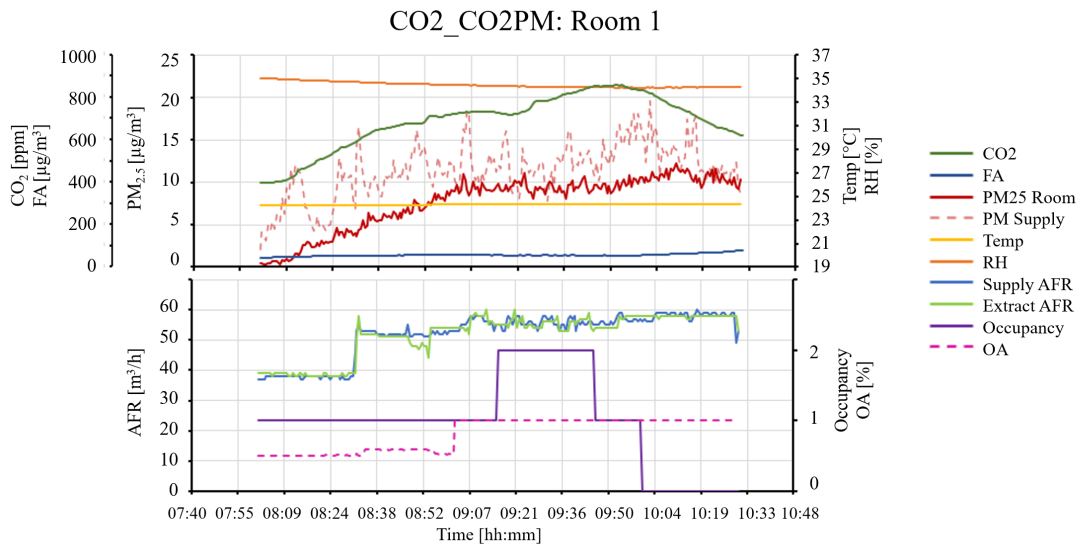


Figure B.10: CO2 control with CO2 and PM recirculation control in room 1.

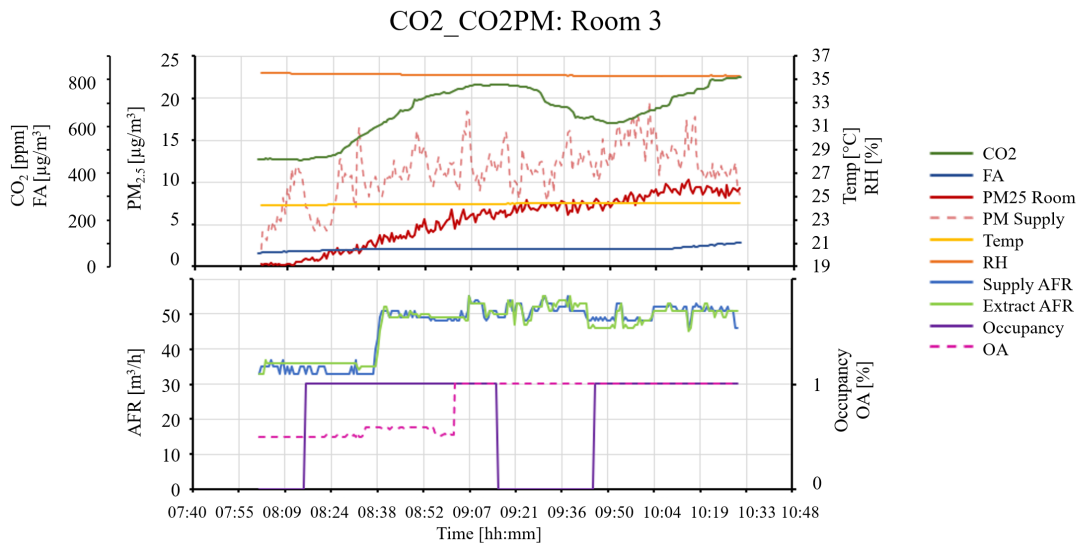


Figure B.11: CO2 control with CO2 and PM recirculation control in room 2.

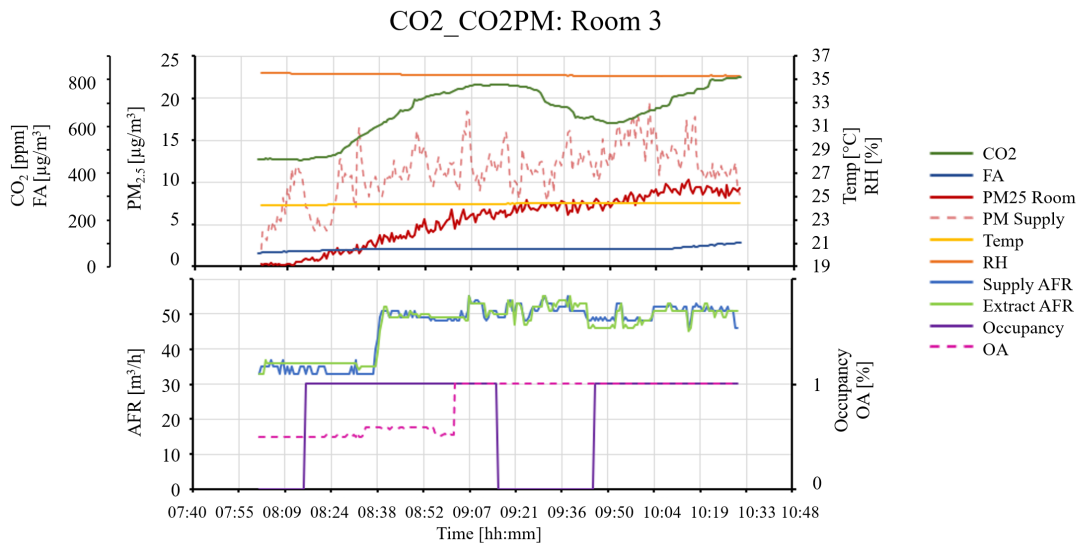


Figure B.12: CO2 control with CO2 and PM recirculation control in room 3.

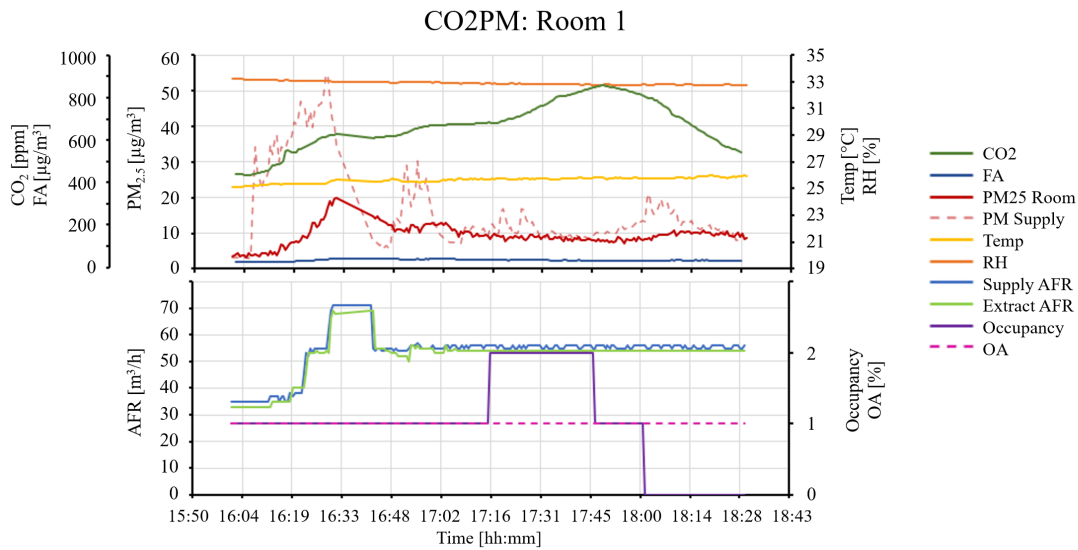


Figure B.13: CO2 and PM control without recirculation in room 1.

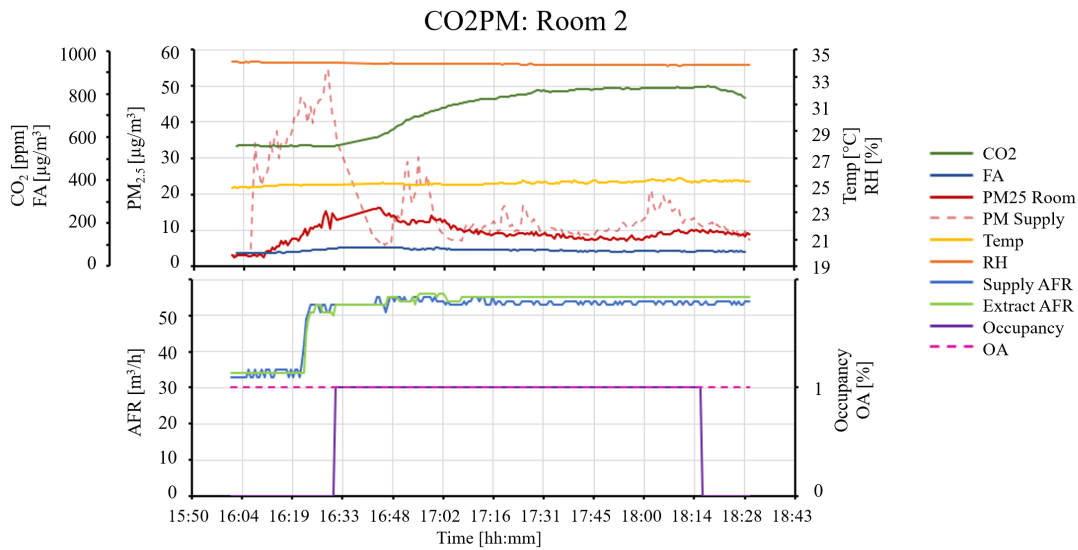


Figure B.14: CO2 and PM control without recirculation in room 2.

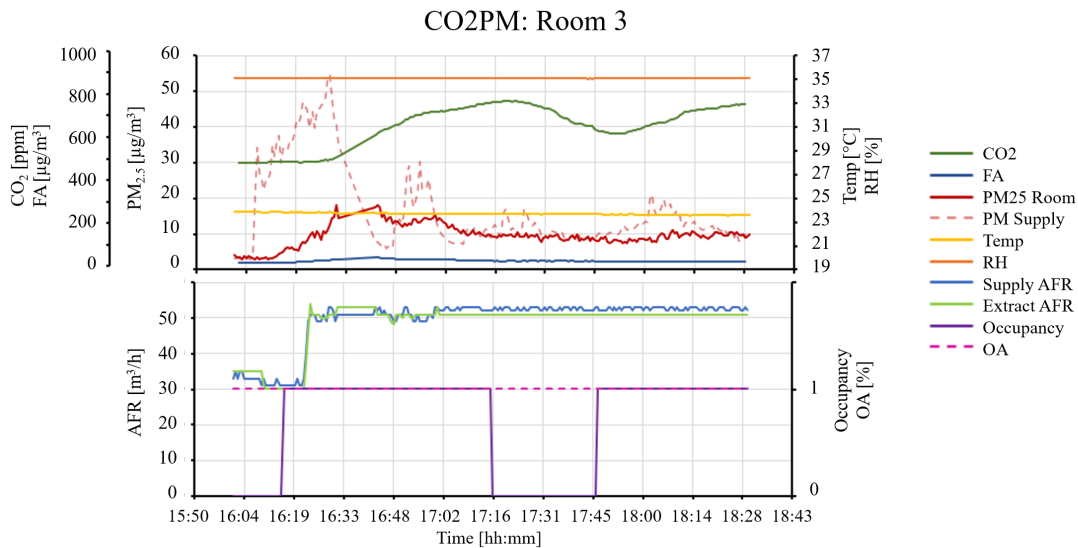


Figure B.15: CO2 and PM control without recirculation in room 3.

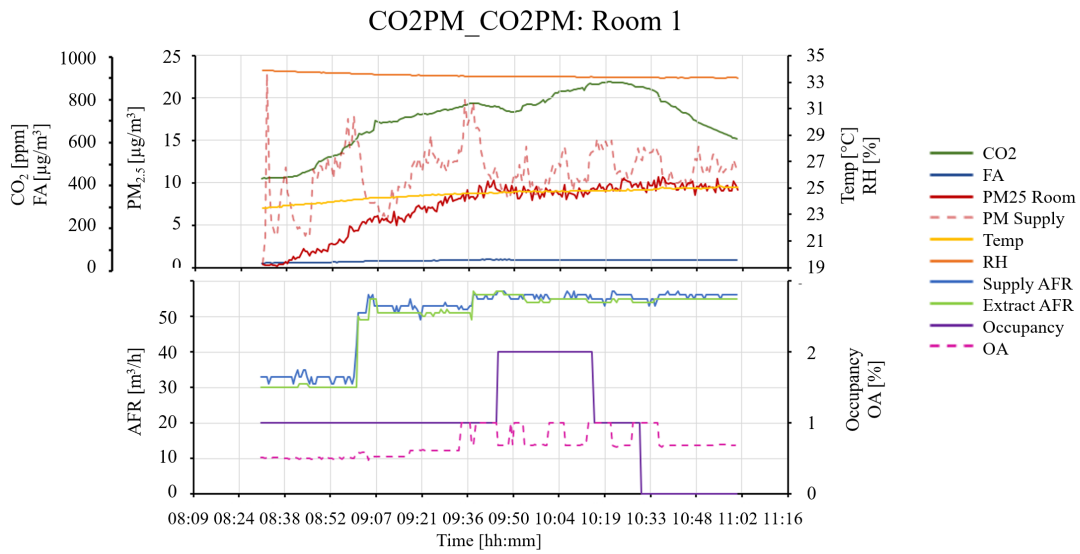


Figure B.16: CO₂ and PM control with CO₂ and PM recirculation control in room 1.

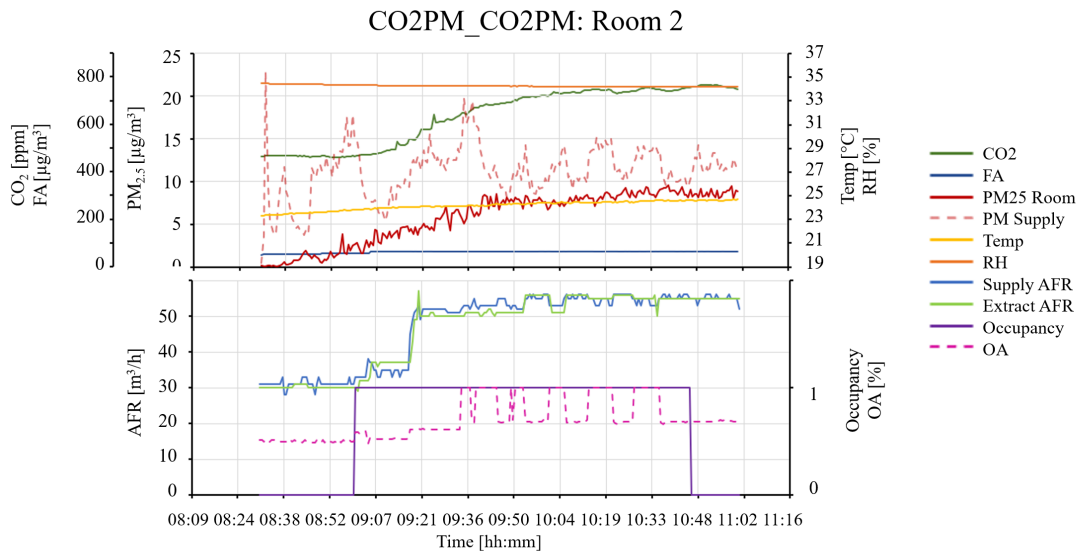


Figure B.17: CO₂ and PM control with CO₂ and PM recirculation control in room 2.

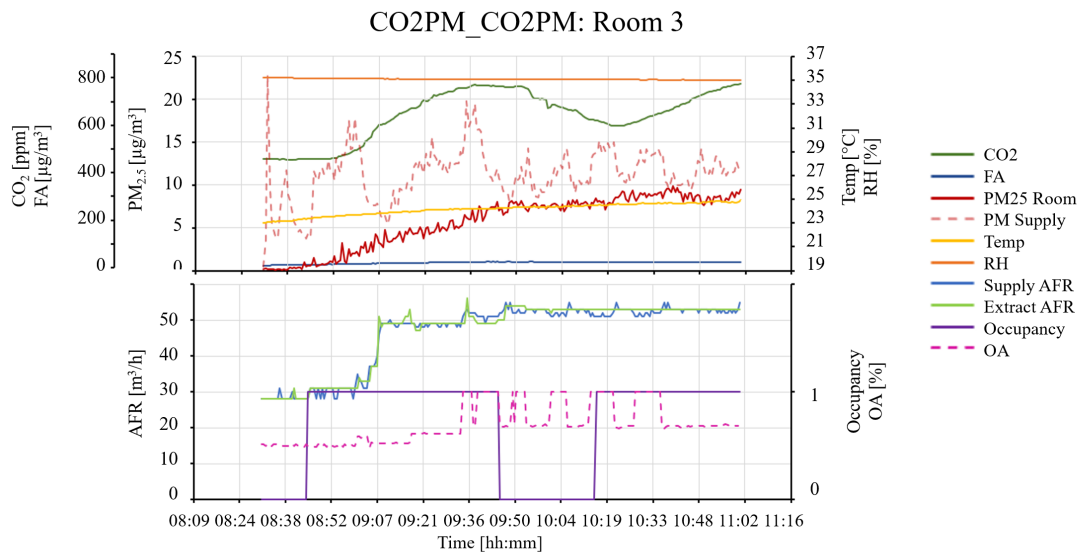


Figure B.18: CO₂ and PM control with CO₂ and PM recirculation control in room 3.

Appendix C

Results: Simulations Trondheim.

All figures from the simulations using Trondheim weather and outdoor concentration of pollutants is presented. Figure C.1-C.16 presents the various boxplots for each contaminant for all control strategies. Figure C.17 gives an overview of the annual energy use for each control strategy.

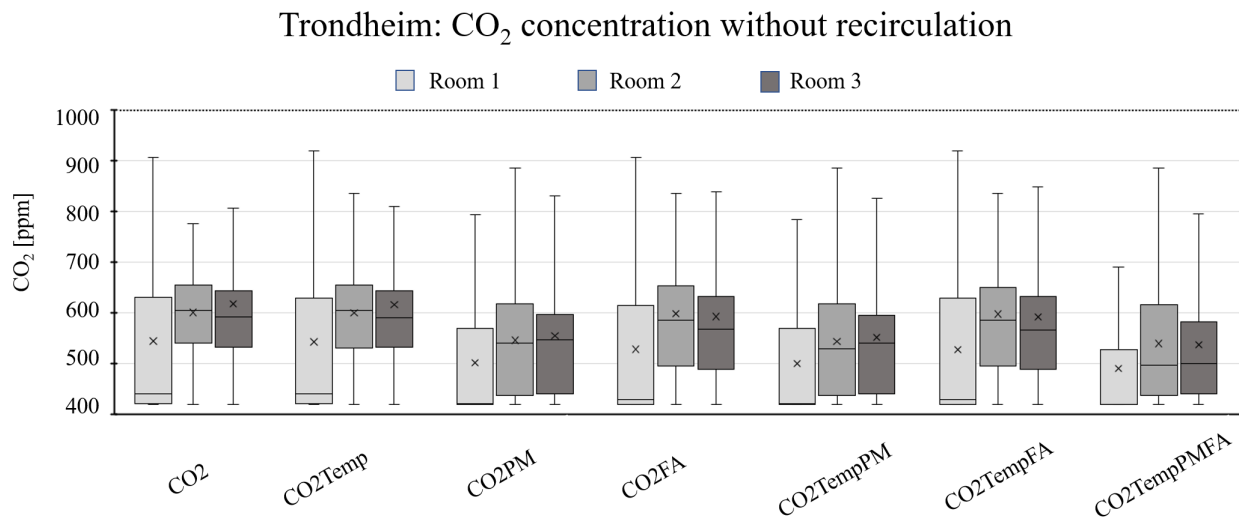


Figure C.1: CO₂ concentration over a year for room control strategies without recirculation.

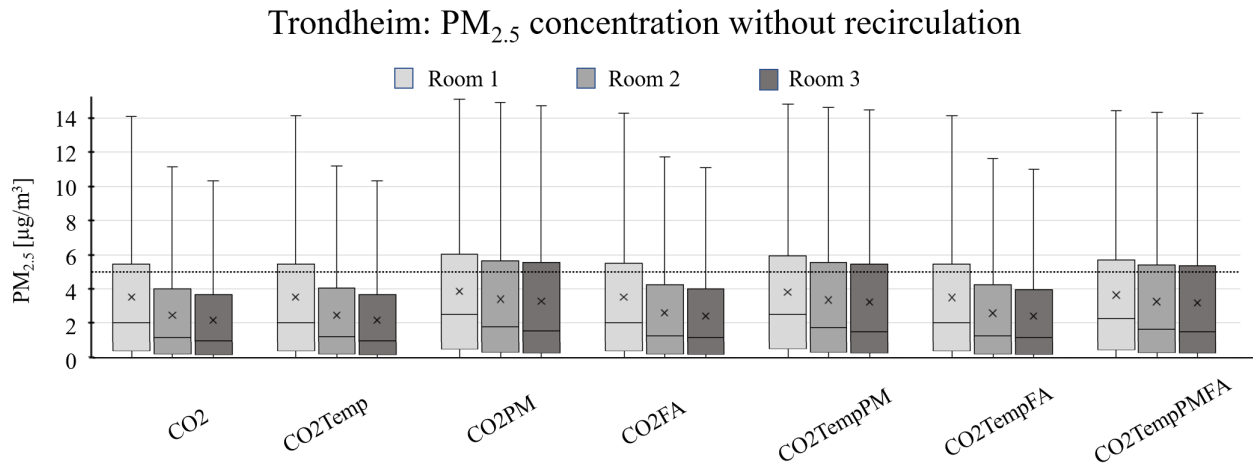


Figure C.2: PM_{2.5} concentration over a year for room control strategies without recirculation.

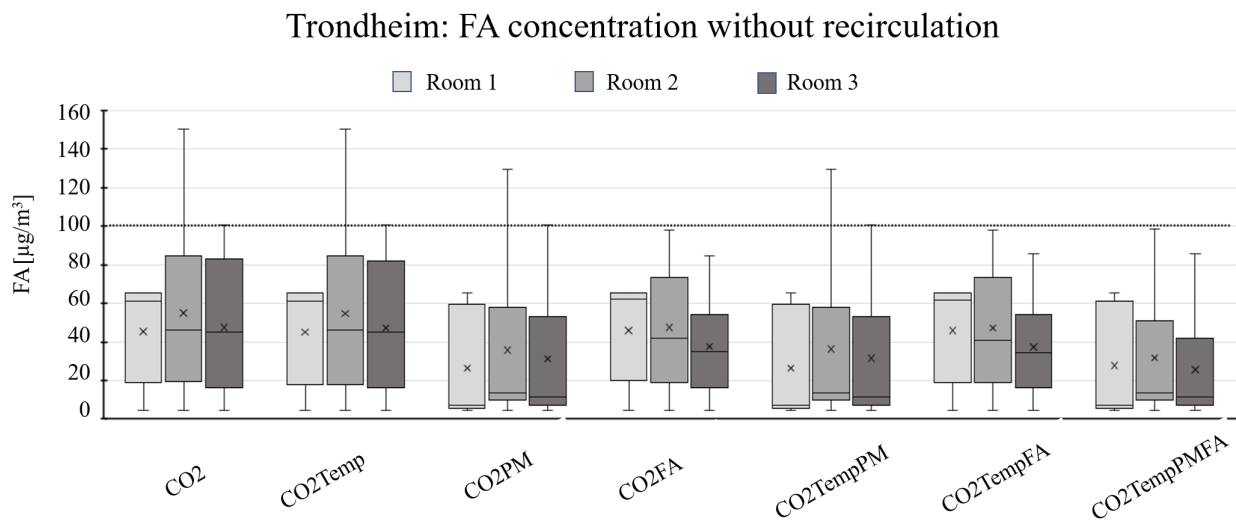


Figure C.3: FA concentration over a year for room control strategies without recirculation.

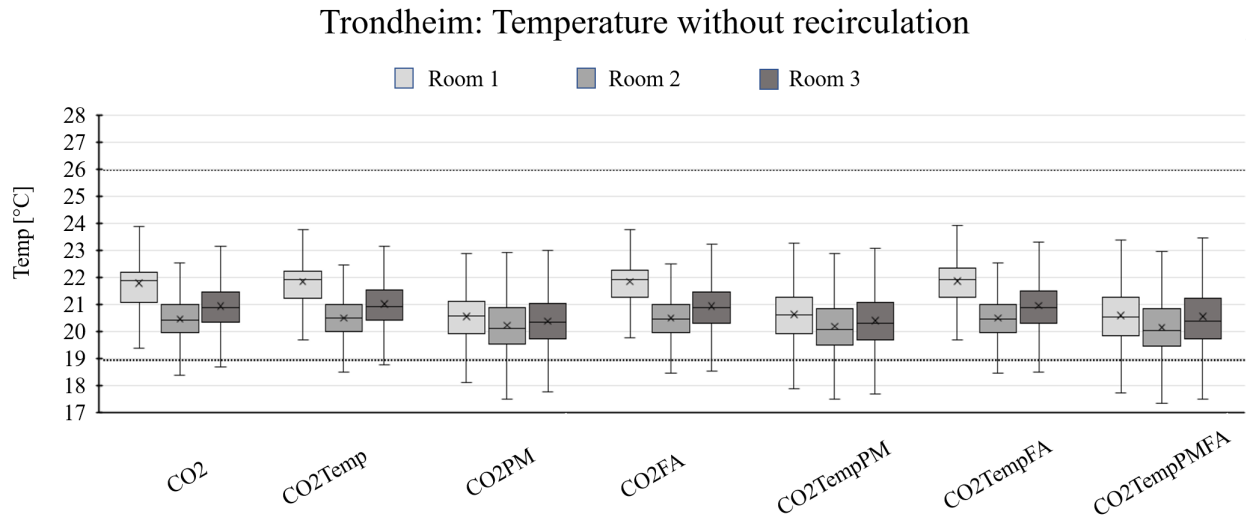


Figure C.4: Temperature over a year for room control strategies without recirculation.

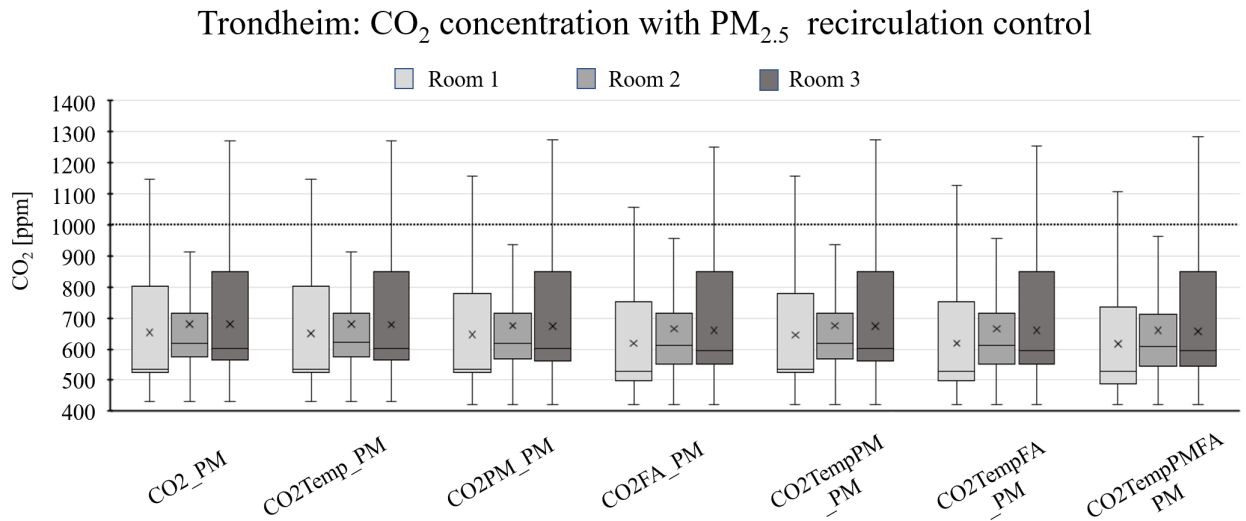


Figure C.5: CO₂ concentration over a year for room control strategies with PM_{2.5} as control parameter for recirculation.

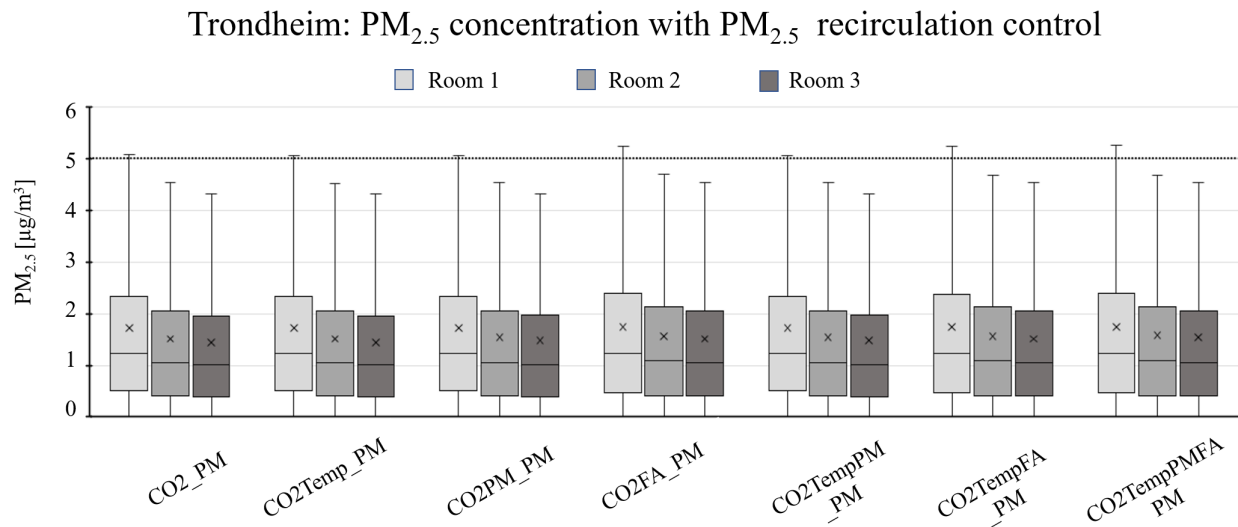


Figure C.6: PM_{2.5} concentration over a year for room control strategies with PM_{2.5} as control parameter for recirculation.

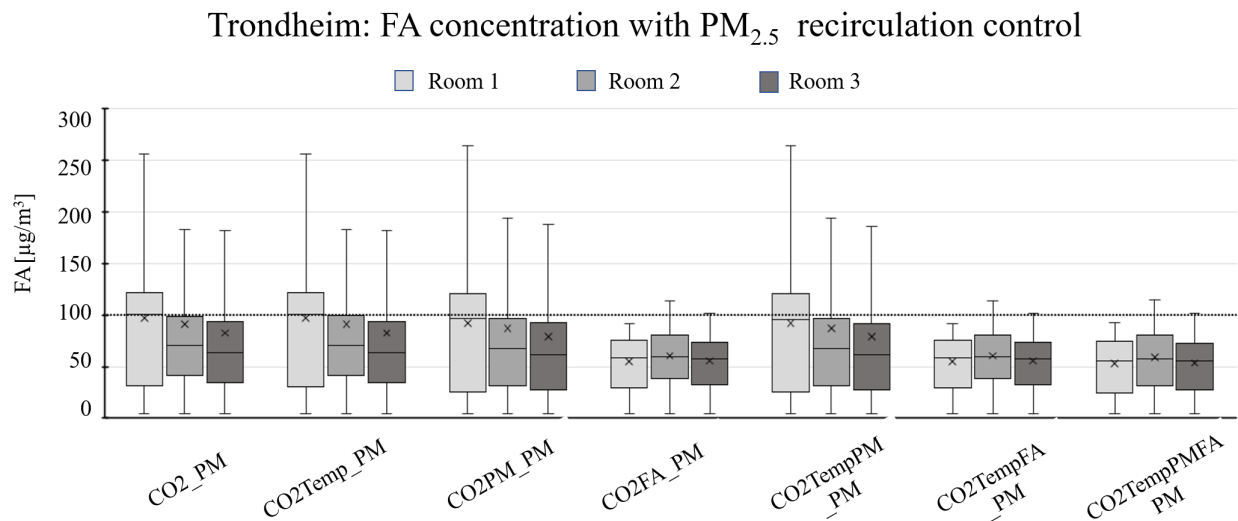


Figure C.7: FA concentration over a year for room control strategies with PM_{2.5} as control parameter for recirculation.

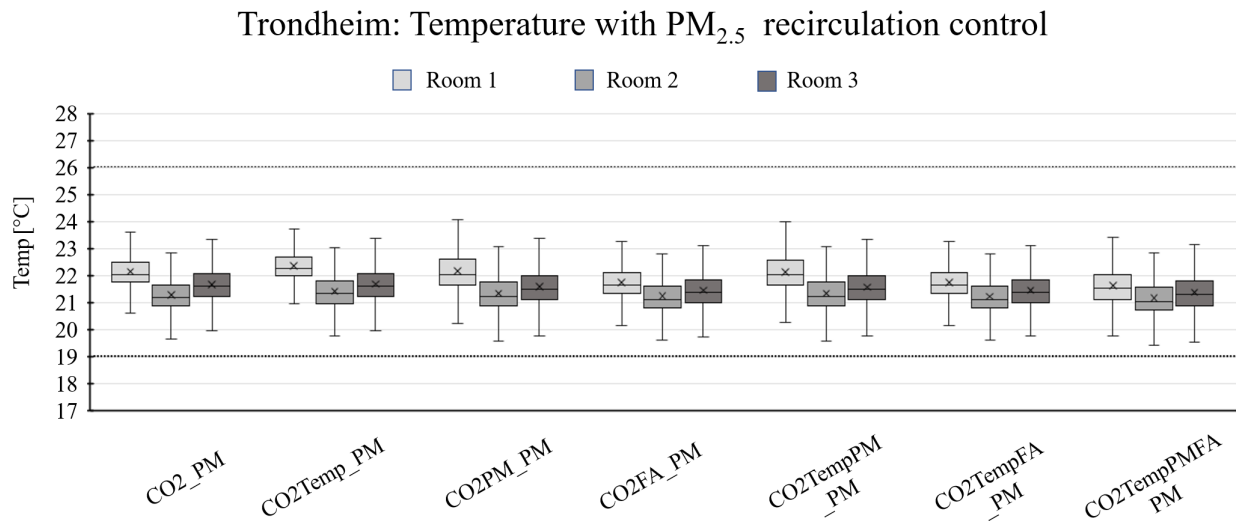


Figure C.8: Temperature over a year for room control strategies with PM_{2.5} as control parameter for recirculation.

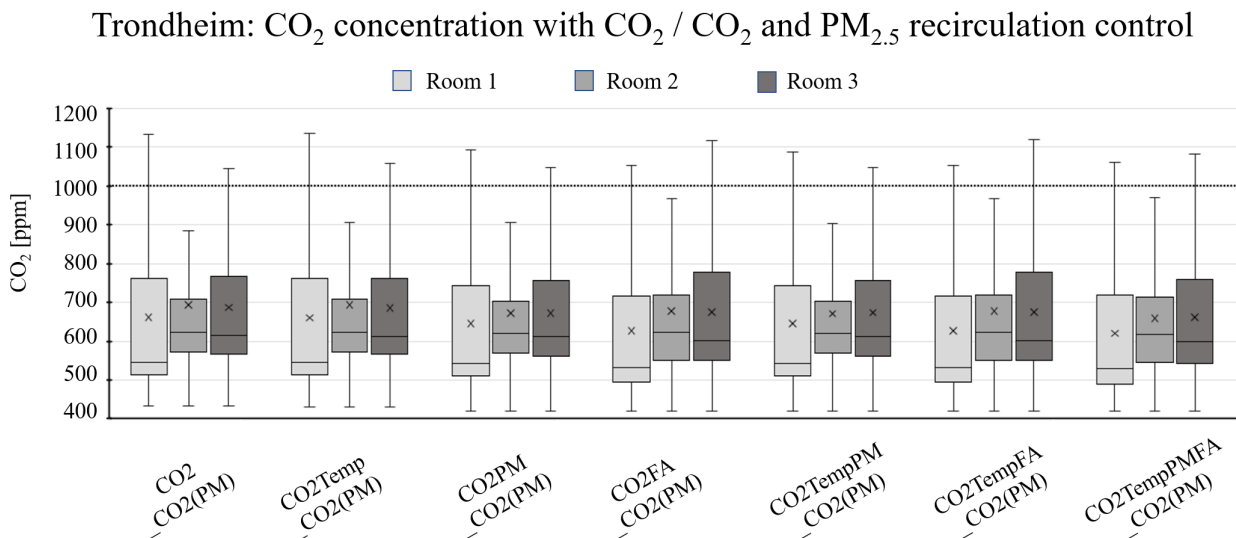


Figure C.9: CO₂ concentration over a year for room control strategies with CO₂ or CO₂ and PM_{2.5} as control parameters for recirculation.

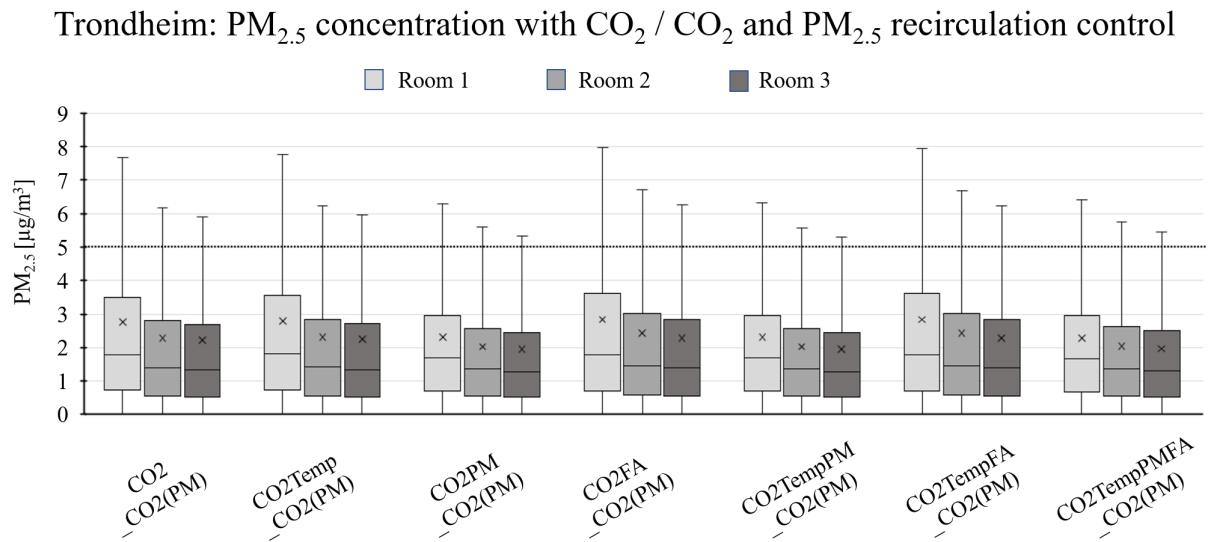


Figure C.10: PM_{2.5} concentration over a year for room control strategies with CO₂ or CO₂ and PM_{2.5} as control parameters for recirculation.

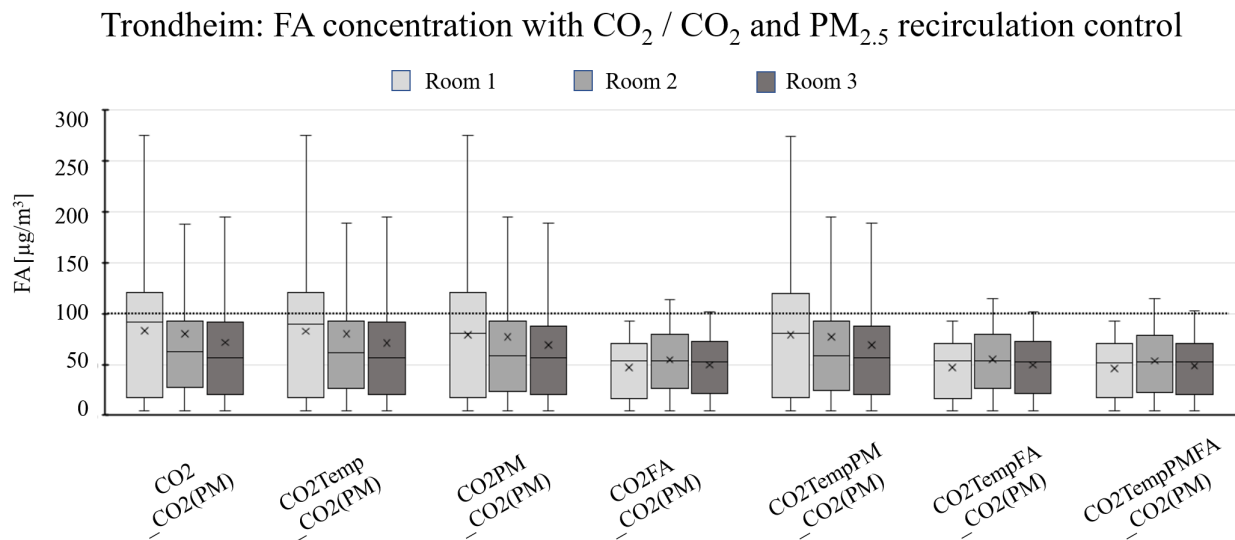


Figure C.11: FA concentration over a year for room control strategies with CO₂ or CO₂ and PM_{2.5} as control parameters for recirculation.

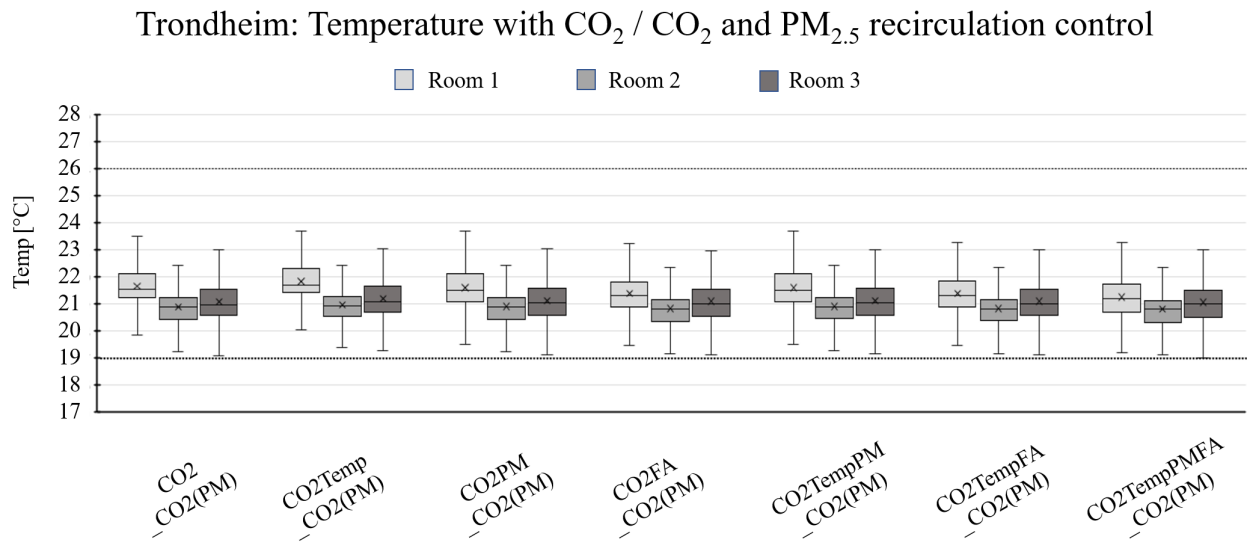


Figure C.12: Temperature over a year for room control strategies with CO₂ or CO₂ and PM_{2.5} as control parameters for recirculation.

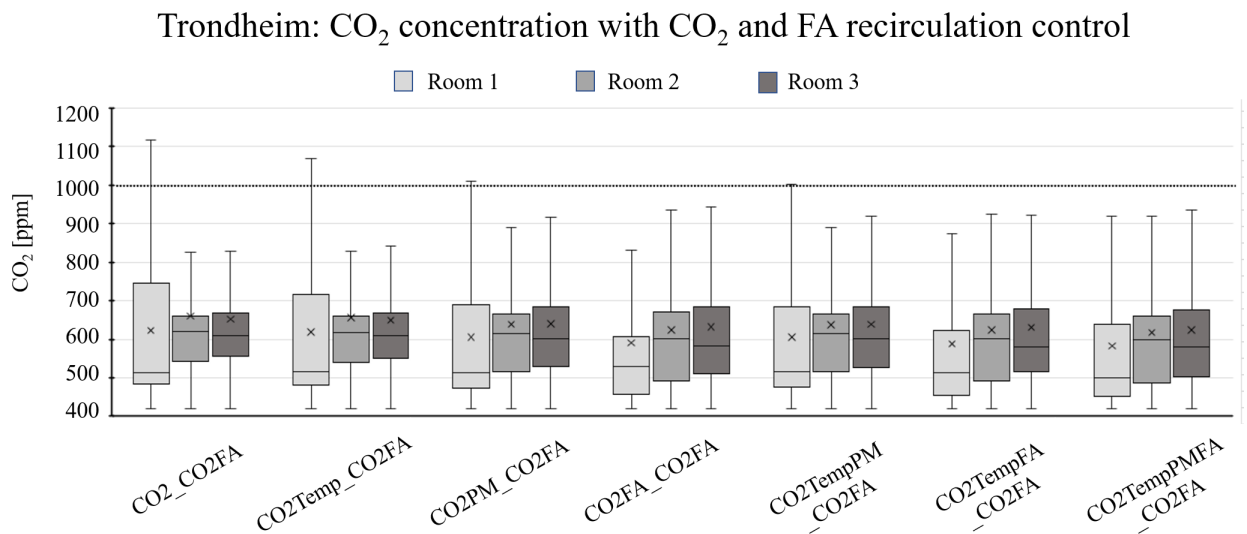


Figure C.13: CO₂ concentration over a year for room control strategies with CO₂ and FA as control parameter for recirculation.

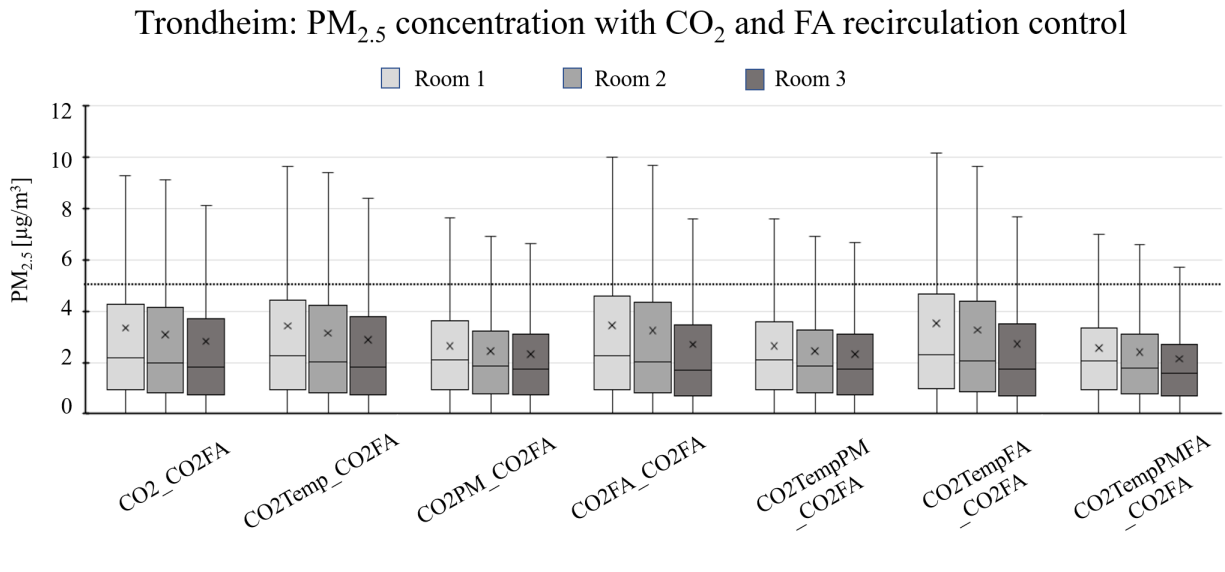


Figure C.14: PM_{2.5} concentration over a year for room control strategies with CO₂ and FA as control parameter for recirculation.

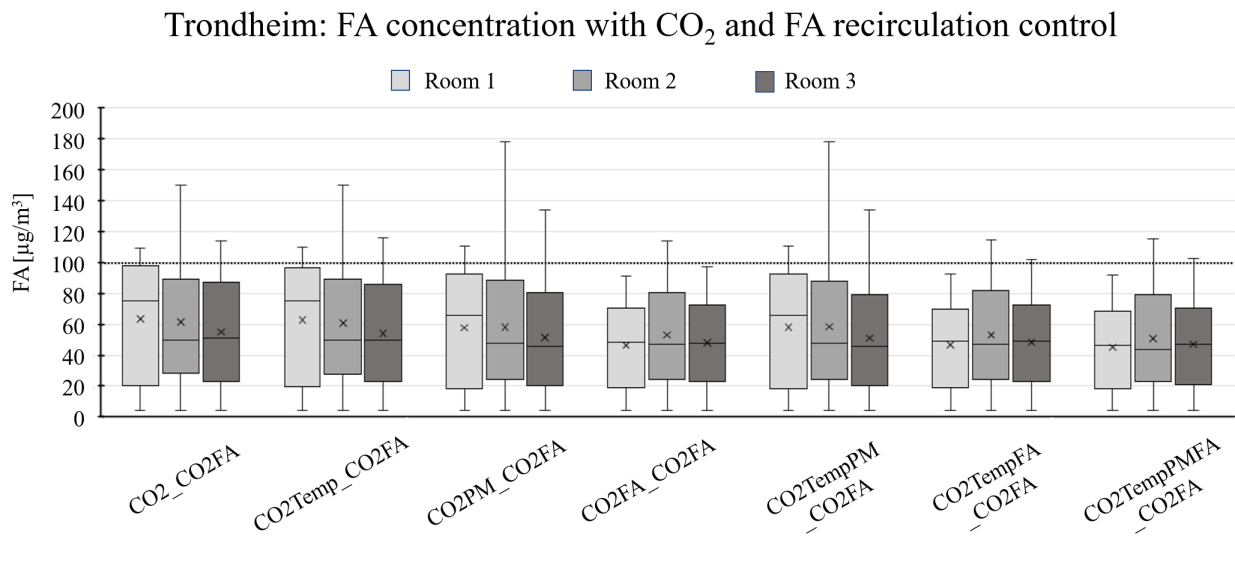


Figure C.15: FA concentration over a year for room control strategies with CO₂ and FA as control parameter for recirculation.

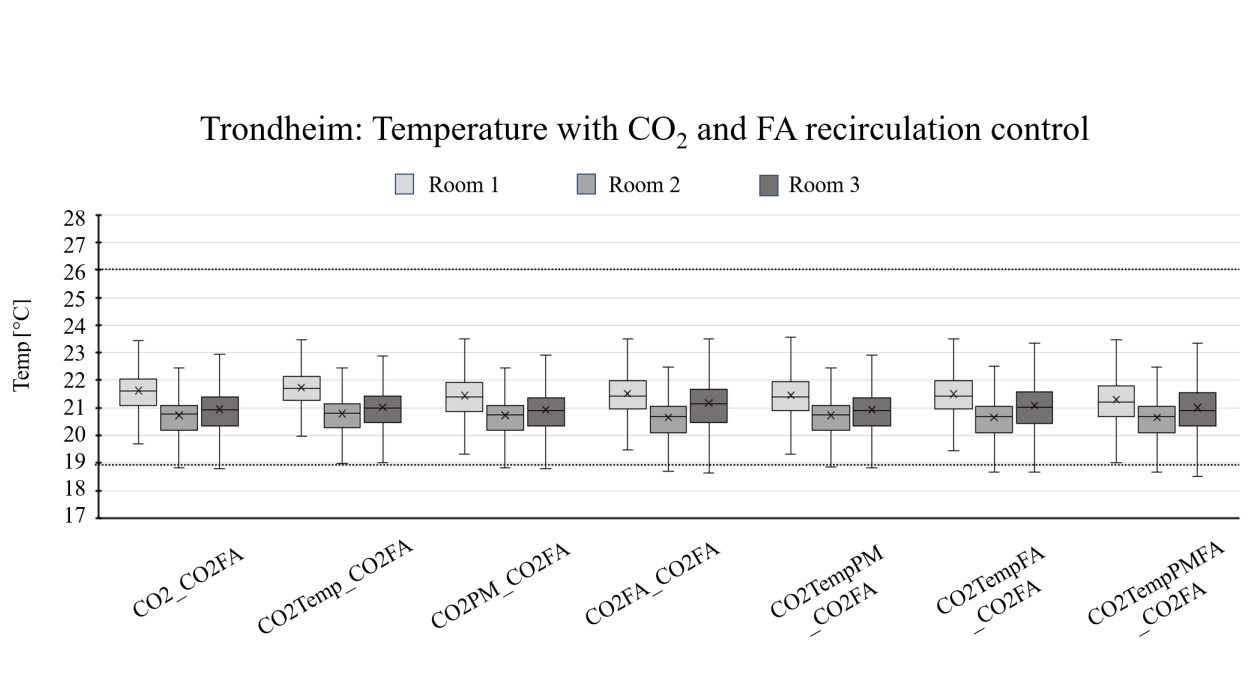


Figure C.16: Temperature over a year for room control strategies with CO₂ and FA as control parameter for recirculation.

Total Annual Energy Consumption in Trondheim [kWh]

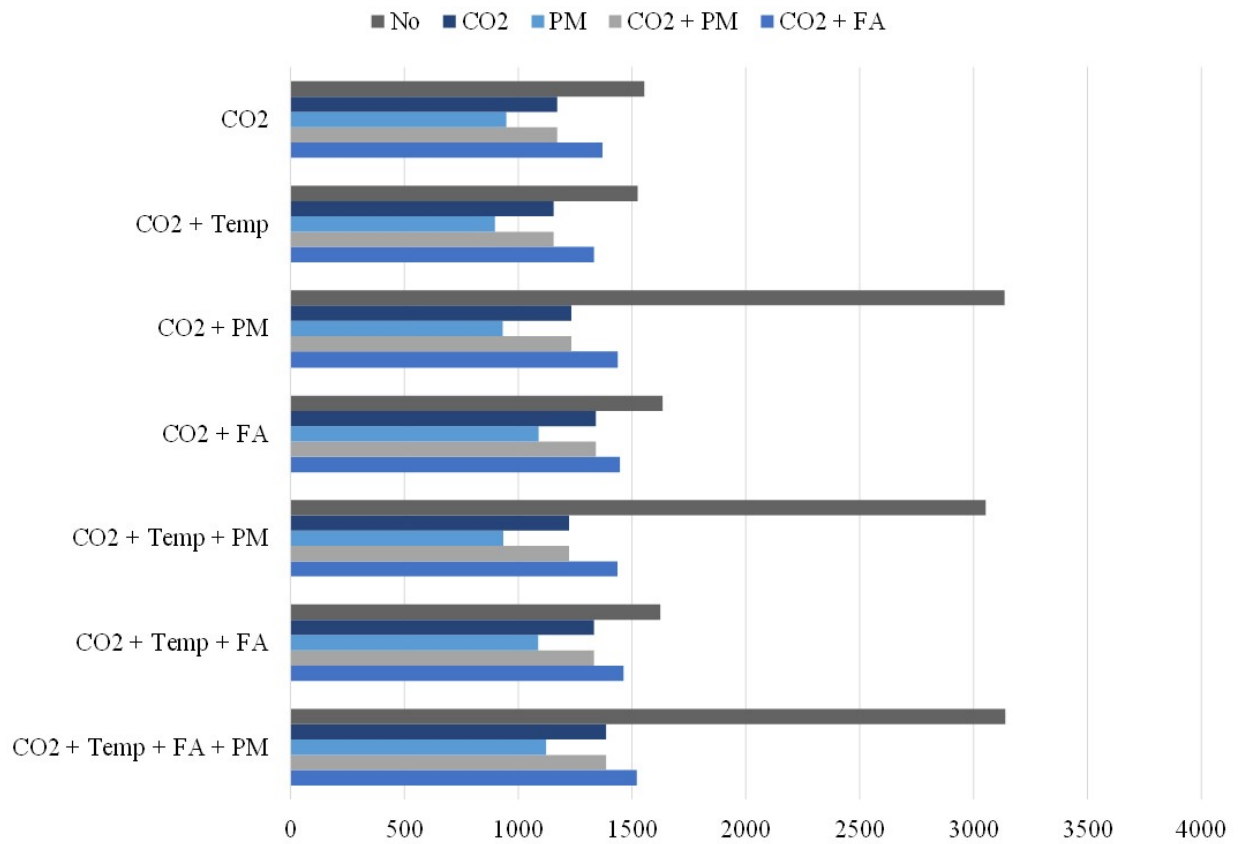


Figure C.17: Total yearly energy consumption for simulations using Beijing weather and outdoor pollution levels.

Appendix D

Formaldehyde

The experiments showed high FA concentrations in room 2 compared to room 1 and 3. Thus, a test was conducted to compare the three sensors in each room to see if the reasons for high concentrations in room 2 were due to sensor differences or if it is actually higher concentrations in room 2 than in the others. During the test, the three sensors that were placed in the various rooms during the control strategy experiments were all placed together on the table in room 2. The results of this test are presented in Figure D.1. The results show that the sensor which was placed in room 2 during the control strategy experiments measured higher concentrations than the two others.

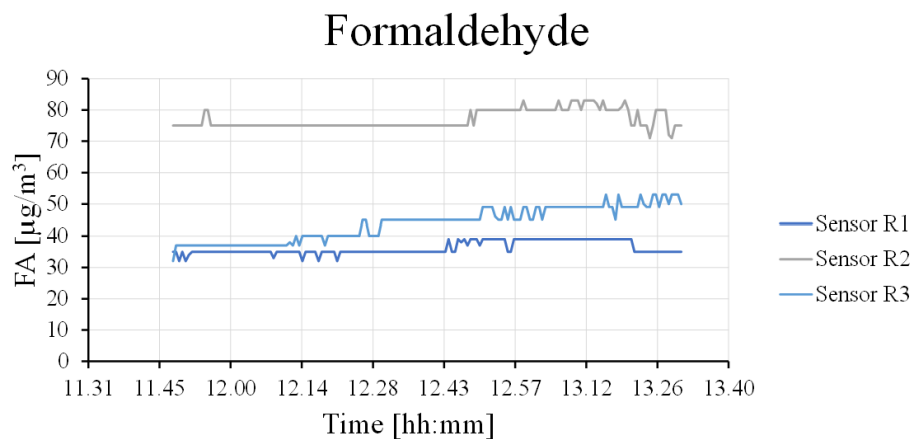


Figure D.1: FA measured at same place for three different sensors.

Appendix E

Datasheets

E.1 Datasheets for the Ventilation System Components

In the following the relevant pages from datasheets for the main components of the ventilation system is presented.

E.1.1 Air Handling Unit

UNI 3 Luftbehandlingsaggregat



Ventilasjonsaggregat for småhus, eneboliger og mindre næringsbygg.

A

700040, 700041, 700042, 700043

- Temperaturvirkningsgrad i varmegjenvinner opp til 85 %.
- Spesifikk vifteeffekt i ventilasjonsanlegg (SFP) lavere enn 1,5.
- Ekstra stillegående.
- Enkel betjening, enkelt filterbytte og vedlikehold.
- Gir balansert ventilasjon med et svært godt inneklima.
- Mulighet for kommunikasjon via modbus.
- Moderne design.
- Effektiv og driftssikker - også i kulde.

	NOBB	GTIN	Modell
700040	43836217	7023677000404	UNI 3 RER høyremodell, EC-vifter, med el.batteri
700041	43836255	7023677000411	UNI 3 REL venstremodell, EC-vifter, med el.batteri
700042	43836395	7023677000428	UNI 3 R R høyremodell, EC-vifter, uten batteri
700043	43836414	7023677000435	UNI 3 R L venstremodell, EC-vifter, uten batteri

Tekniske data

	UNI 3 RE	UNI 3 R
Merkespenning	230v 50Hz	230v 50Hz
Sikringsstørrelse	10A	10A
Merkestrøm total	6,16 A	1,4 A
Merkeeffekt total	1 416 W	216 W
Merkeeffekt elbatteri	1 200W	
Merkeeffekt vifter	2x106W	2x106W
Merkeeffekt forvarme	-	-
Viftetype	B-hjul	B-hjul
Viftemotorstyring	0-10V	0-10V
Viftehastighet - max. turtall	3 390 rpm	3 390 rpm
Automatikk standard	CU60	CU60
Filtertype (TIL/FRA)	ePM1 55% (F7)	ePM1 55% (F7)
Filtermål (BxHxD)	419x192x31 mm	419x192x31 mm
Vekt	67kg	67kg
Kanaltilkobling	Ø160 mm*	Ø160 mm*
Høyde	700 mm	700 mm
Bredde	720 mm	720 mm
Dybde	520 mm	520 mm

*Kjøkkentilkobling Ø125mm

Energiklasse:



CTRL 0,65

LOKAL BEHOVSTYRING

Styring med sensor for ulike soner

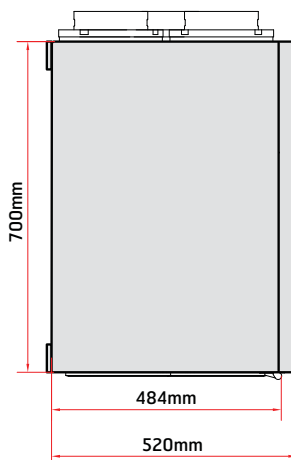
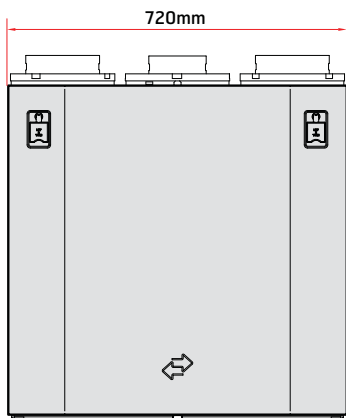
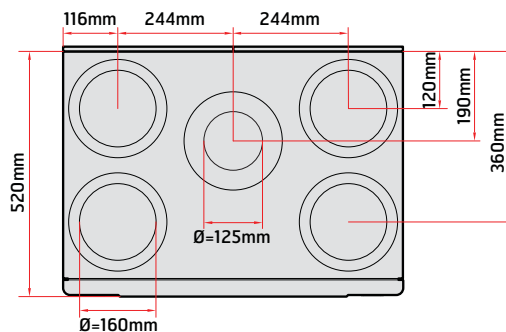
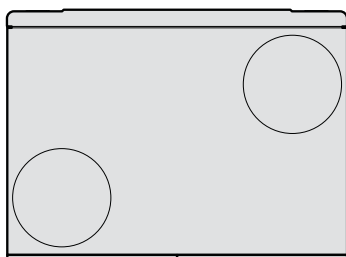
Tilbehør: Avansert panel +

CO₂-føler/ bevegelsesvakt + spjeld

Resultat: Økt luftmengde i soner som har behov

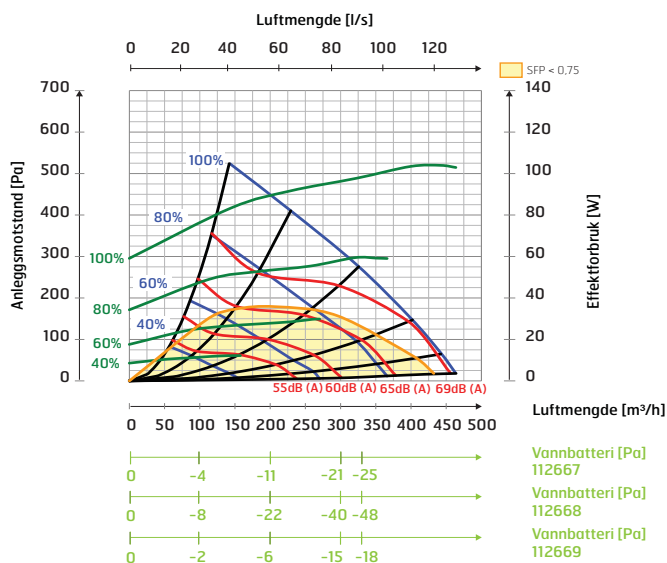
www.flexit.no

Målskisse

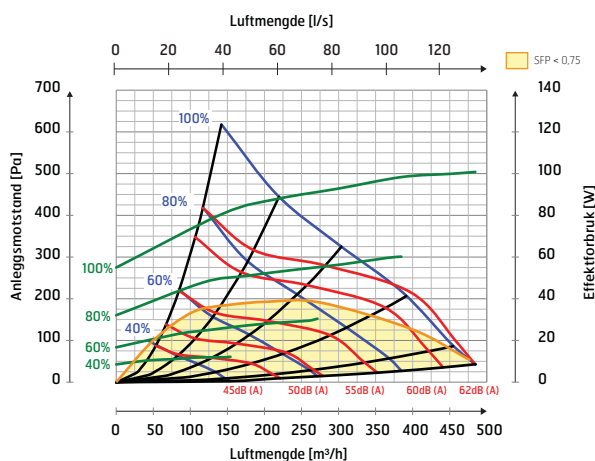


Kapasitetsdiagram/Lyddata

Tilluftside



Avtrekkside



Korreksjonsfaktor for Lw

Hz	63 Lw(dB)	125 Lw(dB)	250 Lw(dB)	500 Lw(dB)	1000 Lw(dB)	2000 Lw(dB)	4000 Lw(dB)	8000 Lw(dB)	LwA (dBA)
Tilluft	7	5	4	-2	-9	-13	-23	-28	
Avtrekk	8	8	0	0	-15	-21	-31	-32	
Avstrålt	-17	-10	-13	-29	-38	-38	-41	-37	-19

Forklaring til diagram

Lyddata er angitt som lydeffektnivå LwA i kapasitetsdiagrammene (dette er lyd til kanal). Disse verdiene kan korrigeres ved hjelp av tabellen for de ulike oktavbåndene om man ønsker å se på Lw (uten tilpasning til A-bånd).

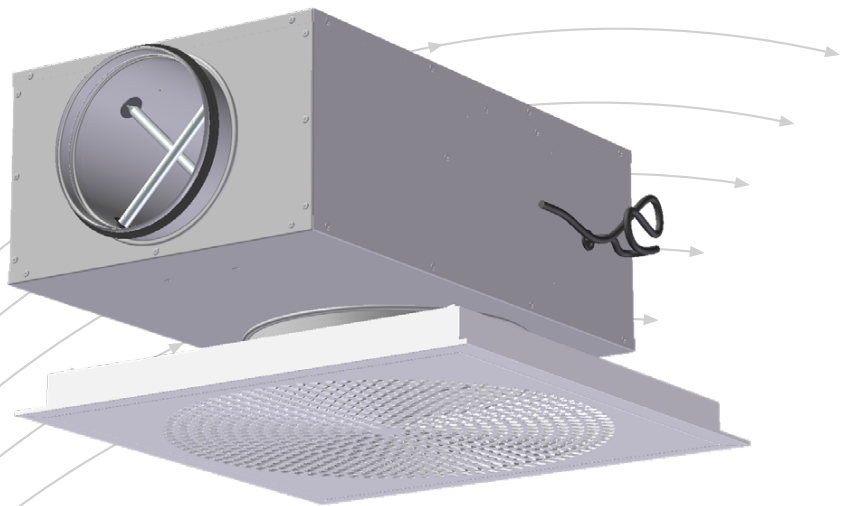
Korreksjonstabellen for respektive oktaver er angitt i Lw, noe som innebærer at man etter omregning pr. oktav for tilluft og avtrekk, får disse verdiene i Lw.

Avstrålt lyd fra aggregatet skal beregnes ut fra tilluftsdiagrammet.

E.1.2 Onrion LØV with Sirius Supply diffuser

Orion-LØV with Sirius

VAV box for supply diffuser



- Unique damper function
- Extensive working range
- Belimo MP-Bus
- MOD/BACnet
- LONWORKS
- Belimo KNX

TROX[®] TECHNIK

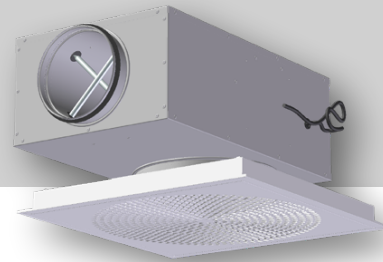
 **Auranor**

TROX Auranor Norge AS

PO Box 100
NO-2712 Brandbu

Telephone: +47 61 31 35 00
Fax: +47 61 31 35 10
E-mail: firmapost@auranor.no
www.trox.no

Orion-LØV with Sirius



APPLICATION

Orion-LØV with Sirius is a diffuser unit with VAV function, and is used as volume flow controller and diffuser in ventilation systems to enable air flow rates to be set as per requirements. Orion-LØV offers excellent induction, and is ideal for variable air flow rates.

FUNCTION

Orion-LØV with Sirius has a built-in VAV controller for adjustment of air flow rates according to requirements. The damper solution will choke the pressure at high flow rates and will maintain a low sound level. This may reduce the need for additional dampers and sound attenuators in a duct system. Orion-LØV with Sirius is delivered with Belimo MP-bus, LON, MOD/BACnet or Belimo KNX for direct BUS communication to SD systems.

Deviation for working range 10 - 20% of V_{nom} : $\pm 25\%$
 20 - 40%: of V_{nom} $< \pm 10\%$
 40 - 100%: of V_{nom} $< \pm 4\%$

If T-pipes are used, a spacing of at least $5 \times \varnothing D$ is recommended in order to maintain the measurement accuracy.

The diffuser front can be supplied with integrated motion sensor or motion/temperature sensor.

Motion/temperature sensor is only to be used together with X-AIRCONTROL

Product sheet for Motion and motion/temperature sensor can be found by following this link:

https://www.trox.no/en/downloads/34aa782bc9b95f08e/Orion-X-Sense-GB-.pdf?type=product_info

DESIGN

Orion-LØV with Sirius is a complete measuring and control unit where the air flow rates in ventilation systems can be set as required. At the measuring station, the differential pressure is measured by using measuring rods integrated in the unit. Sirius is equipped with LHV.D3 VAV controller from Belimo. Controller specifications are provided in the table below.

Full technical documentation can be downloaded from www.belimo.eu. Orion-LØV features a removable front panel with LØV perforation, and is suitable for a range of ceiling systems.

Actuator	LHV-D3-MP / MOD/BACnet / LON
Operating voltage	AC 24 V 50/60 Hz, DC 24 V
Power drain	2,5W
Dim. effect	4.5VA (max.8 A @5 ms)

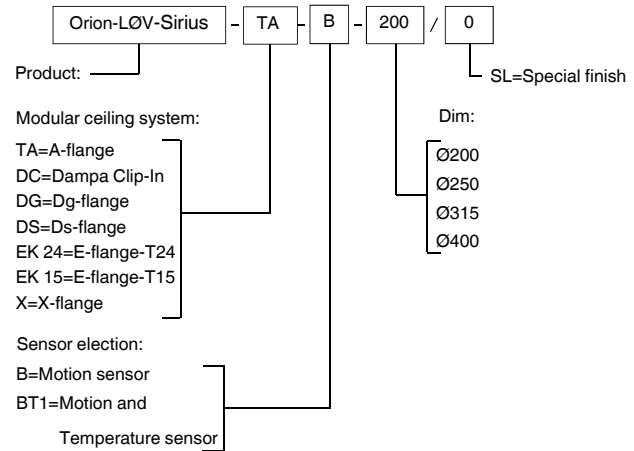
Table 1: Technical specifications, Belimo VAV controller

MATERIALS AND SURFACE COATING

Sirius comes in a galvanised steel design. The measurement unit is in aluminium, and hoses and nipples are in plastic.

The damper is equipped with polyester material, and the connection collar is fitted with EPDM rubber gasket.

ORDER CODE, diffuser - Orion-LØV Sirius



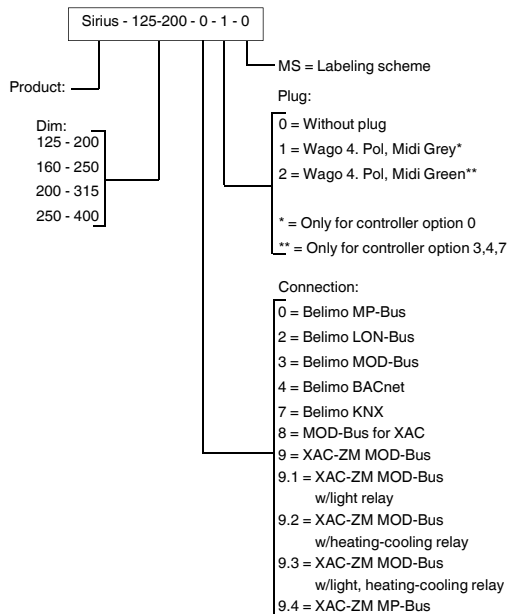
Example:

Orion-LØV-Sirius-TA-B-200/0

Explanation:

Orion-LØV-Sirius supply diffuser with A flange for T-profile ceiling system, motion sensor in diffuser front, spigot Ø200

ORDER CODE, Sirius



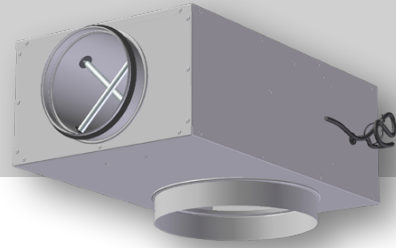
Example:

Sirius-125-200-0-1-0

Explanation:

Sirius with Ø125 inlet and Ø200 outlet, with Belimo MP-Bus, Wago-plug mounted, without labeling scheme.

Orion-LØV with Sirius



QUICK SELECTION, Orion-LØV with Sirius

Sirius dim.	[open] m ³ /h		
	25dB(A)	30dB(A)	35dB(A)
125	155	184	220
160	256	310	374
200	374	446	529
250	526	626	749

Sirius dim.	(75Pa) m ³ /h		
	25dB(A)	30dB(A)	35dB(A)
125	144	184	220
160	234	295	374
200	367	443	529
250	342	569	734

Table 2: Quick selection, Orion-LØV with Sirius

Sirius ØD.	(m ³ /h)	
	Minimum	Maximum
125	26	265
160	43	434
200	70	700
250	106	1060

Table 3: Adjustment range for VAV controller, air flow rate in m³/h.
See calculation diagram for sound power level and pressure drop.

DIMENSIONS AND WEIGHT, Orion-LØV with Sirius

Dim.	D	DA	B	H	L	L1	Weight Sirius [kg]	Weight Sirius with valve [kg]
125-200	124	202	325	175	645	386	8	12
160-250	159	252	360	210	645	402	9	13
200-315	199	317	400	240	645	435	10,5	14,5
250-400	249	402	450	290	645	392	12	16

Table 4

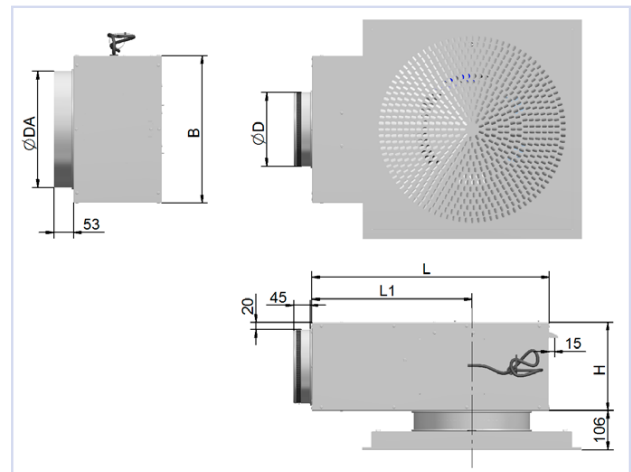


Fig. 1: Dimensions, Orion-LØV with Sirius

Orion-LØV with Sirius



ACOUSTIC DATA

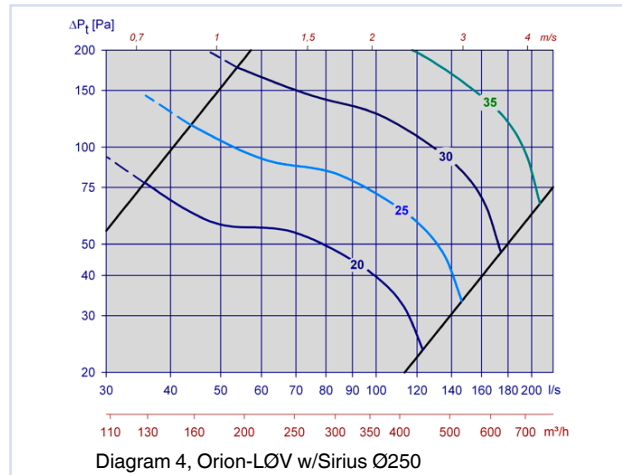
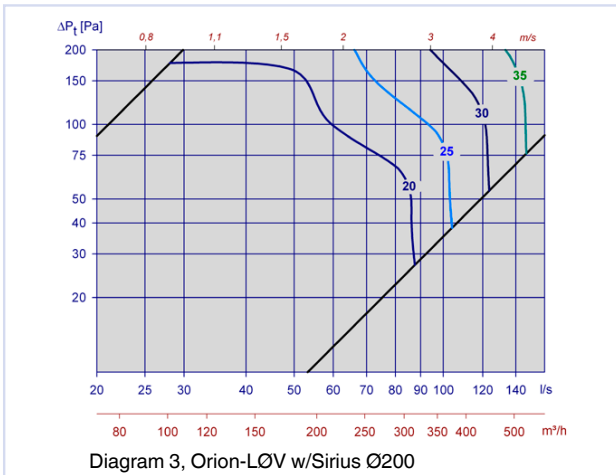
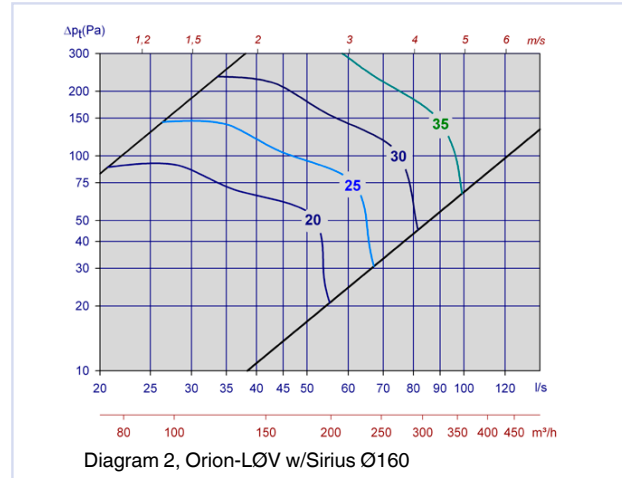
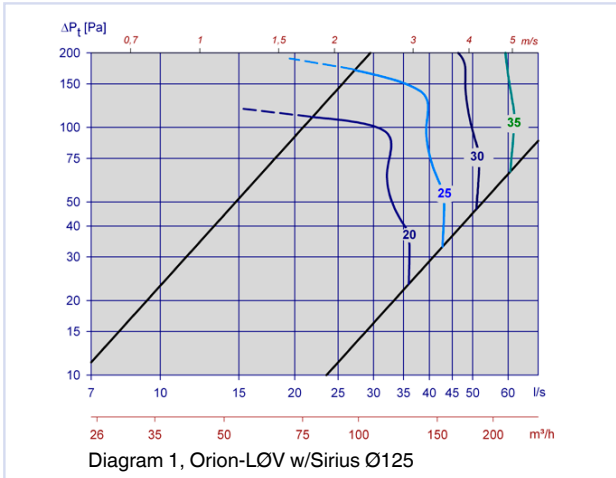
The diagrams provide a summary of the A-weighted sound power level from diffuser, L_{WA} . Correction factors in table 5, page 5, are used to calculate emitted sound power level at the respective frequencies, $L_W = L_{WA} + KO$. A room with absorption equivalent to $10m^2$ Sabine will have a sound pressure level which is 4 dB below the sound power level emitted.

Example:

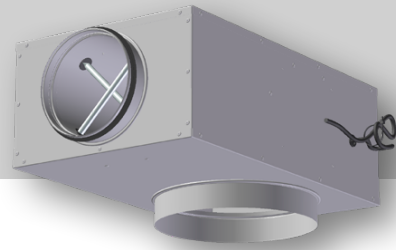
Sirius 125 with Orion-LØV supply diffuser, desired volume flow 50 l/s. From diagram 1, we find that $L_{WA} = 26$ dB(A) with open damper and 45 Pa total pressure drop. The aim is to find the following data:

- Emitted sound power level at 250 Hz
- A-weighted total sound pressure level from diffuser in an office with 4dB room attenuation.
- A-weighted sound pressure level in an office at 75 Pa total pressure loss, i.e. 30 Pa choking with the unit's damper.
 - The correction factor for 250 Hz -2 dB.
Emitted sound power at 250 Hz is then:
 $L_W = L_{WA} + KO = 29 + (-2) = 27$ dB
 - With room attenuation equivalent to 4 dB, A-weighted sound pressure level is: $29 - 4 = 25$ dB(A)
 - At the operating point of 50 l/s and 75 Pa total pressure loss, the diagram indicates 29dB(A). With 4dB room attenuation the sound pressure level in the room will be: $29 - 4 = 25$ dB(A)

CALCULATION DIAGRAM



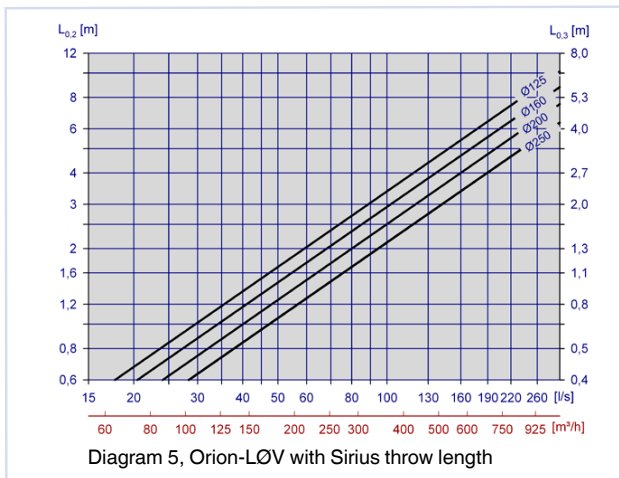
Orion-LØV with Sirius



Sirius dim.	Right pressure drop line (open)								Left pressure drop line (heavily choked)							
	63	125	250	500	1k	2k	4k	8k	63	125	250	500	1k	2k	4k	8k
125	4	-1	-2	-1	-6	-11	-15	-11	2	-3	-4	-9	-6	-6	-8	-9
160	2	1	0	-1	-8	-13	-13	-9	1	-1	-3	-6	-4	-11	-11	-9
200	2	1	-2	-1	-6	-12	-14	-10	1	0	-3	-5	-5	-9	-9	-9
250	3	2	-1	-1	-7	-13	-13	-10	2	2	-1	-3	-6	-11	-10	-9

Table 5: Correction factor, Orion-LØV with Sirius

THROW LENGTH



FLOW PATTERN

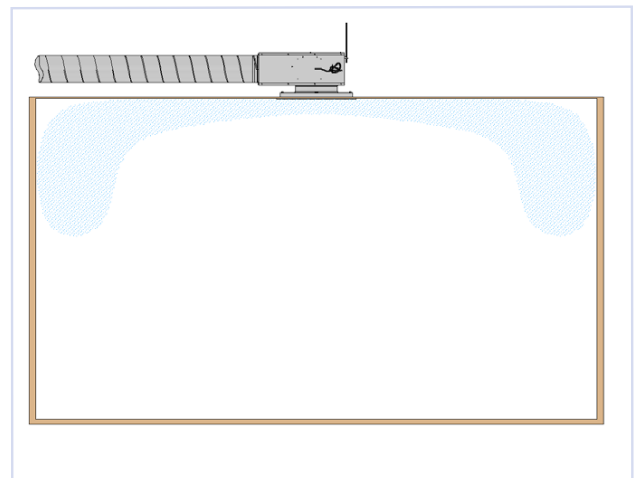


Fig 2: Flow pattern, Orion LØV

Orion-LØV with Sirius	Attenuation [dB]							
Dim.	63	125	250	500	1k	2k	4k	8k
125	14	11	12	12	18	11	14	15
160	12	9	12	11	16	10	14	15
200	10	8	11	12	15	12	12	14
250	8	7	11	12	13	13	13	14

Table 6: Static sound attenuation incl. end reflection, Orion-LØV with Sirius

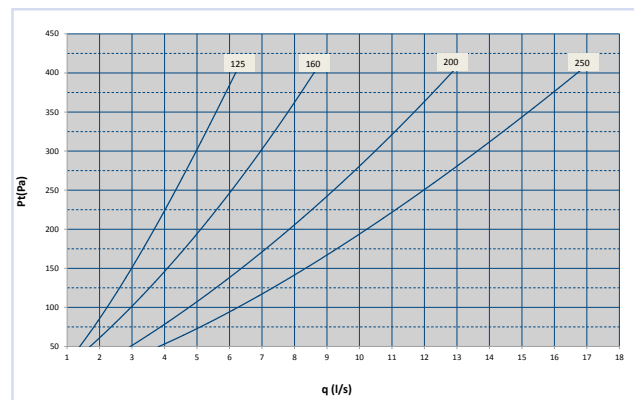


Fig. 3: Sirius, leakage at closed damper

E.1.3 VAV terminal



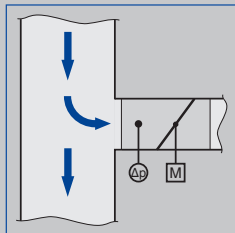
Compact controller



Easy controller



Nozzle for differential pressure measurement



For all upstream conditions



Tested to VDI 6022

VAV terminal units

Type LVC



For low airflow velocities and low duct pressures

Circular VAV terminal units for supply air and extract air systems with variable volume flows, low airflow velocities and low duct pressures

- New measurement principle, optimised for airflow velocities from 0.6 to 6 m/s
- High control accuracy even in case of unfavourable upstream conditions
- Electronic control components for different applications (Easy, Compact)
- Easy handling due to innovative control technique
- Casing length of only 310 mm for all nominal sizes
- Any installation orientation
- Closed blade air leakage to EN 1751, up to class 2
- Casing air leakage to EN 1751, class C

Optional equipment and accessories

- Secondary silencer Type CA, CS or CF for the reduction of air-regenerated noise
- Hot water heat exchanger Type WL and electric air heater Type EL for reheating the airflow

Type		Page
LVC	General information	LVC – 2
	Function	LVC – 4
	Technical data	LVC – 5
	Quick sizing	LVC – 6
	Specification text	LVC – 7
	Order code	LVC – 8
	Attachments	LVC – 9
	Dimensions and weight	LVC – 10
	Product details	LVC – 11
	Installation details	LVC – 12
	Basic information and nomenclature	LVC – 14

Application

Application

- Circular VAV terminal units of Type LVC for the precise supply air or extract air flow control in variable air volume systems with low airflow velocities.
- Closed-loop volume flow control using an external power supply
- For low airflow velocities and low duct pressures
- Effective pressure (differential pressure) as the result of two measurements, one upstream and one downstream of the damper blade
- The relation between damper blade position and differential pressure is stored as a characteristic relationship in the controller

- Shut-off by means of switching (equipment supplied by others)

Special features

- Optimised for low airflow velocities from 0.6 to 6 m/s
- High control accuracy even in case of unfavourable upstream conditions
- Any installation orientation
- Volume flow rate control with Easy or Compact controller
- Casing length of only 310 mm

Nominal sizes

- 125, 160, 200, 250

Description

Parts and characteristics

- Ready-to-commission unit which consists of mechanical parts and control components.
- Plastic nozzle with integral damper blade to measure the volume flow rate
- Easy controller with potentiometers, indicator light, terminals, damper blade position indicator, and protective cover
- Wire clamping bracket
- Double lip seal
- Factory-assembled control components complete with wiring and tubing
- Aerodynamic function testing on a special test rig prior to shipping of each unit
- Set-up data is given on a label or volume flow rate scale affixed to the unit
- High control accuracy even in case of unfavourable upstream conditions

Attachments

- Easy controller: Compact unit consisting of controller with potentiometers, differential pressure transducer and actuator
- Compact controller: Compact unit consisting of controller, differential pressure transducer and actuator

Useful additions

- Secondary silencer Type CA, CS or CF for demanding acoustic requirements

Construction features

- Circular casing
- Spigot with lip seal, for circular connecting ducts to EN 1506 or EN 13180
- Position of the damper blade indicated externally at shaft extension

Easy controller

- Screw terminals for the electrical connection
- Double terminals for looping the supply voltage, i.e. for the simple connection of voltage transmission
- Wire clamping bracket fixed to the casing

Compact controller

- Cable for the electrical connection

Materials and surfaces

- Casing made of galvanised sheet steel
- Nozzle, damper blade, and plain bearings made of ABS plastic, UL 94, flame retardant (V-0)
- Damper blade seal made of TPV (plastic)

Standards and guidelines

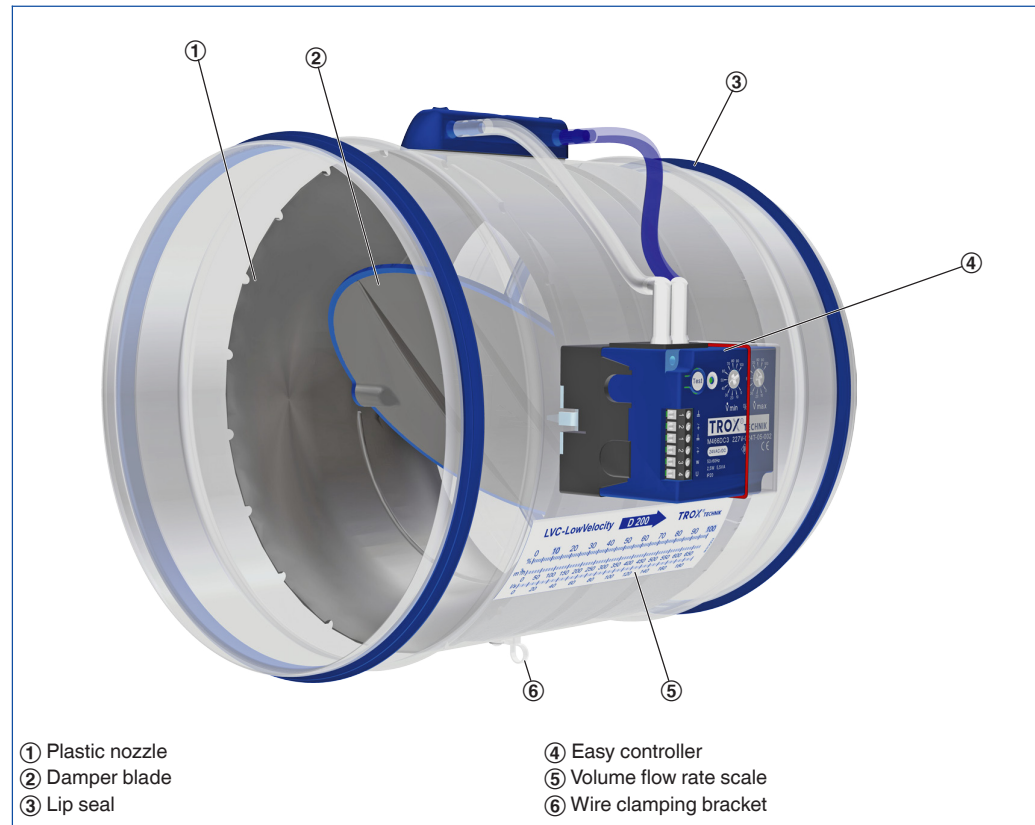
- Hygiene conforms to VDI 6022
- Closed blade air leakage to EN 1751, class 2 (nominal sizes 160 – 250, class 1)
- Nominal size 125 meets the general requirements of DIN 1946, part 4, with regard to the acceptable closed blade air leakage

Functional description

A new measurement principle makes it possible to measure low volume flow rates. The pressure is measured by means of a nozzle with tapings before (upstream) and after (downstream) the damper blade. The Easy controller or the Compact controller of the LVC determines the resulting

differential pressure (effective pressure) and compares it to the stored characteristic. This measurement principle is characterised by small measuring tolerances, and the upstream conditions do not have to meet any special requirements.

Schematic illustration of the LVC



Nominal sizes	125 – 250 mm
Volume flow rate range	8 – 300 l/s or 30 – 1080 m ³ /h
Volume flow rate control range	Approx. 10 to 100 % of the nominal volume flow rate
Minimum differential pressure	5 – 30 Pa
Maximum differential pressure	600 Pa
Operating temperature	10 – 50 °C

Volume flow rate ranges

The minimum differential pressure of VAV terminal units is an important factor in designing the ductwork and in rating the fan including speed control.

Sufficient duct pressure must be ensured for all operating conditions and for all control units. The measurement points for fan speed control must be selected accordingly.

The volume flow rates given for VAV terminal units

depend on the nominal size and on the control component (attachment) that is installed. The table gives the minimum and maximum values for a VAV terminal unit. Some control components may only have a limited volume flow rate range. This applies in particular to control components with a static differential pressure transducer. For volume flow rate ranges for all control components refer to our Easy Product Finder design programme.

LVC, Volume flow rate ranges and minimum differential pressures

Nominal size	①	②	③	④			$\Delta\dot{V}$ ± %
	\dot{V}		$\Delta p_{st\ min}$				
	l/s	m ³ /h	Pa	Pa	Pa	Pa	
125	8	29	5	5	5	5	15
	30	108	5	5	5	6	12
	55	198	16	17	18	19	8
	75	270	30	32	34	35	5
160	12	43	5	5	5	5	15
	50	180	5	5	6	6	12
	85	306	15	16	16	17	8
	120	432	30	32	33	34	5
200	20	72	5	5	5	5	15
	75	270	5	5	5	5	12
	135	486	15	16	16	16	8
	190	684	30	31	32	33	5
250	30	108	5	5	5	5	15
	120	432	5	5	5	5	12
	210	756	15	15	15	16	8
	300	1080	30	31	32	32	5

① LVC

② LVC with secondary silencer CS/CF, insulation thickness 50 mm, length 500 mm

③ LVC with secondary silencer CS/CF, insulation thickness 50 mm, length 1000 mm

④ LVC with secondary silencer CS/CF, insulation thickness 50 mm, length 1500 mm

Quick sizing tables provide a good overview of the room sound pressure levels that can be expected. Approximate intermediate values can be interpolated. Precise intermediate values and spectral data can be calculated with our Easy Product Finder design programme. The first selection criteria for the nominal size are the actual volume flow rates \dot{V}_{\min} and \dot{V}_{\max} . The quick sizing tables are based on generally accepted attenuation levels. If the sound pressure level exceeds the required level, a larger air terminal unit and/or a silencer is required.

LVC, Sound pressure level at differential pressure 50 Pa

Nominal size	\dot{V}	\dot{V}	Air-regenerated noise				Case-radiated noise
			①	②	③	④	①
	l/s	m ³ /h	L _{PA}	L _{PA1}			L _{PA2}
dB(A)							
125	8	29	27	<15	<15	<15	<15
	30	108	35	24	17	<15	17
	55	198	39	30	24	21	21
	75	270	42	34	28	25	23
160	12	43	29	19	<15	<15	<15
	50	180	34	26	23	19	19
	85	306	36	28	23	20	22
	120	432	38	31	26	23	24
200	20	72	31	21	<15	<15	<15
	75	270	35	26	19	17	19
	135	486	36	28	22	20	22
	190	684	36	28	23	21	24
250	30	108	31	24	18	16	17
	120	432	36	28	22	19	25
	210	756	36	28	22	20	28
	300	1080	36	29	23	21	31

- ① LVC
- ② LVC with secondary silencer CS/CF, insulation thickness 50 mm, length 500 mm
- ③ LVC with secondary silencer CS/CF, insulation thickness 50 mm, length 1000 mm
- ④ LVC with secondary silencer CS/CF, insulation thickness 50 mm, length 1500 mm

E.2 Datasheets for the Sensors

In the following the relevant pages from the datasheets for the sensors is presented.

E.2.1 Sensirion SCD30: CO₂, Temperature and Relative Humidity

In the following the datasheet of the Sensirion SCD30 sensor is presented.

Datasheet Sensirion SCD30 Sensor Module

CO₂, humidity, and temperature sensor

- NDIR CO₂ sensor technology
- Integrated temperature and humidity sensor
- Best performance-to-price ratio
- Dual-channel detection for superior stability
- Small form factor: 35 mm x 23 mm x 7 mm
- Measurement range: 400 ppm – 10.000 ppm
- Accuracy: $\pm(30 \text{ ppm} + 3\%)$
- Current consumption: 19 mA @ 1 meas. per 2 s.
- Fully calibrated and linearized
- Digital interface UART or I²C



Product Summary

CMOSens® Technology for IR detection enables carbon dioxide measurements of the highest accuracy at a competitive price.

Along with the NDIR measurement technology for detecting CO₂ comes a best-in-class Sensirion humidity and temperature sensor integrated on the very same sensor module. Ambient humidity and temperature can be measured by Sensirion's algorithm expertise through modelling and compensating of external heat sources without the need of any additional components. The very small module height allows easy integration into different applications.

Carbon Dioxide is a key indicator for indoor air quality. Thanks to new energy standards and better insulation, houses have become increasingly energy-efficient, but the air quality can deteriorate rapidly. Active ventilation is needed to maintain a comfortable and healthy indoor environment and improve the well-being and productivity of the inhabitants. Sensirion sensor solutions offer an accurate and stable monitoring of CO₂ in the air, as well as temperature and humidity. This enables our customers to develop new solutions that increase energy efficiency and simultaneously support the well-being of everyone.

Content

1 Sensor Specifications	2
2 Package Outline Drawing	4
3 Pin-Out Diagram	5
4 Operation and Communication	5
5 Shipping Package	5
6 Ordering Information	5
7 Important Notices	7
8 Headquarters and Subsidiaries	8

1 Sensor Specifications¹

CO₂ Sensor Specifications

Parameter	Conditions	Value
CO ₂ measurement range	I2C, UART PWM	0 – 40'000 ppm 0 – 5'000 ppm
Accuracy ²	400 ppm – 10'000 ppm	± (30 ppm + 3%MV)
Repeatability ³	400 ppm – 10'000 ppm	± 10 ppm
Temperature stability ⁴	T = 0 ... 50°C	± 2.5 ppm / °C
Response time ⁵	$\tau_{63\%}$	20 s
Accuracy drift over lifetime ⁶	400 ppm – 10'000 ppm ASC field-calibration algorithm activated and SCD30 in environment allowing for ASC, or FRC field-calibration algorithm applied.	± 50 ppm

Table 1: SCD30 CO₂ sensor specifications

Humidity Sensor Specifications⁷

Parameter	Conditions	Value
Humidity measurement range	-	0 %RH – 100 %RH
Accuracy ⁸	25°C, 0 – 100 %RH	± 3 %RH
Repeatability ³	-	± 0.1 %RH
Response time ⁵	$\tau_{63\%}$	8 s
Accuracy drift	-	< 0.25 %RH / year

Table 2: SCD30 humidity sensor specifications

Temperature Sensor Specifications⁷

Parameter	Conditions	Value
Temperature measurement range ⁹	-	- 40°C – 70°C
Accuracy ⁸	0 – 50°C	± (0.4°C + 0.023 × (T [°C] – 25°C))
Repeatability ³	-	± 0.1°C
Response time ⁵	$\tau_{63\%}$	> 10 s
Accuracy drift	-	< 0.03 °C / year

Table 3: SCD30 temperature sensor specifications

¹ Default conditions of T = 25°C, humidity = 50 %RH, p = 1013 mbar, V_{DD} = 3.3 V, continuous measurement mode with measurement rate = 2 s apply to values listed in the tables, unless otherwise stated.

² Deviation to a high-precision reference in the calibrated range (400 – 10'000 ppm) of the SCD30. Accuracy is fulfilled by > 90% of the sensors after calibration. Rough handling, shipping and soldering reduces the accuracy of the sensor. Full accuracy is restored with FRC or ASC recalibration features. Accuracy is based on tests with gas mixtures having a tolerance of ± 1.5%.

³ RMS error of consecutive measurements at constant conditions. Repeatability is fulfilled by > 90% of the sensors.

⁴ Average slope of CO₂ accuracy when changing temperature, valid at 400 ppm. Fulfilled by > 90% of the sensors after calibration.

⁵ Time for achieving 63% of a respective step function. Response time depends on design-in, heat exchange and environment of the sensor in the final application.

⁶ CO₂ concentrations < 400 ppm may result in sensor drifts when ASC is activated. For proper function of ASC field-calibration algorithm SCD30 has to be exposed to air with CO₂ concentration 400 ppm regularly.

⁷ Design-in of the SCD30 in final application and the environment impacts the accuracy of the RH/T sensor. Heat sources have to be considered for optimal performance. Please use integrated on-board RH/T compensation algorithm to account for the actual design-in.

⁸ Deviation to a high-precision reference. Accuracy is fulfilled by > 90% of the sensors after calibration.

⁹ RH/T sensor component is capable of measuring up to T = 120°C. Measuring at T > 70°C might result in permanent damage of the sensor.

Electrical Specifications

Parameter	Conditions	Value
Average current ¹⁰	Update interval 2 s	19 mA
Max. current	During measurement	75 mA
DC supply voltage (V _{ddmin} - V _{ddmax})	Min. and max. criteria to operate SCD30	3.3 V – 5.5 V
Interface	-	UART (Modbus Point to Point; TTL Logic), PWM and I ² C
Input high level voltage (V _{IH}) I2C	Min. and max. criteria to operate SCD30	1.75 V - 3.0 V
Input high level voltage (V _{IH}) Modbus	Min. and max. criteria to operate SCD30	1.75 V – 5.5 V
Input low level voltage (V _{IL}) I2C/Modbus	Min. and max. criteria to operate SCD30	- 0.3 V – 0.9 V
Output low level voltage (V _{OL}) I2C/Modbus	I _{IO} = +8 mA, Max. criteria	0.4 V
Output high level voltage (V _{OH}) I2C/Modbus	I _{IO} = -6 mA, Min. criteria	2.4 V

Table 4 SCD30 electrical specifications

Operation Conditions, Lifetime and Maximum Ratings

Parameter	Conditions	Value
Temperature operating conditions	Valid for CO ₂ sensor.	0 – 50°C
Humidity operating conditions	Non-condensing. Valid for CO ₂ sensor.	0 – 95 %RH
DC supply voltage	Exceeding specified range will result in damage of the sensor.	- 0.3 V – 6.0V
Voltage to pull up selector-pin	Max criteria	4.0 V
Voltage to pull up selector-pin	Min criteria	1.75 V
Storage temperature conditions	Exceeding specified range will result in damage of the sensor.	- 40°C – 70°C
Maintenance Interval	Maintenance free when ASC field-calibration algorithm ¹¹ is used.	None
Sensor lifetime	-	15 years

Table 5: SCD30 operation conditions, lifetime and maximum ratings

¹⁰ Average current including idle state and processing. Other update rates for small power budgets can be selected via the digital interface.

¹¹ CO₂ concentrations < 400 ppm may result in sensor drifts. For proper function of ASC field-calibration algorithm SCD30 has to be exposed to air with 400 ppm regularly.

2 Package Outline Drawing

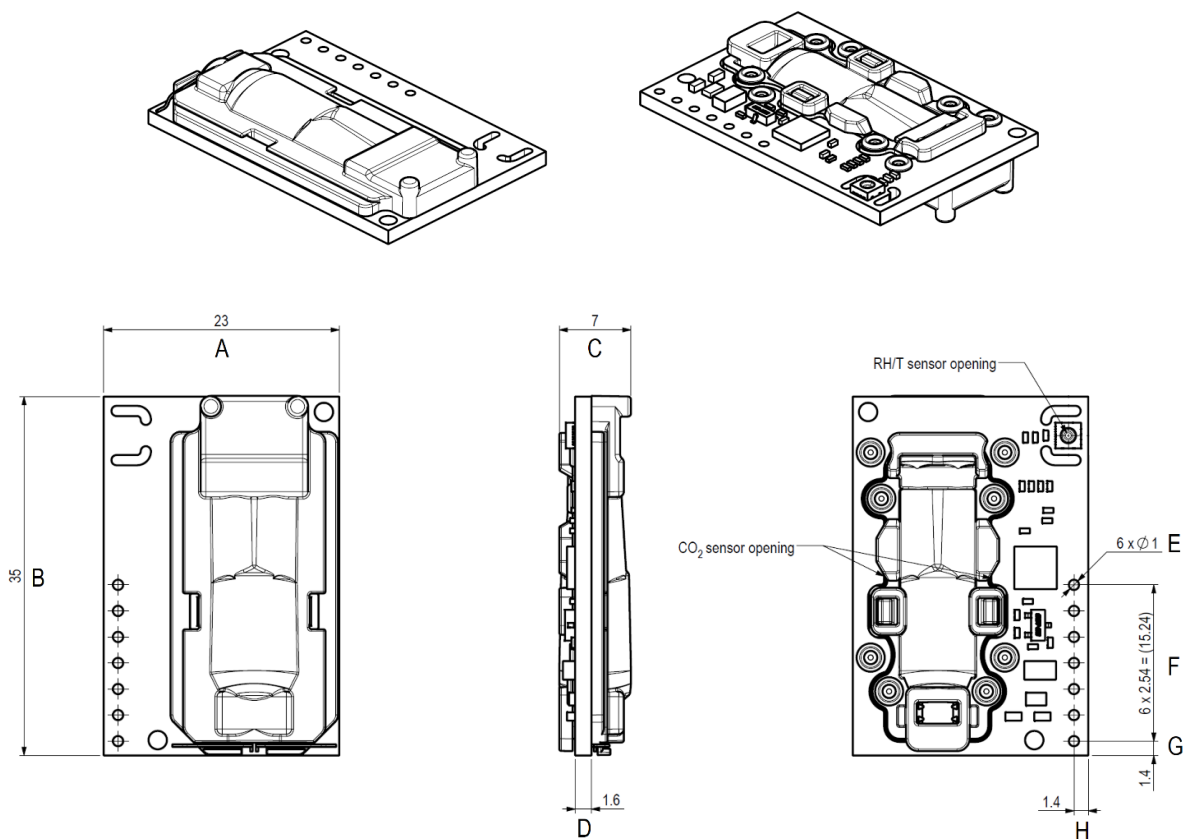


Figure 1 Product outline drawing of SCD30. Pictures on the left show top-view, pictures on the right bottom-view.

Sensor height is 7 mm at the thickest part of SCD30. The weight of one SCD30 sensor is 3.4 g.

Table 6: Nominal dimensions and tolerances SCD30

Dimension	A	B	C	D	E	F	G	H
Nominal [mm]	23.00	35.00	7.00	1.60	1.00	15.24	1.40	1.40
Tolerance [mm]	± 0.20	± 0.20	± 0.70	± 0.20	± 0.15	± 0.30	± 0.15	± 0.15

3 Pin-Out Diagram

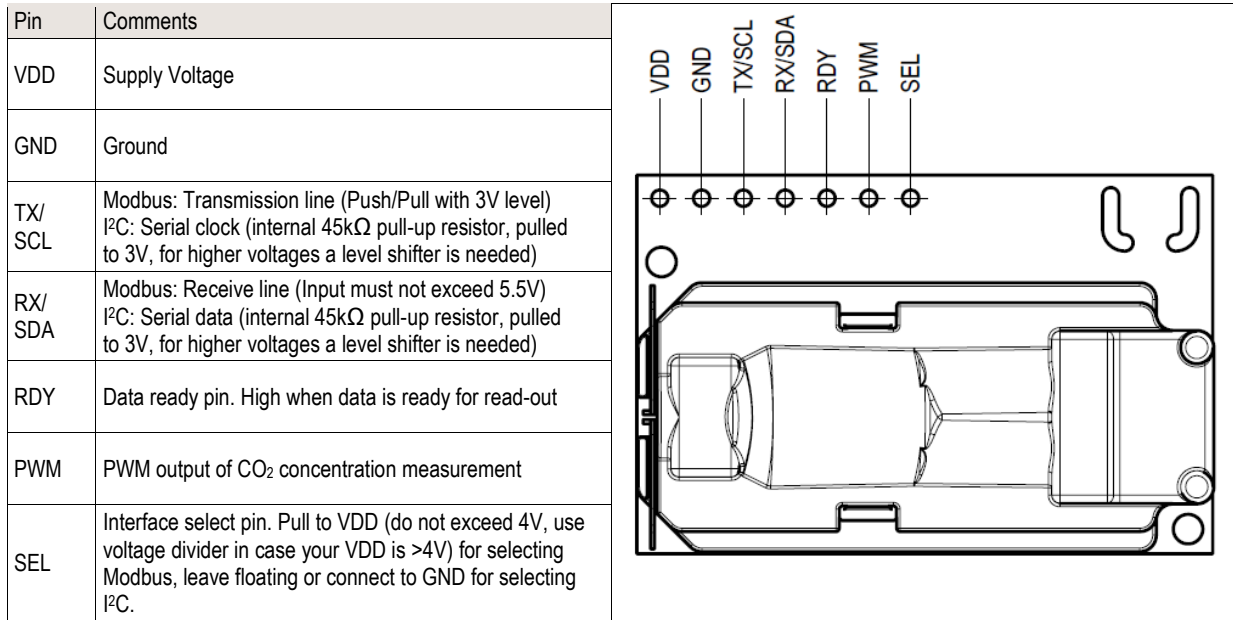


Figure 2: Pin-out of the SCD30.

4 Operation and Communication

Communication lines for I²C have an internal pull-up (45kΩ) to 3V, for higher voltages a level shifter is needed. Check VIH level of your I²C master to determine communication voltage. Please visit the download center of Sensirion webpage for the I²C, Modbus and PWM interface documentation¹².

5 Shipping Package

SCD30 sensor is shipped in stackable trays with 40 pieces each. The tray dimension is 363 mm x 257 mm x 19 mm. Stacking of trays results in an effective tray height of 13 mm.

6 Ordering Information

SCD30 and accessory can be ordered via the following article numbers.

Product	Description	Article Number
SCD30 sensor	CO ₂ , RH and T sensor module	1-101625-10
SEK-SCD30-Sensor	Standalone SCD30 sensor for EvalKit	3.000.061
SEK-SensorBridge	Sensor Bridge to connect SEK-SCD30-Sensor to computer	3.000.124

¹² www.sensirion.com/file/scd30_interface_description

E.2.2 Sensirion SPS30: Particulate Matter

In the following the datasheet of the Sensirion SPS30 sensor is presented.

Datasheet SPS30

Particulate Matter Sensor for Air Quality Monitoring and Control

- Unique long-term stability
- Advanced particle size binning
- Superior precision in mass concentration and number concentration sensing
- Small, ultra-slim package
- Fully calibrated digital output



Product Summary

The SPS30 Particulate Matter (PM) sensor is a technological breakthrough in optical PM sensors. Its measurement principle is based on laser scattering and makes use of Sensirion's innovative contamination-resistance technology. This technology, together with high-quality and long-lasting components, enables precise measurements from its first operation and throughout its lifetime of more than ten years. In addition, Sensirion's advanced algorithms provide superior precision for different PM types and higher-resolution particle size binning, opening up new possibilities for the detection of different sorts of environmental dust and other particles. With dimensions of only 41 x 41 x 12 mm³, it is also the perfect solution for applications where size is of paramount importance, such as wall-mounted or compact air quality devices.

Content

1 Particulate Matter Sensor Specifications	2
2 Electrical Specifications	3
3 Hardware Interface Specifications	4
4 Functional Overview	5
5 Operation and Communication through the UART Interface	8
6 Operation and Communication through the I ² C Interface	16
7 Mechanical Specifications	23
8 Shipping Package	24
9 Ordering Information	24
10 Revision History	24
11 Important Notices	25
12 Headquarters and Subsidiaries	26

1 Particulate Matter Sensor Specifications

1.1 Specification Overview

Parameter	Conditions		Value	Units
Mass concentration range	-		0 to 1'000	µg/m ³
Mass concentration size range	PM1.0		0.3 to 1.0	µm
	PM2.5		0.3 to 2.5	µm
	PM4		0.3 to 4.0	µm
	PM10		0.3 to 10.0	µm
Mass concentration precision ^{1,2} for PM1 and PM2.5 ³	0 to 100 µg/m ³		±10	µg/m ³
	100 to 1000 µg/m ³		±10	% m.v.
Mass concentration precision ^{1,2} for PM4, PM10 ⁴	0 to 100 µg/m ³		±25	µg/m ³
	100 to 1000 µg/m ³		±25	% m.v.
Maximum long-term mass concentration precision limit drift	0 to 100 µg/m ³		±1.25	µg/m ³ / year
	100 to 1000 µg/m ³		±1.25	% m.v. / year
Number concentration range	-		0 to 3'000	#/cm ³
Number concentration size range	PM0.5		0.3 to 0.5	µm
	PM1.0		0.3 to 1.0	µm
	PM2.5		0.3 to 2.5	µm
	PM4		0.3 to 4.0	µm
	PM10		0.3 to 10.0	µm
Number concentration precision ^{1,2} for PM0.5, PM1 and PM2.5 ³	0 to 1000 #/cm ³		±100	#/cm ³
	1000 to 3000 #/cm ³		±10	% m.v.
Number concentration precision ^{1,2} for PM4, PM10 ⁴	0 to 1000 #/cm ³		±250	#/cm ³
	1000 to 3000 #/cm ³		±25	% m.v.
Maximum long-term number concentration precision limit drift ²	0 to 1000 #/cm ³		±12.5	#/cm ³ / year
	1000 to 3000 #/cm ³		±1.25	% m.v. / year
Sampling interval	-		1±0.04	s
Typical start-up time ⁵	number concentration	200 – 3000 #/cm ³	8	s
		100 – 200 #/cm ³	16	s
		50 – 100 #/cm ³	30	s
Sensor output characteristics	PM2.5 mass concentration		Calibrated to TSI DustTrak™ DRX 8533 Ambient Mode	
	PM2.5 number concentration		Calibrated to TSI OPS 3330	
Lifetime ⁶	24 h/day operation		> 10	years
Acoustic emission level	0.2 m	max.	25	dB(A)
Long term acoustic emission level drift	0.2 m	max.	+0.5	dB(A) / year
Additional T-dependent mass and number concentration precision limit drift ²	temperature difference to 25°C	typ.	±0.5	% m.v. / °C
Weight	-		26.3 ±0.3	g

¹ Also referred to as “between-parts variation” or “device-to-device variation”.

² For further details, please refer to the document “Sensirion Particulate Matter Sensor Specification Statement”.

³ Verification Aerosol for PM2.5 is a 3% atomized KCl solution. Deviation to reference instrument is verified in end-tests for every sensor after calibration.

⁴ PM4 and PM10 output values are calculated based on distribution profile of all measured particles.

⁵ Time after starting Measurement-Mode, until a stable measurement is obtained.

⁶ Lifetime is based on mean-time-to-failure (MTTF) calculation. Lifetime might vary depending on different operating conditions.


Laser wavelength (DIN EN 60825-1 Class 1)		typ.	660	nm
--	---	------	-----	----

Table 1: Particulate matter sensor specifications. Default conditions of 25±2 °C, 50±10% relative humidity and 5 V supply voltage apply unless otherwise stated. 'max.' means 'maximum', 'typ.' means 'typical', '% m.v.' means '% of measured value'.

1.2 Recommended Operating Conditions

The sensor shows best performance when operated within recommended normal temperature and humidity range of 10 to 40 °C and 20 to 80 % RH, respectively.

2 Electrical Specifications

2.1 Electrical Characteristics

Parameter	Conditions	Min	Typ	Max	Unit
Supply voltage	-	4.5	5.0	5.5	V
Supply current	Sleep-Mode	-	38	50	µA
	Idle-Mode	300	330	360	
	Measurement-Mode	45	55	65	mA
	Measurement-Mode, first 200ms (fan start)	-	-	80	
Input high level voltage (V _{IH})	-	2.31	-	5.5	V
Input low level voltage (V _{IL})	-	0	-	0.99	
Output high level voltage (V _{OH})	-	2.9	3.3	3.37	
Output low level voltage (V _{OL})	-	0	0	0.4	

Table 2: Electrical specifications at 25°C.

2.2 Absolute Minimum and Maximum Ratings

Stress levels beyond those listed in Table 3 may cause permanent damage to the device. These are stress ratings only and functional operation of the device at these conditions cannot be guaranteed. Exposure to the absolute maximum rating conditions for extended periods may affect the reliability of the device.

Parameter	Min	Max	Unit
Supply voltage VDD	-0.3	5.5	V
Interface Select SEL	-0.3	4.0	
I/O pins (RX/SDA, TX/SCL)	-0.3	5.5	
Max. current on any I/O pin	-16	16	mA
Operating temperature range	-10	60	°C
Storage temperature range	-40	70	
Operating humidity range	0	95	% RH

Table 3: Absolute minimum and maximum ratings.

2.3 ESD / EMC Ratings

Immunity (Industrial level)

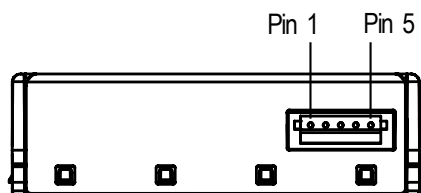
Description	Standard	Rating
Electro Static Discharge	IEC 61000-4-2	±4 kV contact, ±8 kV air
Power-Frequency Magnetic Field	IEC 61000-4-8	30A/m, 50Hz and 60Hz
Radio-Frequency EM-Field AM-modulated	IEC 61000-4-3	80MHz - 1000MHz, 10V/m, 80% AM @1kHz
Radio-Frequency EM-Field AM-modulated	IEC 61000-4-3	1.4GHz – 6GHz, 3V/m, 80% AM @1kHz

Emission (Residential level)

Description	Standard	Rating
Emission in SAC for 30MHz to 230MHz	IEC/CISPR 16	40dB(µV/m) QP @3m
Emission in SAC for 230MHz to 1000MHz	IEC/CISPR 16	47dB(µV/m) QP @3m
Emission in SAC for 1GHz to 3GHz	IEC/CISPR 16	70dB(µV/m) P, 50dB(µV/m) AP @3m
Emission in SAC for 3GHz to 6GHz	IEC/CISPR 16	74dB(µV/m) P, 54dB(µV/m) AP @3m

3 Hardware Interface Specifications

The interface connector is located at the side of the sensor opposite to the air inlet/outlet. Corresponding female plug is ZHR-5 from JST Sales America Inc. In Figure 1 a description of the pin layout is given.



Pin	Name	Description	Comments
1	VDD	Supply voltage	5V ± 10%
2	RX	UART: Receiving pin for communication	TTL 5V and LVTTTL 3.3V compatible
	SDA	I ² C: Serial data input / output	
3	TX	UART: Transmitting pin for communication	TTL 5V and LVTTTL 3.3V compatible
	SCL	I ² C: Serial clock input	
4	SEL	Interface select	Leave floating to select UART Pull to GND to select I ² C
5	GND	Ground	Housing on GND

Figure 1: The communication interface connector is located at the side of the sensor opposite to the air outlet.

Table 4 SPS30 pin assignment.

The SPS30 offers both a UART⁷ and an I²C interface. For connection cables longer than 20 cm we recommend using the UART interface, due to its intrinsic robustness against electromagnetic interference.

Note, that there is an internal electrical connection between GND pin (5) and metal shielding. Keep this metal shielding electrically floating in order to avoid any unintended currents through this internal connection. If this is not an option, proper external potential equalization between GND pin and any potential connected to the shielding is mandatory. Any current through the connection between GND and metal shielding may damage the product and poses a safety risk through overheating.

⁷ Universal Asynchronous Receiver Transmitter.

E.2.3 Sensirion SGP30: Total Volatile Organic Compounds

In the following the datasheet of the Sensirion SGP30 sensor is presented.

Datasheet SGP30

Indoor Air Quality Sensor for TVOC and CO₂eq Measurements

- Multi-pixel gas sensor for indoor air quality applications
- Outstanding long-term stability
- I²C interface with TVOC and CO₂eq output signals
- Very small 6-pin DFN package: 2.45 x 2.45 x 0.9 mm³
- Low power consumption: 48 mA at 1.8V
- Tape and reel packaged, reflow solderable



Product Summary

The SGP30 is a digital multi-pixel gas sensor designed for easy integration into air purifier, demand-controlled ventilation, and IoT applications. Sensirion's CMOSens[®] technology offers a complete sensor system on a single chip featuring a digital I²C interface, a temperature controlled micro hotplate, and two preprocessed indoor air quality signals. As the first metal-oxide gas sensor featuring multiple sensing elements on one chip, the SGP30 provides more detailed information about the air quality.

The sensing element features an unmatched robustness against contaminating gases present in real-world applications enabling a unique long-term stability and low drift. The very small 2.45 x 2.45 x 0.9 mm³ DFN package enables applications in limited spaces. Sensirion's state-of-the-art production process guarantees high reproducibility and reliability. Tape and reel packaging, together with suitability for standard SMD assembly processes make the SGP30 predestined for high-volume applications.

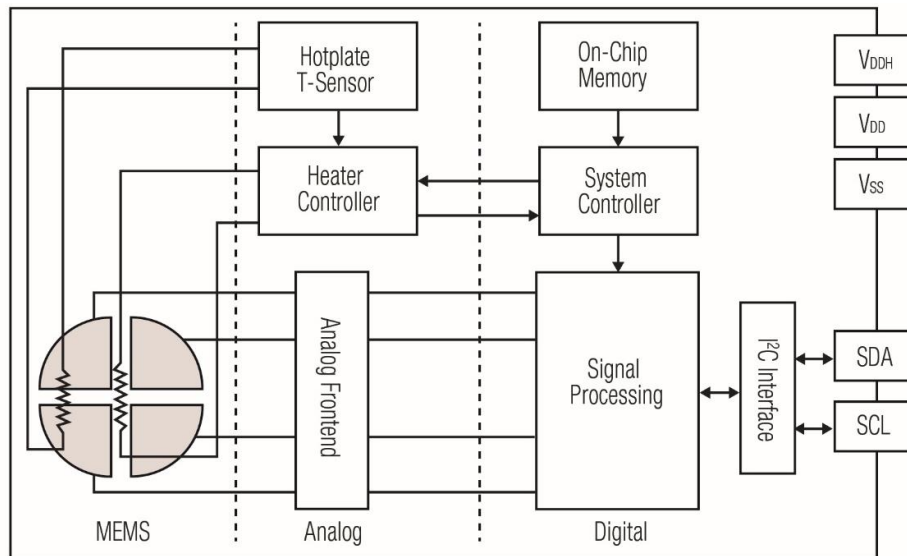


Figure 1 Functional block diagram of the SGP30.

1 Sensor Performance

1.1 Gas Sensing Performance

The values listed in **Table 1** are valid at 25°C, 50% RH and typical VDD.

Parameter	Signal	Values	Comments
Measurement range ¹	Ethanol signal	0 ppm ² to 1000 ppm	
	H ₂ signal	0 ppm to 1000 ppm	
Specified range	Ethanol signal	0.3 ppm to 30 ppm	The specifications below are defined for this measurement range. The specified measurement range covers the gas concentrations expected in indoor air quality applications.
	H ₂ signal	0.5 ppm to 3 ppm	
Accuracy ³	Ethanol signal	see Figure 2 typ.: 15% of meas. value	Accuracy is defined as $\frac{c - c_{set}}{c_{set}}$ with <i>c</i> the measured concentration and <i>c_{set}</i> the concentration set point. The concentration <i>c</i> is determined by $c = c_{ref} \cdot \exp\left(\frac{S_{ref} - S_{out}}{512}\right)$
	H ₂ signal	see Figure 3 typ.: 10% of meas. value	with <i>S_{out}</i> : Ethanol/Hydrogen signal output at concentration <i>c</i> <i>S_{ref}</i> : Ethanol/Hydrogen signal output at 0.5 ppm H ₂
Long-term drift ^{3,4}	Ethanol signal	see Figure 4 typ.: 1.3% of meas. value	Change of accuracy over time: Siloxane accelerated lifetime test ⁵
	H ₂ signal	see Figure 5 typ.: 1.3% of meas. value	
Resolution	Ethanol signal	0.2 % of meas. value	Resolution of Ethanol and Hydrogen signal outputs in relative change of the measured concentration
	H ₂ signal		
Sampling frequency	Ethanol signal	Max. 40 Hz	Compare with minimum measurement duration in Table 10
	H ₂ signal		

Table 1 Gas sensing performance. Specifications are at 25°C, 50% RH and typical VDD. The sensors have been operated for at least 24h before the first characterization.

¹ Exposure to ethanol and H₂ concentrations up to 1000 ppm have been tested. For applications requiring the measurement of higher gas concentrations please contact Sensirion.

² ppm: parts per million. 1 ppm = 1000 ppb (parts per billion)

³ 90% of the sensors will be within the typical accuracy tolerance, >99% are within the maximum tolerance.

⁴ The long-term drift is stated as change of accuracy per year of operation.

⁵ Test conditions: operation in 250 ppm Decamethylcyclopentasiloxane (D5) for 200h simulating 10 years of operation in an indoor environment.

Accuracy ethanol signal

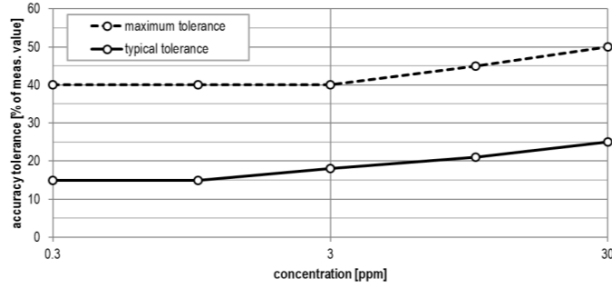


Figure 2 Typical and maximum accuracy tolerance in % of measured value at 25°C, 50% RH and typical VDD. The sensors have been operated for at least 24h before the characterization.

Accuracy H₂ signal

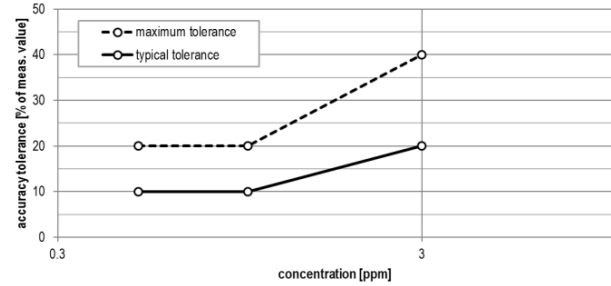


Figure 3 Typical and maximum accuracy tolerance in % of measured value at 25°C, 50% RH and typical VDD. The sensors have been operated for at least 60h before the characterization.

Long-term drift Ethanol signal

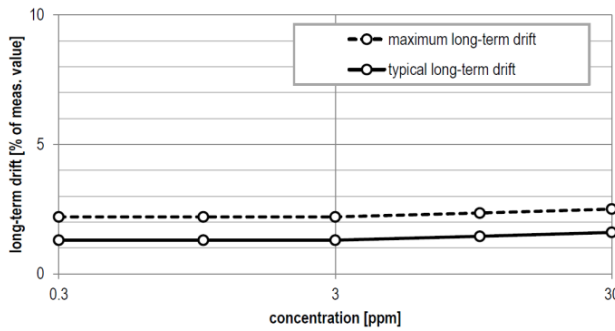


Figure 4 Typical and maximum long-term drift in % of measured value at 25°C, 50% RH and typical VDD. The sensors have been operated for at least 24h before the first characterization.

Long-term drift H₂ signal

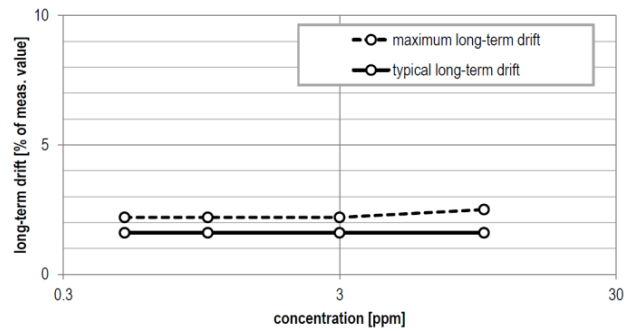


Figure 5 Typical and maximum long-term drift in % of measured value at 25°C, 50% RH and typical VDD. The sensors have been operated for at least 60h before the first characterization.

1.2 Air Quality Signals

Air quality signals TVOC and CO₂eq are calculated from Ethanol and H₂ measurements using internal conversion and baseline compensation algorithms (see **Figure 6**).

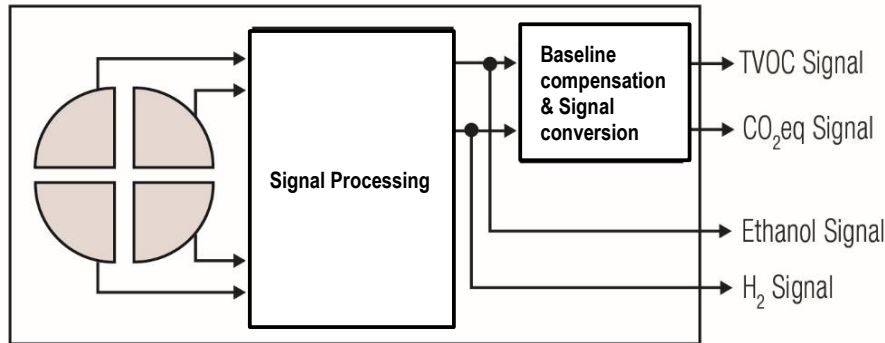


Figure 6 Simplified version of the functional block diagram (compare **Figure 1**) showing the signal paths of the SGP30.

Specifications of air quality signals are shown in **Table 2**.

Parameter	Signal	Values		Comments
Output range	TVOC signal	0 ppb to 60000 ppb		Maximum possible output range. The gas sensing performance is specified for the measurement range as defined in Table 1
	CO ₂ eq signal	400 ppm to 60000 ppm		
		Range	Resolution	
	TVOC signal	0 ppb - 2008 ppb	1 ppb	
		2008 ppb - 11110 ppb	6 ppb	
		11110 ppb - 60000 ppb	32 ppb	
	CO ₂ eq signal	400 ppm - 1479 ppm	1 ppm	
		1479 ppm - 5144 ppm	3 ppm	
		5144 ppm - 17597 ppm	9 ppm	
17597 ppm - 60000 ppm		31 ppm		
Sampling rate	TVOC signal	1 Hz		The on-chip baseline compensation algorithm has been optimized for this sampling rate. The sensor shows best performance when used with this sampling rate.
	CO ₂ eq signal	1 Hz		

Table 2 Air quality signal specifications.

1.3 Recommended Operating and Storage Conditions

Gas Sensing Specifications as detailed in **Table 1** are guaranteed only when the sensor is stored and operated under the recommended conditions. Prolonged exposure to conditions outside these conditions may accelerate aging.

The recommended temperature and humidity range for operating the SGP30 is 5–55 °C and 4–30 g m⁻³ absolute humidity, respectively (see **Figure 7** for the corresponding translation into relative humidity). It is recommended to store the sensor in a temperature range of 5–30 °C and below 30 g m⁻³ absolute humidity (see **Figure 8** for the corresponding translation into relative humidity). The sensor must not be exposed towards condensing conditions (i.e., >90 % relative humidity) at any time. To ensure a stable performance of the SGP30, conditions described in the document SGP Handling Instructions have to be met. Please also refer to the Design-in Guide for optimal integration of the SGP30 into the final device.

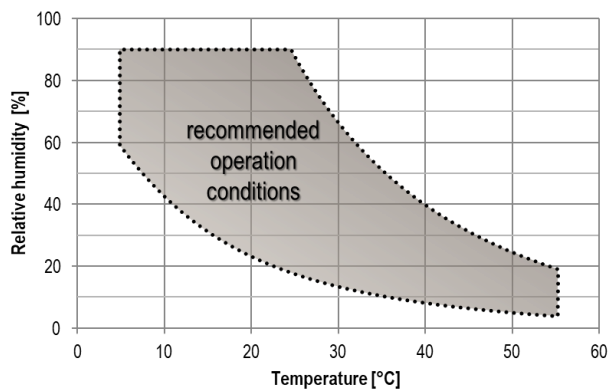


Figure 7 Recommended relative humidity and temperature for operating the SGP30.

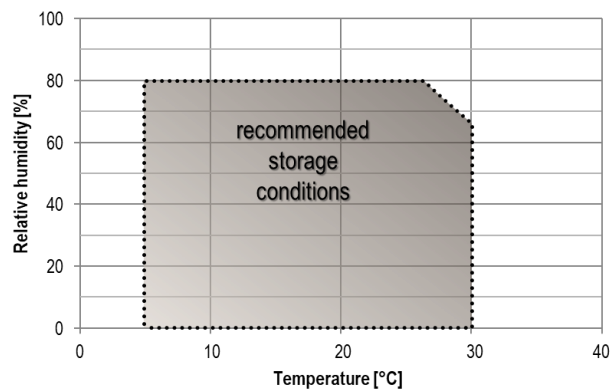


Figure 8 Recommended relative humidity and temperature for storing the SGP30.

2 Electrical Specifications

Parameter	Min.	Typ.	Max.	Unit	Comments
Supply voltage V_{DD}	1.62	1.8	1.98	V	Minimal voltage must be guaranteed also for the maximum supply current specified in this table.
Hotplate supply voltage V_{DDH}	1.62	1.8	1.98	V	
Supply current in measurement mode ⁶		48.8		mA	The measurement mode is activated by sending an "sgp30_iq_init" or "sgp30_measure_raw" command. Specified at 25°C and typical VDD.
Sleep current		2	10	μA	The sleep mode is activated after power-up or after a soft reset. Specified at 25°C and typical VDD.
LOW-level input voltage	-0.5		0.3*VDD	V	
HIGH-level input voltage	0.7*VDD		VDD+0.5	V	
V _{hys} hysteresis of Schmitt trigger inputs			0.05*VDD	V	
LOW-level output voltage			0.2*VDD	V	(open-drain) at 2mA sink current
Communication	Digital 2-wire interface, I ² C fast mode.				

Table 3 Electrical specifications.

3 Interface Specifications

The SGP30 comes in a 6-pin DFN package, see **Table 4**.

Pin	Name	Comments
1	V_{DD}	Supply voltage
2	V_{SS}	Ground
3	SDA	Serial data, bidirectional
4	R	Connect to ground (no electrical function)
5	V_{DDH}	Supply voltage, hotplate
6	SCL	Serial clock, bidirectional

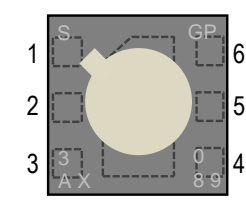


Table 4 Pin assignment (transparent top view). Dashed lines are only visible from the bottom.

⁶ A 20% higher current is drawn during 5ms on V_{DDH} after entering the measurement mode.

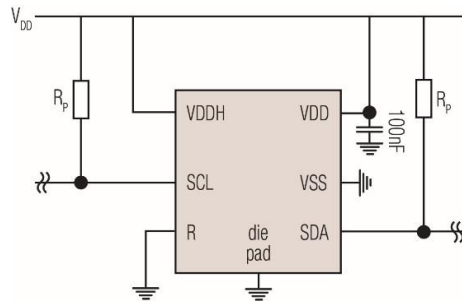


Figure 9 Typical application circuit (for better clarity in the image, the positioning of the pins does not reflect the positions on the real sensor).

The electrical specifications of the SGP30 are shown in **Table 3**. The power supply pins must be decoupled with a 100 nF capacitor that shall be placed as close as possible to pin VDD – see **Figure 9**. The required decoupling depends on the power supply network connected to the sensor. We also recommend VDD and VDDH pins to be shorted⁷.

SCL is used to synchronize the communication between the microcontroller and the sensor. The SDA pin is used to transfer data to and from the sensor. For safe communication, the timing specifications defined in the I²C manual⁸ must be met. Both SCL and SDA lines are open-drain I/Os with diodes to VDD and VSS. They should be connected to external pull-up resistors. To avoid signal contention, the microcontroller must only drive SDA and SCL low. The external pull-up resistors (e.g. $R_p = 10\text{ k}\Omega$) are required to pull the signal high. For dimensioning resistor sizes please take bus capacity and communication frequency into account (see for example Section 7.1 of NXP's I²C Manual for more details⁸). It should be noted that pull-up resistors may be included in I/O circuits of microcontrollers.

The die pad or center pad is electrically connected to GND. Hence, electrical considerations do not impose constraints on the wiring of the die pad. However, for mechanical stability it is recommended to solder the center pad to the PCB.

4 Absolute Minimum and Maximum Ratings

Stress levels beyond those listed in **Table 5** may cause permanent damage to the device. These are stress ratings for the electrical components only and functional operation of the device at these conditions cannot be guaranteed. Exposure to the absolute maximum rating conditions for extended periods may affect the reliability of the device.

Parameter	Rating
Supply voltage V_{DD}	-0.3 V to +2.16 V
Supply voltage V_{DDH}	-0.3 V to +2.16 V
Storage temperature range	-40 to +125°C
Operating temperature range	-40 to +85°C
Humidity Range	10% - 95% (non-condensing)
ESD HBM	2 kV
ESD CDM	500 V
Latch up, JESD78 Class II, 125°C	100 mA

Table 5 Absolute minimum and maximum ratings.

Please refer to Handling Instructions for Sensirion Gas Sensors on Sensirion webpage for full documentation.

⁷ If VDD and VDDH are not shorted, it is required that VDD is always powered when VDDH is powered. Otherwise, the sensor might be damaged.

⁸ http://www.nxp.com/documents/user_manual/UM10204.pdf

E.2.4 The Dart Sensors WZ-S: Formaldehyde

In the following the datasheet of The Dart Sensors WZ-S sensor is presented.

Dart Sensors WZ-S formaldehyde module

Operation Manual

DART SENSORS

ProSense Technologies Co., Ltd.

Brief Introduction

WZ-S formaldehyde module from global detection expert DART SENSORS combines novel HCHO sensor with advanced electronic control technology, converting HCHO concentration into PPM directly. Once HCHO arrives at working electrode (anode) it is oxidized instantaneously to generate an electrical signal. The electrical signal is then acquired and processed by microprocessor into a PPM value and is output by standard digital signal. WZ-S HCHO module is pre-calibrated in the factory and can be integrated into your system directly.

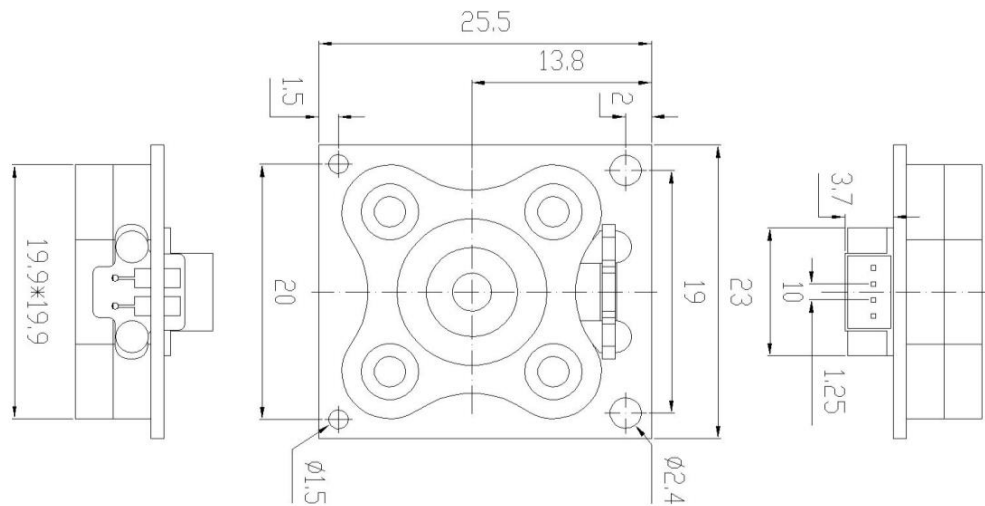
Typical Applications

- Smart home
- Portable devices
- Wearable devices
- Air conditioners
- Air cleaners
-

Key Features

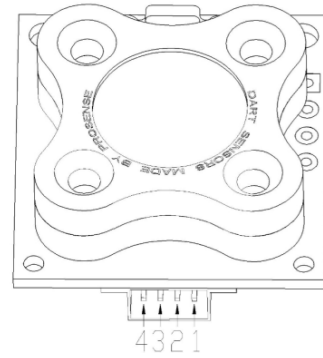
- High precision
- Fast response
- Long service life
- Low power consumption
- High stability
- Pre-calibrated

Diagram



Definition of Pins

PIN	DEFINITION
Pin1	Vin(5V)
Pin2	GND
Pin3	RXD (0~3.3V data input)
Pin4	TXD(0~3.3V data output)



Technical Specification

MODEL	WZ-S
Detection Principle	Micro fuel cell
Detectable Gas	HCHO
Detection Range	0-2ppm
Overload	10ppm
Input Voltage	5-7V
Warm up time	<3min
Response Time (T90)	<40S
Recovery Time (T10)	<60S
Resolution	0.001ppm
Operating temperature range	-20°C~50°C
Operating Humidity Range	10%~90%RH (non-condense)
Storage Condition	0~20°C
Lifetime	5 years in air
Warranty Period	12 months
Weight	4g

Communication Protocol

➤ General Settings

Module makes use of serial communication.

Communication configuration parameters are:

Baud rate	9600
Data bits	8 bits
Stop bit	1 bit
Parity bit	None

➤ Communication Command

There are two communication types: active upload type and Q&A type. The default type is active upload and it sends gas concentration once every second. Commands are as follow:

0	1	2	3	4	5	6	7	8
Start	Gas	Unit ppb	No decimal byte	Concentration (High byte)	Concentration (low byte)	Full range (high byte)	Full range (low byte)	Check sum
0xFF	CH2O=0x17	Ppb=0x04	0x00	0x00	0x25	0x07	0xD0	0x25

Gas concentration = concentration (high byte)*256 + concentration (low byte)

Switch to Q&A mode:

0	1	2	3	4	5	6	7	8
Start	Reserved	Switch command	Q&A	Reserved	Reserved	Reserved	Reserved	Checksum
0xFF	0x01	0x78	0x41	0x00	0x00	0x00	0x00	0x46

Switch to active upload mode:

0	1	2	3	4	5	6	7	8
Start	Reserved	Switch command	Active upload	Reserved	Reserved	Reserved	Reserved	Checksum
0xFF	0x01	0x78	0x40	0x00	0x00	0x00	0x00	0x47

To read gas concentration:

0	1	2	3	4	5	6	7	8
Start	Reserved	Command	Reserved	Reserved	Reserved	Reserved	Reserved	Checksum

0xFF	0x01	0x86	0x00	0x00	0x00	0x00	0x00	0x79
------	------	------	------	------	------	------	------	------

To return:

0	1	2	3	4	5	6	7	8
Start	Command	Concentration (High byte) (ug/m3)	Concentration (low byte) (ug/m3)	Reserved	Reserved	Concentration (High byte) (ppb)	Concentration (low byte) (ppb)	Checksum
0xFF	0x86	0x00	0x2A	0x00	0x00	0x00	0x20	0x30

Gas concentration = concentration (high byte)*256 + concentration (low byte)

Checksum calibration

```
/******
```

*Function name: unsigned char FucCheckSum(uchar *i,uchar ln)

*Function description: checksum calibration[Take Not(Byte1+Byte2+...Byte7) +1]

*Note: Take Not(Byte1+Byte2+...ByteX (X>2)

```
*****/
```

```
unsigned char FucCheckSum(unsigned char *i, unsigned char ln)
```

```
{
    unsigned char j, tempq=0;
    i+=1;
    for(j=0; j<(ln-2); j++)
    {
        tempq+=*i;
        i++;
    }
    tempq=(~tempq)+1;
    return(tempq);
}
```

Notes

- Avoid changing or moving sensor on the module.
- Avoid moving or changing electronic elements on PCB.
- Avoid exposure to organic vapour, organic solvent、 high gas concentration.
- Protect from excessive vibration and shock.

No recommended for industrial safety/personal monitoring, refer to 2-FP5.



ProSense Technologies Co., Ltd.

Add:Room206, Building4, Lianjian S&T Park, LonghuaDistrict,Shenzhen,China;

Tel: +86 755 3669 0079

Email: sales@szprosense.com

Appendix F

Risk Analysis

A risk assessment was performed in order to do the experiments in the test facility. The assessment is included in the following.

NTNU		Prepared by	Number	Date
		HSE section	HMSRV2801E	09.01.2013
HSE		Approved by		Replaces
Hazardous activity identification process		The Recorder		01.12.2008
				

Unit: Department of Energy and Process Engineering

Date: 21.07.22

Line manager: Terese Lovås

Participants in the identification process (including their function): Hans Martin Mathisen (supervisor), Maria Justo Alonso (co-supervisor), Stine Flage Marman (Student)

Short description of the main activity/main process: Master project for student Stine Flage Marman. "Experimental Development of Control Strategies for Demand Controlled Ventilation using IoT".

Is the project work purely theoretical? (YES/NO): NO Answer "YES" implies that supervisor is assured that no activities requiring risk assessment are involved in the work. If YES, briefly describe the activities below. The risk assessment form need not be filled out.

Signatures: Responsible supervisor:



Student: Stine F. Marman

ID nr.	Activity/process	Responsible person	Existing documentation	Existing safety measures	Laws, regulations etc.	Comment
1	Use of CO ₂ bottle	Stine Flage Marman		Sensors are used for monitoring CO ₂ concentrations. Thoroughly ventilating the rooms in between experiments. The bottle is secured using chains to prevent it from tipping over.	Forurensningsloven: http://www.lovdata.no/cgi-wit/idles?doc=/sfs/sf-20010430-0443.html Kjemikalieforskriften: http://www.lovdata.no/all/hl-19810313-006.html#6	CO ₂ bottle is used to supply CO ₂ to the rooms for measurements. Risk of leakage must be evaluated.
2	Mosquito coil	Stine Flage Marman		The mosquito coil is placed on a metal plate, with a metal cylinder around it, to prevent any ember from getting in touch with anything flammable.		Mosquito coils are used as PM sources. This requires combustion, and the risk of fire must therefore be evaluated.

NTNU	Risk assessment			Prepared by	Number	Date
				HSE section	HMSRV2803E	04.02.2011
HSE/MS				Approved by		Replaces
				The Rector		01.12.2008
						

Unit: Department of Energy and Process Engineering

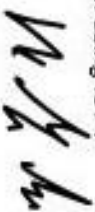
Date: 21.07.22

Line manager: Terese Lovås

Participants in the identification process (including their function): Hans Martin Mathisen (supervisor), Maria Justo Alonso (co-supervisor), Stine Flage Marmann (Student)

Short description of the main activity/main process: Master project for student Stine Flage Marmann. "Experimental Development of Control Strategies for Demand Controlled Ventilation using IoT"

Signatures: Responsible supervisor:



Student: Stine F. Marmann

Activity from the identification process form	Potential undesirable incident/strain	Likelihood: (1-5)	Consequence:			Risk Value (human)	Comments/status Suggested measures
			Human (A-E)	Environment (A-E)	Economy/material (A-E)		
Use of CO ₂ bottle	CO ₂ leakage	1	C	B	A	C1	
Mosquito coil	Fire	1	C	C	C	C1	

Likelihood, e.g.:

1. Minimal
2. Low
3. Medium
4. High
5. Very high

Consequence, e.g.:

- A. Safe
- B. Relatively safe
- C. Dangerous
- D. Critical
- E. Very critical

Risk value (each one to be estimated separately):

Human = Likelihood x Human Consequence
 Environmental = Likelihood x Environmental consequence
 Financial/material = Likelihood x Consequence for Economy/material

Potential undesirable incident/strain

Identify possible incidents and conditions that may lead to situations that pose a hazard to people, the environment and any materiel/equipment involved.

Criteria for the assessment of likelihood and consequence in relation to fieldwork

Each activity is assessed according to a worst-case scenario. Likelihood and consequence are to be assessed separately for each potential undesirable incident. Before starting on the quantification, the participants should agree what they understand by the assessment criteria.

NTNU	Risk assessment			Prepared by	Number	Date
				HSE section	HMSRFV2803E	04.02.2011
HSE/ES				Approved by		Replaces
				The Recorder		01.12.2008
						

Likelihood

Minimal 1	Low 2	Medium 3	High 4	Very high 5
Once every 50 years or less	Once every 10 years or less	Once a year or less	Once a month or less	Once a week

Consequence

Grading	Human	Environment	Financial/material
E Very critical	May produce fatalities	Very prolonged, non-reversible damage	Shutdown of work > 1 year.
D Critical	Permanent injury, may produce serious health damage/sickness	Prolonged damage- Long recovery time.	Shutdown of work 0.5-1 year.
C Dangerous	Serious personal injury	Minor damage- Long recovery time	Shutdown of work < 1 month
B Relatively safe	Injury that requires medical treatment	Minor damage- Short recovery time	Shutdown of work < 1week
A Safe	Injury that requires first aid	Insignificant damage- Short recovery time	Shutdown of work < 1day

The unit makes its own decision as to whether opting to fill in or not consequences for economy/material, for example if the unit is going to use particularly valuable equipment. It is up to the individual unit to choose the assessment criteria for this column.

Risk = Likelihood x Consequence

Please calculate the risk value for "Human", "Environment" and, if chosen, "Economy/material", separately.

About the column "Comments/status, suggested preventative and corrective measures":

Measures can impact on both likelihood and consequences. Prioritise measures that can prevent the incident from occurring, in other words, likelihood-reducing measures are to be prioritised above greater emergency preparedness, i.e. consequence-reducing measures.

NTNU		Risk matrix		prepared by	Number	Date
				HSE Section	HMSRV2604	8 March 2010
HSE/HS				approved by	Page	Replaces
				Revisor	4 of 4	9 February 2010



MATRIX FOR RISK ASSESSMENTS at NTNU

		CONSEQUENCE					LIKELIHOOD				
		Extremely serious	E1	E2	E3	E4	E5	Very low	Low	Medium	High
CONSEQUENCE	Extremely serious	E1	E2	E3	E4	E5					
	Serious	D1	D2	D3	D4	D5					
	Moderate	C1	C2	C3	C4	C5					
	Minor	B1	B2	B3	B4	B5					
	Not significant	A1	A2	A3	A4	A5					
		Very low	Low	Medium	High	Very high					

Principle for acceptance criteria. Explanation of the colours used in the risk matrix.

Colour	Description
Red	Unacceptable risk. Measures must be taken to reduce the risk.
Yellow	Assessment range. Measures must be considered.
Green	Acceptable risk. Measures can be considered based on other considerations.

